Technical University of Munich
TUM School of Medicine

Identification and functional characterization of the transcription factor CEBPB as a novel hub gene and disease driver in chronic inflammatory skin disorders

Menatullah Sameh Sameeh Mubarak

Complete reprint of the dissertation approved by the TUM School of Medicine of the Technical University of Munich for the award of the

Doktorin der Naturwissenschaften doctoral degree (Dr.rer.nat.).

Chair: Prof. Dr. Julia Jellusova

Examiners:

1. Prof. Dr. Stefanie Eyerich
2. Prof. Dr. Dr. Fabian Theis

The dissertation was submitted to the Technical University of Munich on 22 May 2023 and accepted by the TUM School of Medicine on 20 June 2023.

Summary

Transcription factors represent key nodes that integrate numerous environmental cues and signaling pathways to drive a plethora of downstream cellular responses. Their contribution to a multitude of human diseases like cancer and inflammatory disorders, as well as their great therapeutic potential has therefore been well-recognized. Also in chronic inflammatory skin diseases (CISD), different transcription factors have emerged as crucial players in the pathogenesis. CISDs represent a major global health burden and are characterized as highly diverse, complex diseases, whose pathogenesis is driven by a multitude of factors like genetic predisposition, environmental cues, impaired epithelial function and dysregulated cutaneous immunity.

The CCAAT/enhancer-binding protein beta (CEBPB) is a well-known transcription factor that is sensitive to various immunogenic stimuli. Although its function has been extensively characterized in different tissues, its role in the human skin remained so far unexplored. In this study, we investigate CEBPB as a novel master transcription factor in keratinocytes and aim at dissecting its functional role in-depth within skin inflammation. Using a novel biocomputational approach, we identified CEBPB as a hub gene differentially regulated in the lesional skin of CISD patients. In spatial transcriptomics, bulk RNA Seq and IHC analysis, CEBPB was significantly upregulated in the lesional skin of Lichen planus and Psoriasis patients compared to non-lesional skin, with the strongest levels in Psoriasis. Single-cell RNA Seq analysis revealed keratinocytes among high expressing cell populations for CEBPB in the lesional skin. Similarly, *in vitro* stimulated primary human keratinocytes showed significant CEBPB induction under Psoriasis- and Lichen-type microenvironments, implying a potential role for CEBPB in these diseases. Indeed, bulk RNASeq of CEBPB-knockout keratinocytes revealed regulation of various disease-relevant pathways, such as keratinization, antimicrobial peptide production, IL-17 signalling and chemokine secretion for psoriatic-type inflammation, and different cell death pathways, IL-1 family signalling and IFN- γ response for lichenoid-type inflammation. Using a 3D psoriatic skin model, we show that loss of CEBPB completely inhibited keratinocytes proliferation and IL22-induced acanthosis. Additionally, CEBPB-knockout keratinocytes showed reduced mitochondrial metabolism and ATP levels with downregulated metabolic fitness. Moreover, CEBPB-knockout reduced secretion of neutrophil attracting chemokines and inhibited neutrophil migration. In line, CEBPB levels positively correlated with the clinical scores of acanthosis and neutrophil infiltration in CISD patients. Finally, the generated CEBPB target gene signature could be traced back in patients showing a positive enrichment in Psoriasis.

Besides, its role in Psoriasis disease pathology, we show that CEBPB is also involved in type 1 skin inflammation. Here, using 3D Lichen skin models, we show that CEBPB-knockout inhibited apoptosis, indicating its involvement in cell death mediation under type 1 inflammatory conditions. Moreover, CEBPB-knockout significantly reduced the secreted IL-1ß levels, while increasing cell viability. Its role in apoptosis was also confirmed. In addition, we generated an extensive CEBPB target gene signature under type 1 inflammatory conditions showing downregulation of various disease markers, mainly IFN-γ response genes, as well as inflammatory cytokines and chemokines, upon CEBPB loss. In line, we demonstrate a positive correlation between the lesional expression of CEBPB and the clinical score of interface dermatitis in Lichen patients. Finally, this CEBPB target gene signature could also be traced back in Lichen patients.

Altogether, we show that CEBPB is associated with various pathogenic hallmarks of inflammatory skin diseases, hence proposing it as a novel regulatory node in skin inflammation and a control point for the pathogenic epithelial response in both Psoriasis and Lichen. In summary, we assign CEBPB a critical role in Psoriasis, where it regulates cell proliferation, drives acanthosis and neutrophil infiltration, as well as the expression of various disease-relevant factors in keratinocytes. In Lichen, we assign CEBPB a role in regulating the IFN-γ response, promoting apoptosis under type 1 conditions and driving the expression of various disease-relevant factors in keratinocytes, hence contributing to the clinical manifestation of interface dermatitis in lichenoid skin diseases.

This work also provides an extensive keratinocyte-specific CEBPB transcriptional landscape under different inflammatory conditions and can be exploited for the identification of novel downstream disease markers. These new CEBPB-mediated mechanisms thus expand the molecular view on transcription factors as disease drivers in the epidermis. Finally, our findings hold substantial promise for the use of CEBPB as new therapeutic target in skin inflammation.

Zusammenfassung

Transkriptionsfaktoren integrieren zahlreiche Umweltreize und Signalwege, um eine Vielzahl von nachgeschalteten zellulären Reaktionen anzutreiben. Ihre Rolle in einer Vielzahl menschlicher Erkrankungen, wie Krebs und entzündlichen Krankheiten, sowie ihr großes therapeutisches Potenzial, wurden daher allgemein anerkannt. Auch bei chronisch entzündlichen Hauterkrankungen (CISD) haben sich verschiedene Transkriptionsfaktoren als entscheidende Akteure in der Pathogenese herausgestellt. CISDs stellen eine große Herausforderung für die globale Gesundheit dar. Sie sind als sehr vielfältige, komplexe Krankheiten charakterisiert, deren Entstehung von einer Vielzahl von Faktoren wie genetischer Veranlagung, Umwelteinflüssen, beeinträchtigter Epithelfunktion und fehlregulierter kutaner Immunität bestimmt wird.

Das CCAAT/enhancer-binding protein beta (CEBPB) ist ein bekannter Transkriptionsfaktor, der auf verschiedene Immunstimuli reagieren kann. Seine Funktion in verschiedenen Geweben wurde schon umfassend untersucht, doch seine Rolle in der menschlichen Haut blieb bislang unerforscht. Im Rahmen dieser Studie untersuchen wir CEBPB als neuer Master-Transkriptionsfaktor in Keratinozyten mit dem Ziel, seine funktionelle Rolle in der Hautentzündung zu untersuchen. Mit Hilfe eines bioinformatischen Ansatzes, haben wir CEBPB als ein Hub-Gen identifiziert. Anhand von ‚spatial transcriptomics', Bulk RNASeq- und IHC-Analysen haben wir gezeigt, dass CEBPB in der Läsionshaut von Patienten mit Lichen planus und Psoriasis im Vergleich zur nicht-läsionalen Haut signifikant hochreguliert war, mit den stärksten Effekten in der Psoriasis. Keratinozyten wurden zudem anhand von Single cell RNASeq unter den stark exprimierenden Zellpopulationen für CEBPB in der Läsionshaut nachgewiesen. *In vitro* Stimulation von primären menschlichen Keratinozyten mit Psoriasis-und Lichen-spezifischen Stimuli bewirkte eine signifikante CEBPB-Induktion, was auf eine potenzielle Rolle von CEBPB in diesen Krankheiten hindeutete. In der Tat zeigte Bulk RNASeq Analyse von CEBPB-Knockout Keratinozyten eine Regulation von verschiedenen krankheitsrelevanten Pathways, wie ‚Verhornung' (keratinization), ‚Antimicrobial peptide-Produktion' ‚IL-17-Signalweg' und Ausschüttung von Chemokine für Entzündungen vom Psoriasis-Typ, und verschiedene Zelltodwege, IL-1-Familie Signalwege und IFN-γ-Antwort für Entzündungen vom lichenoiden Typ. Anhand eines 3D-Psoriasis-Hautmodells zeigen wir, dass der Verlust von CEBPB die Keratinozytenproliferation und die IL-22-induzierte Akanthose vollständig hemmen kann. Darüber hinaus zeigten CEBPB-Knockout Keratinozyten einen stark reduzierten mitochondrialen Metabolismus und gerinerge ATP-Produktion mit verringertem metabolischen Fitness. Darüber hinaus inhibierte der CEBPB-Knockout die Sekretion von Chemokinen, die Neutrophile anlocken, und hemmte somit die Migration von Neutrophilen.

Entsprechend korrelierten die CEBPB-Expressionswerte in der läsionalen Haut positiv mit den klinischen Scores von Akanthose und neutrophiler Infiltration bei CISD-Patienten. Schließlich konnte die generierte CEBPB-Gensignatur bei Pso Patienten mit positiver Anreicherung zurückverfolgt werden.

Neben seiner Rolle in der Psoriasis Pathologie zeigen wir, dass CEBPB auch an Typ-1-Hautentzündungen beteiligt ist. Hier zeigen wir anhand von 3D-Hautmodellen, dass CEBPB KO die Apoptose hemmte, was auf seine Beteiligung an der Zelltodvermittlung unter Typ-1-Entzündungsbedingungen hinweist. Zudem reduzierte CEBPB-Knockout signifikant die sezernierten IL-1ß-Spiegel, wobei die Viabilität der Zellen erhöht war. Auch seine Rolle in der Apoptose wurde bestätigt. Darüber hinaus haben wir eine umfassende CEBPB-Zielgensignatur unter Typ-1-Entzündungszuständen generiert, die durch eine Inhibierung verschiedener Krankheitsmarker, hauptsächlich IFN-γ response Gene, sowie entzündlicher Zytokine und Chemokine, charakterisiert war. In Übereinstimmung mit diesen Daten konnten wir eine positive Korrelation zwischen der läsionalen CEBPB Expression und dem klinischen Score von Interface Dermatitis bei Lichen-Patienten zeigen. Schließlich konnte diese CEBPB-Zielgensignatur auch bei Lichenpatienten zurückverfolgt werden.

Insgesamt zeigen wir in diesem Projekt, dass CEBPB mit verschiedenen pathogenen Merkmalen entzündlicher Hauterkrankungen assoziiert ist, und schlagen es daher als neuer regulatorischer Checkpoint bei entzündlichen Hauterkrankungen und als hub Gen für die pathogene Epithelreaktion sowohl bei Psoriasis als auch bei Lichen vor. Zusammenfassend weisen wir CEBPB eine entscheidende Rolle bei der Psoriasis zu, wo es die Zellproliferation, Akanthose und Neutrophileninfiltration reguliert, sowie die Expression verschiedener krankheitsrelevanter Faktoren in Keratinozyten antreibt. Im Lichen weisen wir CEBPB eine entscheidende Rolle bei der Regulierung der Zelllebensfähigkeit, der Förderung von Apoptose unter Typ-1-Bedingungen und der Steuerung der Expression verschiedener krankheitsrelevanter Faktoren in Keratinozyten zu, die letztendlich zur klinischen Manifestation von Interface Dermatitis bei lichenoiden Hauterkrankungen beitragen.

Diese Arbeit liefert auch eine umfangreiche Keratinozyten-spezifische Transkriptionslandschaft für CEBPB unter verschiedenen Immunbedingungen und kann für die Identifizierung neuer Krankheitsmarker genutzt werden. Diese neuen CEBPB-vermittelten Mechanismen erweitern somit die molekulare Sicht von Transkriptionsfaktoren als Krankheitstreiber in der Epidermis. Schließlich könnten unsere Ergebnisse für die Verwendung von CEBPB als neues therapeutisches Ziel bei chronischen Hautentzündungen vielversprechend sein.

Table of Contents

Table of Figures

List of Tables

List of Abbreviations

Abbreviation	Definition
AD	Atopic Dermatitis
AE	Atopic Eczema
AIM2	Absent in melanoma
AML	Acute myeloid leukemia
AMP	Antimicrobial peptide
AMPK	AMP-dependent protein kinase
ANOVA	Analysis of Variance
APC	Antigen presenting cell
ARG	Arginase
ASS 1	Argininosuccinate synthase 1
ATF	Activating transcription factor
ATP	Adenosine triphosphate
CASP	Caspase
CCNB	Cyclin B
CCNE	Cyclin E
CDC	Cell dividion cycle
CDK	Cyclin-dependent kinase
CEACAM	CEA cell adhesion molecule
CEBPB	CCAAT enhancer binding protein beta (human)
Cebpb	CCAAT enhancer binding protein beta (mouse)
CIDEC	Cell Death Inducing DFFA Like Effector C

CISD	Chronic inflammatory skin disease
CNS	Central nervous system
COPD	Chronic obstructive pulmonary disease
COX	Cyclooxygenase
CRE	cAMP response elements
CREB	AMP response element-binding protein
CRISPR	Clustered Regularly Interspaced Short Palindromic Repeats
CRP	C-reactive protein
CSF	Colony stimulation factor
CXCL	CXC motif chemokine ligand
DAMP	Death associated molecular pattern
DAPK	Death associated protein kinase
DBD	DNA binding domain
DC	Dendritic cell
DD	Dimerization domain
DEG	Differentially expressed gene
DHFR	Dihydrofolate reductase
DNA	Deoxyribonucleic acid
DSC	desmocollin
EAE	Experimental autoimmune encephalomyelitis
ECM	Extracellular matrix
EDN	Endothelin
ELISA	Enzyme-linked Immunosorbent Assay
EMP	Epithelial membrane protein
ETC	Electron transport chain
FA	Fatty acid
FABP	Fatty acid binding protein
FACS	Fluorescence activated cell sorting
FAO	Fatty acid oxidation
FFA	Free Fatty acid
FLG	Filaggrin
GBP	Guanylate binding protein
GC	Glucocorticoid
GSEA	Gene set enrichment analysis
HBV	Hepatitis B virus
HCV	Hepatitis C virus
HFD	High-fat diet
HIF	Hypoxia induced factor
HPV	Human papilloma virus
HS	Hidradenitis suppurativa
HSC	Hematopietic stem cell
IAP	Inhibitor of apoptosis
ICAM	Intercellular Adhesion Molecule

ID	Interface dermatitis
IF	Immunofluorescence
IFIT	Interferon Induced With Tetratricopeptide Repeats
IFITM	Interferon induced transmembrane
IFN	Interferon
IHC	Immunohistochemistry
IL	Interleukin
ILC	Innate lymphoid cell
IRF	Interferon response factor
ISG	Interferon stimulated gene
ITGAM	Integrin subunit alpha M
JAK	Janus activated kinase
KO	Knockout
KRT	Keratin
LAP	Liver activating protein
LC	Langerhans cell
LCE	Late cornified envelope
LCN	Loricrin
LE	Lupus erythematosus
LEP	Leptin
LIP	Liver inhibitory protein
LP	Lichen planus
LPS	Lipopolysaccharide
MACS	Magnetic activated cell sorting
MCM	minichromosome maintenance
MEFV	MEFV Innate Immunity Regulator, Pyrin
MFI	Median fluorescence intensity
MIP	Major intrinsic protein
MMP	Matrix metalloproteinases
MOA	Mode of action
MS	Multiple sclerosis
MYB	MYB Proto-Oncogene, Transcription Factor
MYC	MYC Proto-Oncogene, BHLH Transcription Factor
NDUF	NADH:Ubiquinone Oxidoreductase
NES	Normalized enrichment score
NFKB	Nuclear factor kappa B
NGS	Next-generation sequencing
NK	Natural killer
NL	Non-lesional
NLR	NOD-like receptor
NLRP	NOD, Leucine rich Repeat and Pyrin domain containing
NLS	Nuclear localization signal
NOD	Nucleotide-binding oligomerization domain

NOS	Nitric oxide synthase
OCR	Oxygen consumption rate
OE	Overexpression
OIS	Oncogene-induced senescence
ORA	Overrepresentation analysis
ORF	Open-reading frame
OS	Oxidative stress
OXPHO	Oxidative phosphorylation
PA	Pathway analysis
PAMP	Pathogen-associated molecular pattern
PARP	Poly (ADP-ribose) polymerase
PCNA	Proliferating cell nuclear antigen
PCR	Polymerase chain reaction
PFA	Paraformaldehyde
PG	Prostaglandin
PIM	Pim-1 proto-oncogene, proviral integration site 1
PPAR	Peroxisome Proliferator-Activated Receptor
PRODH	Proline dehydrogenase
PTGS	Prostaglandin-Endoperoxide Synthase
QC	Quality control
RA	Retinoic acid
RAR	Retinoic acid receptor
RAS	Ras proto-oncogene, Rat sarcoma
RIPK	Receptor Interacting Serine/Threonine Kinase
RNA	Ribonucleic acid
RNP	Ribonucleoprotein
ROS	Reactive oxygen species
RT	Room temperature
SAA	Serum amyloid A
SC	Stratum corneum
SERPIN	Serine proteinase inhibitor
SLE	Systemic Lupus Erythematosus
SMAC	second mitochondrial-derived activator of caspases
SN	Supernatant
SOD	Superoxide dismutase
SPRR	Small proline-rich protein
SRC	Spare respiratory capacity
STAT	signal transducer and activator of transcription
SZ	SMAC, ZVAD
TAD	Tranactivation domain
TCS	T-cell supernatant
TF	Transcription factor
TGF	Transforming growth factor

TK	Thymidine kinase
TLR	Toll-like receptor
TMEM	Transmembrane
TNF	Tumor necrosis factor
UMAP	Uniform Manifold Approximation and Projection
UMI	Unique molecular identifier
UQCRC	Ubiquinol-Cytochrome C Reductase Core Protein
US	Unstimulated
WB	Western blot
XAF	XIAP Associated Facto
ZVAD	Pan-Caspase inhibitor Z-VAD-FMK

1. Introduction

1.1. The skin- structure and immunological function

1.1.1. The skin- a complex, multi-functional organ

The skin is the largest organ of the body and its primary interface with the environment (Kupper and Fuhlbrigge 2004; Nestle et al. 2009). It is responsible for balancing body temperature and moisture, restricting water loss, transmitting sensation, protecting from UV light and providing mechanical integrity (S. Eyerich et al. 2018; Kabashima et al. 2019). As the outermost organ of the body, it is constantly exposed to physical, chemical and microbial insults and has thus evolved to act as the body's first line of defense. This protective barrier function of the skin is not restricted to the historically well-characterized mechanical properties, where the skin was viewed as inert tight barrier that inhibits the entry of potentially harmful environmental substances and pathogens, but is rather reinforced by a complex and versatile system of active cutaneous immune surveillance (Kupper and Fuhlbrigge 2004; S. Eyerich et al. 2018).

1.1.2. Skin structure and overview of skin components

The skin consists of two major compartments, the epidermis and the connective tissue (Figure 1), with keratinocytes being the main and most numerous cell type in the epidermal compartment (Pasparakis, Haase, and Nestle 2014). Epidermal keratinocytes are highly specialized epithelial cells with the main physiological function of maintaining the physical barrier of the skin by forming its outermost layer known as the stratum corneum (SC) (Kabashima et al. 2019; Eckert and Rorke 1989). The formation of the SC is achieved by keratinocytes passing through three different epidermal layers as they mature to finally become corneocytes by terminal differentiation (Figure 1 A). First, the basal layer (stratum basale) lies at the border with the underlying dermis and contains proliferating keratinocytes (epidermal stem cells), which express the keratins K5 and K14 (Bikle, Xie, and Tu 2012; Moll et al. 1982). As the keratinocytes leave the stratum basale and start to differentiate, they switch to expressing the keratins K1 and K10 (early differentiation markers) in the stratum spinosum (Bikle, Xie, and Tu 2012; Eichner, Sun, and Aebi 1986). The stratum granulosum is the uppermost nucleated layer below the SC and contains keratinocytes with dense granules of filaggrin (FLG) and loricrin, as well as laminar bodies (LB) with lipids that are important for tight junction formation (Mehrel et al. 1990; Steven et al. 1990; Matsui and Amagai 2015; S. Eyerich et al. 2018). Finally, keratinocytes reach terminal differentiation becoming corneocytes in the SC layer. The corneocytes are characterized as flattened, denucleated

"dead" cells with their plasma membrane being replaced by a 'cornified envelope', that consists of crosslinked keratin filaments enclosed with a lipid envelope (Egawa and Kabashima 2016; Candi, Schmidt, and Melino 2005; S. Eyerich et al. 2018). The net result is a resilient impermeable structure providing protection and barrier function.

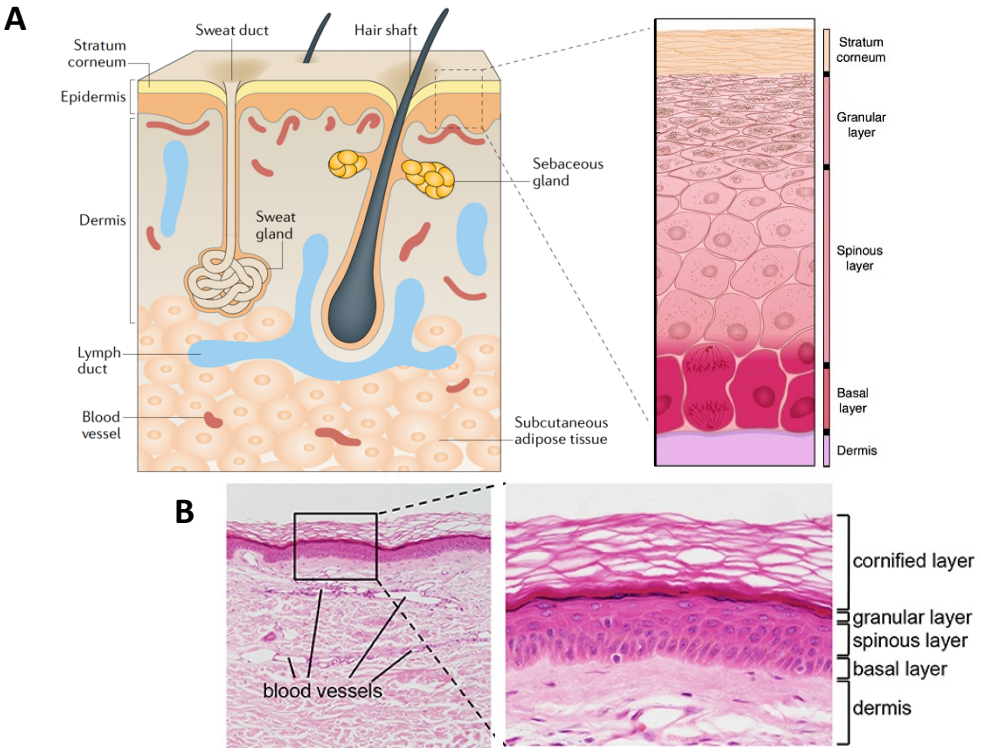

Figure 1: Structure of the human skin. A) Structural components of the human skin showing the epidermis with its stratum corneum (SC) and the dermis with integrated sweat and sebaceous glands, hair shafts, lymph and blood vessels, as well as underlying subcutaneous adipose tissue. A zoom-in (right) shows the different epidermal layers formed by keratinocytes in distinct differentiation states, as they go from mitotically active basal cells to spinous cells then enucleated granular cells, resulting finally in differentiated, cross-linked corneocytes in the SC. **B)** H&E stained section of healthy human skin at a magnification of ×10 (left panel) and ×40 (right panel), showing the histological appearance of epidermis and underlying dermis (left) and a zoom-in on the epidermis with its four main layers (right). Adapted and modified from (Kabashima et al. 2019; Segre 2006; Martin et al. 2021).

In contrast to the relatively simple anatomy of the epidermis, the underlying dermis is anatomically more complex with a greater cell diversity (Nestle et al. 2009). The dermis contains fibroblasts and other stromal cells, as well as nerve endings, and is rich in extracellular matrix (ECM) comprising collagen and elastin fibers (Pasparakis, Haase, and Nestle 2014; S. Eyerich et al. 2018). In addition, lymphatic and vascular vessels are present in the dermis, allowing the migration and recruitment of different immune cells (Kabashima et al. 2019).

1.1.3. The skin as an active immune organ

Innate immune cells and T-cells in the skin

Immunosurveillance of a large and exposed organ like the skin represents a unique challenge in its complexity and regulation. In the epidermis, Langerhans cells (LCs), which are a unique subset of antigen-presenting cells (APCs) with a dendritic cell (DC)-like phenotype, represent the main skin-resident immune cell type (Figure 2). (Kabashima et al. 2019; Nestle et al. 2009). Additionally, T-cells, mainly CD8+ T-cells can be found in the lower epidermal layers (Krueger and Stingl 1989). The dermis, on the other hand, contains more specialized immune cells such as different subsets of DCs, macrophages, mast cells, innate lymphoid cells (ILCs), NKT cells and CD4+ T-helper (Th) cells (Kabashima et al. 2019; Tong et al. 2015; Pasparakis, Haase, and Nestle 2014). Here, T-cells are preferentially residing beneath the epidermal-dermal junction (Bos and Kapsenberg 1993; Nestle et al. 2009). At steady-state in healthy skin, CD4+ and CD8+ T-cells are usually present in equal numbers in the dermis with most being skin-specific resident memory T-cells. These cells support DCs, mast cells and macrophages in the dermal innate immune sensing of danger signals (e.g. pathogen components) via activation of different innate immune receptors (PRRs) such as Toll-like (TLRs) and NOD-like (NLRs) receptors, as well as various innate immune pathways such as the inflammasome activation and antimicrobial peptides (AMPs) secretion (Volz, Kaesler, and Biedermann 2012; de Koning et al. 2012; S. Eyerich et al. 2018; Kupper and Fuhlbrigge 2004). Finally, these dermal immune cell populations are highly dynamic and undergo drastic changes during an inflammatory immune response, leading to the recruitment of further effector T-cells, as well as different granulocytes.

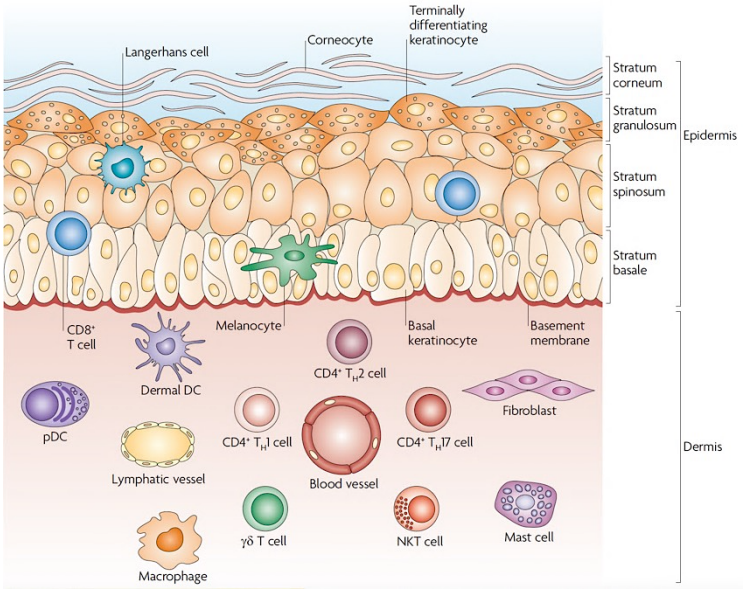

Figure 2: Immunological skin anatomy and cellular effectors. Specialized cells in the epidermis are shown: mainly melanocytes, which produce pigment (melanin) and Langerhans cells and more rarely CD8+ cytotoxic T cells, can be found in the stratum basale and stratum spinosum. Various specialized cells in the dermis include dendritic cells (dermal DCs and plasmacytoid DCs (pDCs)), different T cell subsets (CD4+ T helper 1 (Th1), Th2 and Th17 cells, γδ T cells) and natural killer T (NKT) cells. Additionally, fibroblasts, macrophages and mast cells and are present. From (Nestle et al. 2009).

Keratinocytes as immune sentinels

Keratinocytes are not merely barrier components, but rather important and often under-appreciated participants in cutaneous immune responses. In fact, together with the previously described LCs they represent epidermal innate immune sentinels that express several TLRs and are capable of sensing pathogen-associated molecular patterns (PAMPs) (Nestle et al. 2009; Lebre et al. 2007). During skin infection by pathogens, keratinocytes are key producers of AMPs like ß-defensins (Gilliet and Lande 2008; Lai and Gallo 2009). Additionally, keratinocytes can sense danger-associated molecular patterns (DAMPs) such as toxins leading to inflammasome activation and the production of active pro-inflammatory cytokines IL-1ß and IL-18 via cleavage from their precursors (Martinon, Mayor, and Tschopp 2009; Nestle et al. 2009). Keratinocytes also produce large amounts of other cytokines like IL-1α, TNF and IL-6, thus stimulating both local and systemic immune responses (Cristina Albanesi et al. 2005). Furthermore, activated keratinocytes are an important source of chemokines and therefore actively shape the immune response by selectively recruiting different immune cell types from the blood into the skin. Interestingly, although keratinocytes cannot directly prime naïve T-cells, they are capable of inducing functional recall immune responses in antigen-experienced memory T-cells (Black et al. 2007). Thus, keratinocytes can act both as innate immune sentinels and pro-inflammatory effector cells to initiate and amplify immune responses in the skin under infection and inflammation.

1.2. Chronic inflammatory skin disorders and their immune response patterns

1.2.1. Chronic inflammatory skin diseases (CISDs)

As an active immune organ, the skin serves as an arena for a wide variety of immune processes that are orchestrated by T-cells and ILCs (Pasparakis, Haase, and Nestle 2014; Ho and Kupper 2019; Sabat et al. 2019). Imbalance of the cutaneous immune system with uncontrolled or misdirected immune activity is implicated in the development of various pathologic conditions such as chronic inflammatory skin diseases (CISDs), including Psoriasis, Atopic and Allergic contact dermatitis, Lichen planus, Cutaneous lupus and Vitiligo. These skin disorders constitute a major global health burden due to their frequency and association with a severe loss of quality of life, as well as a high risk for various comorbidities such as Allergic asthma, Arthritis, metabolic syndromes and cardiovascular diseases (Kadunce and Krueger 1995; Galli et al. 2003; González et al. 1998; Porter et al. 1997; Kupper and Fuhlbrigge 2004). Additionally, they are connected with enormous socio-economic costs, thereby adding to the overall burden inflicted by these diseases (Nestle, Kaplan, and Barker 2009; Augustin et al. 2012; Finlay 2009).

CISDs are further characterized as highly diverse and complex diseases, whose pathogenesis is driven by a multitude of factors such as genetic predisposition, environmental cues, impaired epithelial function and dysregulated cutaneous immunity (C. Albanesi and Pastore 2010; Kilian Eyerich, Eyerich, and Biedermann 2015). In addition, intricate communication between epithelial and immune cells plays a critical role in the dynamic regulation of cutaneous immune responses and is hence implicated in the pathogenesis of inflammatory skin diseases (Bernard et al. 2012; Kupper and Fuhlbrigge 2004). In this frame, keratinocytes have elaborate immunoregulatory functions and play active roles in both the initiation and amplification of skin inflammation. Heterogeneity on disease and patient level further add another layer to this complexity (K. Eyerich and Eyerich 2018; Quaranta et al. 2014). In fact, more than 100 different CISDs have been historically described based on clinical and histological phenotype, making disease classification complex and often misleading.

1.2.2. Immune response patterns in CISDs

Different umbrella phenotypes have been since defined based on the immune response patterns to group CISDs into different types according to the dominating T-cells, as these represent the detrimental drivers of the skin pathogenic processes. In this frame, different T-helper (Th) cell subsets and their innate counterparts, together with their produced signature cytokines, act as molecular switches to regulate cutaneous inflammation, by dictating drastic molecular changes in the local tissue cells (e.g. keratinocytes), thereby leading to specific skin alterations of both microscopic and macroscopic nature (K. Eyerich and Eyerich 2018; Quaranta et al. 2014). This immune classification can be hence summarized into following six patterns (Figure 3): **(1)** lichenoid pattern, caused by type 1 immune cells and characterized by a strong immune cytotoxic reaction against basal keratinocytes **(2a)** eczematous pattern, caused by type 2 immune cells and defined by impaired epidermal barrier and increased infection, **(2b)** bullous pattern, caused by type 2 immune cells and defined by loss of epithelial integrity, **(3)** psoriatic pattern, caused by type 3 immune cells, where a strong neutrophil infiltration, high metabolic activity and epidermal thickening (so-called acanthosis) are main features, **(4a)** fibrogenic and **(4b)** granulomatous, caused by a dysbalance of regulatory T-cells (Tregs) resulting in either dermal thickening with atrophic epidermis or formation of granulomas, respectively (K. Eyerich and Eyerich 2018). Such classification is critical not only for appropriate diagnosis, but also for rational choice of therapy, especially with the advances made in immune-mediated therapeutics (K. Eyerich and Eyerich 2018; Noda, Krueger, and Guttman-Yassky 2015).

The patterns 1, 2a and 3, representing the main patterns of most common CISDs, were the focus in this project and will therefore be described with their associated diseases into more detail in the following sections.

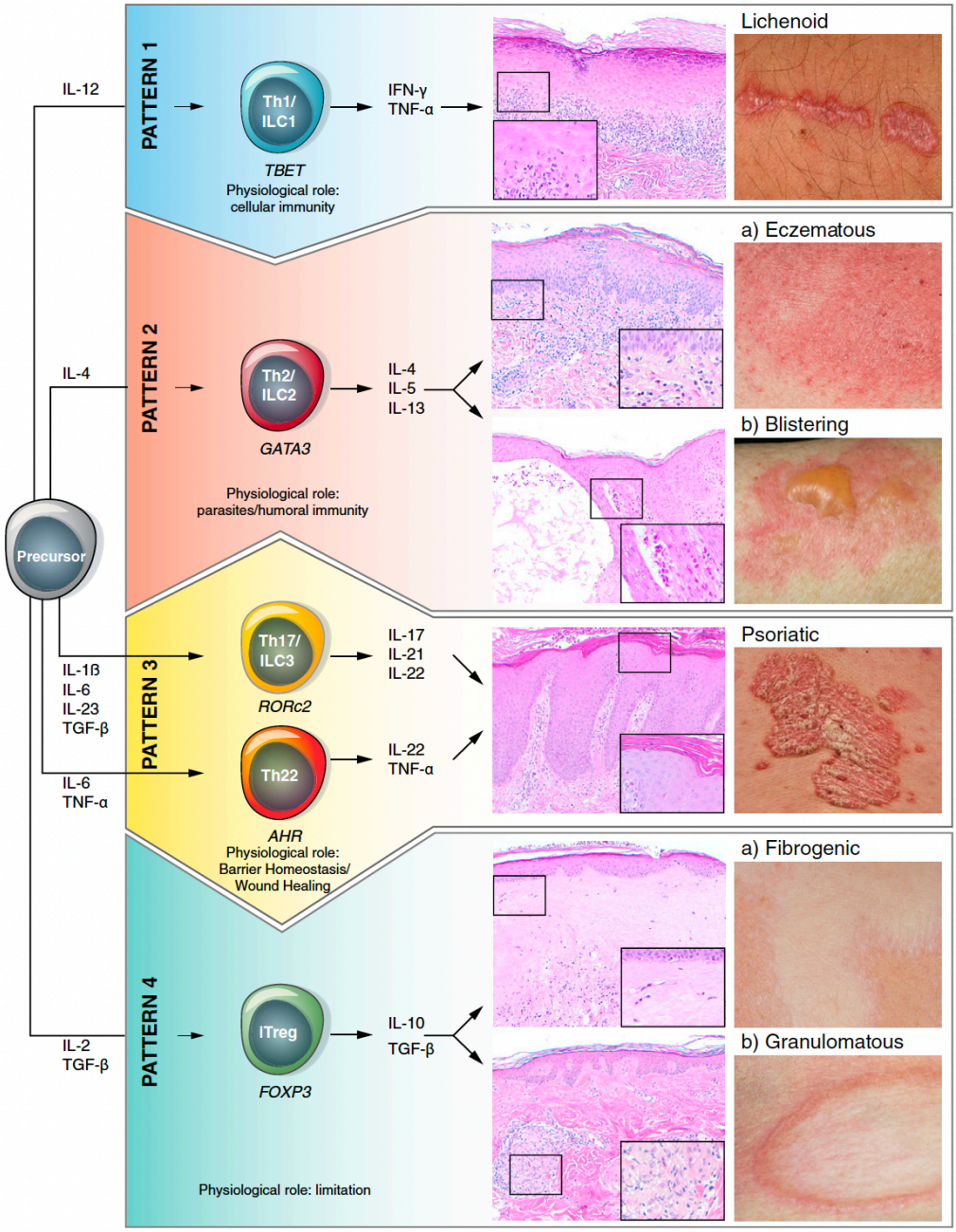

Figure 3: Lymphocyte subsets drive different immune response patterns in the skin. The main T-helper (Th) subgroups differentiate from a common precursor under specific stimuli as indicated. The derived Th subsets are characterized by the depicted master transcription factors and the key cytokines they produce as part of their effector functions. These secreted cytokines elicit six distinct cutaneous immune response patterns, with different histological and clinical pictures as shown for each pattern. Lichenoid inflammatory skin diseases thus follow a Th1, eczematous skin diseases a Th2, psoriatic skin diseases a Th17/Th22 and fibrogenic skin diseases a Treg pattern. The displayed clinical pictures highlight the heterogeneity of CISDs. Adapted from (K. Eyerich and Eyerich 2018).

1.2.3. The Lichenoid/ type 1 pattern and Lichen planus

The major physiological role of the cytotoxic immune response found in the lichenoid pattern is removal of potentially infected or (pre)-carcinogenic cells (K. Eyerich and Eyerich 2018). In type 1

inflammatory skin disorders, this reaction is dysregulated and directed against healthy keratinocytes of the basal layer leading to 'interface dermatitis' (ID), the hallmark histological feature of these diseases. ID is characterized by a band-like immune cell infiltrate along the basal membrane of the epidermis and cell death in keratinocytes, which show typical vacuolization and cell swelling (Sontheimer 2009). Lupus erythematosus (LE) and Lichen planus (LP) represent two classical Interface dermatitis positive inflammatory skin diseases (K. Eyerich and Eyerich 2018; Lauffer et al. 2018).

LP is a rare dermatosis with a prevalence of 0.22-1% and significant association with several other diseases like thyroid disease, vitiligo, alopecia areata and systemic viral infections such as with Hepatitis C and B virus (HCV, HBV) and human papilloma virus (HPV) (Vičić et al. 2023; Li et al. 2017; Lodi, Pellicano, and Carrozzo 2010; Wang and Hung 2021; Della Vella et al. 2021; Ioannides et al. 2020). In fact, viral components are proposed among the key environmental factors that can trigger LP by modification of self-antigens on the surface of basal keratinocytes leading to host immune response dysregulation (Shengyuan et al. 2009; Boch et al. 2021) .

At the center of the immunopathogenesis of these diseases are cytotoxic CD8+ T-cells (Tc1), CD4+ Th1 cells, ILC1, NKT and NK cells (Figure 4B) (K. Eyerich and Eyerich 2018; Boch et al. 2021). Other cell types like mast cells, macrophages and plasmacytoid DCs (pDCs), but also Th17, Th9 and Tfh cells are involved (Aghamajidi et al. 2021; Żychowska, Woźniak, and Baran 2021; Vičić et al. 2023). On the molecular level, IFN-γ as the master cytokine and regulator of type 1 lymphocytes drives this cytotoxic reaction and dictates the molecular alterations in keratinocytes. Besides cell death by apoptosis or necroptosis, keratinocytes contribute to disease progression and chronicity by production of different cytokines such IL-1ß, IL-6 and TNF-α, and chemokines like CXCL9, CXCL10 and CXCL11, which attract more type 1 lymphocytes into the skin, as well as the upregulation of various cell adhesion molecules like ICAM-1 and VCAM-1, again promoting immune cell migration to the inflammation site (Farley, Wood, and Iordanov 2011; Aghamajidi et al. 2021; Vičić et al. 2023; K. Eyerich and Eyerich 2018) . Moreover, apart from IFN-γ, the release of other cytotoxic molecules by type 1 lymphocytes like perforin, granzyme B and granulysin, together with Fas-FasL mediated cell death of keratinocytes contributes to the basement membrane disruption, epidermal injury and consequent development of chronic lichenoid lesions (K. Eyerich and Eyerich 2018; Vičić et al. 2023; Prpić Massari et al. 2004; Grassi et al. 2009; Chung et al. 2008). Additionally, other cytokines that have been implicated in type 1-disease pathogenesis are IFN-α, TNF- α and IL-1ß, as well as the Th17 cytokines IL-17A and IL-22 (Boch et al. 2021; Vičić et al. 2023). Finally, clinically, these molecular and histological changes result in planar,

polygonal papules and plaques with shiny desquamation and common pruritus, with erosions in extreme cases (Figure 4A) (K. Eyerich and Eyerich 2018).

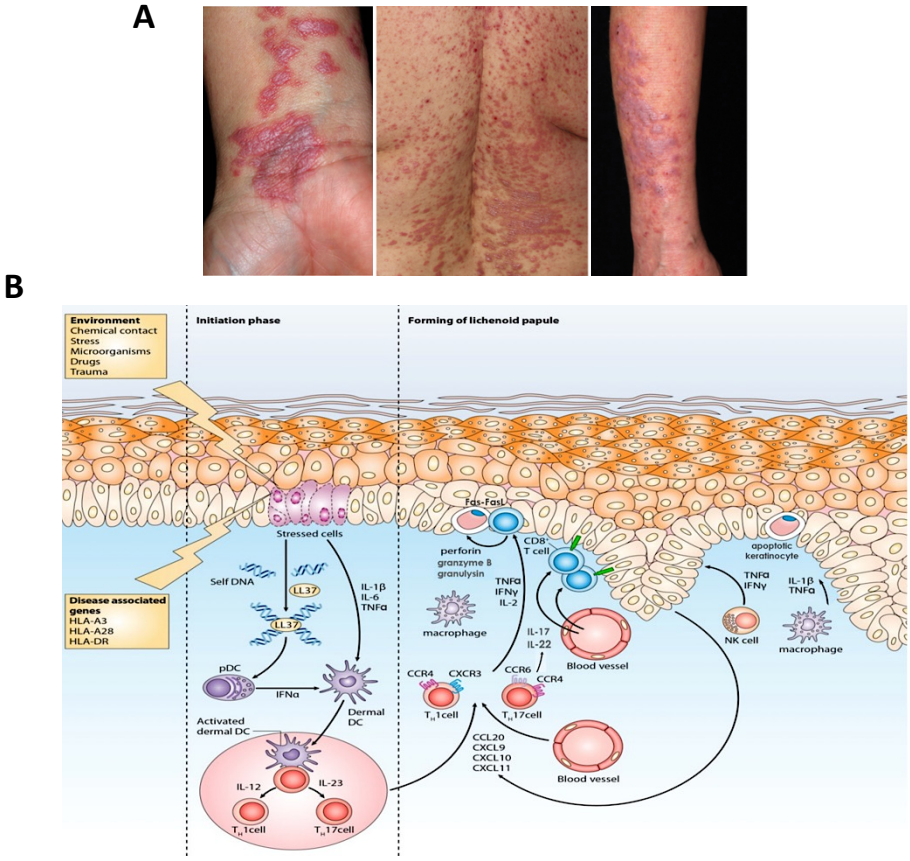

Figure 4: Lichen planus: clinical manifestation and immunopathogenesis. A) Cutaneous Lichen planus (LP) patients with typical clinical picture (Boch et al. 2021). **B)** LP immunopathogenesis with major effector cells and signaling pathways. LP inflammation begins as an antigen-directed reaction, caused by different environmental and genetic factors, finally resulting in the differentiation and activation of effector T-cells (mainly Th1, but also Th17). T-cells are recruited into the skin via the action of depicted chemokines and secrete key inflammatory cytokines such as IFN-γ, while effector CD8+ T-cells mediate keratinocytes cell death by the Fas-FasL receptors and cytotoxic mechanisms through granule exocytosis of perforin, granzyme B, and granulysin. An LP lesion is formed and maintained by other inflammatory cells such as DCs, macrophages and NK cells. From (Vičić et al. 2023).

1.2.4. The Eczematous/ type 2 pattern and Atopic dermatitis

The major physiological role of the eczematous pattern is host defence against extracellular parasites, a process that is dysregulated in Atopic dermatitis (AD) (also called Atopic eczema (AE)) (K. Eyerich and Eyerich 2018). AD is the most common chronic inflammatory skin disease with a prevalence of 10-30% in children and 2-3% in adults (Hay et al. 2014; Kilian Eyerich, Eyerich, and Biedermann 2015). It is often associated with other type 2-mediated disorders like food allergies, allergic rhinitis and asthma. AD-affected patients suffer from skin lesions with papules, scaly plaques, erythema, dry skin and

intense pruritus (K. Eyerich and Eyerich 2018; Kilian Eyerich, Eyerich, and Biedermann 2015). On the cellular level, these lesions are dominated mainly by Th2 and ILC2 cells (type 2 lymphocytes) secreting high levels of IL-4, IL-13, IL-5 and IL-31 with various effects on the epidermis. Other cell types like mast cells and eosinophilic granulocytes are also common in the AD immune infiltrate. IL-4, IL-13 and IL-31 all interfere with keratinocytes differentiation leading to the downregulation of epidermal differentiation genes like filaggrin (*FLG*), thereby inhibiting barrier function and resulting in dry skin (Howell et al. 2007; Cornelissen et al. 2012). In fact, loss-of-function mutations in the *FLG* gene represent the strongest genetic association with AD development (Palmer et al. 2006). An important immune function of keratinocytes under such type 2 microenvironment, is the upregulation of various immune mediators like IL-25, IL-33 and TSLP, which are critical drivers of type 2 immune responses (Otsuka et al. 2017; S. Eyerich et al. 2018). Additionally, IL-31 functions a main mediator of itch (pruritus) (Dillon et al. 2004; Sabat et al. 2019). IL-4 and IL-13 also inhibit cutaneous immunity with deficient epidermal production of AMPs in keratinocytes, which ultimately leads to atypical colonization of the skin of AD patients with *Staphylococcus aureus* or other microbes with an overall increased risk of cutaneous pathogen infections (Ong et al. 2002; S. Eyerich et al. 2011). IL-5, on the other hand, is responsible for the activation of mast cells, eosinophils and basophils, which release mediators that lead to further influx of immune cells, itch and oedema (K. Eyerich and Eyerich 2018). Altogether, these type 2 immune changes result in histological hallmarks such as spongiosis in the acute phase and irregular epidermal thickening (acanthosis) in the chronic phase.

1.2.5. The Psoriatic/ type 3 pattern and Psoriasis

The physiological role of the immune reaction found in the psoriatic pattern is the host defense against extracellular pathogens and maintenance of homeostasis at epithelia of barrier organs (K. Eyerich and Eyerich 2018). This is driven by type 3 lymphocytes, mainly by CD4+ Th17 and Th22 cells, but also by Tc17 and ILC3 cells, producing the disease signature cytokines IL-17A, TNF-α, IL-22 and IL-23.

Psoriasis (Pso) is the most common skin inflammatory disease dominated by this cytokine axis. With a prevalence of 2-3%, Psoriasis is a common disease frequently associated with metabolic disorders, cardiovascular diseases, colitis and joint disease (psoriatic arthritis) (Parisi et al. 2013; Sterry et al. 2007; Henes et al. 2014; Takeshita et al. 2017). Both genetic and external life-style factors such as smoking are involved in the development of Psoriasis (Sabat et al. 2019). Additionally, autoantigens like LL-37 and the melanocytic protein ADAMTSL5 are described as potential triggers (Schäkel, Schön, and Ghoreschi 2016). Clinically, classic psoriatic lesions manifest as sharply demarcated, raised plaques with thick desquamation and scaling (Figure 5A) (K. Eyerich and Eyerich 2018). Microscopically,

psoriatic skin lesions are characterized by massively thickened epidermis (acanthosis), increased stratum corneum (hyperkeratosis), reduced stratum granulosum (hypogranulosis) and the presence of cell nuclei in the stratum corneum (parakeratosis) (K. Eyerich and Eyerich 2018; Sabat et al. 2019). Other histological hallmarks include the accumulation of neutrophils (micro-abscesses) in the upper layers of the epidermis, a strong lymphocytic dermal infiltrate with T-cells, DCs and macrophages, as well as dilated dermal blood capillaries.

On the molecular level, these histological changes are caused by hyperactive epidermal metabolism accompanied by keratinocytes hyperproliferation and increased migration, on the one hand, and inhibited differentiation on the other hand, as well as by activation of innate immune pathways (Figure 5B) (K. Eyerich and Eyerich 2018). IL-17A induces keratinocytes secretion of various chemokines like CCL20, which attracts Th17/Th22 cells and CXCL1, CXCL5 and CXCL8, which are all strong attractants for neutrophils, as well as the production of several AMPs (e.g. LL-37, S100A7/A8/A9) and of VEGF, which stimulates vascularization (S. Eyerich et al. 2010; Furue et al. 2020; K. Eyerich and Eyerich 2018; Sabat et al. 2019). Like IL-17A, IL-22 is also involved in the induction of AMPs in keratinocytes. Moreover, IL-22 is mainly responsible for the impaired cornification process by increasing keratinocytes proliferation, while inhibiting their terminal differentiation, thereby leading to the described acanthosis and parakeratosis (K. Eyerich and Eyerich 2018; Zheng et al. 2007; S. Eyerich et al. 2010). IL-23 is central for promoting IL-17A and IL-22 expression by immune cells and for inducing a pathogenic inflammatory Th17 phenotype (Ghoreschi et al. 2010; Sabat et al. 2019). Finally, the pleiotropic cytokine TNF-α synergizes with the other mentioned cytokines and drives multiple pro-inflammatory effects leading to the production of more inflammatory cytokines/ chemokines, endothelial activation and recruitment of more immune cells (Sabat et al. 2019).

A

B

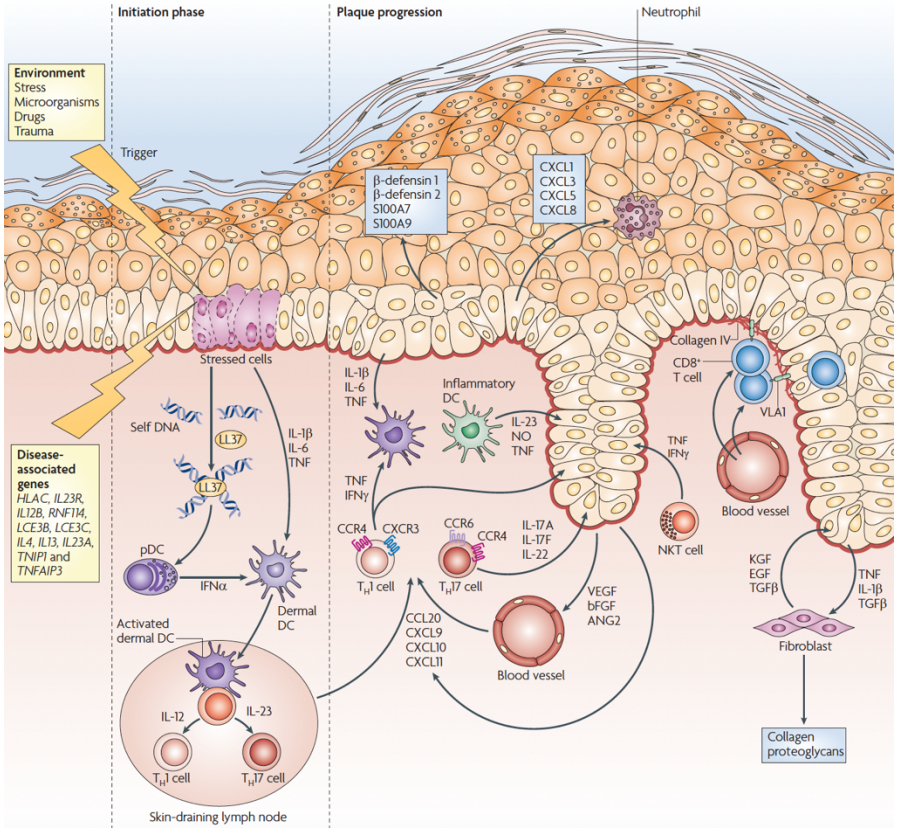

Figure 5: Psoriasis: clinical appearance and immunopathogenesis. A) Typical clinical manifestation of plaque-type Psoriasis (Pso) with patients suffering from the occurrence of red or shiny well-demarcated scaly skin lesions. Modified from (Boehncke and Schön 2015; Griffiths et al. 2021). **B)** Immune processes underlying Pso initiation and plaque formation with the main cellular immune mediators indicated. Pso is triggered in genetically predisposed individuals via environmental factors depicted, upon which stressed keratinocytes release self-DNA that complexes with the AMP LL-37 leading to the activation of plasmacytoid dendritic cells (pDCs). Keratinocyte-derived IL-1β, IL-6 and TNF-α together with pDC-derived IFN-α activate dermal DCs, which in return activate T-cells promoting the differentiation of mainly Th1, Th17 and (not shown) Th22 cells, which migrate into the skin via the action of indicated keratinocyte-derived chemokines and secrete their effector cytokines (mainly IL-17A, IL-17F and IL-22) driving keratinocytes proliferation while inhibiting terminal differentiation, as well as shown AMP and chemokine secretion, the latter leading to attraction of neutrophils into the skin. Adapted from (Nestle et al. 2009).

1.3. The CCAAT/enhancer binding protein beta (CEBPB)- structure, function and regulation

1.3.1. Transcription factors as key regulatory nodes

Transcription factors represent key nodes that integrate signaling pathways to drive a plethora of downstream cellular responses. Their contribution to a wide variety of human diseases like cancer, cardiovascular, metabolic and inflammatory disorders, as well as their promising therapeutic potential is therefore well-recognized (Parisi et al. 2013; Sterry et al. 2007; Takeshita et al. 2017; Henes et al.

2014). Also in CISDs, different transcription factors have emerged as crucial players in the pathogenesis such as the AP-1 members, JUN and FOS, as well as NFκB and different STATs, especially STAT1 and STAT3 (Pasparakis, Haase, and Nestle 2014; Sano et al. 2005; Zenz et al. 2008). Nevertheless, the complex transcription factor networks that specifically regulate human keratinocytes proliferation, differentiation and inflammatory response still remain poorly understood. Moreover, given the plasticity of the phenotypes in skin diseases, it is tempting to hypothesize that investigating the transcriptional machinery can provide answers critical to the regulatory switches in the complex disease pathogenesis.

1.3.2. CEBPB- transcription factor family, structure and isoforms

The CCAAT/enhancer-binding protein beta (CEBPB or CEBP/ß, historically TCF5 or NF-IL6) is a well-known transcription factor of the basic-leucine zipper (bZIP) family, which regulates the expression of hundreds of target genes (Akira et al. 1990; Tsukada et al. 2011). The CEBP family consists of six members (CEBPA, CEBPB, CEBPD, CEBPE, CEBPG, CEBPZ) that bind to the CCAAT promotor consensus sequence TT (G) N(A/G) N(C/T) G N(A/T) AAT(G) (Akira et al. 1990) (Figure 6A, B). Structurally, CEBPB consists of four main elements (Figure 6 A, C) (Tsukada et al. 2011): **(1)** a C-terminal leucine-zipper (ZIP), which is responsible for dimerization and lies directly adjacent to **(2)** a basic DNA-binding domain (DBD), which determines DNA-specificity and serves as primary nuclear localization signal (NLS), both forming together the highly conserved bZIP domain (Williams, Angerer, and Johnson 1997). **(3)** The C-terminal tail region is important for protein-protein interactions, which are central for CEBPB function. Indeed, CEBPB functions either as a homo- or heterodimer with other CEBP members or bZIP proteins like FOS, JUN and ATF, directing binding to AP1 and CRE sites, respectively (Williams, Cantwell, and Johnson 1991; Hsu et al. 1994; Vallejo et al. 1993). **(4)** The N-terminus contains different effector domains that mediate either transactivation (transactivating domain, TAD) or repression (negative regulatory domain, Reg).

CEBPB is encoded by an intronless gene that is transcribed into a single mRNA by a mechanism of alternative translation initiation at three different consecutive start codons regulated by a short upstream open reading frame (uORF), thereby yielding three protein isoforms: LAP*, LAP and LIP (Descombes and Schibler 1991; Calkhoven, Müller, and Leutz 2000) (Figure 6C). The longer LAP isoforms (liver activating protein, LAP) are gene activators, while the truncated LIP (liver inhibitory protein, LIP) isoform, lacking the TAD domain, has been assigned a main role as trans-dominant gene repressor, although it can still activate a number of targets in specific cellular contexts (Ossipow, Descombes, and Schibler 1993; Wassermann-Dozorets and Rubinstein 2017).

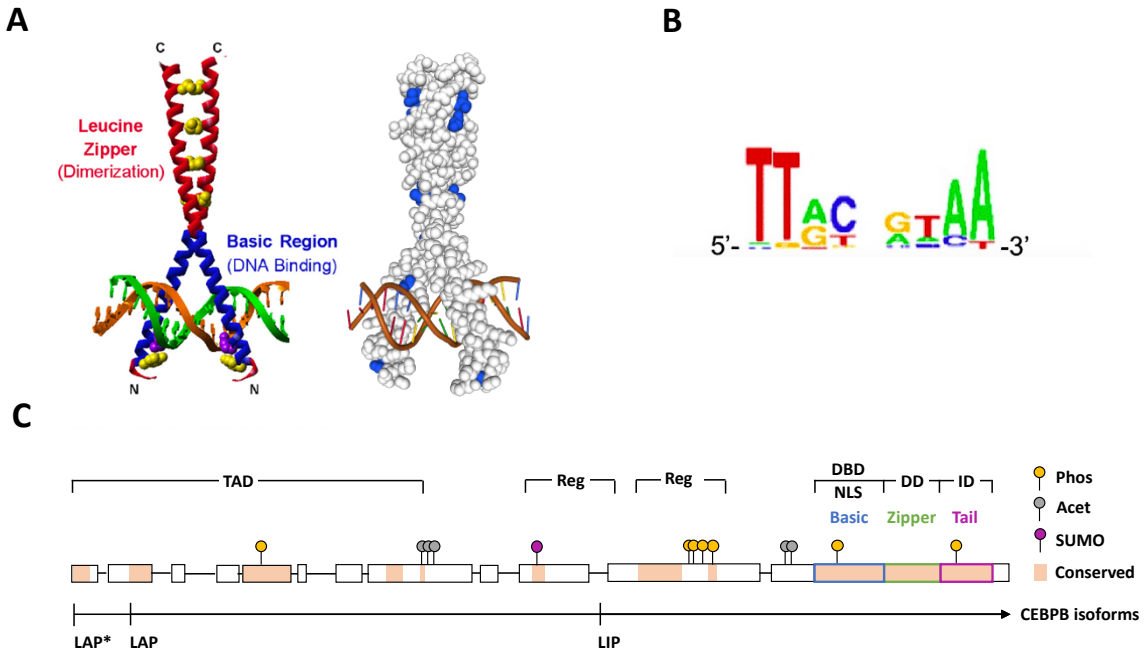

Figure 6: CEBPB structure, DNA consensus and isoforms. A) Structure of CEBPB homodimer-DNA complex with secondary and tertiary structures (left) and predicted crystal structure (right). Leucine zippers are shown as red helix and the basic regions of the DNA binding domain as blue helix. In the crystal structure key Ser/Thr residues are indicated in blue. The space-filled crystal structure was generated by the Swiss-Model Software (Expasy). **B)** Consensus DNA motif for the C/EBP palindrome. **C)** Amino acid sequence and isoforms of C/EBPß presented as scaled graphics displaying inter-isoform conservation as pink shaded regions. Stick figures represent sites of indicated post-translational modifications, while lines with arrows locate alternative translation initiation sites for the generation of the three different isoforms LAP*, LAP and LIP. Key regions are labelled depicting the following domains: Transcription activation Domain (TAD), Regulatory domain (Reg), DNA-binding domain (DBD), nuclear translocation signal (NLS), Dimerization Domain (DD) and Interaction Domain (ID). Modified from (Tsukada et al. 2011).

1.3.3. CEBPB regulation- key triggers and upstream signaling pathways

CEBPB expression and function is regulated on several levels including gene transcription, alternative translation, posttranslational modification and protein-protein interactions (Ramji and Foka 2002; Huber et al. 2012). *CEBPB* expression is regulated by various transcription factors like ATF, SP1, RARα, MYB, STAT3 and NFκB (Niehof, Streetz, et al. 2001; LeClair, Blanar, and Sharp 1992; Mink et al. 1999; Duprez et al. 2003; Berrier, Siu, and Calame 1998). In addition, the action of various cytokines, nutrients and bacterial components, is a crucial part of the CEBPB expression regulation.

Cytokine signaling constitutes one of the main pillars upstream of CEBPB, rendering it sensitive to various immunogenic stimuli like LPS, IL-1ß, IL-6, TNF-α and IFN-γ (Poli, Mancini, and Cortese 1990; Tengku-Muhammad et al. 2000; Zhang and Rom 1993). IL-1ß and TNF-α, are believed to mediate their effects on CEBPB induction via signaling through MAPK and NFκB, while IL-6 mediates its effects via

the JAK/STAT3- pathway (Poli, Mancini, and Cortese 1990; Poli 1998; Akira and Kishimoto 1997). In return, CEBPB then acts as part of these cytokine pathways to induce the expression of the respective response genes, which has been best studied for the IL-6 response. Additionally, CEBPB constitutes a critical component in the IL-17 signaling pathway (Cortez et al. 2007; Patel et al. 2007; Shen et al. 2006). On one hand, IL-17 acts upstream of CEBPB to induce its expression and regulate its activity, and on the other hand, IL-17-induced CEBPB then functions to regulate the gene expression of various IL-17-responsive genes, hence suggesting a positive feedback loop. Moreover, remarkably, CEBPB was found to even partially substitute for IL-17 signaling effects, further pinpointing its importance within this pathway (Ruddy et al. 2004; Shen et al. 2005).

Metabolically, CEBPB can be regulated by different pathways such as Akt-mTOR and AMPK, thereby rendering it sensitive to metabolic changes and environmental cues (Calkhoven, Müller, and Leutz 2000; Smink and Leutz 2010; Choudhury et al. 2011). Finally, CEBPB has also the ability to further stimulate its own transcription, hence conferring autoregulation (Niehof, Kubicka, et al. 2001).

1.3.4. CEBPB function- a pleiotropic transcription factor with multi-faceted roles

CEBPB is involved in different signaling pathways

Having been induced by the described pathways, CEBPB then mediates the expression of a myriad of genes, which in return are involved in various signaling pathways. Few examples for CEBPB-signaling pathways include a TGFß1-SMAD3 signaling pathway for ECM regulation (Du et al. 2016), an IFNγ-ATF6 pathway controlling cell death (Gade et al. 2012) and MyD88-dependent TLR signaling for bacterial defense (Lu et al. 2009). Apart from cytokine-dependent signaling, CEBPB has been also implicated in glucocorticoid (GC) and prostanoid signaling pathways (Roos and Nord 2012). Altogether, CEBPB truly exhibits striking variability and plasticity with respect to the signaling pathways it takes part in.

The multi-faceted functions of CEBPB

CEBPB regulates a wide variety of cellular processes including cell survival, proliferation, differentiation, apoptosis and senescence in many tissues like fat, bone, liver and skin (Atwood and Sealy 2010; Buck, Turler, and Chojkier 1994; Gade et al. 2008; Wu et al. 1995; Ramji and Foka 2002). Moreover, it controls metabolism and hematopoiesis, as well as immune and inflammatory responses (Hirai et al. 2015; Poli 1998; Satake et al. 2012; Ackermann et al. 2019). While CEBPB is expressed in nearly all cells, it shows prominent expression specifically in the liver , where it was originally identified,

as well as in the intestine, lung, adipose tissue and spleen (Wedel and Ziegler-Heitbrock 1995; Descombes and Schibler 1991; Cao, Umek, and McKnight 1991). Hence, the functional properties of CEBPB have been most studied in adipocytes, hepatocytes and immune cells of the myeloid lineage. With respect to the skin, knowledge about the role of CEBPB comes mainly from mouse models (described under section '4. Discussion'), however, little is known about the regulation and function of CEBPB specifically in the human skin.

A role for CEBPB in cell survival, proliferation and differentiation

CEBPB can promote both proliferation and differentiation in a cell-type and context-specific manner. For instance, it has a pro-mitotic effect on many cell types such as hepatocytes and adipocytes (Calkhoven, Müller, and Leutz 2000; Buck et al. 1999; Guo, Li, and Tang 2015). Moreover, it regulates epithelial cell development, as seen from *Cebpb -/-* mice with impaired ductal morphogenesis based on defective mammary epithelial cells (MECs) proliferation and differentiation (Robinson et al. 1998). Additionally, CEBPB is an important regulator of cell-cycle exit and Ras-induced senescence in primary human fibroblasts and mouse embryo fibroblasts (MEFs) (Sebastian et al. 2005).

A role for CEBPB in metabolism

CEBPB plays important roles in metabolism and energy homeostasis. It enhances aerobic glycolysis and fatty acid oxidation (FAO), hence contributing to a higher respiratory capacity of the affected cells (Ackermann et al. 2019). CEBPB carries out these metabolic effects by regulating the gene expression of a number of metabolic genes, such as PPARγ, especially in liver and adipose tissue (Desvergne, Michalik, and Wahli 2006; Lefterova et al. 2008). Given this role of CEBPB in adipogenesis, *Cebpb* knockout mice were found to be protected against HFD-induced obesity (Millward et al. 2007).

A focus on CEBPB's role in immunity and inflammation

Within the hematopoietic system, CEBPB carries out crucial functions in the regulation of both the myeloid and lymphoid cell lineages. CEBPB is upregulated and required for driving the stress-induced granulopoiesis (Hirai et al. 2006). This is based on sustaining STAT3-dependent G-CSF-responsive proliferation of granulocytes. Another well-established function of CEBPB during hematopoiesis, is the regulation of the development and function of monocytes and macrophages (Natsuka et al. 1992; Cain et al. 2013; Tanaka et al. 1995). Here, *Cebpb -/-* mice showed lower numbers of peripheral blood monocytes (Tamura et al. 2015). At the level of HSCs, it has been shown that CEBPB-deficient cells are impaired in their cell cycle progression and subsequent differentiation under stress conditions.

Owing to its role in controlling the expression of a myriad of factors implicated in host defense such as cytokines, chemokines, and their receptors, as well as acute phase response proteins and AMPs, CEBPB is central to the regulation of immune responses with both pro-and anti-inflammatory functions (Poli 1998; Ramji and Foka 2002; Tsukada et al. 2011).

Loss of CEBPB in mice showed a remarkable myelo-/lymphoproliferative disorder with an imbalance in T-helper immune responses, defective activation and function of macrophages, compromised IL-12 production and disturbed IL-6 levels (Screpanti et al. 1995). Given that, *Cebpb -/-* mice showed higher susceptibility to infections with various pathogens including *Salmonella*, *Listeria monocytogenes* and *Candida albicans* (Screpanti et al. 1995; Tanaka et al. 1995). Furthermore, CEBPB was found to be involved in the transcriptional activation of various pro-inflammatory genes downstream of TLR9, which senses both bacterial and viral unmethylated CpGs, hence implicating CEBPB also in the immune response to viral infections (Yamamoto et al. 2017). As a key regulator of monocyte/ macrophage responses to inflammation, CEBPB is significantly induced during macrophage differentiation, where it regulates multiple genes including growth factors (*G-CSF, GM-CSF, M-CSF*), differentiation-specific genes (*MCP-1*), inflammatory cytokines/ chemokines (*IL1B, TNFA, IL6, IL8, IL12, MIP1*) and effector molecules (*NOS2, COX2,* lysozyme genes) (Tanaka et al. 1995; Dunn et al. 1994; Bretz et al. 1994; Wedel and Ziegler-Heitbrock 1995; Matsumoto, Sakao, and Akira 1998; Natsuka et al. 1992; Akira and Kishimoto 1997; Poli 1998; Huber et al. 2012). Hence, CEBPB loss in macrophages abolishes their bacterial killing properties, as well as their cytotoxic abilities. Using a model of *Mycobacterium tuberculosis* (Mtb) infection, CEBPB was found to be pivotal in governing the M1/M2 balance (Sahu et al. 2017; Veremeyko et al. 2018). Besides its role in myeloid immune responses, CEBPB has been also implicated in the regulation of T-cell responses. For instance, CEBPB is required for oral immunity against candidiasis by inducing the expression of ß-defensin 3 (Simpson-Abelson et al. 2015).

Finally, one of the best studied immunological roles of CEBPB is within the acute phase response to inflammation, where it drives the expression of the serum amyloid A (SAA) and P (SAP), C reactive protein (CRP) and complement C3, and is believed to be involved in both the induction and maintenance of the acute phase inflammatory reaction (Poli and Cortese 1989; Alam et al. 1993; Ray, Hannink, and Ray 1995). Overall, CEBPB thus represents a key regulator of immunity and inflammation on multiple levels.

1.4. Project Aim

Transcription factors are accepted as critical molecular switches in complex disease pathogenesis. Therefore, investigating the transcriptional machinery within the context of inflammatory skin diseases can unravel novel disease mechanisms and expand our understanding of the pathogenic epithelial response on the molecular level. Moreover, such studies can identify new unappreciated disease drivers that can be used either as biomarkers or therapeutic targets, hence representing a step towards precision medicine in the field of CISDs.

In this project, we aim to expand the knowledge on the transcriptional networks specifically regulating human keratinocytes response under different inflammatory conditions and assess their contribution to disease phenotypes. For this, we focus on the pleiotropic transcription factor CEBPB, whose function has been well-described in various tissues, yet detailed knowledge of its effects in human skin under healthy and disease conditions is still missing. In this study, we identify CEBPB as a key transcriptional regulator in the skin via a translational biocomputational approach. Using different transcriptomics technologies and a wide variety of functional assays, we aim to investigate CEBPB as a novel master transcription factor in keratinocytes and focus at dissecting its functional role in-depth in different patterns of skin inflammation.

More specifically, in this project, the following research questions will be addressed:

1) How is CEBPB regulated on gene and protein level in patients suffering from different inflammatory skin conditions?

2) How is CEBPB regulated in human keratinocytes under homeostatic and immunogenic microenvironments?

3) Does CEBPB affect skin inflammation in different skin diseases, e.g. Psoriasis, Lichen planus and Atopic dermatitis? And how?

4) What are potential CEBPB-downstream target genes and pathways implicated in disease pathology?

5) Is CEBPB contributing to specific clinically relevant disease hallmarks? If yes, how can that be explained on the molecular level?

2. Materials and Methods

2.1. Materials

2.1.1. Buffers and solutions

Buffer	Usage	Recipe
10x TBS	Western Blot	152 mM Tris-HCl, 46 mM Tris-base, 1.5 M NaCl, pH 7.6
1x TBS-T	Western Blot	1x TBS, 0.1% Tween-20
20x NuPage MOPS SDS Running Buffer	Western Blot	1 M MOPS, 1 M Tris-base, 35 mM SDS, 10 mM EDTA, pH 7.7
20x NuPage Transfer Buffer	Western Blot	500 mM Bicine, 500 mM Bis-Tris, 20 mM EDTA, pH 7.2
1x Final Transfer Buffer	Western Blot	1x NuPage Transfer Buffer, 10% Methanol
6x SDS sample buffer (Laemmli buffer)	Western Blot	300 mM Tris-HCl, 60% Glycerol, 12% SDS, 12.5% ß-mercaptothanol, 0.12% Bromphenol blue, pH 6.8
Blocking buffer	Western Blot	5% milk powder in 1x TBS
Primary Antibody diluent (BSA-based)	Western Blot	5% BSA in 1x TBS-T
Primary Antibody diluent (milk-based)	Western Blot	5% milk powder in 1x TBS-T
Secondary Antibody diluent	Western Blot	5% milk powder in 1x TBS-T
FACS buffer	FACS, IF	PBS w/o $Ca^{2+}Mg^{2+}$, 5% FCS, 0.02% sodium azide solution
4% PFA fixation solution	IF	4% PFA powder in pre-warmed PBS, 1N NaOH (until solution clears), pH 7.0 (HCl)
Boiling buffer (Citrate-based)	IHC	10 mM sodium citrate (citric acid monohydrate 4.2g in 2l/ Tri-sodium citrate dihydrate 5.88g in 2l), 0.05% Tween-20, pH 6.0 (HCl)
10x Tris Washing buffer	IHC	0.5 M Trizma base, 9% NaCl, pH 7.6 (HCl)
20x PBS	ELISA/ IHC	110 mM KCl, 58 mM KH_2PO_4, 33 mM Na_2PO_4, 5.5 M NaCl
Coating buffer (BD)	ELISA	0.1 M sodium carbonate (Na2CO3), pH 9.5
Blocking buffer (BD)	ELISA	10% FCS in PBS w/o $Ca^{2+}Mg^{2+}$
Blocking buffer (R&D)	ELISA	1% BSA in PBS w/o $Ca^{2+}Mg^{2+}$
Washing buffer	ELISA	1x PBS, 0.05 % Tween-20, pH 7.2 - 7.4
Citrate buffer	ELISA	190 mM citric acid monohydrate, pH 3.9
TMB stock solution	ELISA	100 mM TMB in 50% EtOH, 50% DMSO
Substrate Solution	ELISA	1 mM TMB, 0.05 % H_2O_2 in citrate buffer
Stop Solution	ELISA	2 N H_2SO_4
Sorting buffer	scRNA Seq	PBS + 0,5 % BSA + 2 mM EDTA

2.1.2. Media and supplements

Table 1: Media components.

Media/ Supplements	Identifier (Cat#)	Source
DermaLife Basal Medium	LM-0004	Cellsystems
DermaLife K LifeFactors Kit	LL-0007	Cellsystems
DMEM (1X)	41966-029	GIBCO
RPMI medium 1640 (1X)	21875-034	GIBCO
OPTI-MEM (1X)	31985-062	GIBCO
FBS Superior stabil	FBS.S0615	Bio&Sell
Human serum	H4522-100ML	SIGMA
MEM-NEAA (100x)	11140-035	Gibco Life Technologies
L-Glutamine 200 mM (100x)	25030-024	Gibco Life Technologies
Sodium pyruvate 100mM (100x)	11360-039	Gibco Life Technologies
Penicillin/Streptomycin (P/S) (100x)	15140-122	Gibco Life Technologies
FCS	SV30160.02	GE Healthcare
0,5 % EDTA pH 8,0	11568896	Invitrogen Life Technologies

Table 2: Media composition.

Medium	Composition
Keratinocyte Medium for 2D	DermaLife Basal Medium ± Supplements ± HC ± P/S
Keratinocyte Medium for 3D	DermaLife Basal Medium + Supplements ± HC ± P/S + $CaCl_2$ ± Vitamin C
Fibroblast Medium	DMEM + 20% FCS + 1% (1x) P/S
T-cell medium (5% HS)	RPMI + 1% (1x) P/S + 1% (1x) L-Glutamine + 1% (1x) NEAA+ 1% (1x) sodium pyruvate + 5% Human serum
Freezing medium T-cells/ PBMCs	RPMI + 40% FCS+ 10% DMSO

2.1.3. Chemicals, reagents and enzymes

Table 3: Chemicals.

Chemicals	Identifier (Cat#)	Source
Acetone		
Bicine		ChemCruz
Bis-Tris		
Bovine Serum Albumin (BSA)		Sigma-Aldrich
$CaCl_2$	C-7902	Sigma-Aldrich
Citric acid monohydrate		Roth
Collagen type I solution	C3867-1VL	Sigma-Aldrich
Dithiothreitol (DTT)	A1101	AppliChem
Dimethylsulfoxid (DMSO)		AppliChem

EDTA UltraPure 0.5 M		Invitrogen by Life Technologies
Ethanol (C2H5OH)(96% and 70%)	1085430250	Merck
Formaldehyde solution 3,6-3,7 %	PZN02652965	Fischer
Glucose		
Hydrogen peroxide 30% solution (H2O2)	216763	Sigma-Aldrich
Isopropyl alcohol (C3H7OH)		
Methanol (CH3OH)		Merck
MOPS		AppliChem
Non-fat dried milk powder		AppliChem
Paraformaldehyde		Sigma-Aldrich
Sodium azide (NaN3)		Merck
Sodium carbonate (Na2CO3)		Merck
Sodium chloride (NaCl)		Roth
10 % Sodium dodecylsulfate (SDS)		Gibco Life Technologies
Sulfuric acid (H2SO4)		Merck
Tetramethylbenzidine (TMB)		Sigma-Aldrich
Triton-X100		Sigma-Aldrich
Trizma base		Sigma-Aldrich
Tween-20 Detergent		EMD Millipore
Vitamin C	A5960-25G	Sigma-Aldrich
Xylol		

Table 4: Reagents.

Reagents	**Identifier (Cat#)**	**Source**
Bond Primary Antibody diluent	AR9352	Leica
Dextran solution	D8802	Sigma-Aldrich
Hematoxylin counterstain (BOND Polymer Refine Red Detection)	DS9390	Leica
IDTE buffer	11-01-02-02	IDT
LymphoPrep	1114547	Progen Biotechnik
Page Ruler	26616	Thermo Scientific
Perm/WashTM buffer (10X)		BD
QIAzol Lysis Reagent	79306	Qiagen
RNAlater Solution	1018087	Qiagen
S.p. HiFi Cas9 Nuclease	1081061	IDT
SuperSignal West Femto Chemiluminescence substrate	88620	Thermo Fisher
Trypan Blue Stain (0,4%)		Gibco Life Technologies
Trypsin	25300-054	Gibco Life Technologies

2.1.4. Cells, biological samples and patients cohorts

Experimental Model	Source
Primary human keratinocytes	AG Eyerich, different donors, suction blister
Neutrophils	AG Eyerich, different donors, blood

Table 5: Patient cohort generated within this study.

Disease	Number of Patients	Collected Biomaterial
Lichen Ruber	5	Skin biopsies 4 mm and 6 mm Blood (PBMCs and Serum) Skin T-cells
Atopic Dermatitis	4	
Psoriasis	7	

2.1.5. Antibodies

Antibody	Dilution	Usage	Identifier (Cat#)	Source
Rabbit anti-CEBPB (E299)	1:1000/ BSA	WB	ab32358	Abcam
Rabbit anti-Vinculin	1:1000/ BSA	WB	4650S	Cell Signaling
Mouse anti-α-Tubulin (DM1A)	1:1000/ BSA	WB	3873T	Cell Signaling
Mouse anti-β-Actin	1:1000/ BSA	WB	A2228	Sigma-Aldrich
Rabbit anti-PARP	1:1000/ BSA	WB	9542S	Cell Signaling
Rabbit anti-phospho-Stat3 (Tyr705) (D3A7)	1:1000/ BSA	WB	9145S	Cell Signaling
Rabbit anti-pRIPK1	1:1000/ BSA	WB	65746	Cell Signaling
Rabbit anti-RIPK3	1:2000/ milk	WB	ab72106	Abcam
Rabbit anti-cleaved Caspase 3	1:500/ BSA	WB	9661	Cell Signaling
Rabbit anti-GAPDH (D16H11)	1:1000/ BSA	WB	5174	Cell Signaling
Rabbit anti-TRAF6 (D21G3)	1:1000/ BSA	WB	8028S	Cell Signaling
Rabbit anti-PIM1	1:200/ BSA	WB	2907S	Cell Signaling
Mouse anti-PIM1 (12H8)	1:200/ BSA	WB	sc-13513	Santa cruz
Mouse anti-rabbit-HRP	1:10.000/ milk	WB	sc-2357	Santa Cruz
Goat anti-mouse-HRP	1:10.000/ milk	WB	115-035-166	Jackson
Mouse anti-CEBPB (H-7)	1:50	IHC	sc-7962	Santa Cruz
Rabbit anti-CEBPB (LAP)	1:50	IHC	3087S	Cell Signaling
Rabbit anti-Ki67		IHC	RBK027	Zytomed
alkaline phosphatase (AP)-linked anti-rabbit antibody (BOND Polymer Refine Red Detection)		IHC	DS9390	Leica
Mouse CD45- BV421 (HI30)	1:100	FACS	563879	BD Bioscience
Mouse CD4- APCCy7 (RPA-T4)	1:20	FACS	557871	BD Bioscience
Mouse CD8- Bv711 (RPA-T8)	1:200	FACS	301044	BioLegend

Recombinant human CD3- PEVio770 (REA613)	1:50	FACS	130-113-702	Milteny
Mouse IFNg- BV605 (B27)	1:100	FACS	562974	BD Biosciences
Mouse IL4- PerCpCy5.5 (8D4-8)	1:20	FACS	561234	BD Bioscience
Mouse IL17A- PE (SCPL1362)	1:50	FACS	560436	BD Bioscience
Mouse IL22- eFluor660 (22URTI)	1:20	FACS	50-7229	ebioscience
Mouse TNFa- AF700 (MAb11)	1:50	FACS	557996	BD Bioscience
Rat IL13- V450 (JES10-5A2)	1:10	FACS	561158	BD Bioscience
Rat IL10- FITC/ Vio-515 (JES3-9D7)	1:10	FACS	130-108-135	Miltenyi
Rat GM-CSF- PE/ Dazzle594 (1)	1:50	FACS	502317	Biolegend

2.1.6. Kits and commercial assays

Kits/ Assays	**Identifier (Cat#)**	**Source**
BioPlex Pro Human Cytokine 27-Plex	M500KCAF0Y	Bio-Rad Laboratories
BioPlex Pro Human Chemokine Single Plex assays for: CXCL1 CXCL2 CXCL5 CCL22	 171-BK22MR2 171-BK23MR2 171-BK14MR2 171-BK41MR2	Bio-Rad Laboratories
Human IL-1β ELISA Set II	557953	BD Bioscience
BD OptEIA Set Human IL-4	555194	BD Bioscience
BD OptEIA Set Human IL-6	555220	BD Bioscience
Human IL-17 DuoSet ELISA (DY317)	DY317	R&D Systems
Human INF-γ DuoSet ELISA (DY285B)	DY285B	R&D Systems
Human IL-22 DuoSet ELISA (DY782)	DY782	R&D Systems
Human TNF-α DuoSet ELISA (DY210)	DY210	R&D Systems
DuoSet ELISA hIL13 (DY213-05)	DY213-05	R&D Systems
Pierce BCA Protein Assay Kit	23227	Thermo Fisher Scientific
ChemoTx Disposable Chemotaxis System	101-5	Neuroprobe
CellTiter 96 Aqueous Non-Radioactive Cell Proliferation Assay	G5421	Promega
Luminescent ATP Detection Assay Kit	ab113849	Abcam
MitoTracker Deep Red FM Kit	M22426	Thermo Fisher
Seahorse XFp Cell Mito Stress Test Kit	103010-100	Agilent
miRNeasy Mini Kit	217004	Qiagen
RNeasy Plus Mini Kit	74136	Qiagen
TruSeq Stranded Total RNA Kit (Bulk RNA Seq)	20020597	Illumina
Chromium Next GEM Single Cell 3' GEM, Library & Gel Bead Kit v3.1 (Single cell Seq)	PN-1000121	10x Genomics
Visium Spatial Gene Expression Slide & Reagent Kit (Spatial transcriptomics)	PN-1000184	10x Genomics

P3 Primary Cell 4D-Nucleofector™ X Kit S/ L	V4XP-3032/ V4XP-3024	Lonza
Vector TrueVIEW autofluorecence quenching kit + VECTASHIELD Vibrance™ Antifade Mounting Medium	SP-8400 H-1800	VECTOR Laboratories
IHC-P with Permanent AP Red Kit	ZUC001-125	Zytomed
Applied Biosytems High Capacity cDNA Reverse Transcription Kit	4368814	Thermo Fisher Scientific
Fast Start Universal SYBRGreen Master (Rox)	04913914001	Roche
RIPA Lysis Buffer System	sc-24948	Santa Cruz Biotechnology
Agilent High Sensitivity DNA Kit	5067-4626	Agilent
Agilent RNA 6000 Nano Kit	5067-1511	Agilent
Lipofectamine 3000 Reagent Kit	L3000001	ThermoFisher
Whole skin dissociation kit, human	130-101-540	Miltenyi
Cytofix/Cytoperm Fixation/Permeabilization Solution Kit	544722	BD Bioscience
LIVE/DEAD Fixable Aqua Dead Cell Stain Kit	L34957	Thermo Fischer Scientific
SuperSignal West Femto Chemiluminescence substrate	88620	Thermo Fisher

2.1.7. Cytokines and cell culture treatment reagents

Cytokine/ Stimulant	**Identifier (Cat#)**	**Source**
Recombinant human IL-17A	317-ILB-050	R&D systems
Recombinant human TNF-α	210-TA-005	R&D systems
Recombinant human IL-22	782-IL-010	R&D systems
Recombinant human IL-4	130-093-921	Miltenyi
Recombinant human IL-13	213-ILB-005	R&D systems
Recombinant human IFN-γ	285-IF-100/CF	R&D systems
Recombinant human IL-6	C-61625	PromoKine
Recombinant human TGF-ß	C-63503	PromoKine
Recombinant human IL-ß	C-61120	PromoKine
GolgiPlug (Brefeldin A)	555029	BD Bioscience
GolgiStop (Monensin)	554715	BD Bioscience
Ionomycin	I0634	Sigma-Aldrich
Phorbol-12-myristat-13-acetat (PMA)	P8139	Sigma-Aldrich
Z-VAD(OMe)-FMK	60332S	Cell Signaling
SMAC (B-9135 Birinapant)	B-9135	LC Laboratories

2.1.8. Primers

Target	**Direction**	**Sequence (5'-3')**
hCEBPB	fw	GGGAGCCCGTCGGTAATTTT
	rev	CATGTGCGGTTGGTTTGGAC

hPIM1	fw	TGGGGAGAGCTGCCTAATGG
	rev	GCCTAATGACGCCGGAGAAA
h18S	fw	GTAACCCGTTGAACCCCATT
	rev	CCATCCAATCGGTAGTAGCG

2.1.9. Oligonucelotides

CRISPR RNAs (crRNAs) and tracr RNAs	**Usage**	**Sequence (5'-3')**	**Company**
Hs.Cas9.CEBPB.1.AB crRNA	CRISPR/Cas9	GGCCAACTTCTACTACGAGG	IDT, predesigned
Hs.Cas9.CEBPB.1.AA crRNA	CRISPR/Cas9	CTCTTCTCCGACGACTACGG	IDT, predesigned
Hs.Cas9.PIM1.1.AD crRNA	CRISPR/Cas9	TTCGACTTCATCACGGAAAG	IDT, predesigned
Hs.Cas9.PIM1.1.AE crRNA	CRISPR/Cas9	CGACCTGCACGCCACCAAGC	IDT, predesigned
CRISPR-Cas9 tracrRNA	CRISPR/Cas9		IDT, #1072534
tracrRNA-ATTO	Transfection control		IDT, #1075928

2.1.10. Softwares and databases

Software	**Company**
Cytoscape	Cytoscape
BD FACSDiva Software	BD
Intas ChemoStar	Intas Science Imaging
Primer blast	NCBI
FlowJo	Tree Star
GraphPad Prism	GraphPad Software
ImageJ	Wayne Rasband
QuantStudio ViiA	Applied Biosystems
Loupe browser	10x Genomics
Seahorse Wave	Agilent
DAVID	Laboratory of Human Retrovirology and Immunoinformatics (LHRI)
ZENBlue Software	Zeiss
STRING protein interactions	STRING DB
Database	**Company**
MSigDB	UCSan Diego, Broad Institute
Reactome	Reactome
KEGG	KEGG, Kyoto University
TRANSFAC	geneXplain
JASPAR	JASPAR

2.1.11. Devices

Device	Company
HiSeq4000	Illumina
NovaSeq6000	Illumina
LSRFortessa flow cytometer	BD Biosciences
4D Nucleofector device: 4D-Nucleofector Core Unit 4D-Nucleofector X Unit	Lonza
Bioanalyzer 2100	Agilent
Chromium Controller	10x Genomics
gentleMACS dissociator (AutoMACS)	*Miltenyi*
MiniBlot Module	Life Technologies
BOND-MAX stainer	Leica
TCS SP8 confocal laser scanning microscope	Leica
EVOS M5000 Imaging System	Thermo Fisher Scientific
Leica SP5 Confocal Microscope	Leica Microsystems
Epoch Luminometer	BioTek
Epoch ELISA reader	BioTek
Hydrospreed ELISA washer	Tecan
Bio-Plex 200 system (Luminex)	BIO-RAD
Applied Biosystems ViiA7 Real-Time PCR system	Thermo Fisher Scientific

2.1.12. Consumables

Here only selected consumables, which might be important for data reproduction and/or are not characterized as standard lab consumables (e.g. plastic ware) are summarized.

Consumables	Identifier (Cat#)	Company
Gels 4-12 % Bolt Bis-TrisPlus	NW04122BOX	Invitrogen
Epredia™ SuperFrost Plus™ Adhesion slides	J1800AMNZ	Thermo Scientific
Millicell Cell Culture Inserts 0,4 µm 12mm Diameter	PIHP01250	Merck Millipore
DAKO Flex IHC Microscope Slides	K8020	Agilent
Menzel X1000 Round Coverslip dia. 15mm #1.5 (0.16-0.19mm)	17284914	Thermo Scientific
Ibidi Treat µ-Slide	80286	Ibidi
Pre-separation filter 70 µm	130-095-823	Miltenyi
GentleMACS C Tubes	130-096-334	Miltenyi
pluriStrainer Mini 40 µm	43-10040-60	pluriSelect

2.2. Methods

2.2.1. Cell culture

2.2.1.1. Thawing and seeding of primary human keratinocytes

To thaw primary keratinocytes, a 50ml falcon was prepared and filled with ~20ml PBS. The cell vial was then thawed shortly, transferred fast into the prepared falcon and the vial washed again with PBS. The falcon was then centrifuged for 10 min at 1200 rpm (4^0C), the supernatant (SN) removed and the pellet resuspended in the desired volume. The keratinocytes were resuspended in 12 ml for seeding into T75 flask or 1-2 ml for cell counting and direct seeding into the respective cell culture plate. Cell counting was done by staining the cells with trypan blue and counting in a hemocytometer. Keratinocytes were seeded at a density of 180.000-200.000 cells/ well in a 6-well plate, and the cell number was down-scaled accordingly when using smaller formats.

2.2.1.2. Cultivation and stimulation of primary keratinocytes

Primary human epidermal keratinocytes were obtained from different donors by suction blister as previously reported in (Eyerich et al. 2019) and cultured in fully supplemented keratinocyte medium (+ supplements + HC+ P/S) (Section 2.2.1., Table 1) at 37 °C, 5 % CO_2. One day after seeding, medium was exchanged to remove dead cells. For 2D experiments, cells were allowed to grow to a confluency of ~70% (3-5 days post-seeding depending on donor) prior to stimulation. For stimulation, cells were first starved for 5 hours in DermaLife Basal Medium (- supplements- HC- P/S) and stimulated in HC-free keratinocyte medium with 50 ng/ml human recombinant cytokines (IL-17A, TNF-α, IL-13, IFN-γ, IL-4, IL-1ß, IL-6 and TGF-ß) alone or in the depicted combinations for ~16h (overnight) for RNA and varying timepoints for Protein (3h-72h). TNF-α, however, was used at a final concentration of 10 ng/ml, when used in combination with IL-17A. Alternatively, keratinocytes were stimulated with patients-derived lesional T-cell supernatants (1:10 diluted) as described under section 2.2.1.4.

2.2.1.3. Harvesting of 2D adherent cells for RNA and protein analysis

To harvest the cells, the SN was sucked-off carefully or collected and frozen at -80^0C for secretome analysis. The cells were first washed with 2ml PBS (6-well plate), then trypsinized with 500 µl pre-warmed Trypsin/EDTA per well and placed in the incubator for 6-8 min. The reaction was then stopped with 1 ml Fibroblast medium and the cell suspension collected into a 2 ml Eppendorf tube. The wells were washed with additional 500 µl PBS to collect residual cells. The cells were pelleted by centrifugation 1200 rpm for 10 min at 4^0C and the SN was removed carefully. For RNA analysis, the pellets were frozen away at -80^0C at this step, or used immediately for RNA isolation as described in section 2.2.2.1. For protein analysis, the pellets were subjected to the steps described under section 2.2.3.1. for the generation of whole cell protein lysates.

2.2.1.4. 3D keratinocyte models culture and stimulation

Culture: Three-dimensional (3D) skin models were cultured in collagen (1 % in PBS, collagen type I, SIGMA) pre-coated polycarbonate inserts (Millipore) in a tissue-culture treated 6-well plate. Briefly, 0.3 x 10^6 primary human keratinocytes were seeded in 500 µl keratinocyte medium supplemented with 1.5 mM $CaCl_2$ (SIGMA) into the insert. 2.5 ml keratinocyte medium supplemented with 1.5 mM $CaCl_2$ was added in the surrounding well. Models were cultured at 37 °C and 5 % CO_2. After two days, keratinocytes were exposed to air-liquid interface by removing the medium inside the insert and the medium in the surrounding 6-well was replaced with 2 ml keratinocyte medium supplemented with 1.5 mM $CaCl_2$ and 50 µg/ml Vitamin C (SIGMA). Every second day the medium was changed. **Stimulation:** Eight days after air-lift, the 3D models were stimulated with human recombinant cytokines (see section 2.2.1.2.) or supernatants of lesional T cells from LE/LP, AD or Psoriasis patients (TCS) (1:10 diluted) in 2 ml keratinocyte medium supplemented with 1.5 mM $CaCl_2$ and 50 µg/ml Vitamin C without hydrocortisone (HC) for 24 hours (for RNA analysis) or 72 hours (for histology) or for differing time points (24, 48, 72h) for WB protein analysis.

2.2.1.5. 3D keratinocyte models harvesting for RNA, protein and histology

RNA: To harvest 3D models, the membrane was cut out carefully from the inserts and divided in half, then placed into an eppi pre-filled with 350 µl DTT-supplemented RLT buffer. The samples were vortexed well to dissolve the cell layer from the membrane. The inserts were then cut into smaller pieces within the lysis buffer, vortexed again for 1 min, pipetted repeatedly up and down and vortexed shortly, then placed on ice till further RNA isolation as described under section 2.2.2.1. **Protein**: For generation of WB lysates from 3D models, the inserts were cut and placed into an eppi pre-filled with 200 µl RIPA buffer and processed similar to RNA samples to dissolve the layer, then subjected to the steps described under 2.2.3.1. **Histology:** The inserts were cut out, divided in half and each half placed between two biopsy sponges into a labelled embedding cassette and transferred into a 4% formaldehyde solution till dehydration.

2.2.1.6. Generation of knockout (KO) using CRISPR/Cas9

Preparation of RNP complexes: Predesigned target-specific CRISPR (cr) crRNA, tracrRNA and S.p. HiFi Cas9 Nuclease were purchased from Integrated DNA Technologies in Alt-R® format. crRNA and tracrRNA were reconstituted to 200 µM with IDTE Buffer. For generation of crRNA-tracrRNA duplex, the oligos were mixed at equimolar concentrations and annealed by heating at 95 °C for 5 min followed by a slow cool-down to room temperature for at least 10 min. For enhanced knockout efficiency, a mixture of two crRNA sequences was applied per target. Finally, for RNP formation, 180 pmol crRNA-

tracrRNA duplex was mixed with 60 pmol Cas9 protein in Nucleofection Buffer P3 (Lonza) and incubated for another 10 min at room temperature. crRNA sequences can be found in section 2.1.9. **Transfection of RNP complexes:** CRISPR knockout (KO) was done by electroporation of RNP complexes with the 4D Nucleofector™ X Unit device (Lonza) using the P3 Primary Cell 4D-Nucleofector™ X Kit S (Lonza). For electroporation, 1.6 x 10^5 keratinocytes cells were resuspended in 16 µl Nucleofection Buffer P3 and mixed with 4 µl RNP complex, generating a total reaction of 20 µl per sample (small cuvette). The transfection mixture was transferred to the Nucleofection™ cuvette strips and electroporated with the pulse DS-138 in the 4D Nucleofector™ X unit. After nucleofection, cells were rested at room temperature for 10 min, followed by resuspension in prewarmed cell culture media. Finally, the cells were seeded in cell culture plates of inserts depending on the application.

2.2.1.7. Isolation of neutrophils and neutrophil migration assay

Primary human neutrophils were isolated from peripheral blood of healthy donors using LymphoPrep™ (Progen) and 2 % Dextran solution (Sigma Aldrich) with a final erythrocyte lysis. Neutrophils were cultured in RPMI 1640 medium supplemented with 1 % human serum, 0.1 mM NEAA, 2 mM L-Glutamine, 1 mM sodium pyruvate and 100 U/ml penicillin/streptomycin at 37 °C, 5 % CO_2. Migration assay was performed by Manja Jargosch (AG Eyerich, PostDoc) using ChemoTx® Disposable Chemotaxis System (neuroprobe). 3 x 10^4 neutrophils were added to the top of a 5 µm pore polycarbonate membrane and migrated to keratinocyte supernatant for two hours. Migrated cells were analysed with an LSRFortessa flow cytometer (BD Biosciences). Migration was performed in triplicates. Additionally, migration assays were performed on the neutrophil-like cell line HL-60 after differentiation.

2.2.1.8. Isolation of lesional T cells from patients and supernatant production

Primary human lesional T cells were isolated and expanded from freshly taken skin biopsies of Lichen Ruber (n=8), Atopic Dermatitis (n=3) and Psoriasis (n=4) patients as previously described (Lauffer et al. 2018). Supernatants of expanded lesional T cells were generated by 3-day stimulation with α-CD3 and α-CD28 as mentioned. Concentrations of IL-4, IL-6, IL-13, IL-17A, IL-22, IFN-γ and TNF-α in the supernatants were determined by ELISA (Table 6). A mixture in equimolar ratio was generated from different patients for each disease group and used for stimulation of keratinocytes.

Table 6: Cytokine profiles of patients derived T-cell supernatants (TCS). Cytokine concentrations measured by ELISA (pg/ml) of chosen patients that were pooled to generate the TCS mixes for cell culture use.

Patient	IL-17A	IL-22	IL-4	IL-13	IL-6	TNF-α	IFN-γ
Pso_1	3940	6163	1016	11031	190	5867	7439
Pso_2	4861	3203	285	29573	0	8568	5452
Pso_3	4912	12026	0	6777	158	4014	6604
Pso_4	2522	3942	0	0	31	1714	4322
AD_1	0	3257	4140	52628	32	2511	0
AD_2	0	8933	4645	73869	0	2720	0
AD_3	0	1734	3733	45729	3	3277	0
LE/LP_1	0	1035	5973	58142	0	6955	1713
LE/LP_2	0	10359	2037	50625	1250	13307	6578
LE/LP_3	0	6499	4036	25442	297	6972	3649
LE/LP_4	0	540	2191	28376	47	5421	4242
LE/LP_5	0	7886	3410	47411	1141	7434	4530
LE/LP_6	0	0	307	1446	69	3113	2851
LE/LP_7	0	0	3217	52377	97	3730	4339
LE/LP_8	16	0	2704	7067	331	7345	4956

2.2.1.9. Cell viability assay

Cell viability was determined with the CellTiter 96® Aqueous Non-Radioactive Cell Proliferation Assay (Promega) based on the reduction of the substrate MTS by viable, metabolically active cells into a formazan product. The absorbance of the formazan can be measured at 490 nm and is directly proportional to the number of living cells within a certain linear range. For this, 40.000 keratinocytes were seeded in a 24-well plate and stimulated at max.70% confluency without starving for 24h using the indicated cytokines and inhibitors (section 2.1.7. and Table 7) and the supernatant were collected for ELISA secretome analysis (IL-1ß). The assay was then performed as instructed, using the MTS/PMS reagent at 1:5 ratio and incubating for 1h (HaCaTs) or 4h (keratinocytes) at 37^0C in the dark prior to absorbance measurement. The readount was analyzed as cell viability in % normalized to either SMAC, Z-VAD or US as the respective control.

Table 7: Stimulation for cell viability assay.

Stimulant	Final working concentration	Dilution (1:x)
IFN-γ	50 ng/ml	2000
TNF-α	50 ng/ml	2000
SMAC	1 µM	100.000
Z-VAD	20 µM	500
LE/LP-TCS mix		10

2.2.2. Molecular biological methods

2.2.2.1. RNA isolation from cell culture cells, 3D models and skin biopsies

RNA from cell culture cells and 3D keratinocyte models was isolated using the RNeasy Plus Kit (Qiagen) according to manufacturer's protocol. For the initial cell lysis, the provided RLT lysis buffer was supplemented with DTT (1:50). For 3D models, the following steps were performed on ice prior to RNA isolation according to the kit: the samples were vortexed 1 min, the cell layer pipetted multiple times for dissolving, then vortexed again for another 1 min and finally filtered through a needle (0.9x40mm needle, 20G, 1 ml injection) several times. The final RNA elution was done in 30 µl (cell culture) or 40 µl (3D models) of RNase-free water and the concentration determined by NanoDrop. RNA from skin biopsies was isolated using QIAzol Lysis Reagent (Qiagen) and miRNeasy Mini Kit (Qiagen) and performed by Kerstin Weber (AG Eyerich, technician) according to manufacturer's protocol.

2.2.2.2. cDNA synthesis

mRNA was reversely transcribed into cDNA with the Applied Biosytems High Capacity cDNA Reverse Transcription Kit according to manufacturer's protocol. 500 ng RNA was used as input in a total reaction volume of 20 µl. For this, the RNA was diluted with DEPC-treated water to a volume of 14.2 µl and kept on ice. Then a cDNA synthesis Master Mix was prepared according to table 8 and 5.8 µl of reaction mix were added to the prepared RNA dilution per reaction. After centrifugating shortly and spinning down, the reactions were incubated according to table 9 for cDNA synthesis. The cDNA was stored at -80 ^{0}C.

Table 8: Composition for one reaction mix for cDNA synthesis.

Substance	Volume [µl]
10x RT buffer	2.0
10x Random primers	2.0
25x dNTP mix (100 mM)	0.8
Reverse Transcriptase (50 U/µl)	1.0

Table 9: cDNA synthesis program steps.

Step	Temperature	Time
1	25 ^{0}C	10 min
2	37 ^{0}C	120 min
3	85 ^{0}C	5 min
4	4 ^{0}C	∞

2.2.2.3. Primer design

Primers used for qPCR analysis were designed using NCBI Primer Blast and ordered from Metabion. Sequences can be found under Materials section 2.1.8.

2.2.2.4. quantitative real-time PCR (qPCR)

Using the Fast Start Universal SYBRGreen Master Rox (Roche) system, gene expression was measured by qPCR. For this, a 10 µl reaction was prepared with 3.4 µl diluted cDNA (8.5 ng, 1:10) and 6.6 µl SYBRGreen Master Mix containing the respective target-specific primers (table 10) to be used in 384-well plates. As a referene, 18S was used as housekeeping gene. The relative expression values were calculated using the $2^{-\Delta\Delta Ct}$ method by first normalizing to the housekeeping gene, then to the relative experimental control and finally displayed as a fold change or log2 expression value.

Table 10: Composition for one reaction mix for qPCR analysis in 384-well plate.

Substance	Final concentration	Volume [µl]
2x FastStart Universal SYBR-Green Master (Rox)	1x	5.0
fw primer (4 µM, 1:25 from 100 µM stock)	320 nM	0.8
rev primer (4 µM, 1:25 from 100 µM stock)	320 nM	0.8
cDNA (1:10)	8.5 ng	3.4

2.2.3. Protein biochemistry and analytical protein methods

2.2.3.1. Protein extraction and generation of whole cell lysates

RIPA buffer (Santa Cruz) was supplemented with 2 mM PMSF (1:100), proteinase inhibitor cocktail (1:75) and 1 mM sodium orthovanadate (1:100) and used for keratinocytes lysis after harvesting the cells as described. All the following steps were performed on ice. First, 200 µl of the prepared lysis buffer were added to the cell pellet and shaken for 30 min (2D) or 45 min (3D) at 4 ^{0}C. For 3D models, the samples were vortexed again prior centrifugation. The lysates were then centrifuged for 10 min at 10.000g, 4 ^{0}C and the supernatants collected. The protein lysates were stored at -80^{0}C.

2.2.3.2. BCA assay

The protein concentration of cell lysates was determined using the “bicinchoninic acid assay (BCA) kit” (Pierce) according to the manufacturer’s instructions. The BSA standard dilution series was measured in triplicates and the samples in duplicates at a 1:10 dilution.

2.2.3.3. SDS Polyacrylamide Gel Electrophoresis (SDS-PAGE)

For downstream analysis by western blot, proteins were first resolved by SDS-PAGE using Bolt 4-12% Bis-TrisPlus Gels and the Mini Gel Tank system. 25 µg of total protein were loaded per well. For this, the protein lysates were supplemented with 6x SDS-sample buffer and diluted to the loading volume of 30 µl, boiled at 96^{0}C for 10 min and spun down. 5 µl of PageRule was loaded as marker. The gels

were run with 1x MOPS running buffer for 10 min at 70 V for initial running and then at 140 V for additional 60 min.

2.2.3.4. Western Blot (WB)

For specific protein detection, proteins separated by SDS-PAGE were transferred from the gels onto a PVDF membrane. For the transfer, the "Mini Tank - Blot system" was assembled and used according to the manufacturer's instructions with all components pre-wet in freshly prepared Transfer buffer (section 2.1.1.). The membranes were activated in 100% MeOH and equilibrated in Transfer buffer prior to blotting. The transfer was performed for a total of 60 min with 15 min at 25V and then another 45 min at 20V. After blotting, the membrane was cut according to the proteins being analyzed, washed in TBS and blocked for at least 1.5h with 5% skimmed milk in TBS at RT while shaking. The appropriate primary antibody diluent, either 5% BSA/TBS-T or 5% milk/TBS-T, was determined for each new antibody. For stainings, the primary antibodies used were diluted as indicated under section 2.1.5. and incubated overnight at 4^0C while shaking, followed then by washing in TBS-T and incubation with the respective secondary antibodies (anti-rabbit/ anti-mouse-HRP, section 2.1.5.) in 5% milk/TBS-T for 1h at RT. The membrane was then washed 3x each 10 min with TBS-T and once for 5 min with TBS prior to detection. For chemiluminescent detection, the SuperSignal West Femto Maximum Sensitivity substrate was diluted 1:1, incubated for 3-5 min in the dark and finally imaged at ECL ChemoCam Imager system (Intas) using appropriate exposure times of 30-90 sec for protein targets and 10 sec for house-keepers.

2.2.3.5. Enzyme-linked Immunosorbent Assay (ELISA)

Supernatants of stimulated cells were subjected to ELISA for secretome analysis. ELISA kits for the following cytokines were used (R&D: IL-17A, IL-22, TNF-α, IFNγ, IL-13; BD: IL-4, IL-6, IL-1β, section 2.1.6.) The ELISAs were performed according the manufacturer's instructions following a similar workflow: For each cytokine, two different antibodies with different epitope specificities were used to perform the "Sandwich-ELISA" principle. First, a 96-well plate was coated with the capture antibody diluted in the kit-recommended buffer overnight, and then blocked prior to adding the samples. The supernatants were either added undiluted or diluted depending on analyte and the type of experiment the SNs were derived from. For detection, a second biotinylated antibody was used, which was then bound by added HRP-coupled streptavidin for the subsequent photometric reaction, where the TMB substrate is converted leading to a color change that can be measured by absorption at a specific wavelength. By comparison to standard curves, the cytokine concentrations of the samples were then determined.

2.2.3.6. Luminex

Alternatively, secretome analysis was performed by multiplexed Luminex assay allowing to measure a number of cytokines and chemokines simultaneously in the cell culture supernatants based on the usage of fluorophore-labelled beads that are coupled to different antibodies. Detection is based biotinylated detection antibodies. In this project, either pre-designed Bio-Plex assays (27-Plex) or custom designed panels (table 11) that were generated from single plex (Bio-Rad Laboratories) were used for secretome analysis according to manufactures' protocols.

Table 11: Custom designed Cytokine and Chemokine panels for the characterization of CEBPB-regulated secretome.

Cytokine assay	Chemokine assay
CXCL8	CCL22
CXCL1	CXCL2
CCL3	CXCL5
CCL5	CCL19
IL-6	
GM-CSF	
CXCL9	
CXCL10	
CCL27	

2.2.3.7. Immunofluorescence (IF)

Keratinocytes were seeded onto collagen pre-coated coverslips (1 % in PBS, collagen type I, SIGMA) or directly into Ibidi µ-Slide chambers (Ibidi) and stimulated according to confluency on the next day as indicated. MitoTracker staining was performed 24h after stimulation as described below (section 2.2.5.3.). For the IF after staining, the cells were washed with PBS and fixed using freshly-prepared 4% PFA in PBS for 15 min at room temperature. Different fixation reagents and conditions were first tested to choose the most convenient one (described under '3. Results', section 3.6.5.). The cells were then washed three times with PBS each 5 min and depending on staining either additionally permeabilized with ice-cold acetone for 5 min at -20 ^{0}C or stained directly with DAPI (ThermoScientific, 1µg/ml) in FACS buffer for 5 min. Finally, the cells were washed three times with PBS each 3 min and mounted onto microscope slides using VECTASHIELD Antifade Mounting Medium. The slides were left to dry overnight at RT, then sealed with nailpolish and kept at 4 ^{0}C in the dark till imaging. Imaging was performed as described below (section 2.2.7.2) immediately or within a couple of days to avoid signal loss.

2.2.4. Histology and immunohistochemistry (IHC)

Histology 3D: For fixation, the inserts were placed in fresh 24-well plates and fixed with 4 % Formaldehyde for 24h at 4 °C. After fixation, the membrane was cut out from the insert, divided in half and each membrane half placed between two biopsy sponges in embedding cassettes. The cassettes were placed and kept in 4% formaldehyde solution bath until dehydration. Dehydration was done by graded alcohol series (Histology lab) to remove water and fixative prior to embedding. For this, the 3D model membranes were placed diagonally standing and filled with paraffin in embedding cassettes. The blocks were then stored at RT and cooled at 20^0C o/n before cutting at the microtome (4µm) and mounting onto microscopy slides for use in H&E and IHC stainings. Prior to stainings, the slides were incubated at 65 °C for at least 30 min for paraffin melting. H&E staining was performed automated by the histology lab. The models were analyzed by imaging at the EVOS microscope (section 2.2.7.1.) and certain histological features quantified as described under 2.2.7.3.

IHC 3D and patient biopsies: For IHC analysis, 3-4 µm sections of paraffin-embedded samples were prepared, air-dried overnight at 37 °C, then dewaxed by incubating for at least 30 min at 65 °C (or o/n at 56°C), followed by rehydration. For this, the slides were subjected to the following alcohol series:

- **Xylol** (**Roticlear®**)**, 2x** for 10 min
- **100% Isopropanol, 2x** for 5 min
- **96% Ethanol, 1x** for 5 min
- **70% Ethanol, 1x** for 5 min
- **ddH_2O, 1x** for 5 min

Heat-activated antigen retrieval was performed in boiling buffer either EDTA (for Ki67) or citrate buffer (for CEBPB) in pressure cooker for exactly 7 min. The slides were then washed three times with Tris buffer (section 2.1.1.) and the staining performed using the Permanent AP Red Kit according to manufacturer's instructions. Shortly, the slides were first incubated with 3% Hydrogen peroxide solution for 15 min at RT for peroxidase blocking and then Protein-Block (Reagent 1) for 5 min at RT. After washing in Tris buffer, the slides were incubated with the primary antibodies (rabbit anti-Ki67 (Zytomed, ready-to-use) or mouse anti-CEBPB (Santa Cruz), followed by a secondary polymeric alkaline phosphatase (AP)-linked antibody. For CEBPB, different antibodies were tested for use in IHC and their concentrations were titrated. Best results were obtained with the mouse anti-CEBPB (Santa Cruz) at 1:50 dilution and was used for all subsequent experiments.

The complex was visualized by the substrate Chromogen Fast Red (Permanent AP Red working solution) after 10 min incubation at the microscope and the reaction stopped after desired staining intensity has been reached. The Slides were finally counterstained with haematoxylin, subjected to dehydrating alcohol series and mounted using a xylol-compatible mounting medium (Eukitt quick-

hardening mounting medium, Sigma Aldrich). Alternatively, for some experiments, stainings were performed by an automated BOND system (Leica) according to the manufacturer's instructions.

2.2.5. Metabolic analysis

All stimulations for metabolic analysis were performed without starving the cells and using cells that were not too confluent (max 70%), since these two aspects can negatively impact the measurements leading to artefacts due to additional metabolic stress of the cells.

2.2.5.1. ATP assay

For measurement of intracellular ATP levels, the Luminescent ATP detection assay (Abcam) was used. For this, keratinocytes were seeded in a 24-well plate with 80.000 cells per well and stimulated without starving for 24h. For the assay, reagents and ATP standard were prepared in the dark according to manufacturer's instructions. The cells were lysed by adding 200 µl detergent and shaking the plate for 5 min at 700 rpm. 200 µl substrate solution were then added, incubated while shaking for 5 min and the prepared cell lysates were transferred in triplicates onto a white flat-bottom 96-well plate. After 10 min incubation in the dark at RT, the luminescence was measured with settle time= 0, integration time= 1000 and 10.000 ms.

2.2.5.2. Seahorse assay

The Seahorse XFp Cell Mito Stress Assay (Agilent Technologies) was used to measure real-time mitochondrial respiration (OXPHO) and assess parameters of mitochondrial function in keratinocytes. 20.000 cells per well were seeded in a collagen pre-coated XFp assay plate, grown for 1 day and stimulated without starving for 24h prior to assay. The assay was carried out according to manufacturer's instructions with the following final compound concentrations titrated for primary human keratinocytes: Oligomycin (1 µM), FCCP (1 µM) and Rotenone with Antimycin A (0.5 µM). After the assay, the cells were lysed with trypsin and counted to obtain the cell numbers needed for normalization. The normalized OCR measurements were used for the calculation of different mitochondrial respiration parameters as described in the Seahorse Assay User Guide and in (Divakaruni et al. 2014).

2.2.5.3. MitoTracker assay

Functional mitochondria were stained in live keratinocytes using MitoTracker Deep Red FM (Invitrogen) according to manufacturer's recommendations. The optimal working concentration was determined for keratinocytes in titration experiments (described in '3. Results') as 200 nM. For staining, the cells were washed once in PBS and stained with MitoTracker in pre-warmed keratinocyte

media for 30 min at 37 °C and 5 % CO_2. After staining, the cells were washed with PBS and used as described for further immunofluorescence (IF) staining. For analysis by flow cytometry, the cells were first harvested and pelleted at 1200 rpm for 10 min at 4 °C. The cell pellets were then resuspended in MitoTracker solution (200 nM) and stained as described. Following staining, the cells were washed, re-pelleted and resuspended in FACS buffer (section 2.1.1.). Directly prior to measurement at the cytometer, DAPI (ThermoScientific, 1µg/ml) was added to the cells.

2.2.6. Sequencing techniques

2.2.6.1. Bulk RNA sequencing

Library preparation and sequencing: Libraries were generated using the TruSeq Stranded Total RNA Kit (Illumina) according to the manufacturer's high sample protocol. Samples were sequenced on an Illumina HiSeq4000 (patients biopsies) or NovaSeq6000 (*in vitro* keratinocytes) as paired-end with a read length of 2x 150 bp and an average output of 40 Mio reads per sample. Sequence alignment was performed using STAR aligner with human genome reference hg38. ***Pre-processing:*** RNAseq count data sets were filtered for protein coding genes and genes with transcripts per million (TPM) and counts greater than 0. After removal of Y-Chromosome genes, count data was normalized using sizefactors, calculated and transformed using variance stabilizing transformation with the parameter blind=FALSE from the Bioconductor package DESeq2. ***DEG generation*****:** For the calculation of differential gene expression (DEGs), the design function for *in vitro* models was 'g ~ Donor + Manipulation', with 'Donor' accounting for heterogeneity between the keratinocytes donors and 'Manipulation' refering to the different stimulations of 2D and 3D *in vitro* models. DEGs were determined according to the thresholds $|log2FC| > 1$ and p-value < 0.05. ***Overrepresentation analysis (ORA):*** Background genes were defined as all genes, which have been measured in the experiment. DEGs have been filtered requiring a $|log2FC| > 1$ and p-value < 0.05 and used as input for the ORA analysis using the Bioconductor package clusterProfiler and visualized with ggplot2. For keratinization analysis (Figure 27A) merged gene sets from Reactome, MSigDB and literature-based predefined keratinocyte pathways were used. ***Gene set enrichment analysis (GSEA):*** GSEA was performed on the patient DEGs ranked by signed p-adjusted values using the gene sets generated from 2D and 3D keratinocytes with the Bioconductor package fgsea. Read mapping, pre-processing and all downstream bioinformatic analysis was performed by collaborating bioinformatician Christina Hillig (AG Michael Menden, Helmholtz Zentrum München).

2.2.6.2. Single cell RNA sequencing

Sample preparation: Patients suffering from LE/LP (n=5), Pso (n=7) and AE (n=5) were recruited for the generation of the scRNASeq cohort. Skin cells from 6 mm punch biopsy were isolated by a 3 h at

37^{0}C digestion using Miltenyi Whole Skin Dissociation Kit (130-101-540) and gentleMACS Dissociator (program h_skin_01_01) from Miltenyi according to manufacturer's protocol. The sample was then filtered using a 70 µm pre-separation filter to remove residual undigested tissue, centrifuged for 10 min at 1200 rpm (4^{0}C), resuspended in PBS and transferred into DNA low binding tube to avoid coating. The retrieved cell number was determined. 250.000 - 500.000 cells were taken for FACS staining (section 2.2.8.1.) as part of patients characterization and the rest of the cells used for sorting. For sorting, the cell suspension was stained with CD45 (1:100) for 20-30 min (4^{0}C, dark) followed by PI staining for dead cell removal. Cells were resuspended in sorting buffer (section 2.1.1.) after staining. Living (PI$^-$) immune (CD45$^+$) and epithelial cells (CD45$^-$) were sorted at FACSAria Fusion. CD45$^+$ and CD45$^-$ cells were then mixed in equimolar ratios and used as input for library generation. **Library preparation and sequencing:** In total 24,000 cells (1:1 of CD45-: CD45+ populations) were used per sample as an input for the GEM generation reaction. To increase the output, two samples were performed per patient when possible. The libraries were prepared using the Chromium Next GEM Single Cell 3' Reagent Kits (10x Genomics) in combination with dual indices according to the manufacturer's protocol. Finally, samples were sequenced on a NovaSeq6000 as paired-end with 28-10-10-90 cycles and sequencing depth of at least 20,000 read pairs per cell. Sequence alignment was performed using STAR aligner with human genome reference hg38. **Quality control (QC) and Pre-processing:** QC revealed a minimum of 30 genes per cell, a minimum and maximum UMI-count of 400 and 80,000, respectively. As cut-off for genes, a gene had to be expressed in at least 20 cells with a minimum UMI-count of 1. Further, cells with a mitochondrial fraction above 25 % were removed and doublets detection was performed using the scrublet pipeline. Highly variable genes (HVG) were determined and the data visualized using UMAP. Further, principal component analysis (PCA) was applied. Subsequently, the data were clustered using Leiden clustering and represented in a 2D UMAP plot. **Annotation:** scNym was used for cell type annotation together with the Haniffa lab dataset from (Reynolds et al. 2021). For further refining, literature- and database-retrieved marker genes were used together with marker genes determined by scanpys function `rank_genes_groups`. **Cell cycle analysis:** Cell cycle genes for cell cycle analysis were taken from (Macosko et al. 2015). QC, pre-processing, annotation and further downstream analysis was performed by Christina Hillig.

2.2.6.3. Spatial transcriptomics

Sample preparation: Lesional skin biopsies (4mm) from patients recruited for single-cell RNASeq were taken and immediately snap frozen in liquid nitrogen. Samples were then stored at -80°C until cryosectioning. For cryosectioning, samples were equilibrated to cryostat (NX70, Thermo Fisher Scientific) chamber temperature for at least 30 mins, covered in optimal cutting temperature compound (OCT) and cut into sections of 10µm and directly placed onto the Visium Spatial Gene

Expression slide (10x Genomics) at the indicated fields. Slides were processed with the Visium Spatial Gene Expression Kit (10x Genomics) according to the CG000239 Visium Spatial Gene Expression User Guide RevA. To perform H&E staining, samples were incubated in Mayer's Hematoxylin for 7 min and undiluted Eosin for 1 min, which was previously tested for optimal tissue staining. **Imaging:** Stained sections were imaged using the scanning microscope Axio Scan.Z1 microscope (Zeiss) with the imaging settings shown in table 12. Raw images were processed using Zenblue Software (Zeiss). **Library preparation and sequencing:** Libraries were prepared according to the manufacturer's guide with a tissue permeabilization time of 14 min, which was previously determined by Alex Schäbitz using the Tissue Optimization protocol. For sequencing, the individual libraries were pooled and sequenced on a NovaSeq6000 using the recommended 28-10-10-120 cycle read setup with a sequencing depth of 150-175 million total read pairs per sample. **Histological sample annotation:** H&E images were evaluated and annotated manually by at least two colleagues independently using Loupe Browser (10x Genomics) for their tissue localization, anatomical structures and specific cell types. In frame of tissue localization, epidermal spots were categorized as "upper epidermis", "middle epidermis" and "basal epidermis" and dermal spots were annotated as "dermis 1" to "dermis 7" indicating the depth of the dermal layer. **Bioinformatic analysis:** Spatial data from the cohort generated by former lab member Alexander Schäbitz, together with the data generated in this cohort, was subjected to the same pre-processing and downstream bioinformatic analysis described in detail in the common publication (Schäbitz et al. 2022) and performed by the collaborating bioinformatician Christina Hillig.

Table 12: Imaging settings for Visium Spatial sections.

Parameter	Settings
objective	20x
Brightfield configuration	2424x2424 pixel resolution White balancing
Imaging system	Tile scanning with automatic stitching Shade correction Extended focus with z-stack
Export	Tiff with 25% resize and compression setting 'loss less'

2.2.6.4. Bioanalyzer

To determine the concentration, quality and average fragment sizes of the libraries for single-cell and spatial transcriptomics, the High Sensitivity DNA assay was used according to manufacturer's guidelines and measured on the Agilent 2100 Bioanalyzer.

2.2.7. Microscopy and image analysis

2.2.7.1. Brightfield microscopy for histology and IHC

Imaging was done using the EVOS microscope (ThermoFisher) for histology, IHC stainings and live imaging for metabolic analysis (MitoTracker staining).

2.2.7.2. Confocal IF microscopy

For high-resolution imaging of immunofluorescence experiments, the Leica SP5 Confocal Microscope was used with the optimized settings summarized in table 13.

Table 13: Confocal imaging settings for imaging of MitoTracker IF experiments.

Parameter	Value	Type
Laser intensity	UV (DAPI): 5-15%, other: 5-30%	Intensity parameters
Gain	600-800V	
Offset	-10	
Objective	63x with glycerol	Imaging parameter
Acquisition mode	xyz	Scan parameters
Acquisition format and speed	512x512 for scanning, 1024x1024 for imaging 400 Hz	
Pinhole	1 Airy Unit	
Line Average	4	
Line Accumulation	1	
Frame Average and accumulation	1	
Sequential scan	Between frames	
z-stack	System optimized (10-15 stacks)	

2.2.7.3. Image analysis and quantification

Quantification of epidermal thickness

The epidermal thickness of 3D skin models was measured from the top of the corneal layer to the bottom of the basal keratinocyte layer with ImageJ (Manja Jargosch). Four sections were measured per sample and the mean was calculated. Next, delta thickness (IL-22 minus unstimulated thickness) was calculated for the knockout to visualize the acanthosis effect. Finally, this delta thickness was displayed in relation to the delta thickness from the electroporated noRNP control sample.

Fluorescence intensity quantification

For quantification of fluorescence intensity of MitoTracker signal from IF experiments, 5 to 10 images per condition were collected. Using ImageJ, the mean fluorescence intensity was quantified in a specified area and the background signal subtracted. Then the number of cells in this area was

determined and used for normalization of the measured intensity, to finally display values of signal intensity per cell.

2.2.8. Flow cytometry

2.2.8.1. Live/dead, surface and intracellular staining

FACS staining using a T-cell panel was performed on cells collected from patients skin biopsies as part of the scRNA Seq cohort characterization. For this, cells were resuspended in T-cell medium with 5% HS and transferred into a 24-well plate for re-stimulation with PMA (1:10.000), Ionomycin (1:1000) and GolgiStop (1:1500). GolgiPlug mix (1:1000) was added after 2h at 37 °C and incubated for further 3h at 37 °C, followed by Aqua live-dead staining using L/D staining solution (Aqua 1:1000 in PBS w/o $Ca^{2+}Mg^{2+}$) for 20 min at 4°C in the dark. Cells were then resuspended in FACS buffer (section 2.1.1.) and stained for surface markers (CD3, CD4 and CD8) using the antibodies listed under section 2.1.5. at the indicated concentrations. 50 µl were used as staining volume. The cells were then fixed using Fix/Perm solution for 30 min at 4°C, washed with 1x Perm solution and stained in a total volume of 10 µl 1x Perm solution containing antibodies for different cytokines (IL-17A, IL-22, TNF-α, IFN-γ, IL-4, IL-13, IL-10, GM-CSF). Staining was done for 30 min at RT in the dark while shaking. Finally, the cells were washed with FACS buffer, then resuspended in FACS buffer and transferred into cluster tubes for acquisition.

2.2.8.2. Flow cytometry analysis

Flow cytometry, also known as FACS (fluorescent-activated cell sorting) analysis, allows the investigation of cells based on their size and granularity, as well as the expression of different surface and intracellular markers in a multi-plexed manner. Parameters like the forward scatter (FSC), which gives information about the size of cells and sideward scatter (SSC), which determines the granularity, were used for gating on different cell populations. For experiments analyzed by FACS, different parameters were collected like frequency of certain cell populations positive for specific markers or mean and median fluorescence intensity (MFI) to quantify specific signals. FACS analysis was performed on the LSR Fortessa flowcytometer (BD Bioscience) and analyzed using the FlowJo software.

2.2.9. Statistical analysis

Data were visualized using GraphPad Prism 6 software (https://www.graphpad.com). Applied significant tests are listed in each figure legend. Significance level was defined as $p<0.05$.

3. Results

3.1. Target identification

To tackle the challenge of personalized medicine in dermatology, great efforts have been directed in our group towards combining deep clinical phenotyping of chronic inflammatory skin diseases with transcriptomics of lesional skin to generate an extensive gene expression- clinical attribute landscape. This landscape is based on clinical metadata- a comprehensive dataset containing 86 clinical characteristics derived from a large patient cohort (n=235 from 13 different CISDs) covering diverse attributes such as family history, histological characteristics, metabolic comorbidities, inflammatory values and medication records. Together with the assigned bulk RNA sequencing (bulk RNA Seq) data from the corresponding skin biopsies, this led to the generation of a molecular transcriptional map (Figure 7A) for the main CISDs. This can be exploited to 1) stratify patients based on their clinical attribute-transcriptional signature, 2) predict the response to a certain treatment regimen and 3) predict the risk for potential comorbidities on the molecular level. Moreover, importantly, it can also be employed for the identification of novel disease drivers contributing to specific pathogenic features of skin inflammation. The latter lead to the identification of CEBPB as a potential factor associated with type 3 disease-relevant attributes, neutrophils and acanthosis (Figure 7A, B).

A

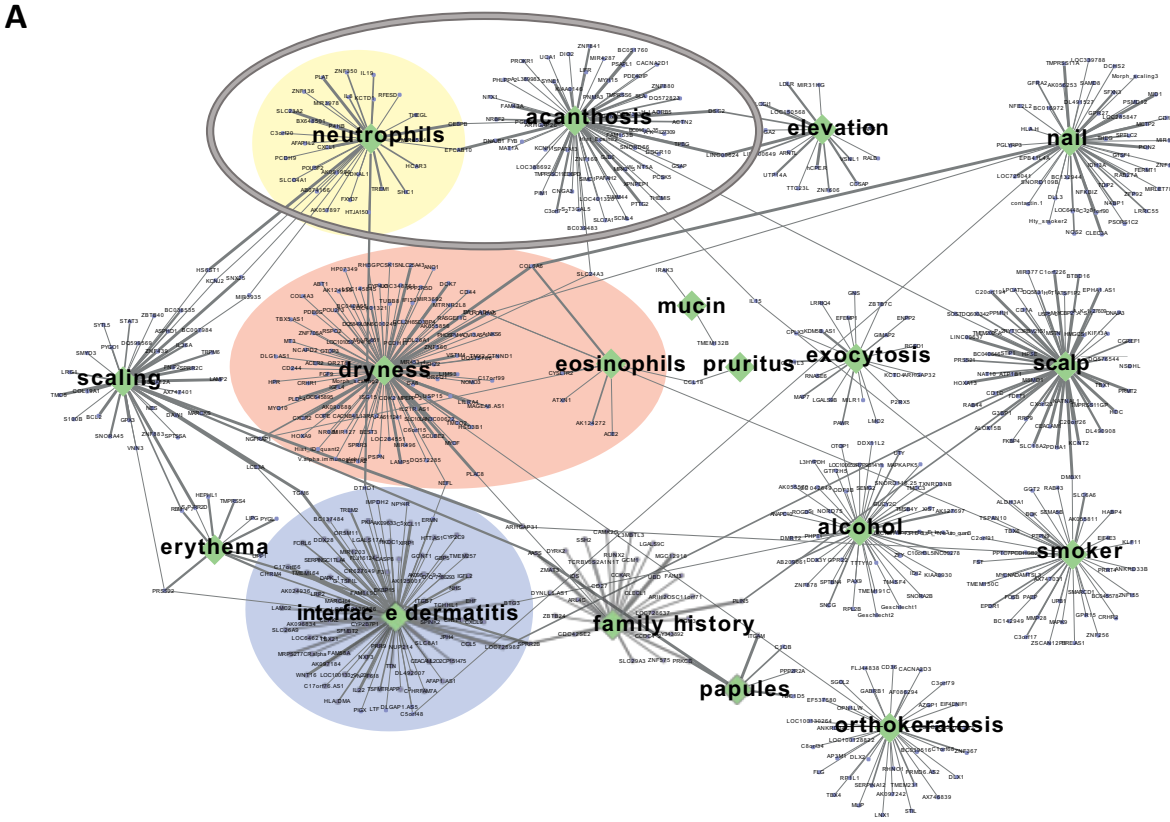

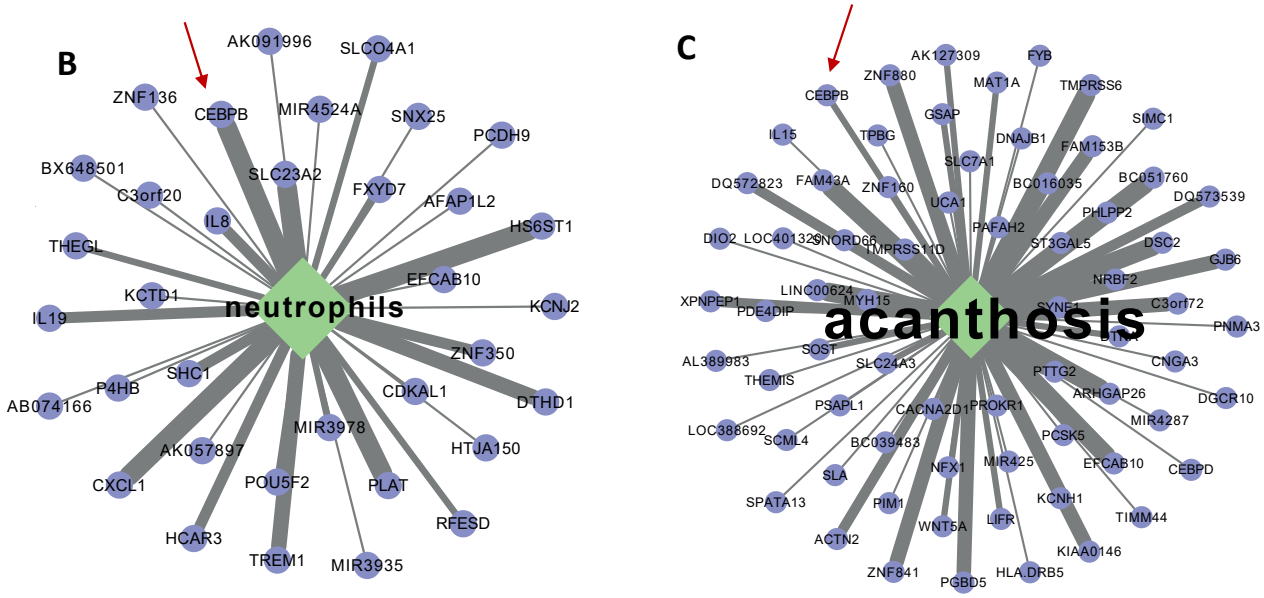

Figure 7: A global gene expression-clincial attribute network for chronic inflammatory skin diseases. **A)** Grouped according to the different disease patterns are key clinical attributes, like acanthosis, neutrophils, dryness and interface dermatitis, displayed as labelled green hubs with surrounding gene signature for each hub. The genes are connected to the clinical characteristics by lines of differing widths corresponding to the strength of association. CEBPB is found as a factor interconnected with both "neutrophils" and "acanthosis". **B)** and **C)** show zoomed-in networks for "neutrophils" and "acanthosis" with the associated genes. Red arrows indicate CEBPB. Figure modified from (Garzorz-Stark et al. 2020).

3.2. Transcription factor profiling reveals CEBPB as a hub gene in psoriatic skin

Transcription factors are key regulators of tissue inflammation and homeostasis. Here, to expand the molecular maps for CISD with a focus on Psoriasis and to identify hidden drivers of pathogenesis, we performed transcription factor profiling on lesional psoriatic skin (n=90) identifying 190 differentially regulated transcription factors (TFs) (0.8 <= log2FC >= -0.8 and padj < 0.05) compared to autologous non-lesional skin. I generated a final network of 135 TFs in Psoriasis based on the number of interactions including only TFs with at least two or more interactions (Figure 8A). Interactions were generated using the STRING protein-protein interaction database including interactions that were either experimentally determined or curated from databases, as well as interactions based on co-expression and text mining, while ruling out all other predicted interactions (e.g. protein homology, gene co-occurrence and gene neighborhood). When ranking transcription factors according to the obtained number of interactions, we identified *MYC*, *SOX2*, *GATA3* and *STAT3* as most connected transcription factors with 55, 47, 35, and 35 interactions, respectively. *CEBPB* was identified as the 5th most connected transcription factor. Whereas the association of these other factors to Psoriasis pathogenesis has been well established, that of *CEBPB* hasn't been characterized in context of skin inflammation yet. *CEBPB* was significantly upregulated in Psoriasis (padj = 6,9E-32) and showed 30 connections with other TFs (Figure 8B). Here, the interaction partners of *CEBPB* comprised multiple

Psoriasis-associated TFs such as *HIF1A*, *STAT1/3*, *JUNB*, *FOSL1* and *NFKB1* indicating a potential involvement of *CEBPB* in the pathogenesis of Psoriasis.

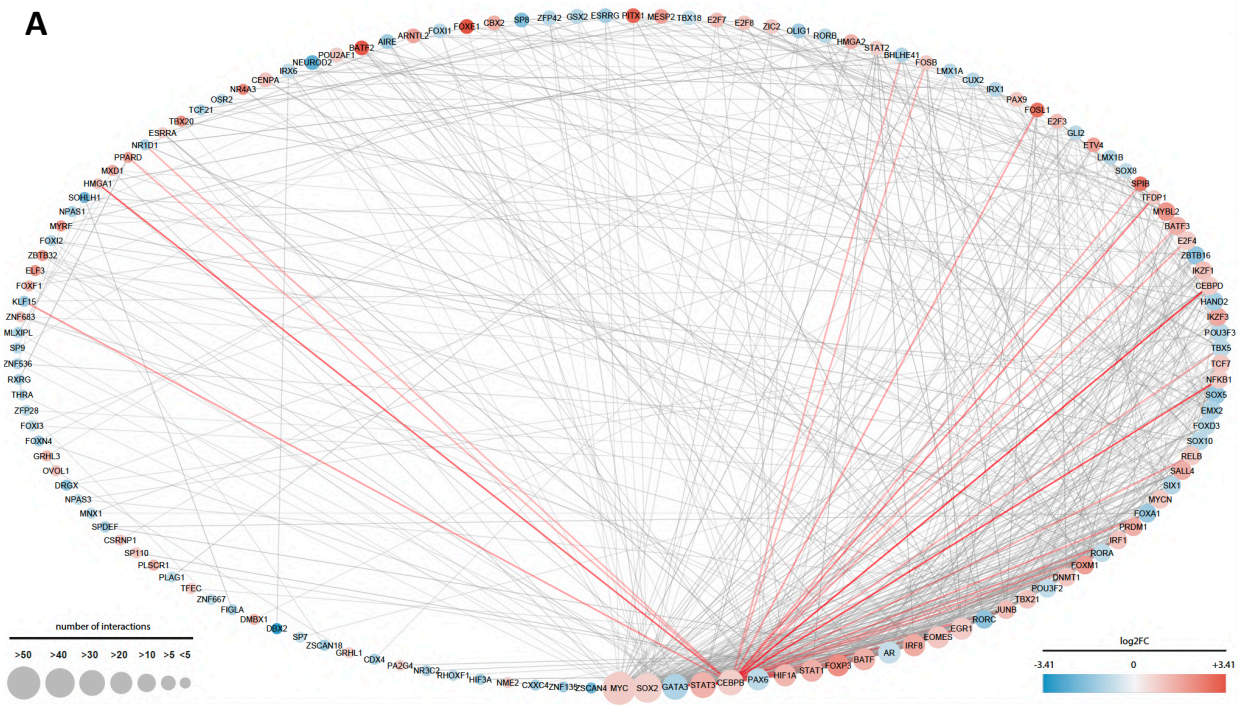

Figure 8: Transcription factors network of psoriatic skin and CEBPB interaction partners. A) TF network of differentially expressed TFs in Psoriasis compared to autologous non-lesional skin (n=90). TFs filtered by GSEA analysis with the 'molecular function' transcription factor. The top differentially expressed TFs within the range -0.8 > log2FC > 0.8 and padj < 0.05 (n=190 without singletons 135) are visualized in a circular STRING PPI-based network using cytoscape. TFs are ordered based on the number of interactions. Node colour indicates log2FC expression values (blue = negative/downregulated, red = positive/upregulated). Node size indicates number of interactions. Edges between nodes indicates STRING protein interactions between TFs with red edges highlighting CEBPB interactions (n=30), which are shown separately in **B).**
TF = transcription factor, FC = fold change, padj = adjusted p-value, PPI= protein-protein interaction.

3.3. CEBPB expression in patients

3.3.1. CEBPB is upregulated in CISD patients with highest levels in Psoriasis via bulk RNA Seq and spatial transcriptomics analysis

To understand the contribution of CEBPB to skin inflammation, I first aimed to evaluate the expression of CEBPB in representative diseases of the three main disease patterns, namely Lichen planus and Lupus erythematosus (LE/LP) as a type 1, Atopic dermatitis (AD) as a type 2 and Psoriasis (Pso) as a type 3 disease. First, using an in-house large bulk RNA sequencing cohort comprising patients with LE/LP (n=41), AD (n=48) and Pso (n=90), CEBPB was significantly upregulated in the lesional skin of LE/LP ($p<0.05$) and Pso ($p<0.0001$), compared to the non-lesional skin, but not in AD ($p=0.0966$). Furthermore, CEBPB expression showed highest levels in psoriatic lesions compared to lichenoid ($p<0.0001$) and AD lesions ($p=0.0019$) (Figure 9A).

To gain insight into the local tissue distribution of CEBPB expression in these skin diseases, I generated in collaboration with other lab members (A. Schäbitz and M. Jargosch) a spatial transcriptomics cohort comprising lesional skin from LE/LP (n= 11), AD (n= 9) and Pso (n= 11), as well as non-lesional skin (n= 14), using the 10X Visium technology (Schäbitz et al. 2022). Here , we observed CEBPB positive spots in the dermis and epidermis of all three lesional conditions (Figure 9 B, C). The non-lesional (NL) skin represented reduced spots number with lower UMI counts/spot (0-5 UMI counts/spot), indicating low basal levels of CEBPB expression in healthy skin. Similarly, AD skin showed only low expressing CEBPB-positive spots with 0-15 UMI counts/spot. In contrast, both LE/LP and Pso showed an enhanced spatial expression of CEBPB with high-expressing CEBPB-positive spots with mainly up to 25 UMI counts per spot in Lichen and up to 30 UMI counts per spot in Pso (Figure 9 B). Notably, the spatial pattern of CEBPB expression showed clear enrichment in the epidermis (3000 (NL), > 7000 (LE/LP), >5000 (AD), >10000 (Pso) UMI counts) compared to the dermis (>500 (NL), > 10 (LE/LP), >2500 (AD), >2500 (Pso) UMI counts) (Figure 9 C). Within the epidermis, CEBPB showed strongest expression mainly in the middle layers.

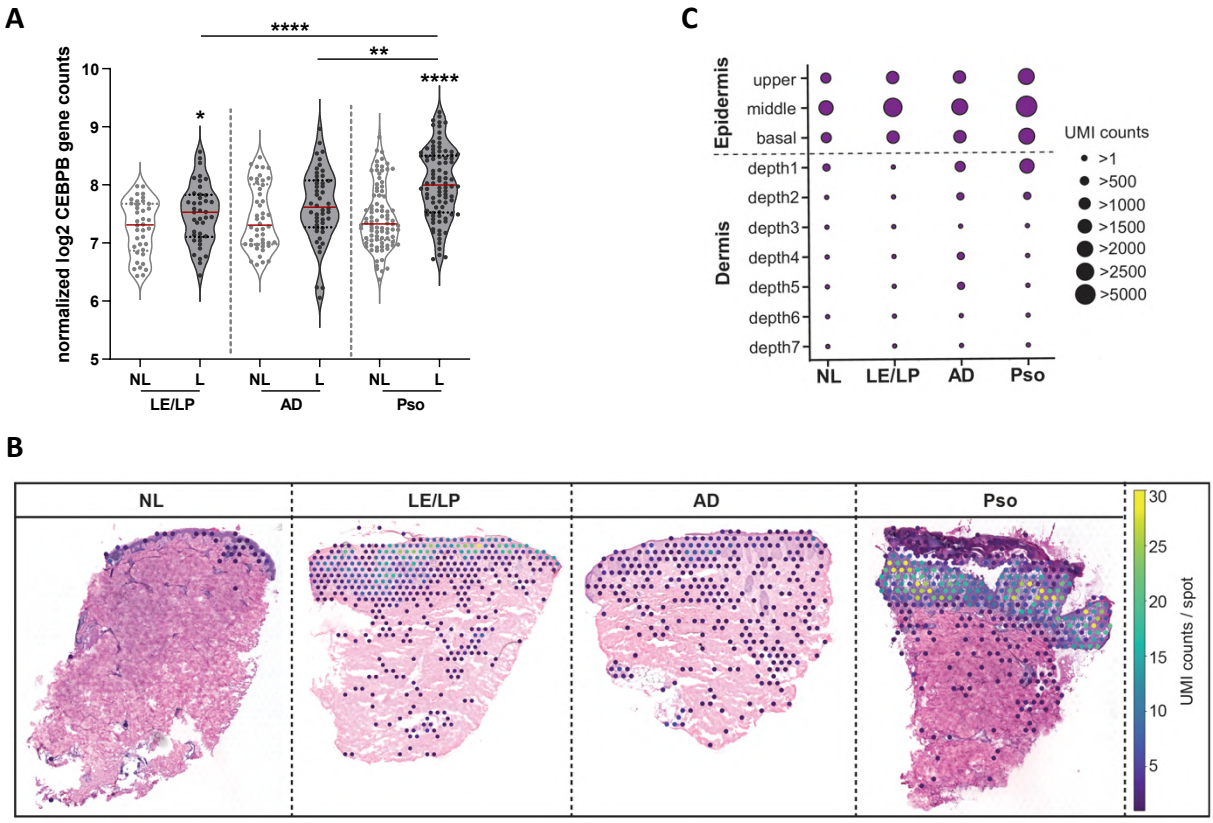

Figure 9: Bulk RNASeq and spatial transcriptomics analysis of CEBPB expression in CISD patients. A) Violin plots of DESeq2 normalized CEBPB gene counts from bulk RNASeq in lesional (L) and non-lesional (NL) skin of Lupus erythematosus/Lichen planus (LE/LP, n= 41), Atopic Dermatitis (AD, n=48) and Psoriasis (Pso, n=90) patients. **B)** Tissue visualization of CEBPB UMI counts per spot for representative H&E stainings of NL (n=14), LE/LP (n=11), AD (n=9) and Pso (n=11) skin from spatial transcriptomics analysis with 55µm spot size. **C)** Quantification of CEBPB UMI counts from the total spatial transcriptomic cohort with classification of skin tissue layers into upper, middle and basal epidermis, as well as 7 different depths for the dermis. Number of UMI counts per tissue layer is given by the different node sizes. Comparison to non-lesional was performed using unpaired t-test with Welch's correction. Comparison of disease groups was performed using Ordinary one-way ANOVA test with Tukey's multiple comparison. *p<0.05, **p<0.01, ****p<0.0001. L = lesional, NL = non-lesional, UMI = unique molecular identifier.

3.3.2. Single-cell RNA Seq analysis of CEBPB expression in Lichen and Psoriasis patients reveals keratinocytes among high expressing cells

Next, to gain better understanding of the CEBPB expressing cell populations in the lesional skin, I performed single-cell RNA Sequencing (scRNA Seq) on LE/LP (n=5), AD (n=5) and Pso patients (n=7). To generate this cohort, I first established the working protocol for scRNA Seq from skin biopsies using the 10X Genomics NextGEM platform. Figure 10 shows the workflow overview with its main steps.

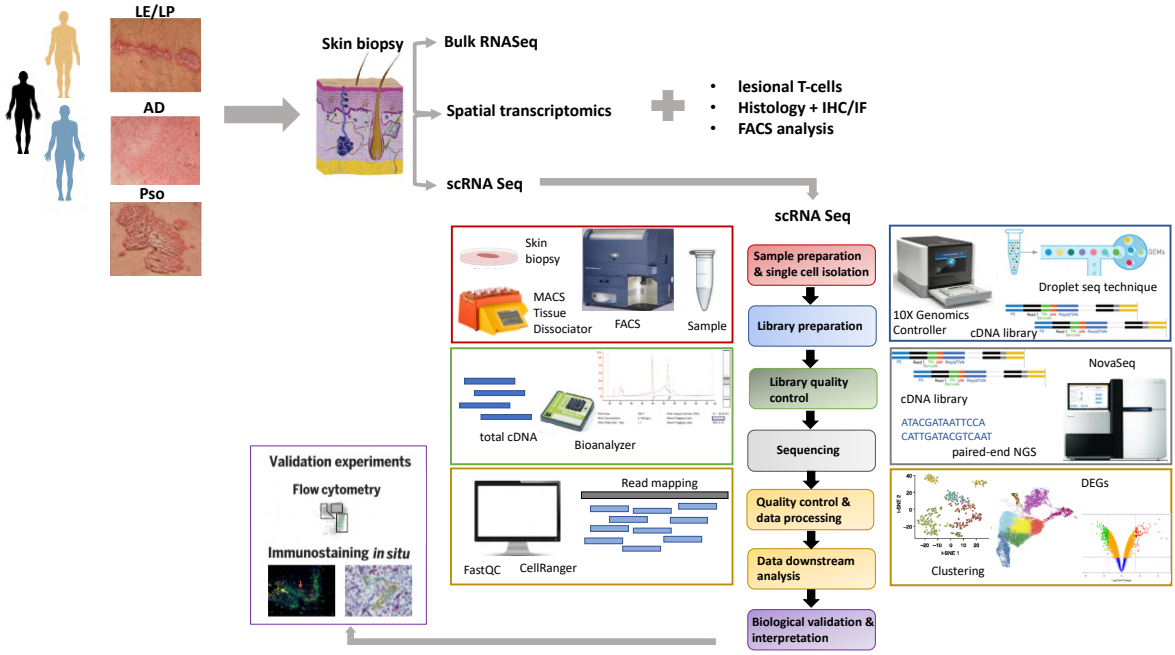

Figure 10: Workflow overview for scRNA Seq analysis of CISD patients. Displayed are the single steps of a scRNA Sequencing experiment, color-coded, with details indicated for each step in the boxes with the respective colors. Skin biopsies are collected from LE/LP, AD and Pso patients as depicted. Besides use for the different transcriptomics analysis, biopsies are also used to isolate lesional T-cells and perform histology, as well as FACS analysis. Upon tissue dissociation and preparation of a single cell suspension, the samples are sorted and used for library generation by the 10X Genomics Droplet technique. The resulting barcoded cDNA libraries are checked for their quality and concentration by Bioanalyzer and then sequenced at a NovaSeq based on the principle of paired-end sequencing. The obtained reads are then mapped to the human reference genome and the data is preprocessed using bioinformatic softwares like FastQC and CellRanger. Downstream analysis is then performed with filtered high quality data to include cell clustering, signature generation and differential gene expression. As a final step, the generated signatures are to be subjected to validation and used to extract biologically relevant information. DEG= differential gene expression, NGS= next-generation sequencing. IHC= immunohistochemistry, IF=immunofluorescence.

As part of the sample preparation step, different sorting strategies have been tested, finally choosing the optimal one depicted in Figure 11 A. This sorting strategy was used throughout the cohort and is based on gating out dead cells by PI staining followed by gating the skin cell populations via CD45 into CD45+ (immune cells) and CD45- (other skin cells e.g. keratinocytes, fibroblasts) populations that were then mixed in equal ratios and used as input for the generation of the single cell libraries. As expected, disease-specific differences in the frequencies of the CD45+ populations were observed, with LE/LP patients having the most prominent amounts, followed by Pso and AD (Figure 11 B). As part of the cohort characterization, I performed FACS analysis with a T-cell panel for each patient validating the cytokine profile (Figure 11 C). As an example, a Lichen patient is shown, where we detected in the CD3+ compartment highest production of the type 1- signature cytokines IFN- γ and TNF-α, followed by IL-13 and IL-22, with no production of IL-17A or IL-4.

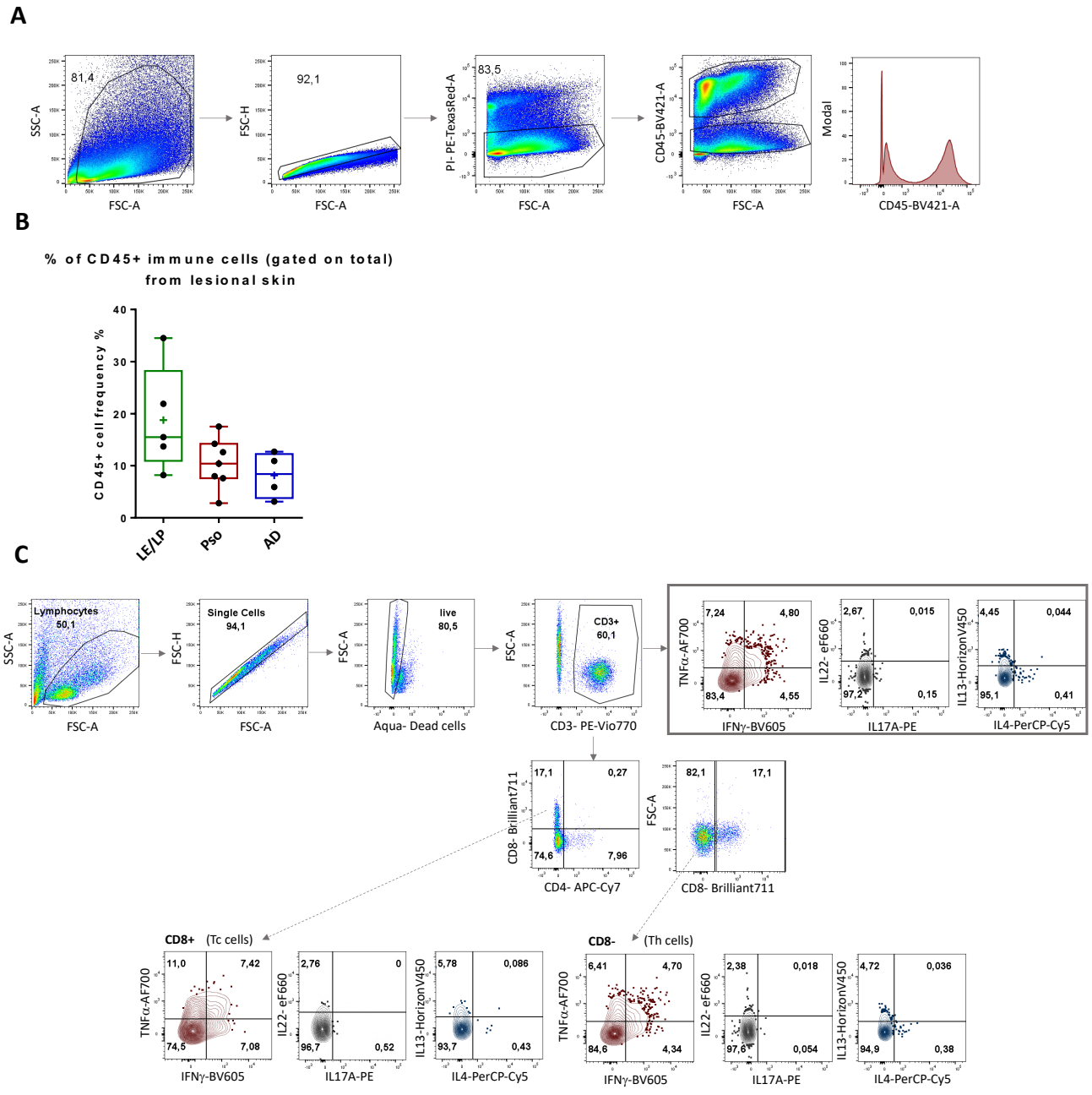

Figure 11: Sample preparation and validation via FACS for the generation of the single-cell RNA Seq cohort. A) FACS sorting strategy used after skin digestion for gating out dead cells via PI-staining and sorting the biopsy cell populations based on CD45 expression into CD45+ (immune cells) and CD45- (other skin cells). The cell populations were then mixed in equal ratios and used as input for the sc library generation. **B)** Percentages of obtained CD45+ cells frequency in Lichen (n=5), Pso (n=7) and AD (n=5) patients from the generated sc cohort. **C)** Example of FACS intracellular staining using a T-cell panel on cells isolated from skin biopsy of a Lichen patient that was subjected to single-cell sequencing. Cells were restimulated with PMA/ Ionomycin for 4h and cytokine secretion was blocked by GolgiStop and GolgiPlug. Production of key cytokines is visualized in the CD3+, CD8+ (Tc cells) and CD8-/CD4+ (Th cells) compartments as part of patients cohort validation. sc= single-cell, Tc= cytotoxic T-cells, Th= T-helper cells.

Using this scRNA Seq cohort, I identified that cells expressing high levels of CEBPB were located in the keratinocytes cluster, followed by fibroblasts, and antigen-presenting cells (APCs), consisting mainly of macrophages and dendritic cells (DCs). Additionally, the lymphocytes and T-cells cluster also contained a moderate number of CEBPB expressing cells (Figure 12). Similar cellular expression patterns were observed for both Lichen and Psoriasis patients.

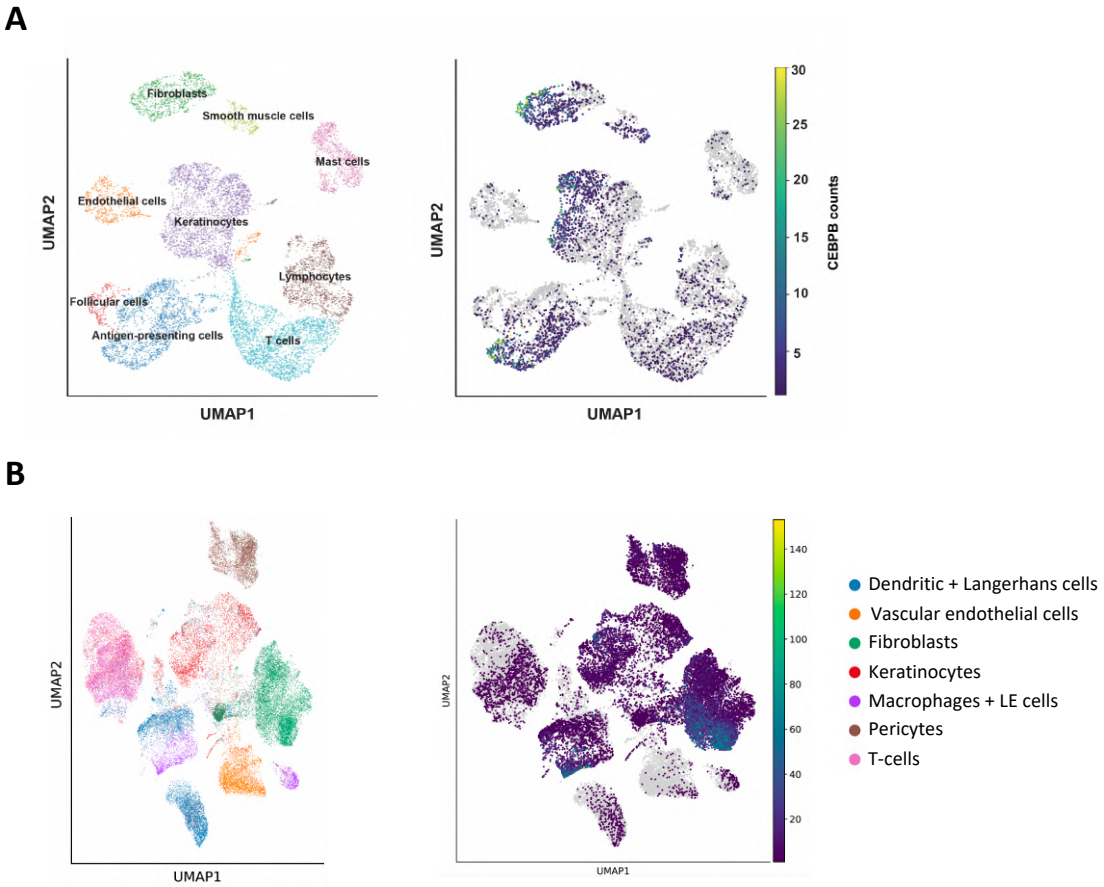

Figure 12: Analysis of CEBPB expression at single-cell level in psoriatic and lichenoid skin shows high expression mainly in keratinocytes, fibroblasts and antigen-presenting cells. A) and **B)** show UMAP plots with annotated cell clusters (left) and CEBPB gene counts (right) obtained from single-cell RNA Seq analysis of lesional skin from psoriatic (A) and lichenoid (B) patients with n=3 (Psoriasis) and n=5 (Lichen). UMAP=Uniform Manifold Approximation and Projection, LE cells= lupus erythematosus cells.

3.3.3. CEBPB protein expression validation in CISD patients

To validate CEBPB expression on protein level, I performed immunohistochemistry in skin biopsies of LE/LP (n=5), AD (n=5) and Psoriasis (n=5) comparing them to non-lesional skin (n=5) (Figure 13). In line with our spatial transcriptomics results, in the non-lesional (NL) skin, CEBPB was detected only at low levels (10.4 ± 5.0 cells per 10x field) confined to the upper epidermal layers. In contrast, CEBPB expression was significantly higher in the lesional skin of all three diseases ($p<0.0001$) with highest

levels in Psoriasis (77.3 ± 14.6 cells/10x field), followed by LE/LP (31.1 ± 9.6 cells/10x field) and AD (24.8 ± 7.9 cells/10x field) (Figure 13 A, B). In the latter, CEBPB expression was mostly found in the upper layers similar to the NL skin, whereas in LE/LP and Pso CEBPB showed strong expression in both basal and upper layers of the epidermis, implying an additional function of CEBPB in the basal keratinocytes under these disease conditions. Moreover, in line with the scRNA Seq findings, the immune infiltrate in LE/LP and Psoriasis also comprised CEBPB positive cells (Figure 13 A).

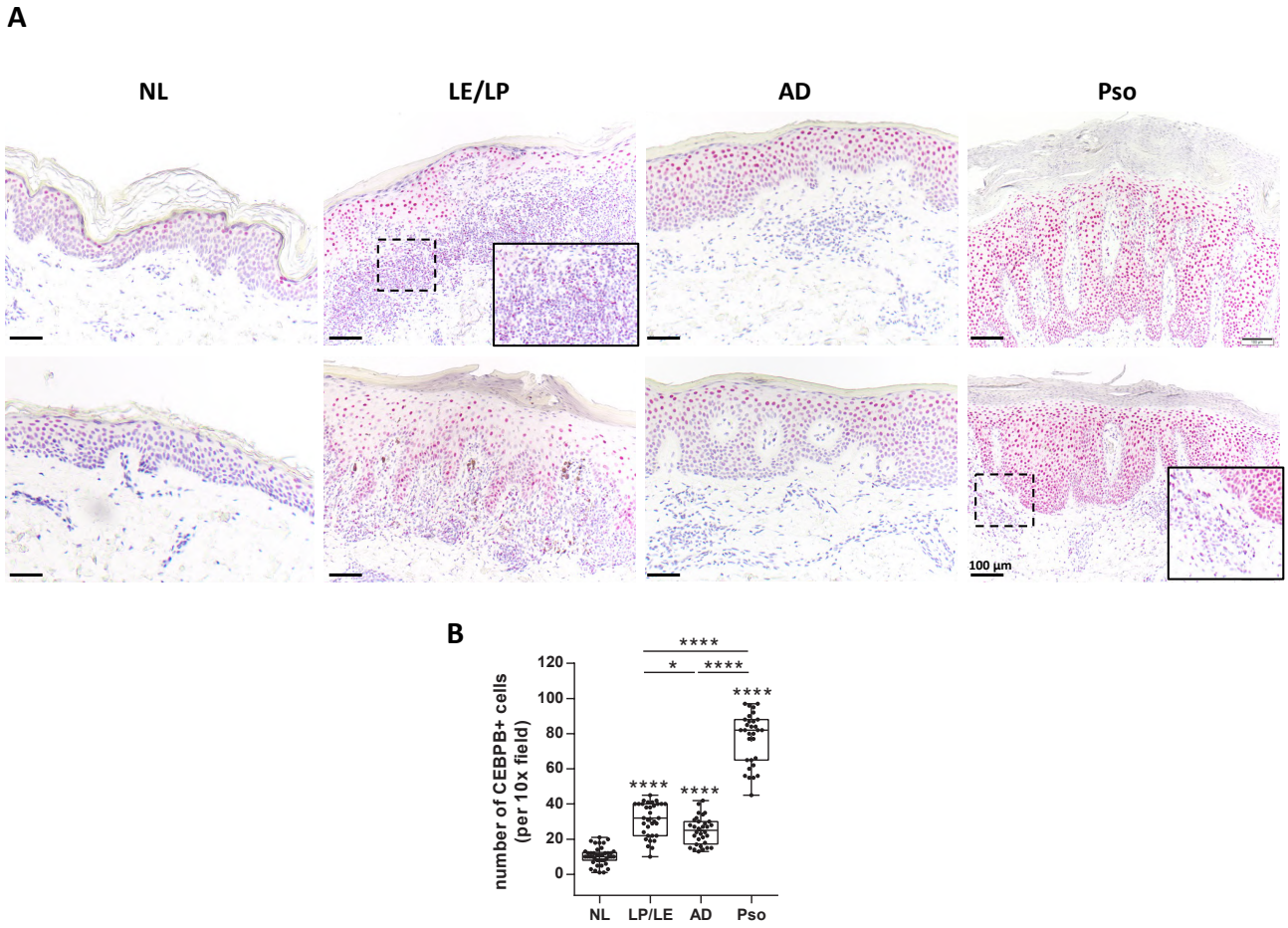

Figure 13: Analysis of CEBPB protein expression in CISD patients via Immunohistochemistry revealing upregulation of CEBPB in psoriatic and lichenoid skin. A) Representative immunohistochemistry (IHC) stainings of CEBPB in NL (n=5), LE/LP (n=5), AD (n=5) and Psoriasis (n=5) patients. Scale bar indicates 100 µm. Zoom-in boxes display the immune infiltrate. **B)** Quantification of the number of CEBPB positive cells per 10x field from IHC staining analysis in (A) (number of quantified fields: NL=41, LE/LP=32, AD=32, Pso=31). Comparison to non-lesional was performed using unpaired t-test with Welch's correction. Comparison of disease groups was performed using Ordinary one-way ANOVA test with Tukey's multiple comparison. *p<0.05, **p<0.01, ****p<0.0001. L = lesional, NL = non-lesional, LE/LP=Lupus erythematosus/ Lichen planus, AD = Atopic Dermatitis, Pso = Psoriasis.

Altogether, these data demonstrate via different transcriptomics methods, as well as protein analysis, the significant upregulation of CEBPB expression in the epidermis of CISD patients compared to the non-lesional skin, showing highest CEBPB induction in Psoriasis followed by Lichen.

3.4. Expression and regulation of CEBPB *in vitro* in primary human keratinocytes

3.4.1. Type 1 and type 3-specific cytokines are capable of inducing CEBPB in 2D keratinocytes

Given the prominent expression of CEBPB in the epidermis, I next aimed to validate these patient findings in an *in vitro* system and check for the regulation of CEBPB under different immunogenic conditions.

For this, 2D primary human keratinocytes were stimulated with various recombinant cytokines to mimic the described immune patterns found in CISDs. *CEBPB* was upregulated with type 1- (IFN-γ+TNF-α), type 2- (IL-4+IL-13) and type 3-related (IL-17A, IL-17A+TNF-α) stimuli compared to the unstimulated (US) control (Figure 14 A). Whereas IFN-γ alone did not evoke a significant upregulation of *CEBPB,* TNF-α and IL-17A alone were sufficient to induce CEBPB expression significantly (fold change (FC) to US: 1.52 ± 0.19, p=0.0137 and 1.42 ± 0.19, p=0.0369). The combination of IL-17A+TNF-α, however, synergistically evoked the strongest induction of *CEBPB* (FC: 2.51 ± 0.32, p=0.0006 to US), which was followed by the combination of IFN-γ+TNF-α (1.82 ± 0.54, p=0.004 to US) and IL-4+IL-13 (1.63 ± 0.18, p=0.0034 to US). Besides these main cytokines, other cytokines were also tested, showing no significant induction of *CEBPB* for TGF-ß and IL-6, whereas a significant moderate induction was observed with IL-1ß (1.6 ± 0.3, p=0.0275 to US) (Figure 14 B). In order to validate these findings on protein level and to visualize the different CEBPB isoforms, Western blot analysis on 2D primary keratinocytes stimulated with different cytokine combinations was performed using different donors and time points (48h, 72h). Figure 14 C shows a representative Western blot with all stimuli included. The LAP isoforms (LAP* + LAP) were differentially regulated under the distinct immune stimuli, with IFN-γ, TGF-ß and IL-6 having inhibitory effects, and TNF-α, IL-17A and IL-1ß with stimulatory effects at the tested time point (48h). Moreover, the strongest induction of the LAPs was obtained with the IL-17A+TNF-α condition. Interestingly, IL-17A increased the LAP* isoform specifically. The LIP isoform, however, showed only weak expression at that time point for most stimuli except IL-1ß.

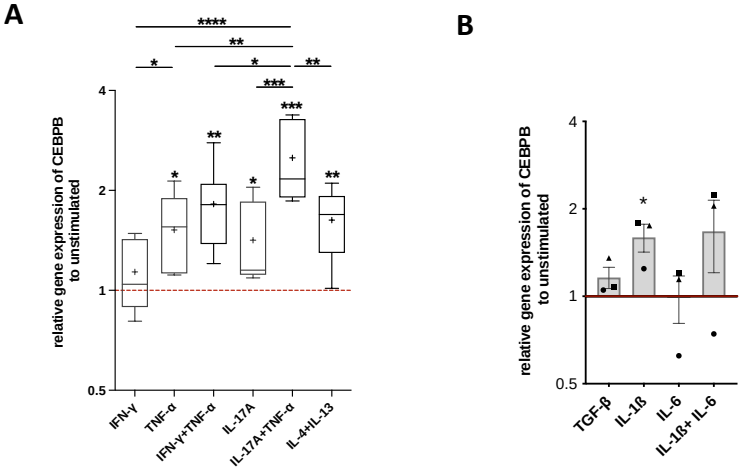

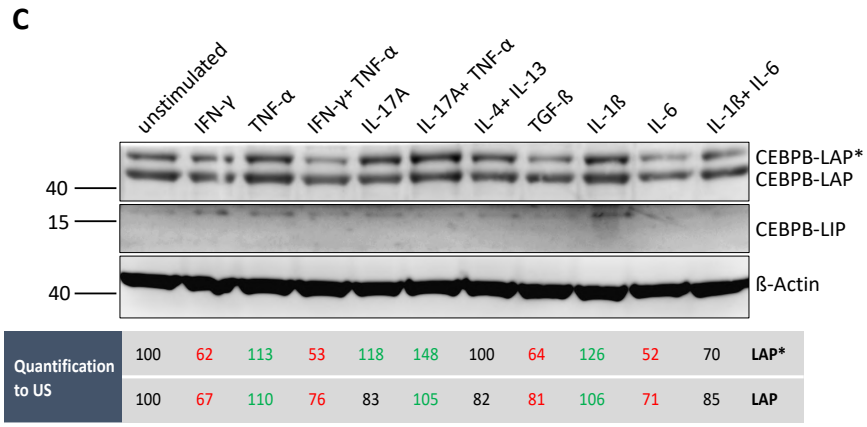

Figure 14: CEBPB is induced by various inflammatory cytokines and most abundantly upregulated by type 3 stimuli. A) and **B)** Relative gene expression of CEBPB in primary human keratinocytes upon o/n stimulation with depicted cytokines representing type 1, type 2 and type 3 inflammatory conditions compared to unstimulated measured by qRT-PCR with n=5-6 (A) and n=3 (B). **B)** Symbols represent different keratinocyte donors. **C)** Western blot analysis of CEBPB expression under different immune stimuli after 48h stimulation. Quantification of the LAP isoforms relative to the unstimulated condition. Comparison to unstimulated sample was performed using unpaired, two-tailed t-test. Comparison within stimuli groups was performed using uncorrected One way ANOVA Fisher's LSD test. *p<0.05, **p<0.01, ***p<0.001, ****p<0.0001.

Next, to understand how CEBPB responds to immunogenic stimuli over time, I performed kinetics experiments focusing on the main cytokine combinations IFN-γ+TNF-α, IL-17A+TNF-α and IL-14+IL-13, revealing that the short isoform LIP is specifically induced by IL-17A+TNF-α only at early time-points (3h, 6h), while the regulation of the LAP isoforms peaks rather at later time-points (24h, 48h) (Figure 15). Here, LAP* was more regulated than LAP, which seemed to be more constitutively expressed. Noteworthy was also that the induction by IFN-γ was delayed and not sustained over time.

Taken together, the RNA and protein data showed compatible results especially for the regulation of CEBPB by the Th17-related stimuli.

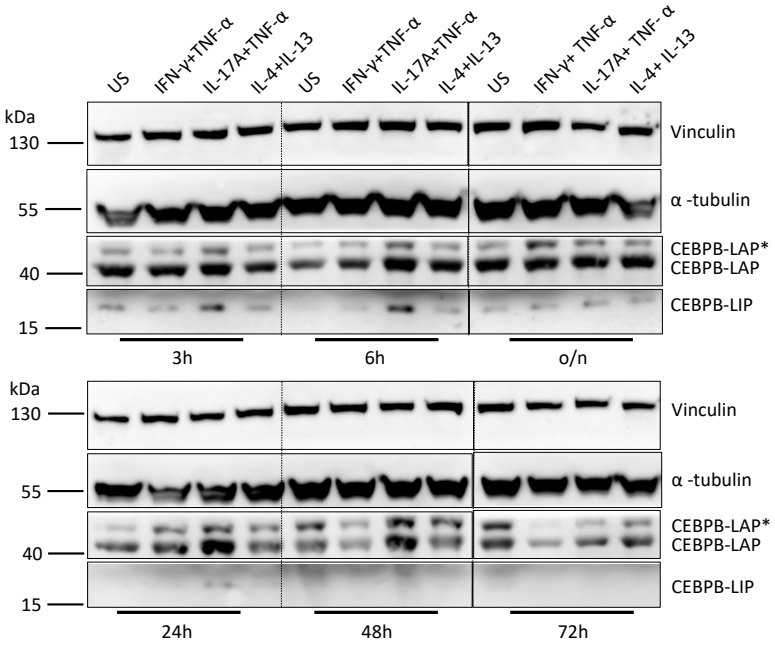

Figure 15: Kinetics of CEBPB expression and differential regulation of the isoforms LAP*, LAP and LIP by type 1, 2 and 3 immunogenic stimuli. Western Blot analysis of CEBPB protein (isoforms LAP*, LAP and LIP) expression in 2D keratinocytes over time after 3, 6, o/n, 24, 48 and 72 h stimulation with the main stimuli for type 1 (IFN-γ+TNF-α), type 2 (IL-4+IL-13) and type 3 (IL-17A+TNF-α). US= unstimulated, o/n= overnight.

3.4.2. Lichenoid and psoriatic microenvironments are capable of inducing CEBPB in 3D keratinocyte skin models

Given that mouse models are not able to fully recapitulate the inflammatory processes in human skin in all its complexity, *in vitro* human skin organoid models or so-called 3D models are a prerequisite in skin research. To get insights on CEBPB regulation at a more physiological level, I therefore aimed next to employ 3D keratinocyte skin models. For this, I first tested different stimulation conditions using both recombinant cytokines, which were titrated to find the optimal concentrations, as well as lesional T-cell supernatant (TCS) mixes derived from skin biopsies of patients suffering from LE/LP, AD or Pso (Figure 16, 17).

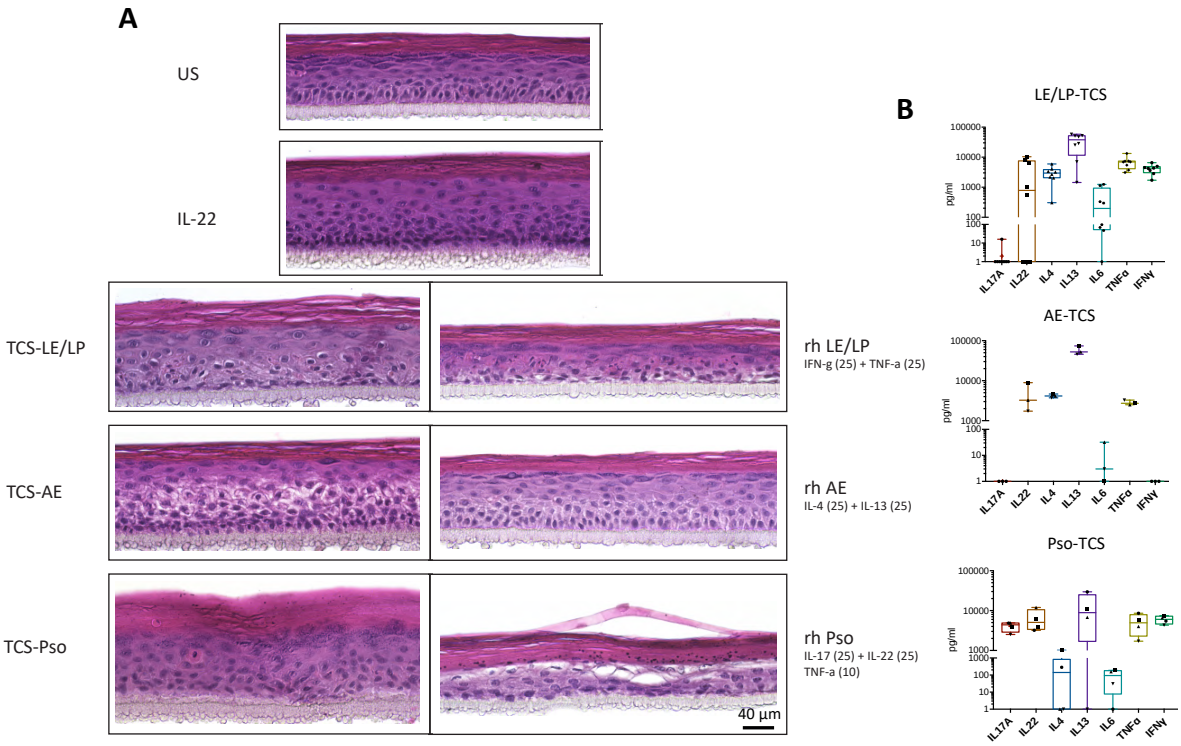

Figure 16: 3D skin models with different stimulations as disease models for LE/LP, AD and Pso. A) H&E staining of 3D keratinocyte models left unstimulated (US), stimulated with IL-22 or stimulated with rh cytokine mixes (concentrations in ng indicated in brackets) in comparison to lesional T-cell supernatants (TCS) derived from LE/LP, AD or Pso patients. Stimulation was performed for 72h. Scale bar= 40 µm. rh= recombinant human. **B)** Cytokine profiles generated by ELISA of the single TCS from LE/LP (n=8), AD (n=3) and Pso (n=4) patients, which were pooled generating the final LE/LP-TCS, AD-TCS and Pso-TCS mixes, respectively, and used throughout the project for stimulations.

Stimulation with IL-22 efficiently induced acanthosis, while stimulation with TCS induced disease-characteristic histological changes like vacuolization of keratinocytes with LE/LP, spongiosis with AD and acanthosis with hyperkeratosis with Pso (Figure 16A). These histological changes were more pronounced with the TCS stimulation than with the rh cytokine mixes for all three disease patterns. Although with the rhLE/LP and rhAD conditions slightly vacuolarized keratinocytes and spongiosis were detected respectively, the rhPso (IL-17A/25 ng + IL-22/25 ng+ TNF-α/10 ng) condition resulted mainly in cell death at this concentration (Figure 16 A). Figure 16 B displays the cytokine profiles of the TCS mixes used for stimulation of all 3D models in this project.

Since stimulation with the described rhPso condition was sub-optimal, we next performed titration experiments to test different concentrations and combinations that could best mimic psoriatic histological features without leading to the observed marked cell death. Characterization of these models revealed the following conditions as most optimal for use in further experiments: IL-22 (50 ng), IL-17A (both 25 ng and 50 ng) and IL-17A (5 ng) + IL-22 (50 ng) (Figure 17).

To sum up, for experiments in this project, 3D models were stimulated mainly with the patients derived TCS mixes, since these displayed the best histological results and represented the most physiological disease models.

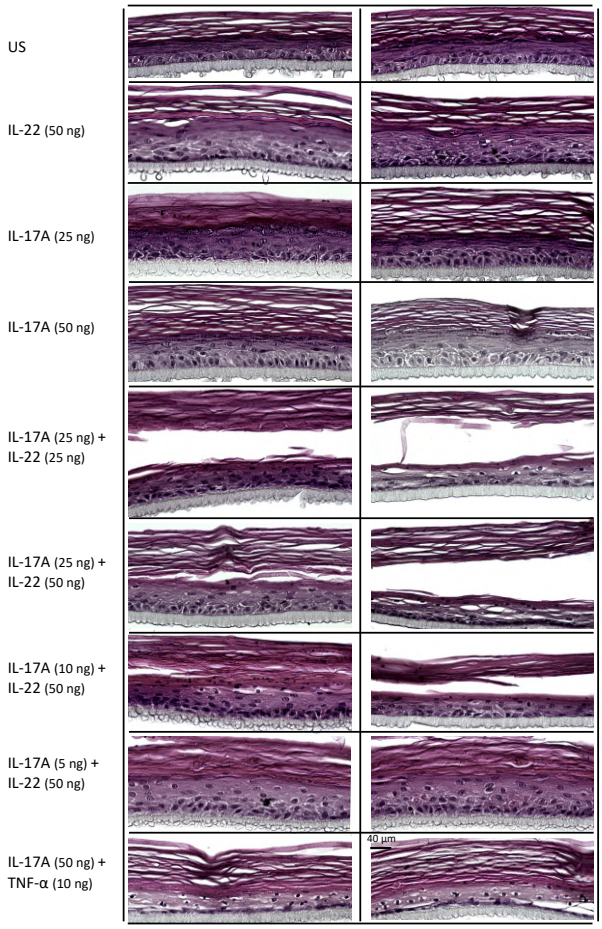

Figure 17: 3D keratinocyte models to test different rh cytokine conditions for Psoriasis. H&E staining of 3D keratinocyte models left unstimulated (US) as control, stimulated with IL-22 or stimulated with different rh cytokine titrations for IL-17A, TNF-α and IL-22. Stimulation was performed for 72h. Two representative images are shown per condition. Scale bar= 40µm. US= unstimulated.

Next, using 3D keratinocyte skin models stimulated with patients derived lesional T-cell supernatants (TCS) as previously described, as well as with IL-22 for acanthosis induction, I detected a significant induction of CEBPB gene expression by the Pso-TCS (FC: 2.07 ± 0.32, p=0.0031). Both IL-22 (FC: 1.79 ± 0.35, p=0.0227) and LE/LP-TCS (FC: 2.01 ± 0.82, p=0.0116) also lead to significant, yet slightly weaker upregulation of CEBPB, whereas stimulation with the AD-TCS showed only a trend towards upregulation with no significant induction of CEBPB (FC: 1.65 ± 0.37, p=0.0580) (Figure 18 A). To validate this on protein level, Western blot analysis was performed on 3D models stimulated for 24h (B) or 48h (C) with either rh cytokine cocktails or lesional TCS (Figure 18 B, C). 24h stimulation was not sufficient to observe significant regulation of the longer LAP isoforms, whereas upregulation of LIP could be observed mainly for the IL-17A+TNF-α stimulus, similar to the 2D findings, followed by IL-17A alone and IL-17A+IL-22 (Figure 18 B). Interestingly, pSTAT3 and thus active STAT3 signaling was most

strongly induced by IL-22 alone and IL-17A+IL-22 in 3D keratinocytes. Noteworthy, CEBPB induction via lesional TCS could be observed only after 48h (Figure 18 C), but not after 24h stimulation as with the rh cytokines (Figure 18 B). Here, strongest induction of all three CEBPB isoforms was observed for the LE/LP-TCS, followed by Pso-TCS, which interestingly mainly induced the LAP* and LIP, and the AD-TCS leading to a moderate upregulation of all three isoforms as well. In contrast to the short stimulation (24h), IL-22 alone lead to a clear LIP induction after 48h stimulation (Figure 18 C). Similarly, in IHC, 3D models stimulated with LE/LP-TCS, Pso-TCS and IL-22 showed a stronger staining for CEBPB with more CEBPB+ cells in basal and upper layers compared to unstimulated (US) models (Figure 18 D). In line with the CEBPB expression results, the AD-TCS model yielded the weakest CEBPB staining among the disease models. Hematoxylin and eosin staining was used to visualize the key characteristic histological features in these models, as previously described.

Thus, taken together, we could recapitulate the patients findings in our 2D and 3D *in vitro* systems confirming once more the upregulation of CEBPB under various immune conditions, with strongest upregulation under Psoriasis-specific stimuli.

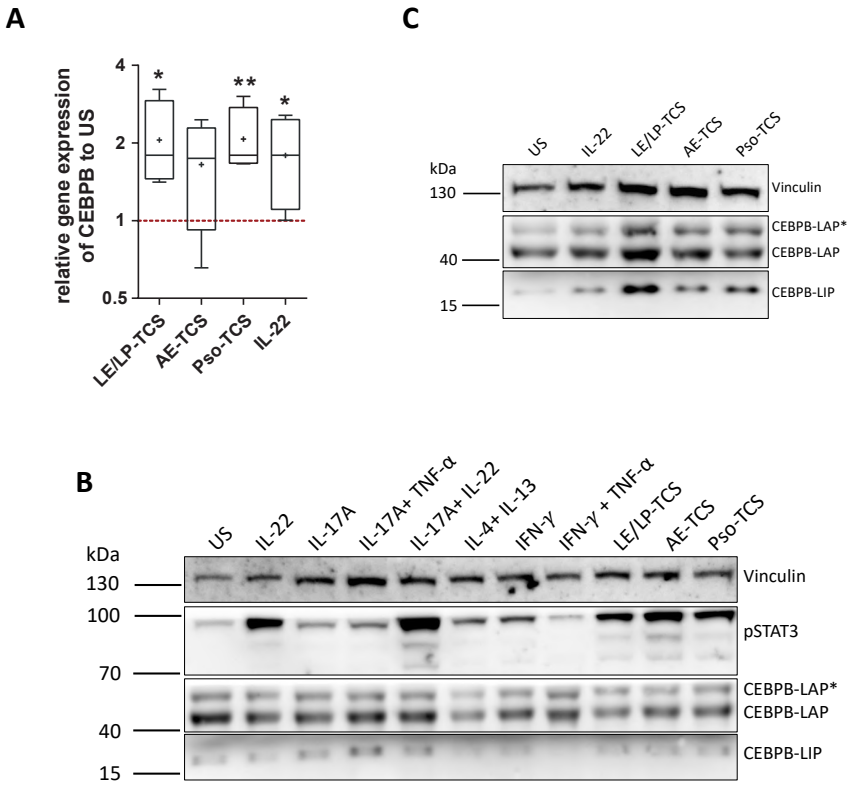

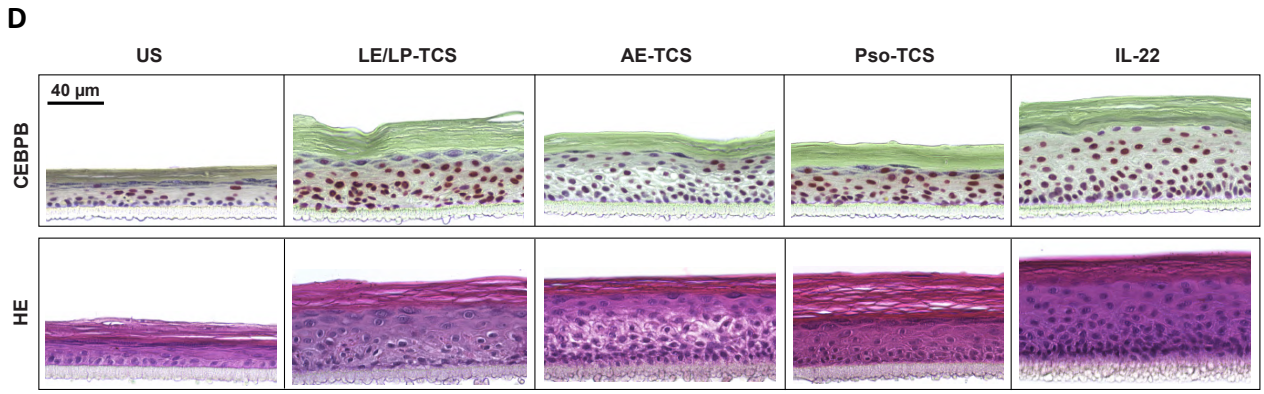

Figure 18: CEBPB is abundantly upregulated under a psoriatic microenvironment in 3D keratinocyte skin models. A) CEBPB relative gene expression in 3D keratinocytes after 24h stimulation with either indicated lesional T-cell supernatants (TCS) from LE/LP, AD and Pso or IL-22 compared to unstimulated measured by qRT-PCR (n=4). **B)** and **C)** Western blot analysis of CEBPB protein levels and isoform expression in 3D models with the depicted stimulations TCS and rh cytokine stimulations for 24h (B) or 48h (C). **D)** IHC staining of total CEBPB protein after 72h stimulation, as well as H&E stainings for visualizing histological characteristics of the stimulated 3D models. Scale bar indicates 40 µm. Comparison to unstimulated sample was performed using unpaired t-test. *p<0.05, **p<0.01. US = unstimulated TCS = T-cell supernatant, H&E = hematoxylin and eosin.

3.5. Generation of a global keratinocyte-specific CEBPB target gene signature under different inflammatory conditions

In order to understand the function of CEBPB in the skin in depth, we next sought to establish a global keratinocyte-specific transcriptional landscape for CEBPB under different immunogenic conditions thereby mimicking the different disease patterns in skin inflammation. For this, I knocked out *CEBPB* in primary human keratinocytes using CRISPR/Cas9, then generating 2D (n=4) and 3D keratinocyte models (n=4) that were either left untreated as a "healthy" control (unstimulated, US) or stimulated with type 1 (IFN-γ+TNF-α (2D/3D), LE/LP-TCS (3D), type 2 (IL-4+IL-13 (2D/3D), AD-TCS (3D)) and type 3 (IL-17A+TNF-α (2D/3D), Pso-TCS and IL-22 (3D)) specific conditions (Figure 19 A). All conditions, except the 3D models stimulated with rh cytokines, were then subjected to bulk RNA seqencing. Additionally, SN was collected from all conditions and WB lysates were generated. The knockout (KO) efficiency was confirmed by Western blot analysis and quantified to be in the range of 80-90 % compared to wild-type keratinocytes (noRNP = pulsed control cells without RNP) (Figure 19 B, C).

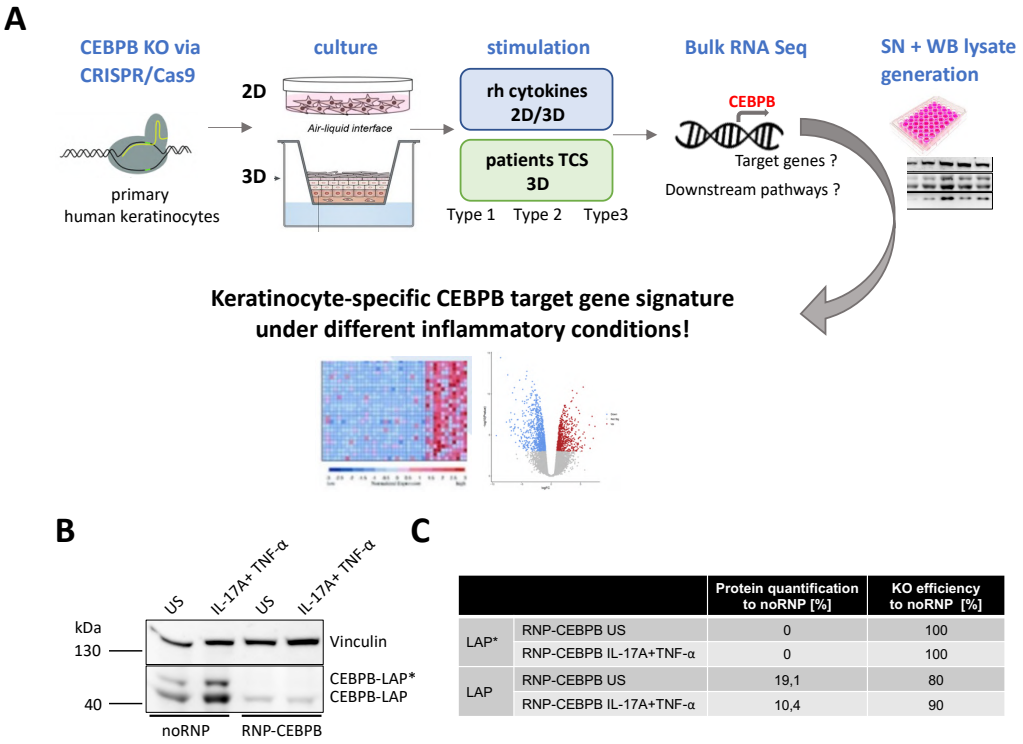

C

		Protein quantification to noRNP [%]	KO efficiency to noRNP [%]
LAP*	RNP-CEBPB US	0	100
	RNP-CEBPB IL-17A+TNF-α	0	100
LAP	RNP-CEBPB US	19,1	80
	RNP-CEBPB IL-17A+TNF-α	10,4	90

Figure 19: Generation of CEBPB-KO keratinocytes disease models for the establishment of a global CEBPB target gene signature under different inflammatory conditions. A) Workflow overview for the generation of a CEBPB target gene signature in skin inflammation: first, CEBPB is knocked-out via CRISPR/Cas9 in primary human keratinocytes, which are then cultured as 2D or 3D models and stimulated for 24h with either rh cytokines or patients derived TCS to mimic type 1, type 2 and type 3 inflammatory conditions. These models are then subjected to bulk RNA Sequencing and analyzed in comparison to the noRNP (only pulsed) control for differential gene expression. Additionally, supernatant (SN) and Western blot (WB) lysates are generated from parallel models stimulated for 48h. **B)** and **C)** CEBPB Knockout (KO) efficiency validation by Western blot analysis showing the longer CEBPB isoforms and their quantification percentages (C) compared to the noRNP control. KO= knockout, rh= recombinant human, TCS= T-cell supernatant, SN= supernatant, WB= Western blot, RNP= Ribonucleoprotein.

3.5.1. CEBPB-regulated transcriptome under type 3/psoriatic microenvironment reveals regulation of various key pathways of Psoriasis pathogenesis

Gene expression of the CEBPB-KO keratinocytes was profoundly altered in all conditions compared to the respective noRNP controls, especially under homeostasis (unstimulated) and type 3 stimulations, as seen from the Volcano plots depicting differentially expressed genes (DEGs, log2FC>=|1|, p<0.05) (Figure 20 A,C).

Starting with the 2D keratinocytes, different metabolic genes such as *ASS1* (FC= -2.3, p= 4,94E-05) and *ARG1* (FC= -6.03, p=0.023) and cytokines such as *IL36G* (FC=- 2.43, p=0,000564) and *IL33* (FC= -2.28, p=0.001) were found among the top differentially downregulated genes in the US condition. Under IL-17A+TNF-α stimulation *SERPINB3/4* (FC=-2.59, p=0.0012/FC= -2.88, p=0.0003), *VNN3* (FC=-2.23,

p=0.0024), a gene known to be upregulated by Th17-cytokines and associated with Psoriasis, and various disease-relevant AMPs like *SAA2/4* (FC= -4.54, p=0.0007) and *S100A7A* (FC=-2.28, p=0.011) and chemokines like *CXCL1* (FC= -1.44, p=0.036) and *CXCL8* (FC= -1.19, p=0.0064) were among the top functionally-relevant suppressed genes in the CEBPB-KO (Figure 20 A). On the other hand, *MMP19, CCL2* and *EDN2* were among the top differentially upregulated genes.

In line with that, pathway analysis performed on these DEGs revealed suppression of various Pso-relevant pathways such as cytokine signaling pathways like 'TNF signaling' (US, IL-17A+TNF-α) and 'IL-17 signaling' (IL-17A+TNF-α) (Figure 20 B). Further features of type 3 pathology are an increased infiltration of immune cells, such as neutrophils into the skin, and overproduction of AMPs. In this context, 'neutrophil degranulation' and 'antimicrobial peptides' were two other disease-relevant pathways that were found to be significantly repressed in CEBPB-KO keratinocytes especially under IL-17A+TNF-α, but also under basal conditions (US) (Figure 20 B).

Comparable to 2D, various AMPs like *S100A8, S100A7* and *S100A7A* were found among the top DEGs to be suppressed in the CEBPB-KO under steady-state (Figure 20 C). However, in contrast to 2D, among the DEGs of 3D keratinocytes various genes involved in keratinization and ECM organization were overrepresented and strongly dysregulated in the CEBPB-KO compared to wild-type keratinocytes. For instance, different keratins like *KRT17* (FC= -4.00, p=9,54E-07), *KRT6A/B* (FC= -2.86, p=0.0056/ FC= -3.41, p=0.0009) and *KRT5* (FC= -2.03, p=0.0022) were detected as top downregulated DEGs under steady-state (Figure 20 C). Moreover, under Pso-TCS stimulation, multiple proliferation genes (e.g. *PRC1, TTK, CDC20, KIF2C* and *TK1*) were represented among the top downregulated DEGs. *ARG1* and *SERPINB3*, two genes that have been associated with Psoriasis, were also strongly downregulated in the CEBPB-KO Pso-TCS stimulated 3D models. Interestingly, on the other hand, various type 2-relevant genes such as *PTGDS, CCL27*, *IL37* and *EDN1* were found among the top upregulated DEGs in the CEBPB-KO models under both unstimulated and Pso-TCS conditions (Figure 20 C), implying a potential shift towards a type 2 phenotype upon loss of CEBPB under these conditions. Similarly, various classical interferon-response genes (e.g. *IFIT1, IFITM3* and *OAS1*) were found among the top upregulated DEGs specifically under Pso-TCS stimulation. Among the top suppressed genes under IL-22, was the neutrophil chemoattractant *IL-19* (FC= -7.76, p=0.0001), the pro-proliferative and anti-apoptotic *SERPINB1*, as well as various MMPs and ECM genes (e.g. *MMP12, MMP19, CEACAM6*) (Figure 20 C). Top upregulated genes here included the RAS oncogene family member *RAB43*, leptin *LEP* and the epidermal growth factor *EREG*, known to be involved in wound healing and tissue repair. Indeed, pathway analysis revealed concomitant results showing significant suppression of 'cell cycle, mitotic' and 'keratinocyte proliferation' pathways in both unstimulated (US) and Pso-TCS stimulated

3D CEBPB-KO skin models (Figure 20 D). Noteworthy, was also the significant suppression of 'neutrophil degranulation' (US, IL-22) and 'IL-17 signaling' (US, IL-22), similar to 2D findings, as well as of 'Cellular response to hypoxia' and 'Cellular senescence' under basal and Pso-TCS conditions, respectively. In contrast, 'IL-10 signaling' was upregulated in CEBPB-KO keratinocytes under psoriatic microenvironment in both 2D (IL-17A+TNF-α) and 3D (Pso-TCS) disease models (Figure 20 B, D), indicating a potential shift towards immunosuppressive cytokine signaling upon loss of CEBPB. In line with the observed upregulation of various type 1/2 genes, 'IL-4 and IL-13 signaling' and 'IFN-α/β/γ signaling' pathways were positively enriched under US and Pso-TCS conditions (Figure 20 D). Interestingly, ECM organization was the most strongly positively enriched pathway under both US and Pso-TCS.

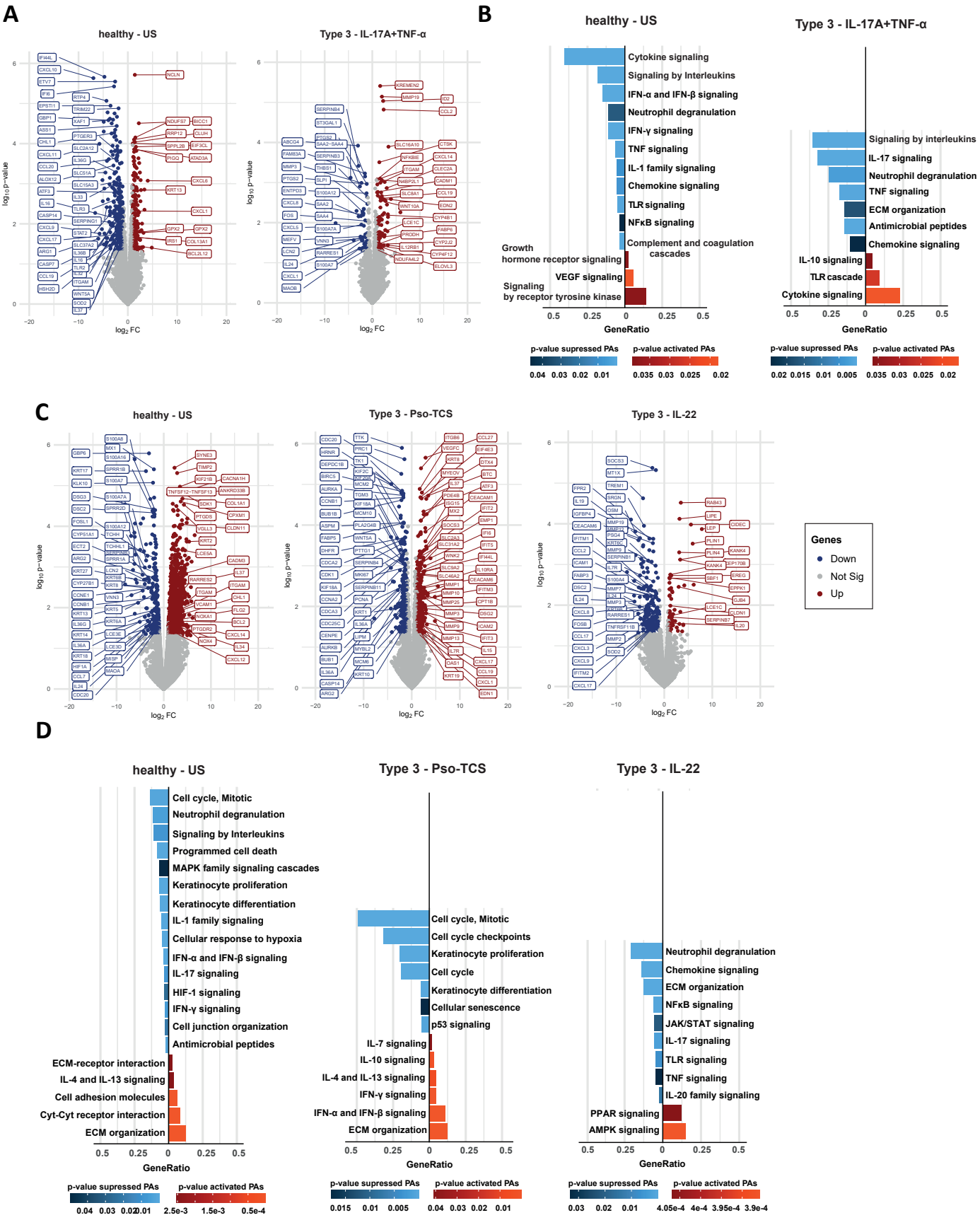

Figure 20: CEBPB regulates key pathways of Psoriasis pathogenesis. A) and **C)** Volcano plots of differentially expressed genes (DEGs) (log2FC >=|1|, p<0.05) in the CEBPB-KO compared to the noRNP control for 2D keratinocytes (n=3-4) (A) and 3D (C) skin models (n=3-4) under type 3 conditions (IL-

17A+TNF-α, Pso-TCS, IL-22) in comparison to unstimulated (US). Highlighted are top differentially regulated genes, as well as other interesting disease-relevant genes that were significantly dysregulated in the CEBPB-KO condition, with red= upregulated, blue= downregulated and grey=not significant. **B)** and **D)** Overrepresentation analysis (ORA) of calculated DEGs shown under (A& C) under healthy (US) and type 3 conditions was performed for 2D (B) and 3D (D) keratinocytes. Displayed are top significantly enriched pathways (PA), as well as further selected functionally-relevant pathways with $p < 0.05$ and the respective gene ratios indicating the percentages of total DEGs in the given PA. US = unstimulated, TCS = T-cell supernatant, FC= fold-change, PA = pathway, DEGs = differentially expressed genes, ORA= overrepresentation analysis.

3.5.2. CEBPB-regulated transcriptome under type 2/eczematous microenvironment

In contrast, most of the downregulated type 3 pathways were upregulated in the CEBPB-KO under type 2 stimulation (Figure 21), implying stimulus-dependent regulatory effects of CEBPB. For instance, AMP genes and their respective pathway were upregulated in both 2D (IL-4+IL-13) and 3D (AD-TCS) conditions. Similarly, various IFN-response genes like *IFNK, IDO1, CXCL9/10/11* and the 'interferon signaling' pathway were found to be upregulated in 2D AD models (Figure 21 A, B), implying a shift towards a type 1 phenotype upon loss of CEBPB under an AD-type microenvironment. Interestingly, in 3D AD-TCS stimulated models, 'keratinocytes differentiation' was downregulated, while 'keratinocytes proliferation' was found to be upregulated on the contrary to Pso (Figure 21 D). All in all, the number of pathways significantly dysregulated upon loss of CEBPB under type 2 stimulation was markedly lower compared to type 3 conditions, further highlighting that CEBPB is likely playing a central role in Psoriasis rather than AD pathogensis.

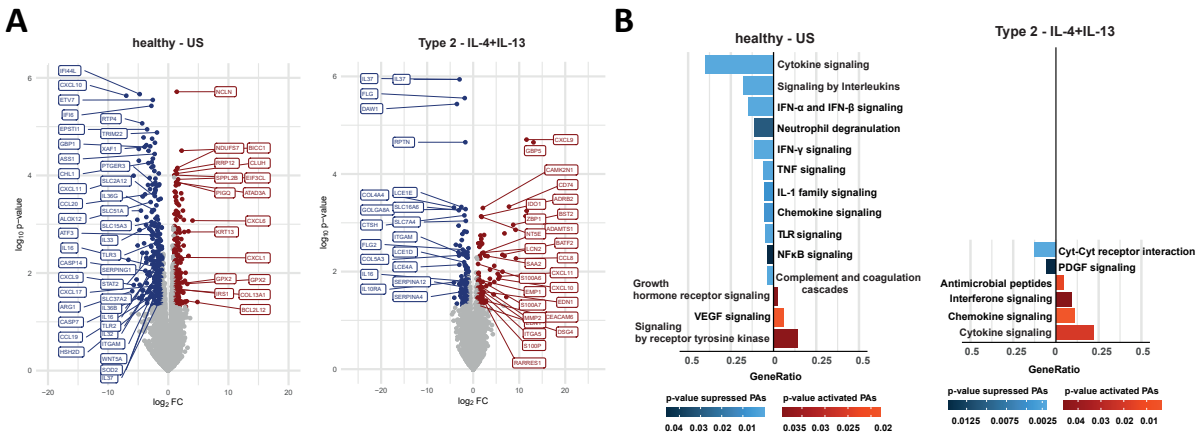

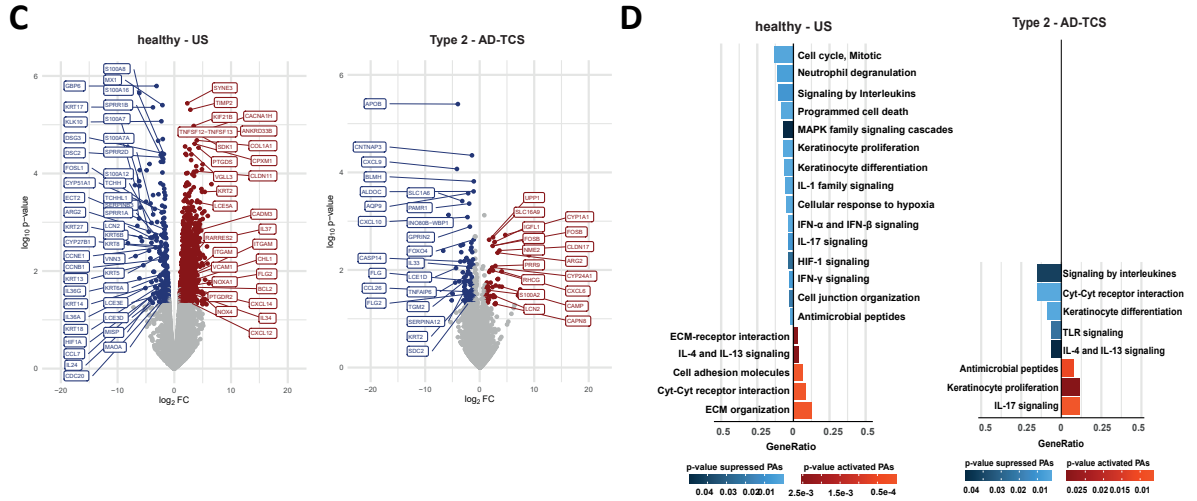

Figure 21: CEBPB-regulated genes and pathways under AD conditions. A) and **C)** Volcano plots of differentially expressed genes (DEGs) ((log2FC >=|1|, p<0.05) in the CEBPB-KO compared to the noRNP control for 2D keratinocytes (n=3-4) (A) and 3D (C) skin models (n=3-4) under type 2 conditions (IL-4+IL-13, AD-TCS) in comparison to unstimulated (US). Highlighted are top differentially regulated genes, as well as other potentially interesting genes that were significantly dysregulated in the CEBPB-KO condition, with red= upregulated, blue= downregulated and grey=not significant. **B)** and **D)** Overrepresentation analysis (ORA) of calculated DEGs shown under (A& C) under healthy (US) and type 2 conditions for 2D (B) and 3D (D) keratinocytes. Displayed are top significantly enriched pathways (PA), as well as further selected functionally-relevant pathways with p < 0.05 and the respective Gene ratios indicating the percentages of total DEGs in the given PA. US = unstimulated, TCS = T-cell supernatant, FC= fold-change, PA = pathway, DEGs = differentially expressed genes, ORA= overrepresentation analysis.

3.5.3. CEBPB-regulated transcriptome under type 1/lichenoid microenvironment reveals regulation of various key disease-relevant pathways for Lichen pathogenesis

Finally, under type 1 conditions, various disease-relevant functional gene groups were overrepresented among the DEGs and strongly dysregulated in the CEBPB-KO compared to wild-type keratinocytes. Indeed, classical IFN-γ response genes such as *IFITM2* (FC= -4.30, p=3E-08), *SERPING1* (FC= -3.17, p=0.001) and the antiviral defense genes *GBPs* (*GBP1, GBP2, GBP3 and GBP5*) were clearly enriched among the top significantly downregulated DEGs of 2D CEBPB-KO keratinocytes under IFN-γ+TNF-α stimulation (Figure 22 A). Additionally, various type 1-relevant chemokines and inflammatory cytokines like *CXCL9, CXCL10, CXCL11 and IL16* were detected among the top downregulated DEGs (Figure 22 A). However, CEBPB-KO upregulated genes under this stimulus were not as abundant, indicating that CEBPB is likely a positive regulator rather than a repressor of gene expression under type 1 inflammation. Nevertheless, one example of a significantly upregulated gene was the AD-associated gene *TSLP* (FC= 2.30, p=0.024).

The CEBPB target gene signature from 3D LE/LP-TCS stimulated keratinocytes showed similar results with multiple IFN-γ response genes such as *ICAM1* (FC= -1.37, p=3,48E-05), *CXCL9* (FC= -3.57, p=0.0002) and *IFITM1* (FC=-1.23, p=0.0004) among the top significantly downregulated DEGs (Figure 22 C). Moreover, various TNF superfamily members *TNFSF* genes (e.g. *TNFSF13B, TNFSF13, TNFSF11*), as well as the Toll-like receptor genes *TLR1* and *TLR2* were detected as top downregulated genes in the CEBPB-KO compared to the noRNP control. Interestingly, transcription factors such as *FOSB, JUNB, FOS* and *ATF3* were also among the top significantly downregulated DEGs under LE/LP-TCS stimulation (Figure 22 C), implying a dysregulation of key transcriptional switches upon loss of CEBPB in those keratinocytes.

In line, pathway analysis on these DEGs was characterized by a negative enrichment of various Lichen-relevant pathways in the CEBPB-KO compared to the noRNP control under both 2D and 3D type 1-stimulations (Figure 22 B, D). For 2D keratinocytes, these downregulated pathways were dominated by 'Interferon signaling' with 'IFN-γ signaling', as well as 'IFN-α/ß signaling', but also 'TNF signaling', all significantly suppressed under both steady-state (US) and IFN-γ+TNF-α stimulation (Figure 22 B). 'IL-1 family signaling' and 'NFkB signaling', which are known to be involved in type 1 responses, were downregulated as well in the CEBPB-KO under basal conditions. For 3D skin models, besides 'signaling by receptor tyrosine kinases' and 'signaling by interleukins' as top suppressed pathways, other disease-relevant pathways like TLR signaling, JAK-STAT, TNF and NFkB signaling pathways were downregulated in the CEBPB-KO (Figure 22 D). Importantly, cell death-related pathways such as 'inflammasomes' and 'NOD-like receptor signaling', which is also involved in the inflammasome pathway and cellular response to stress, together with 'programed cell death' were found to be suppressed in the CEBPB-KO keratinocytes under both steady-state (US) and type 1 conditions (Figure 22 B, D).

In summary, these results provide a global keratinocyte-specific signature of genes regulated by CEBPB under both homeostatic and different inflammatory conditions and reveal a previously unappreciated role for CEBPB as a master transcription factor in keratinocytes.

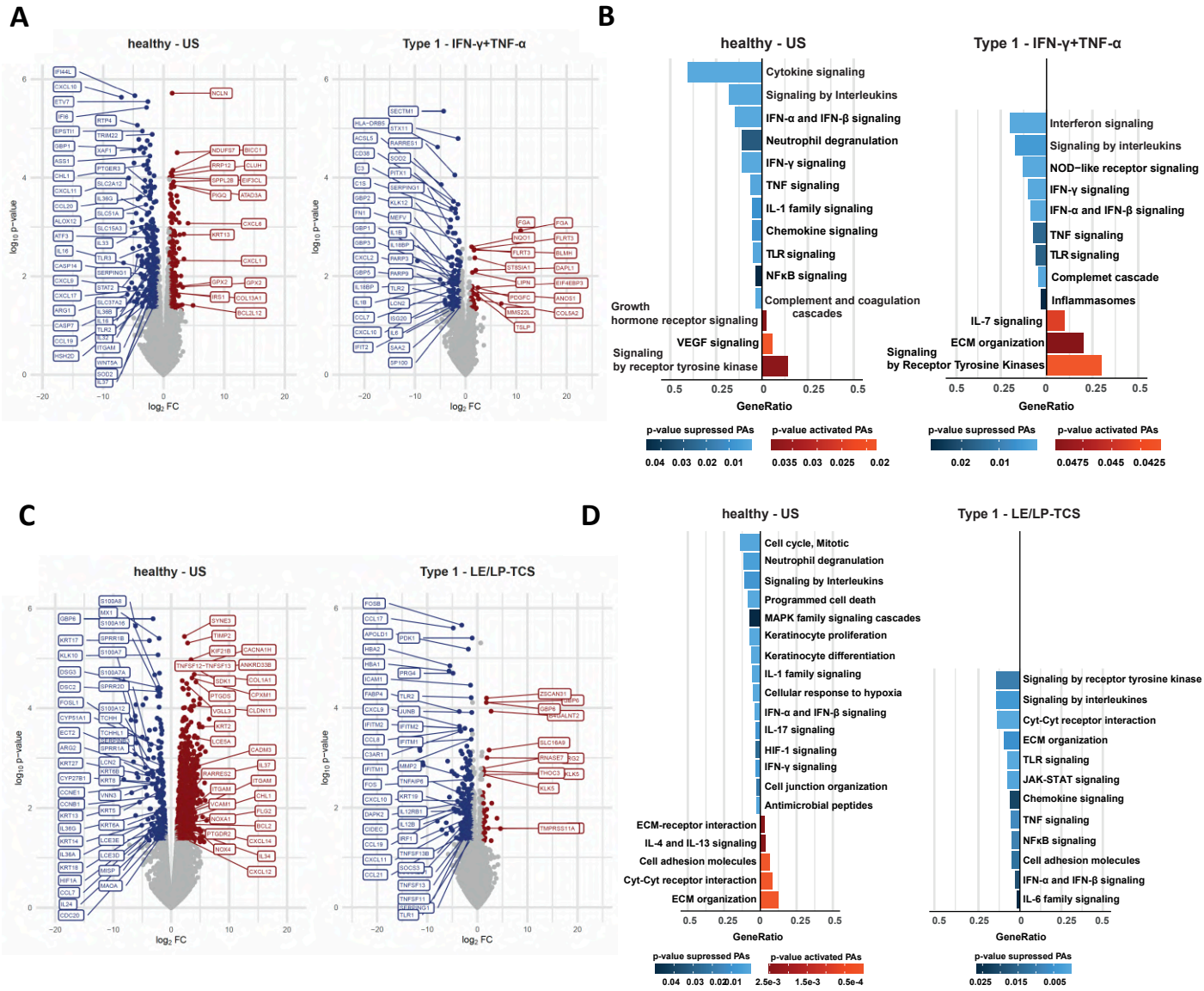

Figure 22: CEBPB regulates key disease-relevant pathways under lichenoid inflammatory conditions. **A)** and **C)** Volcano plots of differentially expressed genes (DEGs) (log2FC >=|1|, p<0.05) in the CEBPB-KO compared to the noRNP control for 2D keratinocytes (n=3-4) (A) and 3D (C) skin models (n=3-4) under type 1 conditions (IFN-γ+TNF-α, LE/LP-TCS) in comparison to unstimulated (US). Highlighted are top differentially regulated genes, as well as other potentially interesting disease-relevant genes that were significantly dysregulated in the CEBPB-KO condition, with red= upregulated, blue= downregulated and grey=not significant. **B)** and **D)** Overrepresentation analysis (ORA) of calculated DEGs shown under (A& C) under healthy (US) and type 1 conditions for 2D (B) and 3D (D) keratinocytes. Displayed are top significantly enriched pathways (PA), as well as further selected functionally-relevant pathways with p < 0.05 and the respective Gene ratios indicating the percentages of total DEGs in the given PA. US = unstimulated, TCS = T-cell supernatant, FC= fold-change, PA = pathway, DEGs = differentially expressed genes, ORA= overrepresentation analysis.

3.6. Functional validation of CEBPB role in Psoriasis

3.6.1. CEBPB is a control point for keratinocytes inflammatory factors secretion and a driver of neutrophil migration

Considering the identified dysregulation of cytokine/ chemokine signaling upon loss of CEBPB and the importance of these pathways for disease pathology, I next investigated the functional role of CEBPB in regulating the inflammatory secretome of keratinocytes on both gene and protein level.

Firstly, on RNA level, CEBPB-KO keratinocytes stimulated with IL-17A+TNF-α showed a significant downregulation of various type 3-relevant factors such as the chemokines *CXCL1* (p=0.0362), *CXCL5* (p=0.0120), and *CXCL8* (p=0.0064), which are all known to be potent neutrophil chemoattractants, as well as the inflammatory cytokine *IL24* (p=0.0190), known to be an autocrine regulator of keratinocytes proliferation and inflammation in Psoriasis (Figure 23 A, C). Similarly, a significant downregulation of *IL24* and the neutrophil chemoattracts *CXCL3, CXCL8* and *IL19* was also observed under IL-22 stimulation, whereas with the Pso-TCS stimulation only *IL36A* as a type 3 factor was significantly reduced (Figure 23A). Also under basal levels, various type 3 (e.g. *IL36A/B/G*), but also type 1-relevant factors (e.g. *IL32, CXCL9/10/11*) were downregulated upon loss of CEBPB compared to the noRNP control (Figure 23A, C). Interestingly, in contrast, multiple type 2-related factors like *CCL2* (p<0.0001), *CCL19* (p=0.0025) and *CCL21* (p=0.0545) were found to be upregulated under type 3 conditions, implying CEBPB's action in skewing the inflammatory response towards type 3 and away from type 2 (Figure 23 A, C). KO of CEBPB under an AD-specific microenvironment (IL-4+IL-13, but not with the AD-TCS) lead mainly to a strong upregulation of type 1-specific chemokines like *CXCL9*, *CXCL10* and *CXCL11*, indicating a potential shift towards a type 1 inflammatory phenotype (Figure 23 A). On the other hand, the expression of the immunosuppressive cytokine *IL37*, which is known to be upregulated in AD and downregulated in Pso, was found to be reduced in the type 2 conditions.

Antimicrobial peptides (AMPs) are one of the most important factors known to be dysregulated in skin inflammation. In this frame, knockout of CEBPB resulted in significant downregulation of key disease-related AMP genes (e.g. *S100A7/8/9* (p<0.0001), *SAA2* (p=0.0069), *SLPI* (p=0.0034), and *SERPINB3* (p=0.0013) under both basal (US), as well as the type 3 conditions (IL-17A+TNF-α and IL-22) (Figure 23 B, D), but interestingly not with the Pso-TCS, which showed only a trend towards downregulation (Figure 23 B, lower heatmap), but no significant effects (Figure 23 B, upper heatmap). Interestingly, on the other hand, most AMPs were upregulated in the CEBPB-KO under type 2 stimulation conditions (Figure 23B, D).

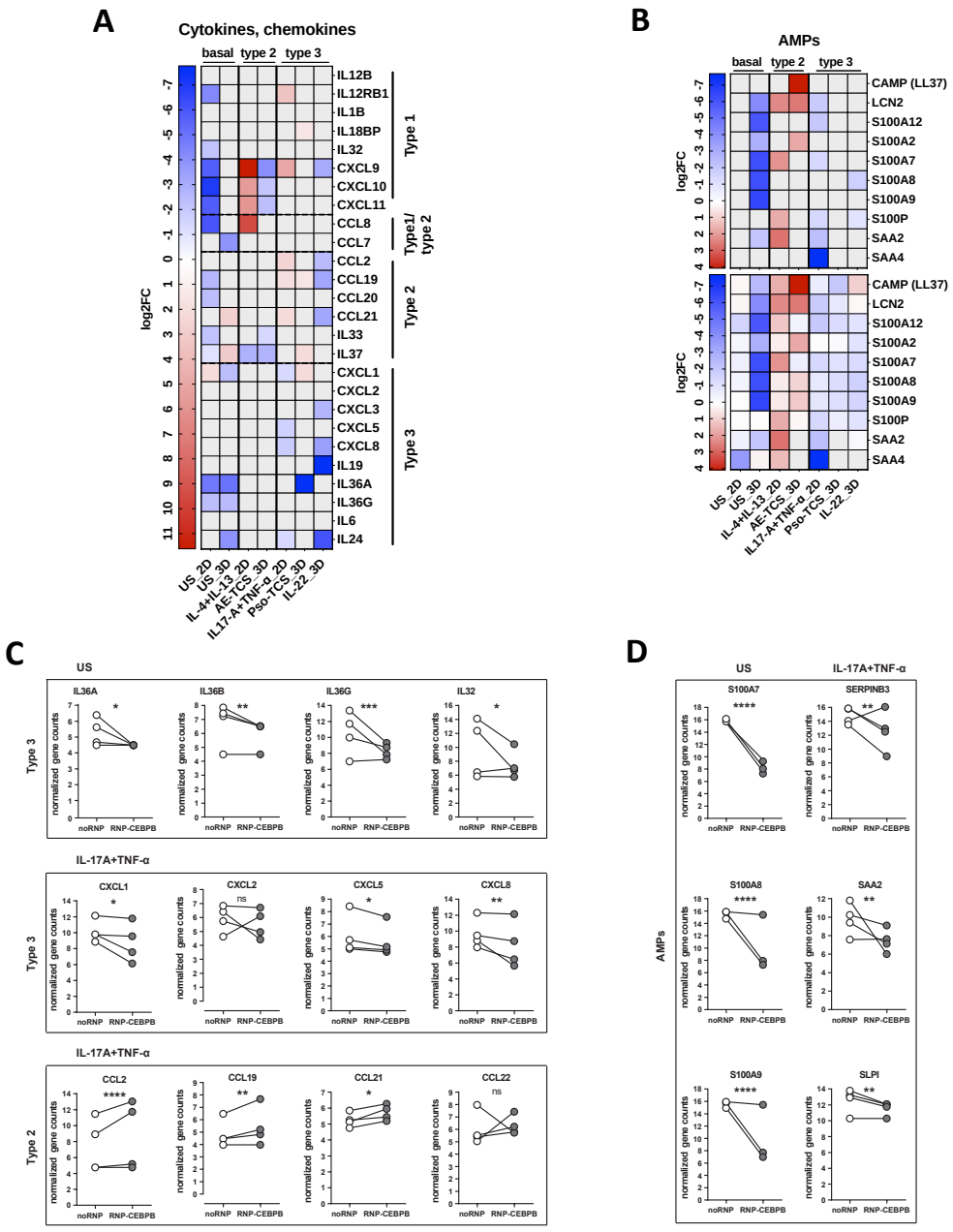

Figure 23: CEBPB is a key regulator of keratinocytes inflammatory secretome gene expression especially under psoriatic conditions. A) and **B)** Heatmaps of differentially expressed genes (DEGs) in the CEBPB-KO compared to the noRNP control for 2D and 3D keratinocytes under depicted type 2 or type 3 stimuli in comparison to unstimulated (US) basal conditions. DEGs were filtered for the functional groups of 'cytokines and chemokines' (A) and antimicrobial peptides 'AMPs' (B) displaying significantly dysregulated genes with red= upregulated, blue= downregulated, white= not regulated and grey=not significant. **B)** Upper heatmap shows only significantly regulated genes (p-value <=0.05), while the lower heatmaps includes all values to show potential yet not significant regulation trends for all stimuli. **C)** and **D)** Normalized gene counts of cytokines and chemokines (C) and AMPs (D) in the CEBPB-KO (RNP-CEBPB) and control (noRNP) 2D keratinocytes under homeostatic (unstimulated, US) and the type 3 condition IL-17A+TNF-α measured by bulk RNAseq (noRNP: n=3, RNP-CEBPB: n=4). Significance calculation for the comparison between RNP-CEBPB and noRNP was performed using DESeq2 for all RNAseq data with *p<0.05, **p<0.01, ***p<0.001, ****p<0.0001. US = unstimulated, FC= fold-change , RNP = Ribonucleoprotein complex, AMPs = antimicrobial peptides, ns =not significant.

To confirm these results on protein level, Luminex analysis was performed for a wide panel of cytokines and chemokines (Figure 24). This confirmed the significant reduction of type 3 factors secretion, with strongest effects observed for the neutrophil chemoattractants CXCL1 (59 %, p=0.0079), CXCL5 (44 %, p=0.0002), IL-8 (63 %, p=0.0014) and the type 3 maintaining pro-inflammatory cytokine IL-6 (49 %, p=0.0002) in the supernatant of IL-17A+TNF-α stimulated CEBPB-KO keratinocytes relative to the noRNP control (Figure 24). Also here, a clear contrasting induction of type 2 factors was detected. The observed higher amounts of the growth factor GM-CSF (196 %, p=0.0030) and the chemokines CCL5 (RANTES, 181 %, p=0.0133), CCL27 (247 %, p=0.0002) and CCL22 (238 %, p=0.0302), imply that loss of CEBPB does not hamper the ability of keratinocytes to promote bone marrow neutrophil maturation, or migration of eosinophils, macrophages and dendritic cells. However, other factors such as VEGF were not regulated, indicating that CEBPB is unlikely to directly affect angiogenesis.

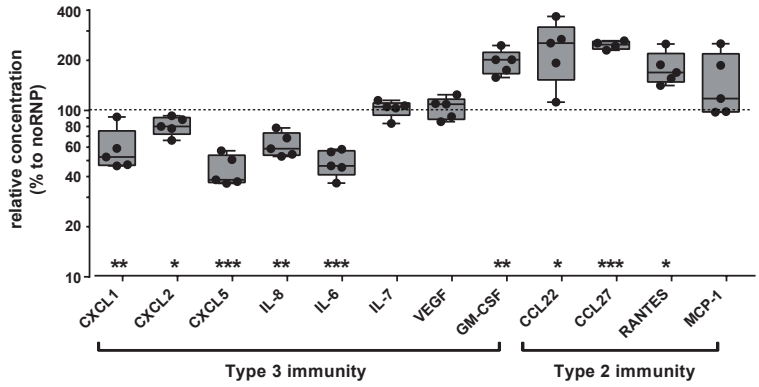

Figure 24: Luminex analysis reveals regulation of type 2 and 3 factors secretion in the supernatants of CEBPB-KO keratinocytes. The supernatant of CEBPB-KO (RNP-CEBPB) and control wild-type (noRNP) 2D keratinocytes (n=5-7) after 48 h stimulation with recombinant IL-17A+TNF-α was analysed for cytokine/chemokine content by multiplex technology (Luminex assay) displaying relative protein concentrations of type 2 and 3-relevant immune factors as percentages compared to the respective noRNP control. Comparison between RNP-CEBPB and noRNP was performed using unpaired t-test with Welch's correction. *p<0.05, **p<0.01, ***p<0.001. RNP = Ribonucleoprotein complex.

Given the strong downregulation of multiple chemokines central for neutrophil attraction and activation, we next attempted to functionally validate CEBPB's effect on neutrophil migration.

For this, a neutrophil trans-well migration assay was performed, revealing a strong reduction in the percentage of migrated human neutrophils (56 %, p=0.0021) towards the supernatant of IL-17A+TNF-α stimulated CEBPB-KO keratinocytes relative to noRNP keratinocyte supernatant, thus confirming that loss of CEBPB inhibits the capacity of keratinocytes to mediate neutrophil infiltration (Figure 25A).

Additionally, knockout of CEBPB in the neutrophil-like HL-60 cell line resulted in diminished migration towards both IL-8 and wild-type (wt) keratinocyte supernatant, implying intrinsic effects of CEBPB on neutrophils activation and migration (Figure 25 B).

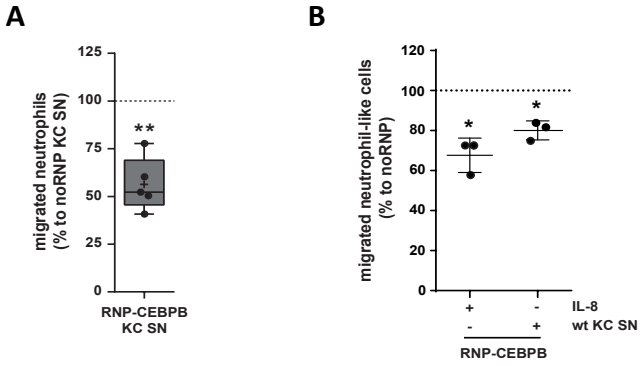

Figure 25: CEBPB is essential for neutrophil migration. A) Relative frequency of human neutrophils that migrated towards the supernatant of CEBPB-KO (RNP-CEBPB) keratinocytes stimulated for 72 h with recombinant IL-17A+TNF-α compared to wild-type (noRNP) keratinocytes (n=5) in a trans-well neutrophil migration assay. **B)** Knockout of CEBPB in differentiated HL60 neutrophil-like cells (n=3) and consecutive migration of these cells compared to noRNP control cells towards IL-8 or supernatant of wild-type keratinocytes (wt KC SN) stimulated with recombinant IL-17A+TNF-α. Shown are the relative frequencies of migrated cells in the trans-well migration assay measured by flow cytometry. Comparison between RNP-CEBPB and noRNP conditions done by unpaired t-test with Welch's correction *p<0.05, **p<0.01. US = unstimulated, RNP = Ribonucleoprotein complex, KC =keratinocyte, wt = wild-type, SN = supernatant.

Taken together, CEBPB acts as a key control point on the keratinocytes inflammatory secretome and is a pivotal regulator of neutrophil biology in the skin, acting both on the keratinocyte and the neutrophil level.

3.6.2. CEBPB effects on ECM organization and cell adhesion

The extracellular matrix (ECM) is an integral component of the skin and plays a central role in both cutaneous homeostasis and skin inflammation, where dysregulated ECM remodeling has been described. Therefore, I next aimed to investigate whether CEBPB loss affected the ECM organization. Indeed, various ECM genes were dysregulated in 3D CEBPB-KO keratinocytes compared to the noRNP control (Figure 26). Under IL-22 stimulation, a clear suppression of various ECM components such as the matrix metallopeptidases *MMP2/3/9/12, ICAM1, DSC2* and the cell adhesion molecules *CEACAM1/6* was observed in the KO. In contrast, under basal and Pso-TCS conditions, ECM genes were mainly upregulated upon loss of CEBPB as seen from the induction of different MMPs (*MMP2/3/9*) and collagens (*COL1A1, COL4A4*), as well as of *VCAM1* and *ITGAM* (Figure 26). *SERPINB3/4*, on the other hand, were strongly downregulated in the CEBPB-KO specifically under the type 3 stimuli (IL-17A+TNF-α, Pso-TCS) and 3D basal (US) condition. Interestingly, the filaggrins *FLG* and *FLG2*, which

are crucial for the stratum corneum (SC) integrity and function, and are suppressed in AD patients, were found to be upregulated under 3D basal conditions, but downregulated in the CEBPB-KO under type 2 inflammatory conditions (*FLG*: IL-4+IL-13 p= 2,78E-06, AD-TCS p= 0,0165, *FLG2*: IL-4+IL-13 p= 0,0036, AD-TCS p= 0,0315), indicating a potential involvement of CEBPB in the skin barrier function. *LCN2* (lipocalin 2), a gene known to be upregulated in Pso and downregulated in AD, is involved in attracting neutrophils to the skin, while inhibiting keratinocytes differentiation. Interestingly, KO of CEBPB lead to significant induction of this gene specifically with AD-type stimuli (IL-4+IL-13 p=0.004, AD-TCS p=0.033), while suppressing it under US (p=0.0012) and IL-17A+TNF-α (p=0.023) conditions, confirming once more the role of CEBPB in driving neutrophil migration and implying CEBPB's potential function in keratinocytes differentiation.

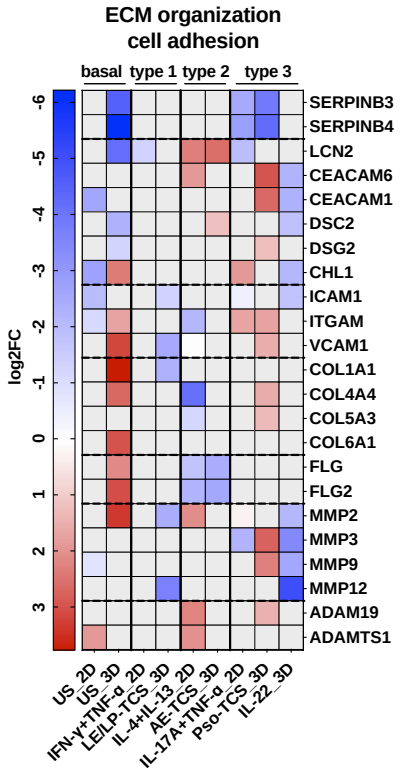

Figure 26: CEBPB loss leads to a dysregulation in cell adhesion and ECM organization. Heatmap of differentially expressed genes (DEGs) in the CEBPB-KO compared to the noRNP control for 2D and 3D keratinocytes under depicted type 1, 2 or 3 stimuli in comparison to unstimulated (US) basal conditions. DEGs are filtered to include genes with function in 'cell adhesion' and extracellular matrix (ECM) 'ECM organization'.
Displayed are significantly dysregulated genes (p<0.05) with red= upregulated, blue= downregulated, white= not regulated and grey=not significant. US= unstimulated, FC= fold-change, DEGs = differentially expressed genes, ECM= extracellular matrix.

3.6.3. Keratinocytes proliferation and pathogenic epidermal hyperplasia is driven by CEBPB

Keratinocytes hyperproliferation and abnormal differentiation with its consequence of acanthosis is a characteristic hallmark of Psoriasis and other CISDs. As previously described, the keratinocyte transcriptome upon knockout of CEBPB showed negative enrichment of various pathways related to cell cycle/ mitosis, keratinocytes proliferation and differentiation (Figure 20).

To investigate this further, we sought to perform keratinization pathway analysis on the 3D CEBPB-KO keratinocyte skin models. However, no keratinization pathway was found in the KEGG database and the one available on Reactome collectively included both proliferation and differentiation genes. Since CEBPB is likely involved in both pathways, as previously described for other tissues, we were interested in investigating its effects separately on proliferation and differentiation processes. Therefore, using publically available datasets on Reactome and MSigDB together with literature research, I generated two separate gene lists for 'keratinocytes proliferation' and 'differentiation', that were subsequently used for the keratinization ORA pathway analysis. Performing this analysis on the 3D CEBPB-KO keratinocyte skin models under type 3 stimulation (Pso-TCS) revealed enriched genes associated with the three main suppressed pathways of 'keratinocytes proliferation', 'cell cycle, mitotic' and 'keratinocytes differentiation', and their differential regulation upon CEBPB loss (Figure 27).

Indeed, various proliferation genes like *AURKA* ($p<0.0001$), *BUB1* ($p=0.0032$), *CCNB1* ($p<0.0001$), *CCNE1* ($p=0.0171$), *CDK1* ($p=0.0002$), *CDCs* and *MCMs* (cell cycle regulation/ mitosis), as well as *MKI67* ($p=0.0011$) and *PCNA* ($p=0.0030$) as classical proliferation markers were enriched and significantly downregulated in CEBPB-KO keratinocytes under Pso-TCS (Figure 27 A, B, C). Similar suppression of proliferation was detected under basal (US) conditions (Figure 27 B). Furthermore, the expression of hyperproliferation-associated keratins, known to be involved in Psoriasis, was strongly suppressed under both basal (*KRT16* ($p=0.0342$), *KRT17* ($p<0.0001$), *KRT6B* ($p=0.0009$)) and Pso-type conditions with Pso-TCS (*KRT6A* ($p=0.05$) and IL-22 (*KRT6B* ($p=0.0138$), *KRT6C* ($p=0.0008$) upon knockout of CEBPB (Figure 27 B, C). On the other hand, anti-proliferative genes such as *EMP1* ($p=0.0007$) and *WNK2* ($p=0.0010$), were upregulated with CEBPB loss under Pso-TCS (Figure 27 B), further highlighting the overall effect of inhibited proliferation in the CEBPB-KO keratinocytes.

Additionally, CEBPB loss altered the expression of various differentiation genes mainly under the Pso-TCS condition. Here, a downregulation of the early differentiation marker keratins (*KRT1* (p=0.0102), *KRT10* (p=0.0328)), as well as of *DSC1* (p=0.0190) and *KLK13* (p=0.0084) (Figure 27A, B). Moreover, various small proline rich proteins genes *SPRRs* encoding envelope proteins of cross-linked differentiated keratinocytes were suppressed under basal and Pso-TCS conditions (Figure 27 B). In contrast, an upregulation of the advanced terminal differentiation keratin *KRT2* (p=0.0003), together with various late cornified envelope genes e.g. *LCE1C* (p=0.0184), *LCE1E* (p=0.0013) and *LCE5A* (p=0.0005), was detected in CEBPB-KO keratinocytes (Figure 27B, C), implying a potential negative involvement of CEBPB in the late cornification process of keratinocytes under both steady state and a psoriatic microenvironment.

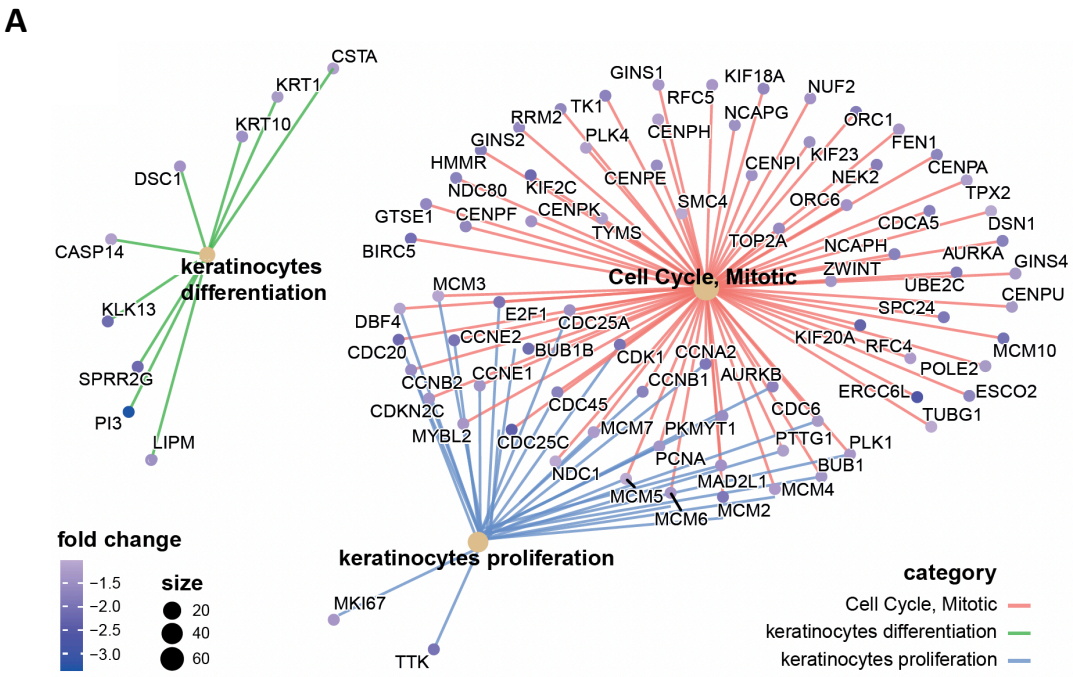

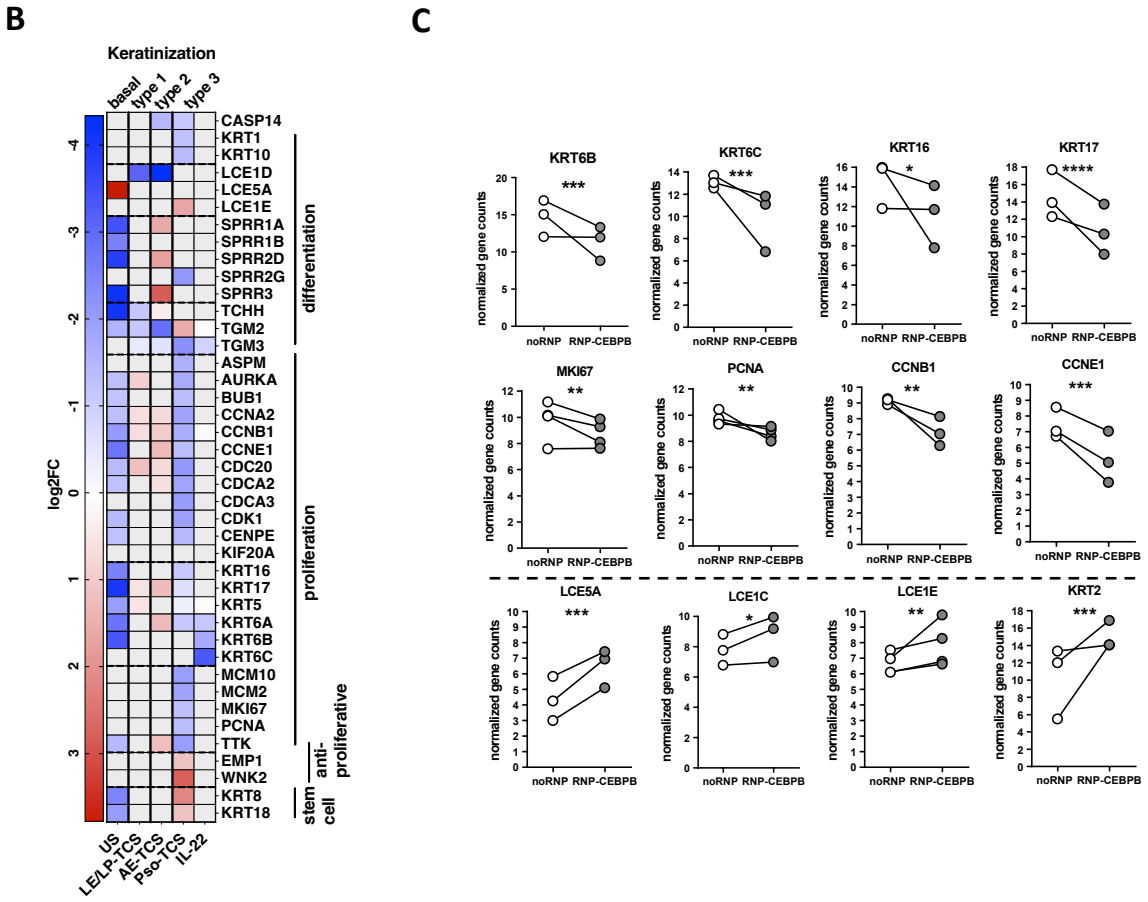

Figure 27: CEBPB is central for the transcriptional regulation of keratinization pathways. A) Cnetplot of keratinization pathway analysis performed on differentially expressed genes (DEGs) obtained by bulkRNA Sequencing of CEBPB-KO (RNP-CEBPB) compared to wild-type (noRNP) 3D keratinocyte skin models (n=4) under Pso-TCS stimulation. Displayed are the top enriched pathways as central nodes with the node size indicating the amount of associated genes shown with their respective color-coded fold changes. **B)** Heatmap of DEGs in the CEBPB-KO compared to the noRNP control for 3D keratinocytes under depicted type 1, 2 or 3 TCS stimulion, as well as IL-22 stimulation, in comparison to unstimulated (US) basal conditions. DEGs are filtered to include genes with function in keratinization and subdivided further into functional groups. Displayed are significantly dysregulated genes (p=0.05) with red= upregulated, blue= downregulated, white= not regulated and grey=not significant. **C)** Normalized gene counts of chosen proliferation and differentiation marker genes in CEBPB-KO (RNP-CEBPB) and wild-type (noRNP) 3D keratinocyte skin models under homeostasis (unstimulated, US), as well as type 3 conditions (Pso-TCS, IL-22) with (US and IL-22: n=3, Pso-TCS: n=4). Comparison between RNP-CEBPB and noRNP was performed using DESeq2 for all RNAseq data. *p<0.05, **p<0.01, ***p<0.001, ****p<0.0001. DEGs = differentially expressed genes, KO = knockout, US = unstimulated, FC= fold-change, RNP = Ribonucleoprotein complex, TCS = T-cell supernatant.

Cell cycle phase analysis on our scRNASeq data from Psoriasis patients further revealed that *CEBPB* expression was significantly higher in the S- and G2/M-keratinocytes compared to those in G1 phase, demonstrating an upregulation of *CEBPB* as the cells progress through the cell cycle towards mitosis, thus again confirming the requirement of CEBPB for driving the process of keratinocytes proliferation (Figure 28 A, B).

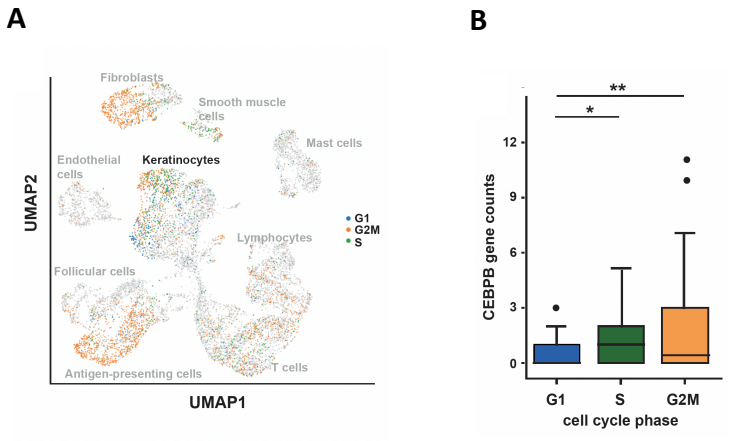

Figure 28: Keratinocytes upregulate CEBPB as they progress through the cell cycle. A) and **B)** Cell cycle phase analysis on scRNAseq data of Psoriasis (n=3 patients). **A)** UMAP plot showing the annotated single cell clusters with cell cycle phases G1 (blue), S (green) and G2/M (orange) highlighted for each cell with the keratinocytes cluster in focus. **B)** CEBPB gene counts of keratinocytes in G1, S and G2/M phases for showing CEBPB expression in correlation to the different cell cycle phases. G1 = Gap1, S = DNA Synthesis, G2/M = Gap2/Mitosis.

Next, to validate the functional effects of the observed dysregulated keratinization gene signature associated with the loss of CEBPB, we generated 3D skin models as previously described and analyzed the epidermal thickness as a proxy for IL-22 induced acanthosis (Figure 29 A). While CEBPB-KO did not alter the cellular morphology or the architecture of the 3D keratinocytes, it notably inhibited the acanthosis development and drastically reduced the relative thickness of the layers ($p<0.0001$) in the CEBPB-KO condition (Figure 29 A, B). Similar results were obtained under Pso-TCS condition (Figure 31C). Also here, the CEBPB-KO showed strongly reduced epidermal thickness and the keratinocytes were deficient in forming as many layers as in the noRNP control. Along this line, the number of $Ki67^{+}$ cells, as a readout for actively proliferating keratinocytes, was markedly reduced in the CEBPB-KO under both steady-state and IL-22, with a reduction from 10 ± 2 to 3 ± 1 cells (US, $p=0.0225$) and from 16 ± 4 to 4.0 ± 1 cells (IL-22, $p=0.0018$), respectively, thus confirming that loss of CEBPB inhibits keratinocytes proliferation (Figure 29 A, C).

In summary, these data show that CEBPB is a key regulator of keratinization pathways, driving keratinocytes proliferation and promoting the development of acanthosis in type 3 skin inflammation.

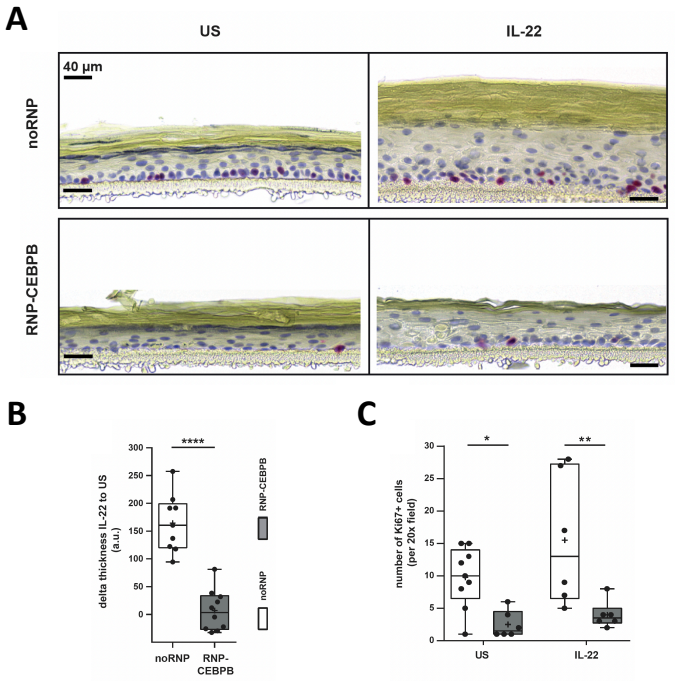

Figure 29: CEBPB knockout inhibits keratinocytes proliferation and alleviates acanthosis. A-C) 3D keratinocyte skin models of CEBPB-KO (RNP-CEBPB) and wild-type (noRNP) cells that were stimulated for 72 h with recombinant IL-22 to induce acanthosis or left unstimulated (US) as a control. Models were stained for the proliferation marker Ki67 by IHC (n=3). Representative IHC stainings are shown in **(A)**. Scale bar indicates 40 µm. **B)** Relative thickness of 3D keratinocyte skin models after IL-22 stimulation is quantified in comparison to the unstimulated control and displayed as Delta thickness (n=10 distances, n=3 donors). **C)** Quantification of Ki67 positive cells per 20x field (n=6-9 fields, n=3 donors). Comparison between RNP-CEBPB and noRNP was performed using unpaired t-test with Welch's correction. *p<0.05, **p<0.01, ****p<0.0001. KO = knockout, US = unstimulated, RNP = Ribonucleoprotein complex, IHC = immunohistochemistry, a.u. = arbitrary unit.

3.6.4. A PIM1-mediated mechanism is potentially involved downstream of CEBPB in acanthosis regulation

In order to further explain the effect of CEBPB on acanthosis at the molecular level, I examined different downstream targets of CEBPB that might be involved in this process. One of these targets is PIM1 (Pim-1 proto-oncogene), a serine/threonine kinase implicated in various cellular processes.

Similar to CEBPB, *PIM1* was found to be upregulated in the lesional skin of Pso patients (Figure 30 A) and significantly induced with type 1 (IFN-γ+TNF-α, FC= 4.50± 1.99, p=0.0016) and type 3 (IL-17A+TNF-α, FC= 2.50± 0.33, p<0.0001) stimuli *in vitro* in primary human keratinocytes on RNA level (Figure 30 A). Comparable regulation patterns were also observed on protein levels, where the active PIM1-S isoform was strongly induced with the IL-17A+TNF-α stimulation condition, as well as with IFN-γ+TNF-α, while the longer PIM1-L isoform was rather constitutively expressed for most tested stimuli (Figure 30 C).

Further kinetics stimulation experiments with the three main stimuli for type 1, 2 and 3, revealed that PIM1-S was most efficiently induced with the type 3 stimulus at later time-points (48h and 72h), while the regulation through type 1 stimuli was happening at earlier time points (o/n) (Figure 30 D). Whereas slightly, but not significantly, higher gene counts could be observed for the LE/LP-TCS stimulation, no upregulation could be detected with Pso-TCS on RNA level (Figure 30 E). Protein analysis of 3D models showed slight induction of the PIM1-S isoform by IL-22 with a downregulation of PIM1-L, while IL-17A+TNF-α stimulated models showed a clear induction of both isoforms (Figure 30F). Altogether, PIM1 expression revealed similar regulation patterns to CEBPB under the different immunogenic stimuli, implying a potential involvement of both factors in the same cellular signaling pathways

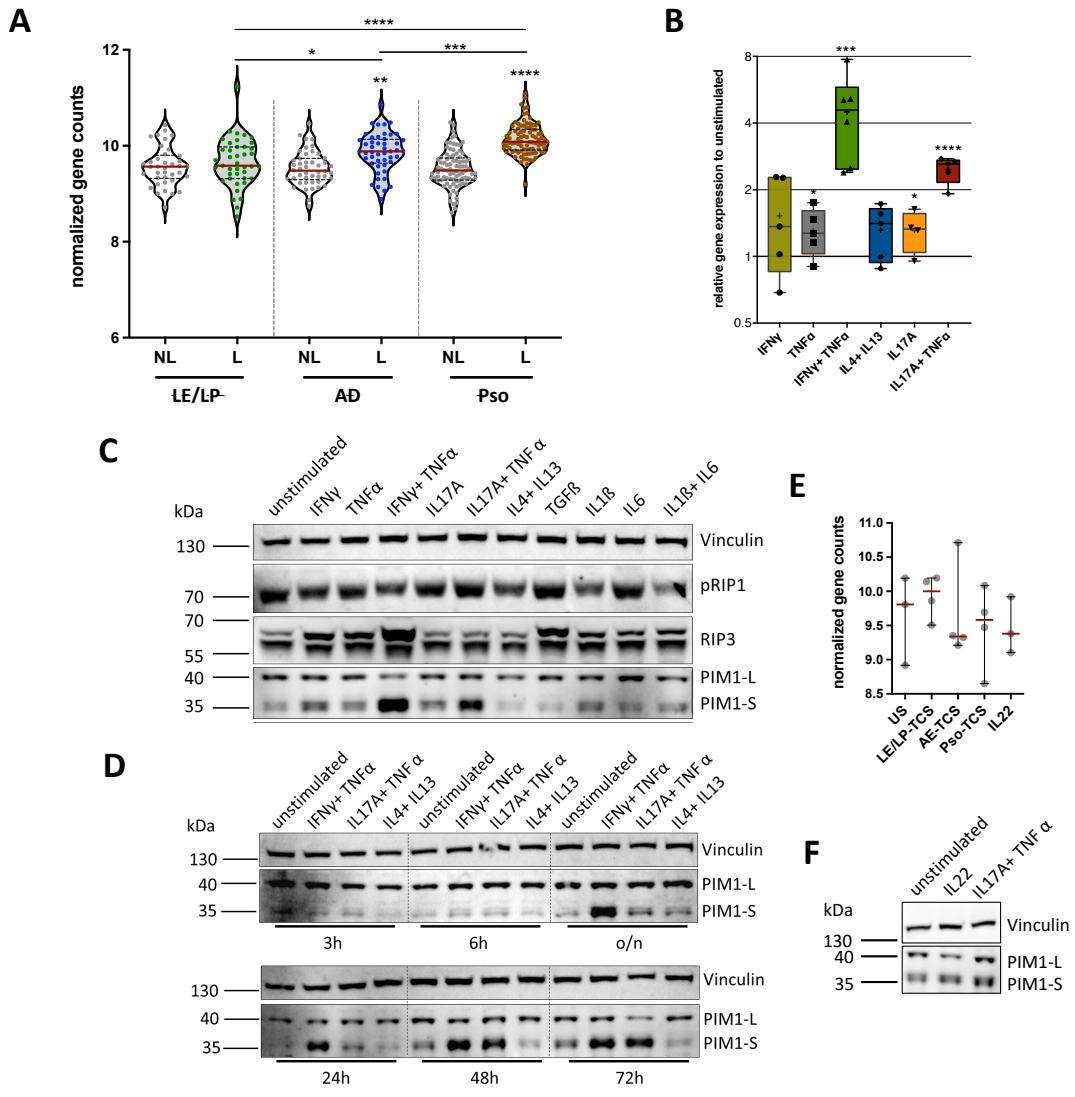

Figure 30: PIM1 is upregulated in the lesional skin of Psoriasis patients and is induced by type 1/ type 3-relevant cytokines *in vitro* in primary human keratinocytes. A) Violin plots of DESeq2 normalized PIM1 gene counts from bulk RNASeq in lesional (L) and non-lesional (NL) skin of Lupus erythematosus/Lichen planus (LE/LP, n= 41), Atopic Dermatitis (AD, n=48) and Psoriasis (Pso, n=90) patients. **B)** qPCR analysis of PIM1 expression in primary human keratinocytes (n=4-5) upon depicted

overnight cytokine stimulations representing type 1, type 2 and type 3 inflammatory conditions. Gene expression is shown relative to the unstimulated control. **C)** Western blot analysis of PIM1 protein expression under different immune stimuli after 48h stimulation showing the different PIM1 isoforms (PIM1-L, PIM1-S). **D)** Kinetics of PIM1 protein expression showing the regulation of the PIM1 isoforms in 2D keratinocytes over time after stimulation with the main stimuli for type 1 (IFN-γ+TNF-α), type 2 (IL-4+IL13) and type 3 (IL-17A+TNF-α). **E)** Normalized gene counts of PIM1 in 3D keratinocyte models after 24h stimulation with either indicated lesional T-cell supernatants (TCS) from LE/LP, AD and Pso or IL-22 compared to unstimulated (n=3-4). **F)** Western blot analysis of PIM1 protein levels in 3D models with the indicated Pso-type stimuli for 48h. Comparison to non-lesional and unstimulated sample was performed using unpaired t-test with Welch's correction. Comparison of disease groups was performed using Ordinary one-way ANOVA test with Tukey's multiple comparison. *p<0.05, **p<0.01, ***p<0.001, ****p<0.0001. L= lesional, NL= non-lesional, US= unstimulated, o/n= overnight, PIM1-L= PIM1 large isoform, PIM1-S= PIM1 small isoform.

Given that and the fact that PIM1 was found in the previously described acanthosis network (Figure 31 A), we were prompted to test this hypothesis of its involvement within the context of the acanthosis pathway.

First, to establish the regulation of PIM1 downstream of CEBPB, the PIM1 protein expression was analyzed in CEBPB-KO keratinocytes revealing a marked reduction, especially of the PIM1-S isoform, upon loss of CEBPB (Figure 31 B). Importantly, similar to CEBPB, loss of PIM1 inhibited the induction of acanthosis in 3D keratinocytes models stimulated with IL-22 or Pso-TCS (Figure 31 C). As expected, the double KO of CEBPB and PIM1 had a synergistic effect on the acanthosis inhibition, yielding 3D models with the thinnest layers compared to the single knockouts. Thus, based on these results, we propose PIM1 as one potential downstream target of CEBPB in the acanthosis axis of Psoriasis disease pathology.

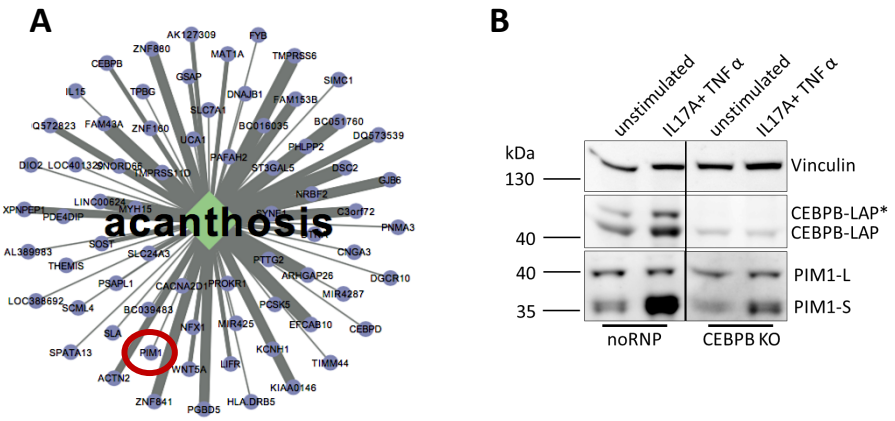

C

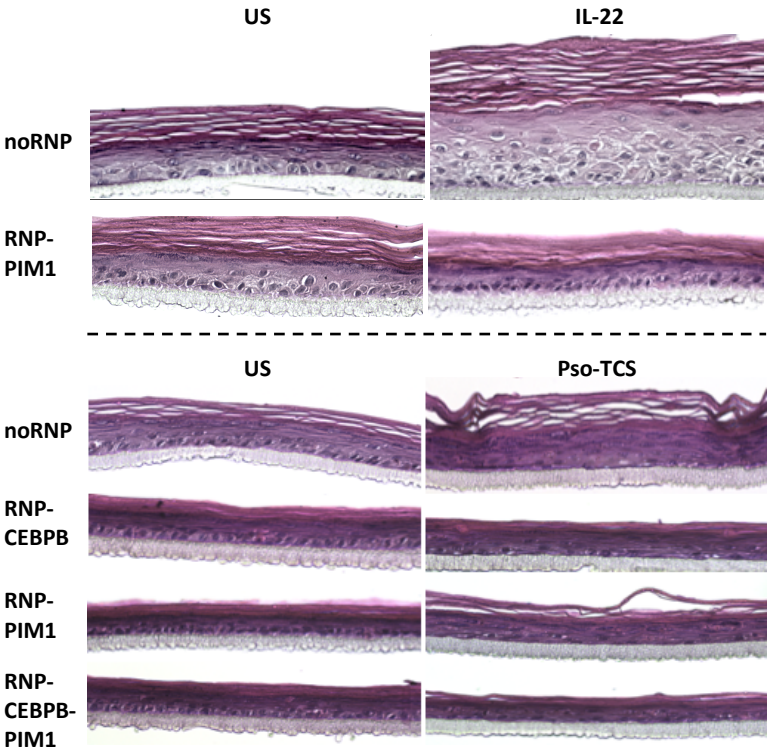

Figure 31: PIM1 is a potential target downstream of CEBPB in the Psoriasis acanthosis axis. A) Network showing genes associated with the attribute "acanthosis" from CISD patients, as previously described, with PIM1 highlighted. **B)** Western blot analysis of PIM1 expression in CEBPB-KO compared to wild-type (noRNP) keratinocytes that were either left unstimulated or treated with IL-17A+TNF-α. CEBPB was stained to confirm KO efficiency. **C)** H&E-stained 3D keratinocyte models of CEBPB-KO (RNP-CEBPB), PIM1-KO (RNP-PIM1) and CEBPB-PIM1 double KO (RNP-CEBPB-PIM1) keratinocytes in comparison to wild-type (noRNP) cells left stimulated for 72 h with IL-22 or Pso-TCS or left unstimulated (US) as a control. US= unstimulated, KO= knockout, RNP= ribonucleoprotein complex, TCS= T-cell supernatant.

3.6.5. CEBPB-deficient keratinocytes undergo metabolic rewiring with downregulated mitochondrial metabolism and reduced metabolic fitness

Psoriatic keratinocytes hyperproliferation requires extensive energy, metabolic fitness and building blocks, hence making keratinocytes metabolism a central, yet under investigated aspect in Psoriasis pathogenesis. We therefore next aimed at examining the role of CEBPB within the context of metabolism focusing on Psoriasis-type conditions.

Gene expression of various metabolic genes was altered in the CEBPB-KO keratinocytes mainly under basal (US) and type 3 conditions (IL-17A+TNF-α , Pso-TCS), but not under IL-22 or type 1/2 conditions (Figure 32 A). Here, CEBPB-KO under Pso-type stimulation resulted in significant repression of various metabolic genes that have been previously described to be induced in psoriatic skin and involved in disease pathogenesis such as *PTGS2* (FC= -1.16, p= 0.001) and *PLA2G4B* (FC= -1.72, p= 0.0007)

(prostaglandin (PG)/lipid metabolism), *FABP5* (FC= -1.8, p= 8,86202E-05) (fatty acid (FA) metabolism), as well as *ASS1, ARG1* and *ARG2* (urea cycle (UC)) (Figure 32 A). Furthermore, *ASS1* and *ARG1* were additionally suppressed under basal conditions. In contrast, various solute carriers (SC) were upregulated with knockout of CEBPB under type 3 conditions. Notably, genes involved in the reactive oxygen species pathway (ROS) together with a number of mitochondrial genes (Mito) constituted two other functional groups that were overrepresented among the dysregulated metabolic genes in the CEBPB-KO compared to the noRNP control (Figure 32 A).

We therefore performed GO term analysis on our gene expression data using as input 'mitochondria' as cellular component. This revealed a significant negative enrichment of various mitochondrial-related terms, both structural (e.g. 'inner/ outer mitochondrial protein complex', 'mitochondrial nucleoid') and functional (e.g. 'respiratory chain complex I', 'respirasome'), in CEBPB-KO compared to wild-type (noRNP) keratinocytes (Figure 32 B). In line, mitochondrial respiratory electron transport chain (ETC) genes like *NDUFA9* (p=0.013), *NDUFB6* (p=0.037), *COA6* (p=0.04), *TMEM177* (p=0.005) and *UQCRC1* (p=0.019) were significantly downregulated upon loss of CEBPB, hence implying potential dysregulation of oxidative phosphorylation in those keratinocytes (Figure 32A, C). In addition, genes contributing to more cellular ROS generation such as *PRODH* (p=0.03), *CYP4B1* (p=0.006) and *NOXA1* (p=0.02) and consequently mitochondrial oxidative stress response genes like *NDUFA4L2* (p=0.04) were upregulated in the CEBPB-KO keratinocytes under basal and Pso-type conditions (Figure 32A, C). On the other hand, genes involved in the removal of ROS like the mitochondrial enzyme *SOD2* (p=0.01) (superoxide dismutase 2) were downregulated, altogether implying an overall increased oxidative stress in keratinocytes upon loss of CEBPB.

Finally, genes encoding key enzymes in nucleotide synthesis (NS) and hence DNA replication such as *TK1* (p=1,67845E-05) and *DHFR* (p=0.0002) were significantly suppressed in the CEBPB-KO keratinocytes under Pso-TCS (Figure 32A, C), coinciding with the observed inhibitory effects on cell proliferation and further confirming CEBPB's central role in regulating keratinocytes proliferation on different levels.

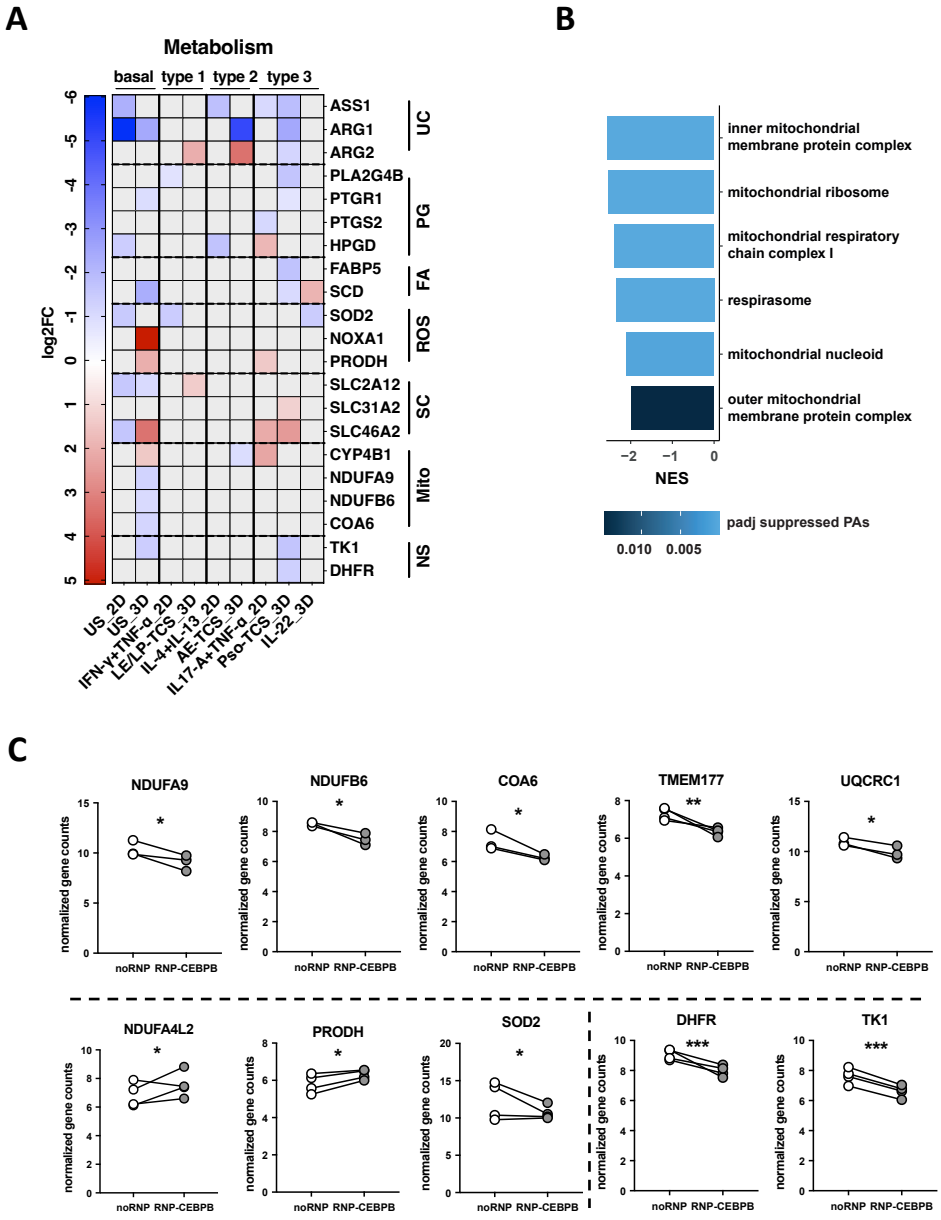

Figure 32: Transcriptional metabolic rewiring of keratinocytes upon loss of CEBPB indicates downregulated metabolic activity. A) Heatmap of differentially expressed genes (DEGs) in the CEBPB-KO compared to the noRNP control for 2D and 3D keratinocytes under depicted type 1, 2 or 3 stimuli in comparison to unstimulated (US) basal conditions. DEGs are filtered to include genes with metabolic function and further subdivided according to their metabolic pathways. Displayed are significantly dysregulated genes (p=0.05) with red= upregulated, blue= downregulated, white= not regulated and grey=not significant. **B)** GSEA analysis with GO term 'cellular component' performed on DEGs of unstimulated CEBPB-KO (RNP-CEBPB) to wild-type (noRNP) 2D keratinocytes (n=3). Displayed are the enriched suppressed GO terms with their enrichment score and adjusted p-values. **C)** Normalized gene counts of metabolic marker genes in CEBPB-KO (RNP-CEBPB) and wild-type (noRNP) keratinocytes (2D and 3D) under basal (unstimulated, US) as well as type 3 conditions (Pso-TCS, IL-17A+TNF-α) (n=3-4). Significance comparison between RNP-CEBPB and noRNP was performed using DESeq2 for all RNAseq data. US= unstimulated, FC= fold-change, DEGs= differentially expressed genes, UC= urea cycle, PG= prostaglandin metabolism, FA= fatty acid metabolism, ROS= reactive oxygen species pathway, SC= solute carriers, Mito= mitochondrial, NS= nucleotide synthesis, KO= knockout, GSEA = gene set enrichment analysis, PA= pathway, NES= normalized enrichment score, padj= adjusted p-value.

To validate these transcriptome findings of metabolic reprogramming, especially of the mitochondrial compartment, I first examined the total cellular ATP levels in primary human keratinocytes using a bioluminescent quantitative ATP assay. A significant reduction of ATP levels in CEBPB-KO cells compared to the noRNP control was observed in a stimulus-dependent manner (Figure 33). Here, IL-17A+TNF-α showed the strongest effect with a decrease of (15 % ± 8%, p=0.0006) followed by IL-17A (14 % ± 7%, p=0.002), unstimulated (US) (10 % ± 6%, p=0.018) and Pso-TCS (9 % ± 7%, p=0.022), whereas under both type 1 (IFN-γ +TNF-α) and type 2 stimuli (IL-4+IL-13) no significant effects could be recorded.

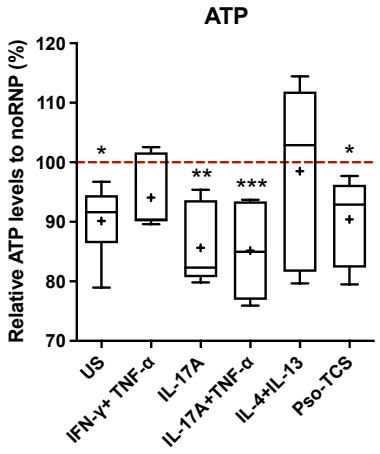

Figure 33: CEBPB regulates cellular ATP levels in keratinocytes under steady-state and psoriatic conditions. Total cellular ATP levels in CEBPB-KO (RNP-CEBPB) 2D keratinocytes relative to noRNP control cells were measured by luminescence ATP assay after 24 h stimulation under type1 (IFN-γ+TNF-α), type 2 (IL-4+IL-13) and type 3 conditions (IL-17A, IL-17A+TNF-α, Pso-TCS) or under basal conditions (unstimulated, US) (n=4). Significance was tested by ordinary one-way ANOVA uncorrected Fisher's LSD. *p<0.05, **p<0.01, ***p<0.001.

Since mitochondrial respiration contributes to most cellular ATP production and is thus crucial for cell proliferation, I next attempted to directly investigate the mitochondrial oxidative phosphorylation (OXPHOS) in CEBPB-KO keratinocytes under homeostasis and type 3 conditions (IL-17A+TNF-α, Pso-TCS) using the Seahorse Cell Mito Stress assay, a widely recognized standard assay for assessing mitochondrial function via multiple parameters.

First, the oxygen consumption rate (OCR) of mitochondrial respiration measured over time showed a clear total reduction in the CEBPB-KO compared to noRNP keratinocytes (Figure 34 A, C). Here, the representative OCR traces demonstrated a lower OCR rate under IL-17A+TNF-α compared to the unstimulated condition for both CEBPB-KO and wild-type keratinocytes (Figure 34 A). Similar effects were observed for the Pso-TCS (Figure 34 C). Basal respiration under steady-state was significantly reduced by 53 % ± 13% (US, p=0.0081) and 38 % ± 10% (IL-17A+TNF-α, p=0.038) in the CEBPB-KO (Figure 34 B). Noteworthy, the maximal respiration (Max) mimicking a high energy demand state and the spare respiratory capacity (SRC), which is an indicator for the ability of cells to respond to the highest energy demand under stress, were even more drastically affected by CEBPB loss, showing significant reductions of (Max: 47% ± 11%, p=0.043, SRC: 55 % ± 11%, p= 0.032) and (Max: 76 % ± 20%,

p= 0.024, SRC: 78 % ± 14%, p=0.012) under IL-17A+TNF-α and unstimulated conditions, respectively (Figure 34 B). Also under Pso-TCS stimulation, a similar, yet non-significant, trend could be observed for the reduction of maximal respiration (Max) (35 % ± 32%) and SRC (58 % ± 38%) (Figure 34 D), thereby altogether indicating the reduced metabolic fitness of CEBPB-KO keratinocytes under stress, under both US and Pso-type conditions. In this frame, the ability of mitochondria to produce ATP (Mito ATP production) via respiration was greatly reduced by 59 % ± 18% (US, p=0.026) and 50 % ± 21% (IL-17A+TNF-α, p=0.064) in the CEBPB-KO keratinocytes (Figure 34 B), coinciding with the previous results obtained by the ATP assay.

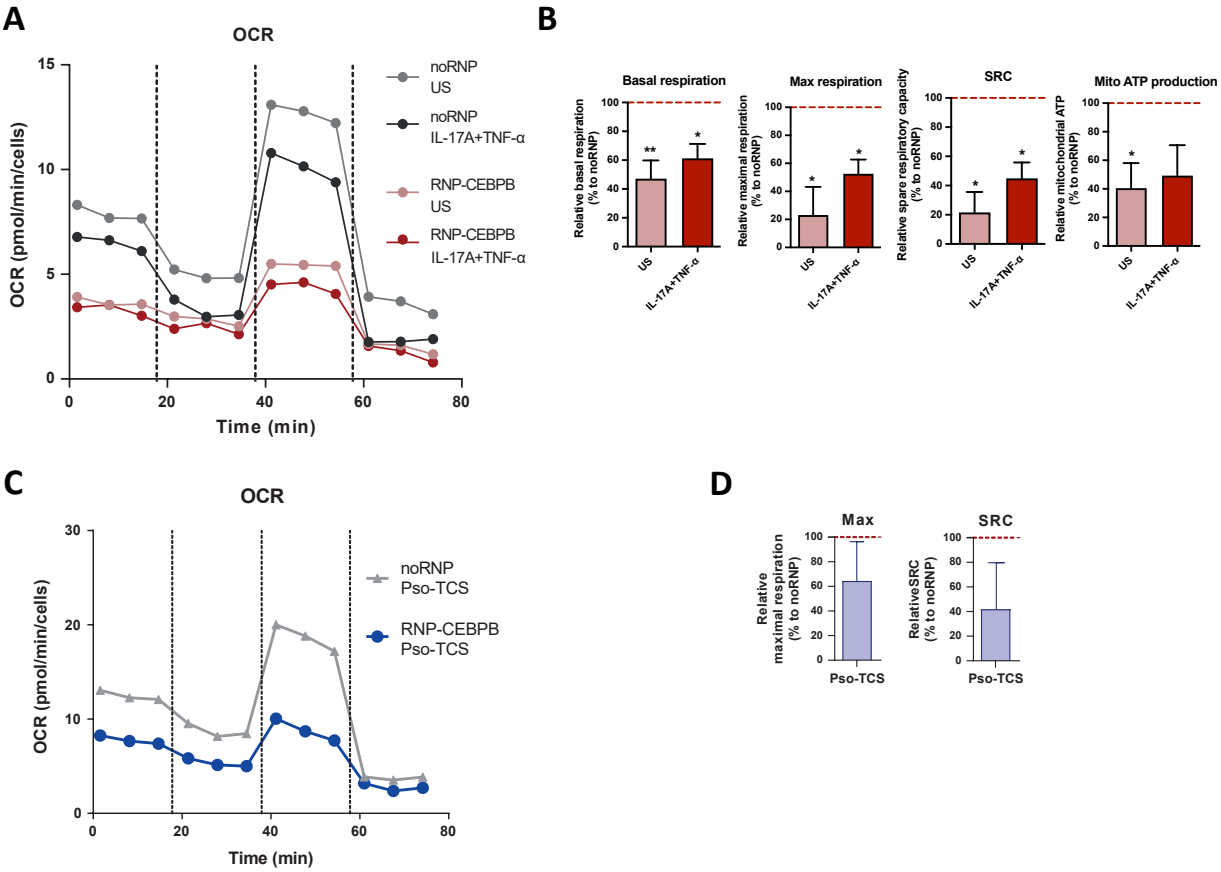

Figure 34: CEBPB loss inhibits mitochondrial respiration and reduces the metabolic fitness in primary human keratinocytes. Seahorse analysis of CEBPB-KO (RNP-CEBPB) and wild-type (noRNP) 2D keratinocytes. Keratinocytes were stimulated for 24 h with IL-17A+TNF-α **(A&B)**, Pso-TCS **(C&D)** or left untreated for basal (US) control, followed by analysis of mitochondrial respiration using Seahorse XF Cell Mito Stress Test (n=3). **A)** and **C)** show representative oxygen consumption rate (OCR) traces that were normalized to cell numbers for each condition as readout for mitochondrial respiration over time at baseline level (0-18 min), after ATP synthase inhibition with Oligomycin (18-38 min), after uncoupling of oxidative phosphorylation with FCCP (38-58 min) and after electron transport chain inhibition with rotenone/antimycin A (58-80 min). **B)** and **D)** show multiple parameters for mitochondrial activity calculated from the OCR traces including basal and maximal respiration, spare respiratory capacity (SRC) and mitochondrial ATP production, all shown as percentages relative to the noRNP control. Comparison between RNP-CEBPB and noRNP was performed using uncorrected Fisher's LSD test. *p<0.05, **p<0.01. US = unstimulated, RNP = Ribonucleoprotein complex, OCR = oxygen consumption rate, Max= maximal, SRC = spare respiratory capacity, Mito= mitochondrial.

These findings prompted us to further examine the mitochondria upon CEBPB loss. For this, I established a mitochondrial staining in primary human keratinocytes using the MitoTracker dye, which specifically and permanently, hence remaining after the cell dies or is fixed, labels mitochondria within live cells utilizing the mitochondrial membrane potential. It thereby provides a readout for both mitochondrial density and function in the cell. First, primary human keratinocytes were stained with different concentrations (50, 100, 200, 300, 400 nM) of the dye testing two different staining times (30, 45 min) and analyzed via FACS or live imaging. Figure 35 shows the results for the 30 min time-point, which was chosen for use in further experiments, since the longer staining time of 45 min did not lead to a change in the signal. The concentration titration showed that with 50 and 100 nM the obtained signal was too weak, especially in imaging, whereas with 400 nM it was relatively high, indicating a saturation already at 300/ 400 nM (Figure 35). The 200 nM concentration was therefore chosen as an optimal condition providing a signal that is strong enough and gives a convenient experimental window, i.e. for potential shifts up or down in the experimental effects. Next, various IF conditions were tested to be able to fix the cells after staining for imaging at the confocal microscope. The following different fixation conditions were tested: **1)** 4% PFA (for 15 min at RT), **2)** 3.5-3.7% formaldehyde (for 15 min at RT) and **3)** MeOH (for 10 min at -20^{0}C), all with or without permeabilization using acetone (for 5 min at -20^{0}C) (results not shown). Fixation with 4% PFA (for 15 min at RT) without additional permeabilization yielded the best results for the MitoTracker staining and was chosen for subsequent IF experiments. Thus, in conclusion, the best staining conditions were determined to be 200 nM for 30 min with DAPI counterstaining for both FACS and imaging.

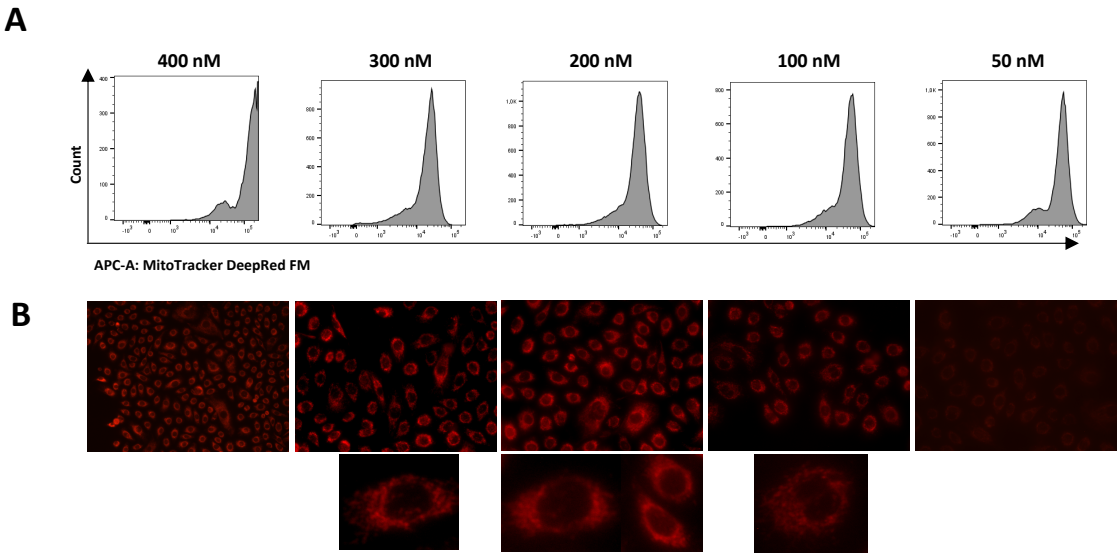

Figure 35: Establishment of MitoTracker staining protocol for staining mitochondria in primary human keratinocytes. A) and **B)** show the single fluorescence intensity histograms (A) and representative microscopy images (B) for each tested concentration after 30 min staining with MitoTracker dye. B) Keratinocytes were imaged live directly after staining using the TexasRed chanel. Lower panel shows zoom-ins on keratinocytes for better mitochondria visualization.

Using the established protocol, we next performed MitoTracker stainings on CEBPB-KO keratinocytes to further examine the mitochondria upon CEBPB loss to reveal potential mitochondrial alterations that might be responsible for the observed downregulated oxidative metabolism. Indeed, the mitochondrial signal intensity per cell was significantly decreased in the CEBPB-KO keratinocytes compared to the noRNP control, namely by approximately 2.5-fold (from 1.8 ± 0.67 a.u. to 0.7 ± 0.29, $p<0.0001$) and 2-fold (from 1.65 ± 0.61 a.u. to 0.86 ± 0.33, $p=0.0015$) in the unstimulated (US) and IL-17A+TNF-α conditions, respectively, thus indicating a clear reduction in the functional mitochondrial mass per cell upon loss of CEBPB under both steady-state and psoriatic microenvironment (Figure 36 A, B). Also here, the effects on the mitochondrial density were slightly more pronounced in the unstimulated compared to the IL-17A+TNF-α condition. Moreover, I verified these findings by flow cytometry, gating on the DAPI-/MitoTracker+ population (Figure 36 C) and detecting once more a reduction in the mitochondrial signal as seen from the shift in the median fluorescence intensity (MFI) of the MitoTracker+ population between the CEBPB-KO and noRNP keratinocytes and the quantified lower MFI of the MitoTracker+ population in the CEBPB-KO under homeostasis (Figure 36 D). In contrast, the frequency of MitoTracker$^+$ population was not significantly reduced, yet a trend towards downregulation could still be observed (Figure 36 E).

In sum, these data demonstrate that CEBPB-deficient keratinocytes undergo extensive metabolic reprogramming leading to enhanced oxidative stress on the one hand, and downregulated mitochondrial respiration, ATP production and metabolic fitness, on the other side, likely due to the observed loss of functional mitochondrial mass.

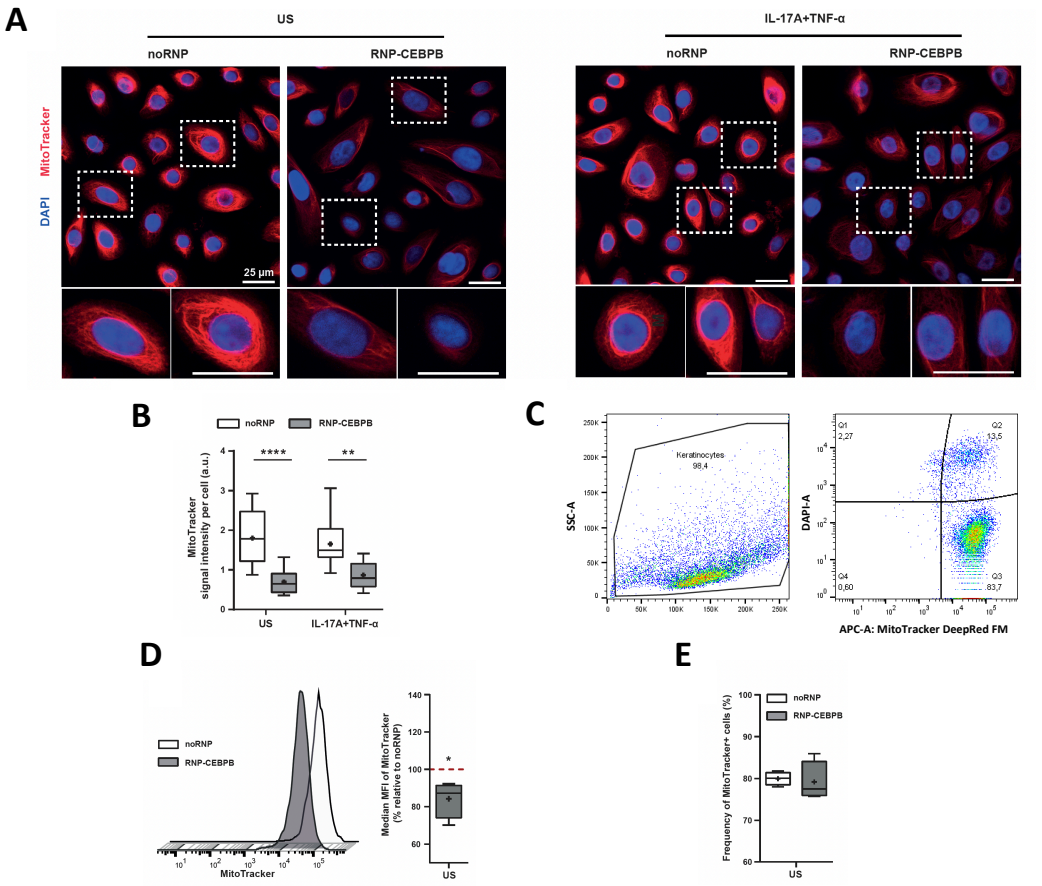

Figure 36: CEBPB knockout reduces the functional mitochondrial density in keratinocytes. MitoTracker analysis of CEBPB-KO (RNP-CEBPB) and wild-type (noRNP) keratinocytes. Keratinocytes were stimulated for 24 h with IL-17A+TNF-α or left unstimulated (US) for basal control (n=3). MitoTracker intensity was measured by immunofluorescence (IF) (A&B) or flowcytometry (FACS) (C-E). **A)** Representative confocal microscopy images of the IF stainings are shown as overlays with DAPI= blue, MitoTracker=red. Scale bar indicates 25 µm. **B)** Quantification of MitoTracker intensity per cell (n=5-7 fields/condition). **C)** Representative FACS staining and gating on DAPI- MitoTracker+ keratinocytes. **D)** MitoTracker fluorescence intensity histograms for one representative donor (D, left) and quantified median fluorescence intensity (MFI) as percentages relative to noRNP control (D, right). **E)** Frequency of MitoTracker-positive populations are displayed. Comparison between RNP-CEBPB and noRNP was performed using uncorrected Fisher's LSD test (B) or unpaired t-test with Welch's correction (D). *p<0.05, **p<0.01, ***p<0.001, ****p<0.0001. KO = knockout, a.u. = arbitrary unit, IF = immunofluorescence, MFI = median fluorescence intensity.

3.6.6. CEBPB levels correlate with key clinical attributes of Psoriasis and its positively regulated genes are enriched in the transcriptomes of Psoriasis patients

To further confirm the relevance of our results in patients, we performed correlation analysis revealing that the expression levels of *CEBPB* in lesional skin of CISD patients (n=261) correlated positively with the clinical scores of the two histological attributes 'acanthosis' (r=0.9682, p=0.0318) and 'neutrophils'

(r=0.9710, p=0.0290), thus highlighting the central role of CEBPB in driving the processes of epidermal hyperplasia and skin neutrophil infiltration in patients (Figure 37 A).

Next, I asked whether the *in vitro* generated CEBPB gene signatures could be traced back in patients suffering from Psoriasis (n=90). Indeed, CEBPB positively regulated (i.e. CEBPB-KO down-regulated) genes were clearly enriched in Psoriasis patients (Figure 37 B). Notably, similar results were obtained for the gene signatures generated from either 2D keratinocytes stimulated with IL-17A+TNF-α or 3D skin models stimulated with Pso-TCS. Conversely, CEBPB negatively regulated (i.e. CEBPB-KO up-regulated) genes showed a trend towards enrichment in the non-lesional skin for 2D, whereas no clear enrichment was observed for the 3D-obtained signatures. All in all, these results further confirm our in vitro data and highlight the role of CEBPB as a key disease driver in the Psoriasis pathogenesis.

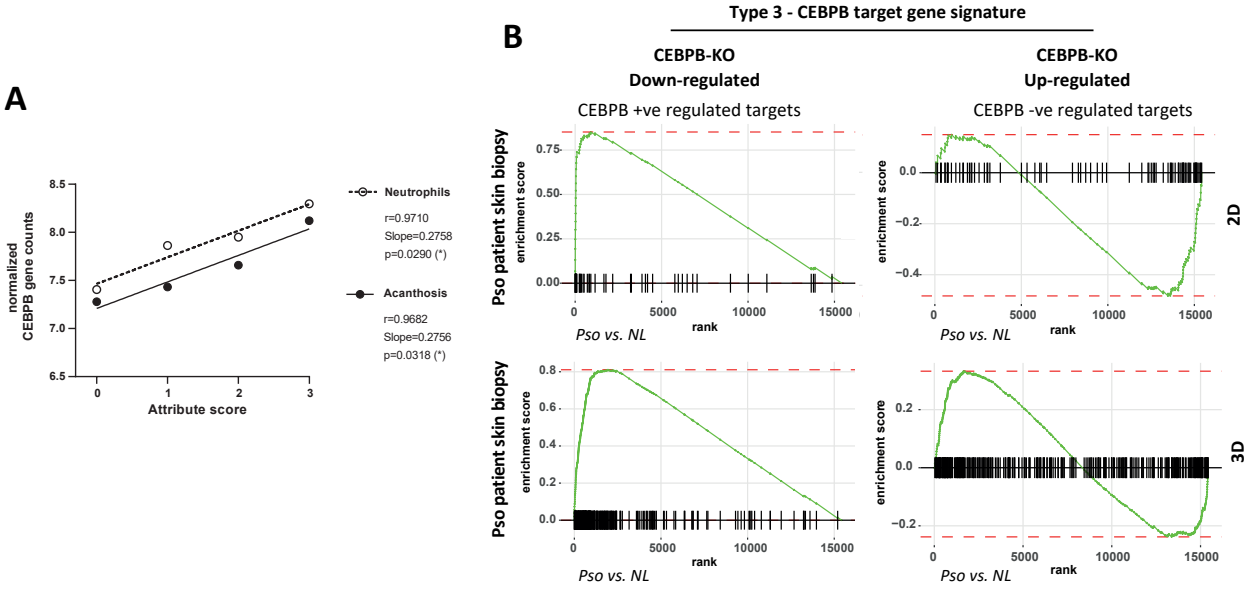

Figure 37: CEBPB correlates with clinical attributes of Psoriasis pathogenesis and its gene signatures are enriched in the transcriptomes of Psoriasis patients. A) Correlation of histological patient scores for the Psoriasis/type 3-associated clinical attributes 'acanthosis' and 'neutrophils' to the CEBPB gene counts from bulk RNAseq of lesional skin from CISD (n=261) patients. Attribute scores were collected from patients biopsies as categorical ordinary data classified as 0 (none), 1 (mild), 2 (moderate) or 3 (severe). Plotted are the means of normalized CEBPB gene counts per attribute score level. Linear regression model was used to test for significance. **B)** GSEA of keratinocyte-specific CEBPB-regulated gene signatures in lesional skin of Psoriasis (n=90) patients. DEGs obtained from 2D and 3D CEBPB-KO keratinocytes under type 3 (IL-17A+TNF-α, Pso-TCS) conditions were used as input for enrichment analysis in the DEGs of lesional skin of Psoriasis (type 3) patients relative to non-lesional (NL) skin. GSEA = Gene set enrichment analysis, TCS = T-cell supernatant, Pso = Psoriasis, KO = knockout, DEGs = differentially expressed genes, NL =non-lesional.

3.7. Functional validation of CEBPB role in Atopic Dermatitis

In contrast to Psoriasis, CEBPB positively regulated genes obtained from AD-TCS stimulated 3D models were negatively enriched in the skin of AD patients (n=48) or showed no clear enrichment for the signatures of 2D IL-4+IL-13 stimulated keratinocytes (Figure 38 A). Interestingly, CEBPB negatively regulated genes from both 2D and 3D AD-disease models, on the other side, were clearly positively enriched in AD patients compared to the non-lesional (NL) skin, implying that CEBPB might be playing a role in suppressing type 2 inflammation rather than driving it like in the case of Psoriasis. Nevertheless, on the contrary to Psoriasis, CEBPB-KO in 3D AD skin models did not show significant histological effects, besides a slight reduction in acanthosis, and was therefore not investigated further (Figure 38 B).

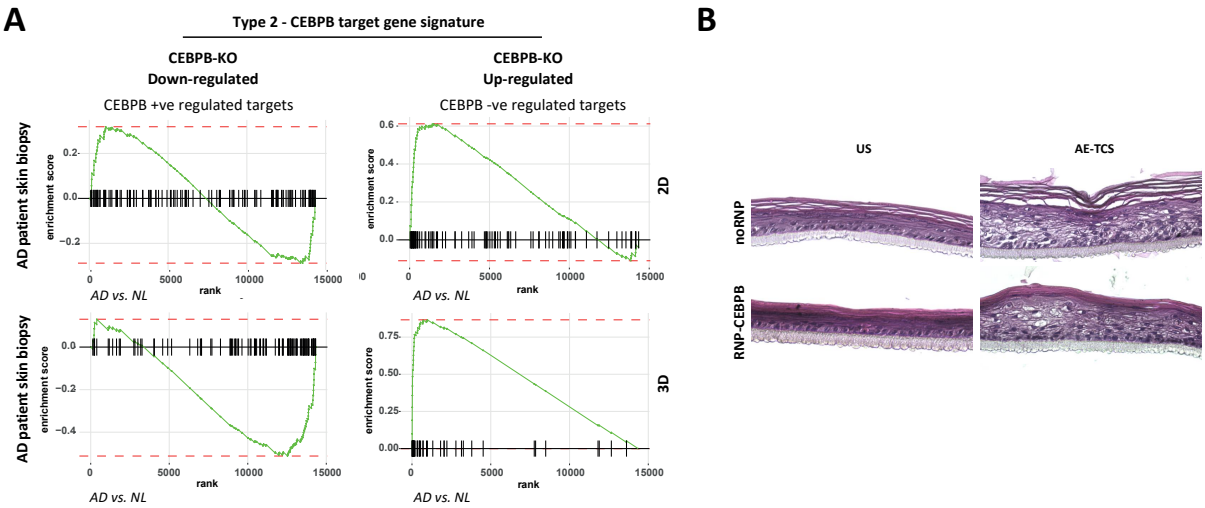

Figure 38: CEBPB negatively regulated target gene signatures are enriched in AD patients and its knockout does not affect 3D AD disease models histologically. A) GSEA of keratinocyte-specific CEBPB-regulated gene signatures in lesional skin of AD (n=48) patients. DEGs obtained from 2D and 3D CEBPB-KO keratinocytes under type 2 (IL-4+IL-13, AD-TCS) conditions were used as input for enrichment analysis in the DEGs of lesional skin of AD (type 2) patients relative to non-lesional (NL) skin. **B)** H&E staining for histological characterization of CEBPB-KO (RNP-CEBPB) 3D models compared to noRNP control under type 2 AD-TCS stimulation. GSEA = Gene set enrichment analysis, TCS = T-cell supernatant, KO = knockout, DEGs = differentially expressed genes, NL =non-lesional, RNP= Ribonucleoprotein complex, H&E= hematoxylin and eosin.

3.8. Functional validation of CEBPB role in Lichen

Finally, we wanted to functionally validate the role of CEBPB in type 1 skin inflammation. Various genes involved in Lichen-relevant pathways such as 'Interferon/ interferon gamma signaling', 'TNF signaling pathway', 'complement cascade' and 'inflammasomes' were negatively enriched in the CEBPB-KO as highlighted by the Cnetplot showing the pathway analysis (PA) performed on CEBPB-KO keratinocytes under IFN-γ+TNF-α stimulation (Figure 39).

3.8.1. Various IFN-γ response genes and type 1-relevant inflammatory factors are dependent on CEBPB

Indeed, CEBPB loss under type 1 conditions (IFN-γ+TNF-α, LE/LP-TCS) led to a clear suppression of various key IFN-γ response genes such as the anti-viral response genes *ISG20* (FC= -1.77, p=0.03), *IFIT2* (FC= -2.07, p=0.03), *IFITM1* (FC= -1.23, p=0.0004) and *IFITM2* (FC= -2.5, p=0.0002), known to be involved in cell cycle arrest and in mediating apoptosis downstream of IFN-γ (Figure 40 A). The intercellular adhesion molecule 1 (ICAM1) is known to be upregulated by IFN-γ in the skin and to act as an important initiator of leukocyte-keratinocyte interactions in many inflammatory skin diseases, potentiating cell adhesion and inflammation, whereas the interferon regulatory factor 1 (IRF1) acts as a master transcriptional activator of interferon-mediated immune responses and apoptosis. Notably, both of these two classical IFN-γ induced genes, were significantly (*ICAM1*, FC= -1.4, p=3,48E-05) and (*IRF1,* FC= -1.4, p=0.015) downregulated in CEBPB-KO 3D skin models specifically with the LE/LP-TCS stimulation compared to the noRNP control, further highlighting CEBPB's role in mediating the classical IFN-γ inflammatory response in keratinocytes (Figure 40 A).

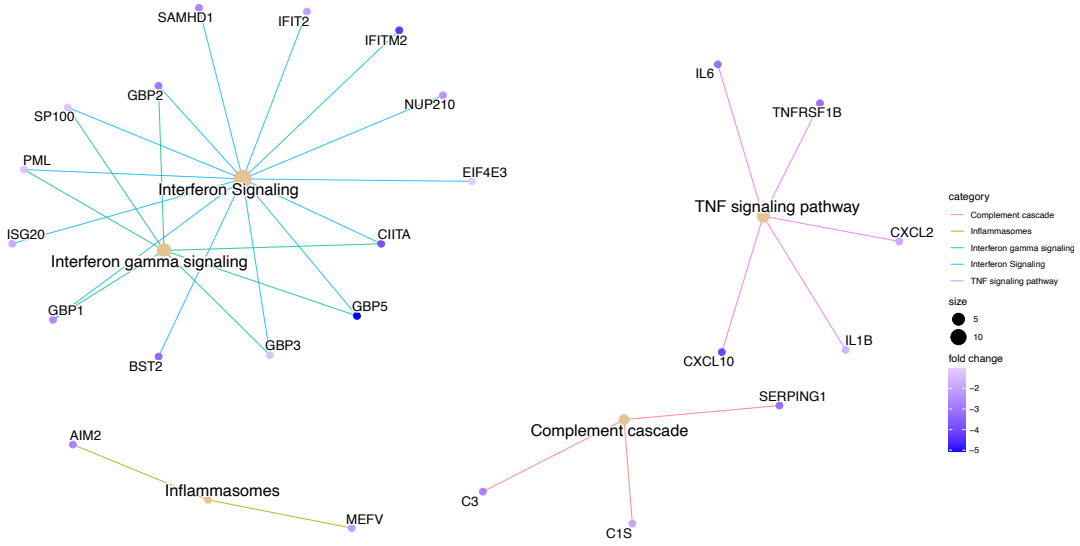

Figure 39: CEBPB regulates the key pathways of IFN, TNF and complement signalling, as well as inflammasomes under type 1 inflammatory conditions. Cnetplot of top significantly enriched pathways (PA) from ORA analysis performed on differentially expressed genes (DEGs) obtained by bulkRNA Sequencing of CEBPB-KO compared to wild-type (noRNP) 2D keratinocytes (n=4) under IFN-γ+TNF-α. Displayed are the top enriched pathways as central nodes with the node size indicating the amount of associated genes shown with their respective fold changes. DEGs = differentially expressed genes, KO = knockout, FC= fold-change, RNP = Ribonucleoprotein complex, PA = pathway, ORA= Overrepresentation analysis.

Focusing on the inflammatory secretome of keratinocytes, we observed that the CEBPB-KO significantly downregulated key Lichen marker chemokines like *CXCL9* (LE/LP-TCS, p=0.0002), known to selectively attract Th1 lymphocytes, as well as *CXCL10* (LE/LP-TCS, p=0.0073) and *CXCL11* (LE/LP-TCS, p=0.02), which are key attractants for CD4+ T-cells, under both basal (US, 2D) and type 1 conditions (IFN-γ+TNF-α, LE/LP-TCS) (Figure 40 B, D). Moreover, similar effects were observed for other type 1-relevant factors like *IL12B*, which favors Th1 responses, *CCL17*, which specifically attracts T-cells, *CCL19*, attracting both lymphocytes and DCs, as well as *CCL8*, which not only attracts lymphocytes, but also monocytes, basophils and eosinophils, all suppressed in the CEBPB-KO keratinocytes compared to the noRNP control (Figure 40 B, D).

As for genes regulated under the 'complement cascade pathway', the expression of *C1S*, *C3* and *SERPING1* was strongly inhibited under both basal and type 1 stimuli (Figure 40 A,C, D). Indeed, the C1 complement inhibitor *SERPING1,* which is known to be strongly induced by IFN-γ, was among the top differentially regulated genes upon loss of CEBPB especially under steady-state yielding a log2FC of -4.33 (US, p=0.003) and log2FC of -3.17 and -1.28 under IFN-γ+TNF-α (p=0.001) and LE/LP-TCS (p=0.0034), respectively (Figure 40 A, C). Notably, the complement C3a receptor 1 *C3AR1,* whose high expression correlated with high immune infiltration in cancer, was significantly suppressed (p=0.0002) specifically in CEBPB-KO 3D skin models under LE/LP-TCS (Figure 40 C, D).

Altogether, these results unravel CEBPB as a key regulator of the keratinocytes inflammatory secretome under type 1 conditions, affecting various key factors for the recruitment of immune cells to the skin.

A

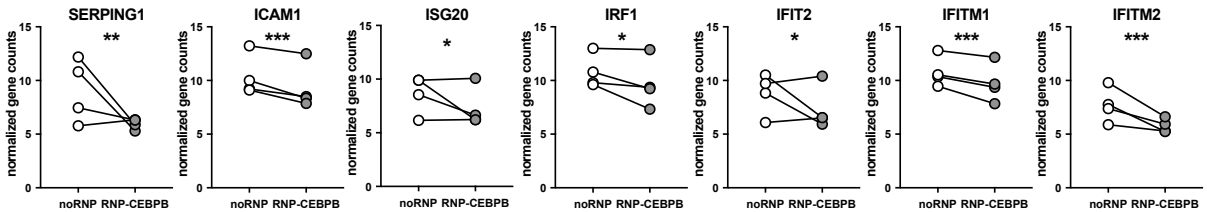

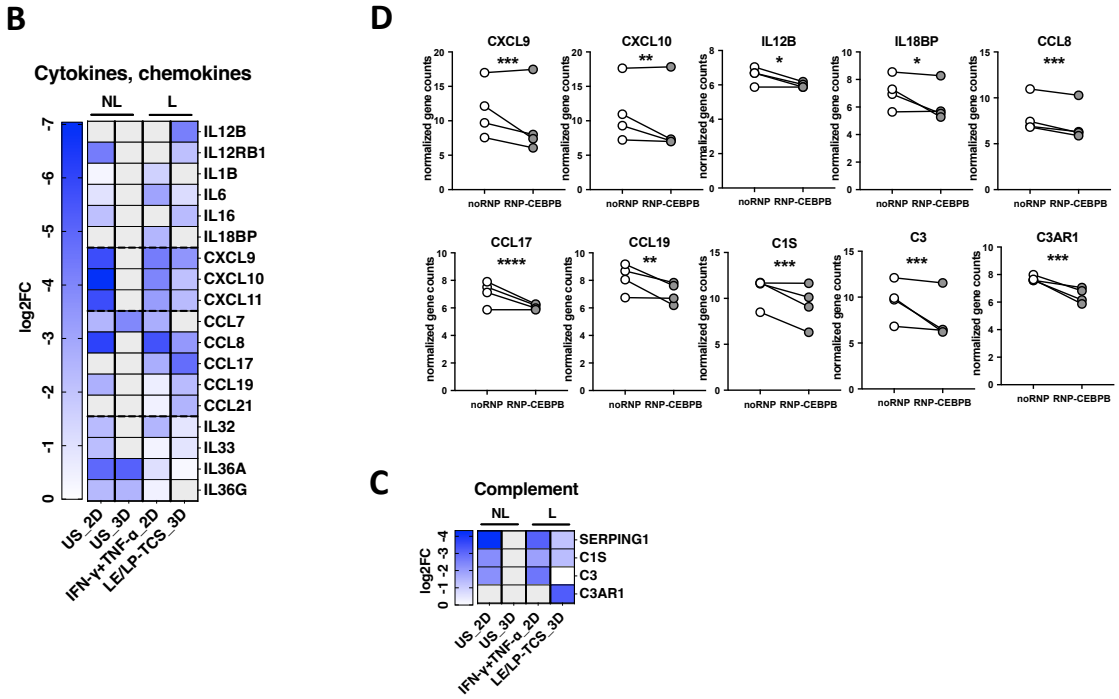

Figure 40: Various IFN-γ response genes and type 1-relevant secreted factors are dependent on CEBPB for their expression. A) and **D)** Normalized gene counts of IFN-γ response genes (A) and cytokines, chemokines and complement factors (D) in the CEBPB-KO (RNP-CEBPB) and control (noRNP) keratinocytes under the type 1 conditions (IFN-γ +TNF-α, LE/LP-TCS) measured by bulk RNAseq (n=4). **B)** and **C)** Heatmaps of differentially expressed genes (DEGs) in the CEBPB-KO compared to the noRNP control for 2D and 3D keratinocytes under depicted type 1 stimuli in comparison to unstimulated (US) basal conditions. DEGs were filtered for the functional groups of 'cytokines and chemokines' (B) and complement factors 'complement' (C) displaying significantly (p-value <=0.05) dysregulated genes with blue= downregulated, white= not regulated and grey=not significant. Significance calculation for the comparison between RNP-CEBPB and noRNP was performed using DESeq2 for all RNAseq data with *p<0.05, **p<0.01, ***p<0.001, ****p<0.0001. US = unstimulated, FC= fold-change, RNP = Ribonucleoprotein complex., TCS= T-cell supernatant.

3.8.2. CEBPB regulates different cell death pathways and drives keratinocytes apoptosis under lichenoid inflammatory conditions

Given the negative enrichment of different cell death pathways like 'Programmed cell death', 'apoptosis' and 'intrinsic pathway for apoptosis' in ORA analysis performed with pre-defined pathways on the CEBPB-KO 3D skin models under LE/LP-TCS stimulation (Figure 41 A), I next aimed to investigate the effects of CEBPB on keratinocytes cell death more closely.

Here, loss of CEBPB led to dysregulation of various genes involved in different cell death pathways under both steady-state (US) and type 1 conditions (Figure 41B). For instance, the inflammasome genes *MEFV* (IFN-γ +TNF-α, FC= -2.10, p=0.0077), *AIM2* (IFN-γ +TNF-α, FC= -2.75, p=0.006) and *CASP1* (US, FC= -1.96, p=0.008) were significantly downregulated upon loss of CEBPB (Figure 41B, C).

Additionally, the autophagy gene *KLK12* (p=0.002), as well as the apoptosis regulating PML bodies genes *SP100* (p=0.04) and *PML* (p=0.04) were significantly suppressed in the CEBPB-KO compared to the noRNP control (Figure 41 B, C). Furthermore, various pro-apoptotic genes like *XAF1* (p=2,84E-05), a key IAP inhibitor and the death-associated kinase *DAPK2* (p=0.007), but also *KLK10* (p=1,61E-07) and *PARP 3/9* (p=0.014/0.02) were downregulated, whereas key anti-apoptotic genes like *BCL2* (p=0.024) and *BCL2L12* (p=0.035) were upregulated in CEBPB-KO keratinocytes, indicating an overall inhibition of apoptosis upon loss of CEBPB (Figure 41 B, C).

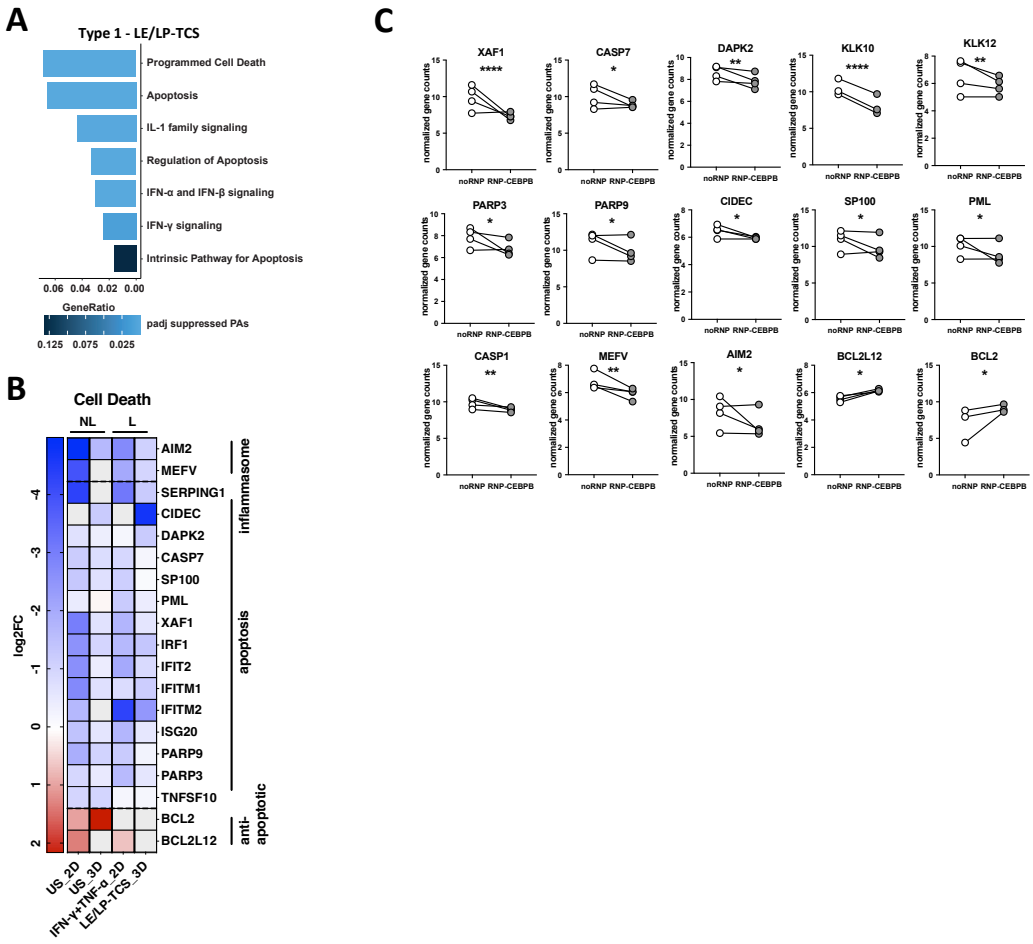

Figure 41: CEBPB regulates various genes involved in different cell death pathways like inflammasomes and apoptosis under type 1 inflammatory conditions. **A)** Top significantly enriched pathways with a function relevant to 'cell death' are displayed from an ORA analysis with prefiltered pathways performed on the DEGs of CEBPB-KO 3D skin models stimulated with LE/LP-TCS compared to noRNP control. **B)** Heatmap of differentially expressed genes (DEGs) in the CEBPB-KO compared to the noRNP control for 2D and 3D keratinocytes under depicted type 1 conditions in comparison to unstimulated (US) basal conditions. DEGs are filtered to include genes with function in 'cell death' and further subdivided according to their role and to the cell death pathways they are involved in. Displayed are significantly dysregulated genes (p=0.05) with red= upregulated, blue= downregulated, white= not regulated and grey=not significant. **C)** Normalized gene counts of cell death genes in the CEBPB-KO (RNP-CEBPB) and control (noRNP) keratinocytes under the basal (US) and type 1 conditions (IFN-γ +TNF-α, LE/LP-TCS) measured by bulk RNAseq (n=3-4). (US): CASP1, XAF1, KLK10, BCL2, BCL2L12, CASP7 and (IFN-γ +TNF-

α): MEFV, AIM2, KLK12, SP100, PML and PARP3/9 and (LE/LP-TCS): DAPK2, CIDEC. US = unstimulated, TCS = T-cell supernatant, FC= fold-change, PA = pathway, DEGs = differentially expressed genes, ORA= overrepresentation analysis, padj= adjusted p-value, RNP = Ribonucleoprotein complex. Significance calculation for the comparison between RNP-CEBPB and noRNP was performed using DESeq2 for all RNAseq data with *p<0.05, **p<0.01, ***p<0.001, ****p<0.0001.

In order to functionally validate the described transcriptome effects, I used 3D Lichen skin models to mimic the processes of apoptosis and necroptosis *in vitro*, where primary keratinocytes were stimulated with the LE/LP-TCS alone for apoptosis/ cell death induction or together with SMAC (S) and Z-VAD (Z), which combined shift the cell death more towards necroptosis (Figure 42 A). While in the noRNP control apoptotic cells were dominantly present upon LE/LP-TCS stimulation, in the CEBPB-KO the induction of apoptosis was completely abolished (Figure 42 A) and the number of quantified apoptotic cells was significantly reduced from 43 ± 5 cells (noRNP) to 3 ± 2 cells (RNP-CEBPB, p<0.0001) (Figure 42B). In the necroptosis model, however, necroptotic cells were still detected after loss of CEBPB (Figure 42 A), indicating that CEBPB is likely mediating keratinocytes apoptosis rather than necroptosis under lichenoid conditions. Consistent with the described CEBPB role in acanthosis, also here under type 1 inflammatory conditions, the thickness of the CEBPB-KO models was reduced when compared to the noRNP counterparts (Figure 42 A).

Additionally, CEBPB loss was found to downregulate the gene expression of pro-inflammatory cytokine *IL1B*, which is an indicator of both cell death and inflammasome activation (Figure 42 C). To further confirm the role of CEBPB in the regulation of cell survival and death, I performed an MTS- cell viability assay on primary keratinocytes treated with apoptosis (IFN-γ+TNF-α+S or LE/LP-TCS+S)- and necroptosis (IFN-γ+TNF-α+SZ or LE/LP-TCS+SZ)- favoring conditions, finding that the CEBPB-KO cells had an overall enhanced viability compared to the noRNP control with the strongest effects observed in the unstimulated (US) condition (Figure 42 D). To confirm the observed RNA effects of *IL1B* on protein level, since IL-1ß is known to be actively secreted by cells undergoing cell death, I measured the IL-1ß levels in the supernatant of these keratinocytes revealing a significant reduction in the CEBPB-KO relative to the noRNP under both apoptosis- favoring conditions (LE/LP-TCS+S: 42% ± 25%, p=0.019), as well as under steady-state (US: 75% ± 7%, p=0.0007), but not under necroptotic conditions (Figure 42 D). Furthermore, the levels of classical apoptosis markers like cleaved caspase 3 were clearly reduced in the RNP-CEBPB apoptosis conditions compared to the control (Figure 42 E). Also, the cleaved PARP protein as a marker for activated caspases was slightly reduced in the CEBPB-KO conditions, while the pRIPK1 levels were rather comparable between the KO and control (Figure 42 E).

Taken together, these results identify CEBPB as a key regulator of cell death pathways and reveal its role in promoting keratinocytes apoptosis under type 1 inflammatory conditions.

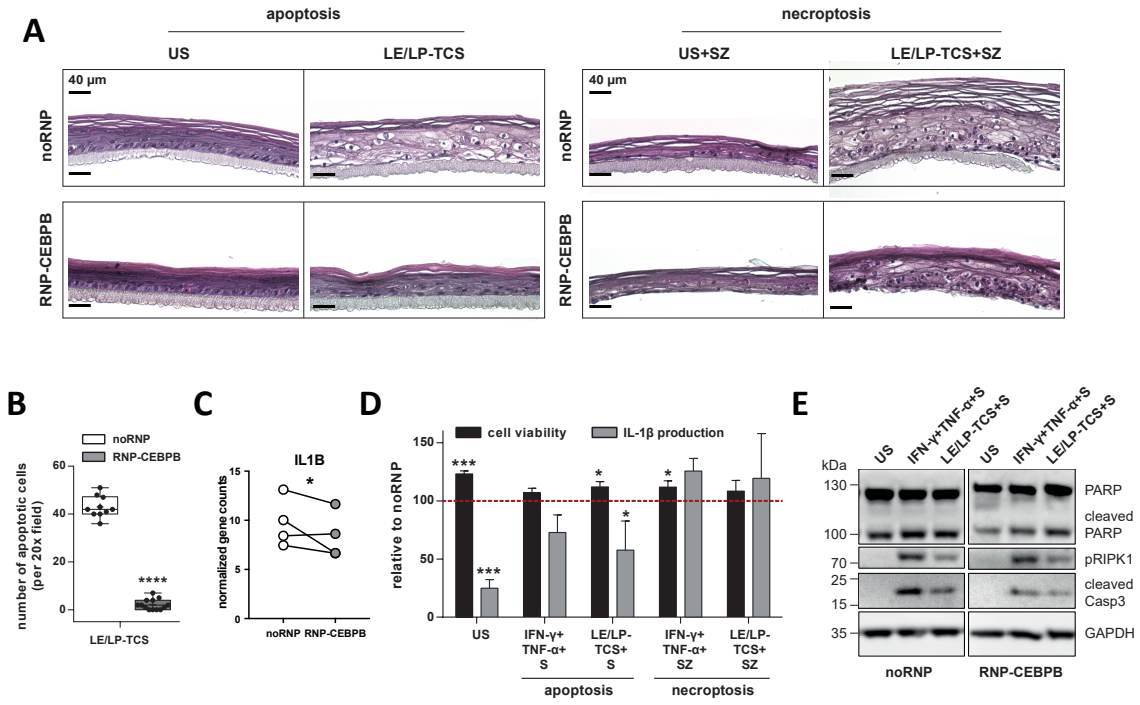

Figure 42: CEBPB-KO keratinocytes fail to undergo apoptosis, have enhanced cell viability and downregulated IL-1ß secretion under lichenoid microenvironment. A) H&E staining of cell death/apoptosis and necroptosis 3D models with wild-type (noRNP) and CEBPB -KO (RNP-CEBPB) keratinocytes left unstimulated (US) or stimulated with the LE/LP-TCS alone or in combination with SMAC and ZVAD for 72h. **B)** Quantification of apoptotic cells from the cell death/apoptosis models with LE/LP-TCS stimulation for the CEBPB-KO compared to noRNP condition (n=11). **C)** Normalized gene counts of *IL1B* in the CEBPB-KO (RNP-CEBPB) and control (noRNP) 2D keratinocytes under IFN-γ +TNF-α condition measured by bulk RNAseq (n=4). **D)** Cell viability, measured by MTS assay, and IL-1ß protein levels, measured by ELISA, of 2D CEBPB-KO keratinocytes stimulated with the indicated apoptosis- or necroptosis-inducing conditions or left unstimulated (US) as a control. Values are shown as percentages relative noRNP. **E)** Western blot analysis of apoptosis markers in noRNP and CEBPB-KO (RNP-CEBPB) keratinocytes stimulated with the depicted apoptosis-favouring conditions (IFN-γ +TNF-α+S, LE/LP-TCS+S) for 24h. Significance calculation for the comparison between RNP-CEBPB and noRNP was performed using DESeq2 for all RNAseq data with *p<0.05. Unpaired t-test with Welch correction (**** p<0.0001) and Ordinary one-way ANOVA uncorrected Fisher's LSD test (*p<0.05, ***p<0.00001) were used for (B) and (D), respectively. S= SMAC, Z= ZVAD, SZ= SMAC+ZVAD, US = unstimulated, TCS = T-cell supernatant, RNP= Ribonucleoprotein complex, KO=knockout, Casp3= Caspase 3.

3.8.3. CEBPB levels correlate with interface dermatitis and its positively regulated target signatures are enriched in Lichen patients

Finally, given that these keratinocytes cell death features make up the clinical attribute of interface dermatitis (ID) at the junction of dermis and epidermis, we checked for a connection of CEBPB levels with this phenotype and indeed detected a positive correlation ($r=0.9514$, $p=0.0246$) between the expression of *CEBPB* in the lesional skin of LE/LP patients (n=41) and the medical score of interface dermatitis collected from those patients biopsies (Figure 43 A).

Additionally, similar to Psoriasis, also here we could trace back our *in vitro* generated CEBPB-target gene signature in Lichen patients showing a clear positive enrichment in the disease compared to the non-lesional (NL) skin for CEBPB positively regulated targets of both 2D IFN-γ+TNF-α stimulated keratinocytes and 3D LE/LP-TCS stimulated skin models (Figure 43 B). CEBPB negatively regulated targets, on the other hand, did not show any enrichment effects.

In summary, we assigned critical roles for CEBPB in regulating type 1 skin inflammation on various levels, hence contributing to the clinical manifestation of interface dermatitis in Lichen patients, and demonstrated an enrichment for CEBPB targets in those patients, further underlining CEBPB's role in Lichen pathogensis.

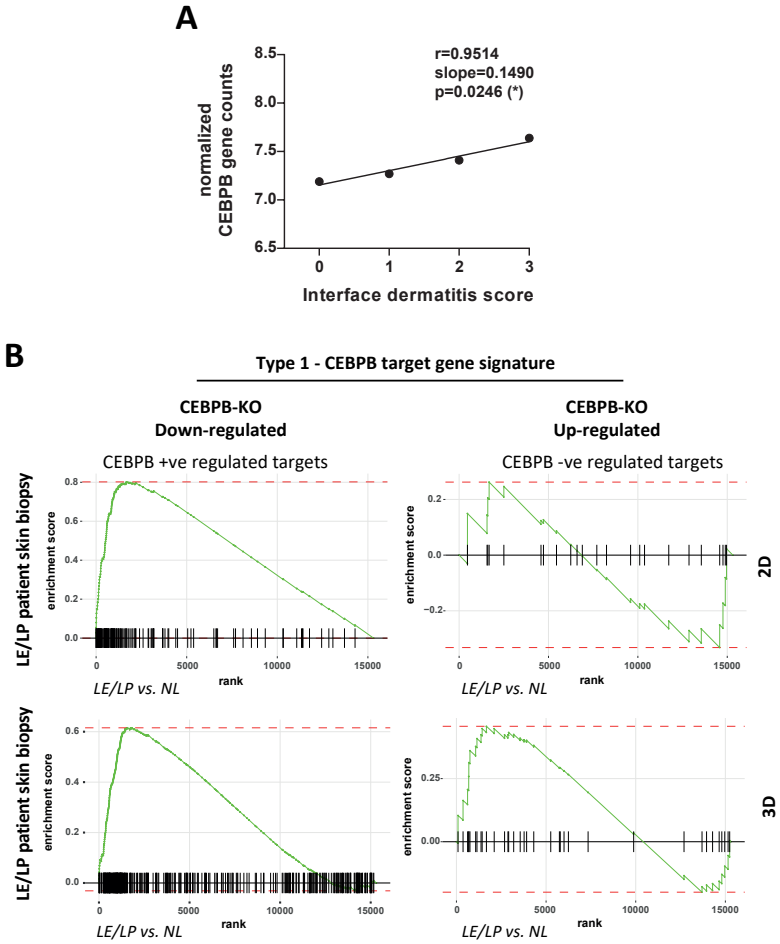

Figure 43: CEBPB levels correlate with interface dermatitis and its positively regulated target gene signatures are enriched in Lichen and Lupus patients. A) Correlation of histological patient scores for the Lichen/type 1-associated clinical attribute 'interface dermatitis' to the CEBPB gene counts from bulk RNAseq of lesional skin from LE/ LP (n=41) patients. Attribute scores were collected from patients biopsies as categorical ordinary data classified as 0 (none), 1 (mild), 2 (moderate) or 3 (severe). Plotted are the means of normalized CEBPB gene counts per attribute score level. Linear regression model was used to test for significance. **B)** GSEA of keratinocyte-specific CEBPB-regulated gene signatures in lesional skin of Lichen and Lupus (LE/LP) (n=41) patients. DEGs obtained from 2D and 3D CEBPB-KO keratinocytes under type 1 (IFN-γ+TNF-α, LE/LP-TCS) conditions were used as input for enrichment analysis in the DEGs of lesional skin of Lichen and Lupus (type 1) patients relative to non-lesional (NL) skin. GSEA = Gene set enrichment analysis, TCS = T-cell supernatant, LE= Lupus erythematosus, LP=Lichen planus, KO = knockout, DEGs = differentially expressed genes, NL =non-lesional.

4. Discussion

4.1. CEBPB as a novel hub transcription factor in psoriatic skin

Transcription factors have evolved as key regulators in multiple diseases. In this project, I investigated CEBPB as a master transcription factor in primary human keratinocytes. CEBPB was identified as one of the most connected transcription factors in psoriatic skin. Analysis of CEBPB interaction partners revealed various key transcription factors that have been assigned a role in skin inflammation such as STAT1/3, JUNB, FOSL1, HIF1A and NFκB. Indeed, as previously mentioned, one of the key characteristics of CEBPB is its ability of interaction and heterodimerization with various proteins, hence expanding its repertoire of target genes. Our results are in line with previous findings showing an interaction of CEBPB with members of the AP1 family, as well as with STAT3 and NFκB (Lee et al. 2021; Swoboda et al. 2021; Akira and Kishimoto 1997; Ramji and Foka 2002). STAT3 is one of the best-studied transcription factors in Psoriasis pathogenesis, where its hyperactivation has been reported in almost every cell type involved in disease initiation and progression. In keratinocytes STAT3 hyperactivation drives proliferation and epidermal hyperplasia, reduces keratinocytes differentiation and promotes the secretion of various pro-inflammatory mediators (Calautti, Avalle, and Poli 2018; Kishimoto et al. 2021; Sano et al. 2005). NFκB is a pleiotropic transcription factor with well-established role in inflammation. Cooperative function of CEBPB with NFκB has been described for driving the expression of several pro-inflammatory cytokine genes like *IL6*, *TNF* and *IL8* (Matsusaka et al. 1993; B. Stein and Baldwin 1993). Transcriptional machinery in Lichen planus is much less studied in comparison to Psoriasis, making the identification of novel transcriptional disease drivers highly relevant. Here, besides NFκB, the IFN-γ responsive transcription factors STAT1 and IRF1 have been described as hubs (Lauffer et al. 2018)

4.2. CEBPB is upregulated in the lesional skin of Lichen and Psoriasis patients

Using bulk RNASeq analysis, I could show that CEBPB is upregulated in the lesional skin of both Psoriasis (Pso) and Lupus/ Lichen (LE/LP) patients compared to the non-lesional skin. Although bulk RNASeq comes with various advantages like lower cost and easier sample library preparation, making it the standard technique for analyzing large patients cohorts, it gives a mixed signal from all cell populations of the skin biopsy for a given gene. Furthermore, it leaves the biologically relevant question of tissue localization unanswered. Therefore, to gain a better understanding of *CEBPB* gene expression within tissue and cellular context, I performed further transcriptomics techniques, namely spatial transcriptomics and single-cell RNASeq (scRNASeq).

CEBPB is enriched in the epidermis and highly expressed by keratinocytes

Spatial transcriptomics allows to study gene expression within the local tissue microenvironment, which can be critical for investigating effects on tissue response, as well as for linking gene expression to certain histological features. The spatial results showed clear epidermal enrichment for the CEBPB expression in lesional skin, indicating the potential role of CEBPB within the epidermal pathogenic response. This was further confirmed at cellular resolution, where scRNASeq analysis revealed keratinocytes among the cell clusters with highest *CEBPB* expression in Psoriasis and Lichen. Other CEBPB-high expressing cell populations were fibroblasts and APCs (Macrophages, Monocytes, DCs), followed by T-cells. Given their role as main disease drivers in the epidermal compartment, on the one hand, and the fact that the expression and function of CEBPB is less-studied there compared to the other cell types, I was prompted to characterize the function of CEBPB specifically in keratinocytes. On protein level, one study showing IHC analysis of CEBPB expression in psoriatic skin, describes preferential expression in differentiated keratinocytes (Chiricozzi et al. 2014), which could not be detected neither in our IHC data, nor on gene level in sc data from Pso patients. In fact, our sc data revealed that proliferating psoriatic keratinocytes undergo changes in their CEBPB expression, upregulating CEBPB as they progress through the cell cycle. Also, our spatial and IHC data showed supporting results, with strong CEBPB protein expression in both basal, as well as differentiated keratinocytes. One explanation could be the specificity of the used CEBPB antibody in either detecting all isoforms (LAP*, LAP, LIP) as in our case or preferentially detecting the longer isoforms (LAP*, LAP), which is likely the case in the described study, hence yielding different isoform-dependent expression patterns for CEBPB. Indeed, internal data generated in this project (data not shown) showed distinct expression patterns for the CEBPB isoforms with the LAPs being preferentially expressed in the upper differentiated layers and LIP in the basal layer of the epidermis, hence supporting this explanation.

CEBPB shows prominent expression in fibroblasts and T-cells

As already described, CEBPB's role has been best-studied in myeloid cells (Y.-C. Lu et al. 2009; Natsuka et al. 1992; Huber et al. 2012; Ramji and Foka 2002). However, it would be interesting to investigate the function of CEBPB specifically in dermal fibroblasts and lesional T-cells in context of skin inflammation. Our results from bulk RNASeq of CEBPB-KO keratinocytes revealed the regulation of various genes involved in ECM organization, cell adhesion and collagen production. Since fibroblasts are the main specialized cells for ECM production, it would be therefore interesting to check the function of CEBPB within this context. Moreover, CEBPB has been assigned a role in tissue repair and fibrosis, however with a focus on the role of myeloid cells. Here, a novel subset of monocytes responsible for mediating fibrosis was described to be under the control of CEBPB for their

differentiation and mice with *Cebpb -/-* hematopoietic cells were indeed resistant to fibrosis (Satoh et al. 2017). Moreover, a TGF-β-CEBPB axis was shown to play a central role in pulmonary fibrosis, where knockdown of CEBPB attenuated myofibroblast differentiation and ECM deposition (Ding et al. 2021). Thus, fibroblast proliferation, deposition of excessive pathological ECM and scar formation represent interesting processes that can be studied in connection to CEBPB in fibroblasts, especially within the context of type 4 fibrogenic inflammatory skin diseases. Additionally, T-cell intrinsic functions of CEBPB have not been characterized in-depth neither in humans nor in mice. So far, the effects described for CEBPB on T-cells derived from mouse models, are not cell-intrinsic, but rather mediated indirectly by macrophages (J. Dai et al. 2017). Together with our sc data, our IHC results showing CEBPB protein expression in the immune infiltrate of Pso and LE/LP patients provide further evidence for the potential role of CEBPB in skin lesional T-cells, which make up most of the immune infiltrate.

4.3. CEBPB is responsive to type 1/3-cytokine microenvironments *in vitro* in primary human keratinocytes

CEBPB has been described to be responsive to various cytokine signals (Cardinaux, Allaman, and Magistretti 2000; Niehof et al. 2001; Tengku-Muhammad et al. 2000). Previous studies showed that IL-17A induces CEBPB and that functional cooperation between IL-17A and TNF-α has been described to be mediated by CCAAT/enhancer binding protein family members (Chiricozzi et al. 2014; Ruddy et al. 2004). In primary human keratinocytes, I could show similar synergistic effects of TNF-α with both IFN-γ and IL-17A in the induction of CEBPB, with the combination IL-17A+TNF-α yielding the strongest upregulation on both RNA and protein levels. Induction of CEBPB by IL-1ß was less strong, however it could still be interesting to follow-up, especially with respect to synergism with IL-17A and TNF-α, within the context of Hidradenitis suppurativa (HS), where IL-1ß is elevated and pathogenic IL-1 family signaling is described (Del Duca et al. 2020).

Kinetics of CEBPB protein expression revealed differential temporal isoform regulation with LIP showing short-term ('fast') dynamic changes in its expression levels, implying that the isoforms might be employing different mechanisms for their transcriptional function. In this frame, LIP reacts to immunogenic stimuli like IL-17A with rapid induction as seen from our data, this likely translates into long-term temporal regulation of its target genes, indicating that low of levels of LIP over a shorter period of time is sufficient for this isoform to mediate its downstream effects, whereas the LAPs, specifically LAP*, seem to employ a 'slow dynamics' approach to gene regulation, requiring their induced levels to be kept longer to mediate their cellular effects. This dynamics approach to gene

regulation has been proposed by different studies for other transcription factors (Swift and Coruzzi 2017; C. Li et al. 2018) and would be interesting to validate for CEBPB.

3D skin equivalents represent a powerful tool in human skin research to model disease pathology in an *in vitro* setting. In this project, stimulation of 3D models with lesional TCS derived from patients compared to rh cytokines yielded better induction of disease-specific histological features and were therefore chosen as a more physiological model to study the expression and function of CEBPB. However, one limitation of these models comes from the heterogeneity of the TCS cytokine composition, which is on the one hand characteristic for CISD diseases, but on the other hand adds another layer of complexity when trying to study the effects of specific cytokines. Therefore, to retrieve this information, 2D keratinocytes were stimulated with rh cytokines, while 3D models were stimulated with the patients TCS to study CEBPB within both contexts. CEBPB was hence similarly induced by LE/LP- and Pso-TCS on both RNA and protein levels. Moreover, clear upregulation of CEBPB was observed with IL-22 alone, which has not been described as an inducer of CEBPB in any tissue so far. IL-22 has important functions in innate host defense at mucosal and epithelial surfaces such as intestine, lung and skin (Shabgah et al. 2017). Importantly, this implicates CEBPB in other pathological conditions, where IL-22 plays a role, such as rheumatoid arthritis (RA), multiple sclerosis (MS) and interstitial lung diseases. Moreover, IL-22 is central for inducing cell proliferation and inhibition of apoptosis, which has positive effects in mediating tissue regeneration, but negative effects contributing to tissue hyperplasia and tumor growth (Shabgah et al. 2017). This implies CEBPB to have a role in both, physiological IL-22 mediated tissue repair and pathogenic hyperplasia, with the latter being confirmed by our results in this project in context of acanthosis.

4.4. A CEBPB-dependent keratinocyte-specific gene signature under different inflammatory conditions

So far, except for few studies, not much is known about the function of CEBPB as a transcription factor in human keratinocytes. For instance, CEBPB has been described to repress p63 during keratinocyte differentiation and to regulate CCL20 gene expression in inflammation (Antonini et al. 2015; Sperling et al. 2012). Therefore, a main aim of this project, was to generate a global overview of CEBPB target genes in keratinocytes and to investigate the transcriptional landscape of CEBPB under both homeostatic and inflammatory conditions. This does not only give valuable insight into the role of CEBPB in keratinocytes, but also reveals multiple downstream targets that might be interesting for further validation either as biomarkers or disease drivers, hence providing a framework for other follow-up studies. Examples of these targets will be discussed for each disease pattern in the following

sections. In general, the results obtained from bulk RNA Seq analysis of CEBPB-KO keratinocytes showed strong stimulus-dependency adding to the complexity of investigating the role of CEBPB within the skin and underlining the multi-functionality of this transcription factor. Importantly, results from this analysis also revealed interesting information concerning which models are more appropriate for studying certain pathways in the skin. For example, cytokine production and metabolism are best-studied in 2D keratinocytes, whereas keratinization, AMP production and ECM organization in 3D keratinocyte models.

4.5. CEBPB in Psoriasis

4.5.1. CEBPB as a control point for keratinocytes inflammatory secretome and driver of neutrophil migration

Loss of CEBPB lead to the downregulation of various type 1 and 3 cytokines and chemokines, while upregulating type 2 factors, highlighting the role of CEBPB as a positive regulator for type 1/3-specific secretome and as a suppressor for type 2-specific secretome in keratinocytes under psoriatic microenvironment. This implies CEBPB's action in skewing the inflammatory response towards type 3 and away from type 2 during Psoriasis pathogenesis. In line, type 3 relevant cytokine pathways like 'TNF signaling' and 'IL17 signaling' were positively regulated by CEBPB. These results are confirmed by similar findings from keratinocytes (Chiricozzi et al. 2014), as well as from other tissues like myeloid tissue (Pope, Leutz, and Ness 1994), bone (Shen et al. 2005), liver and smooth muscle (Akira et al. 1990; Patel et al. 2007) describing CEBPB's role in those two pathways.

Moreover, the suppressive effects observed on the 'neutrophil degranulation' pathway with inhibition of various neutrophil chemoattractants (e.g. CXCL1, CXCL5, CXCL8) on both RNA and protein level were detected specifically under the stimuli IL-17A+TNF-α and IL-22, but not under type 1/ 2 stimuli or with the Pso-TCS, probably due to the described TCS heterogeneity issue. A similar role for CEBPB in neutrophil attraction to the site of inflammation has been described for the lung. Using both murine models and human samples, lung epithelial CEBPB was assigned a role in mediating pulmonary inflammatory immune responses, for example to cigarette smoke, by regulating a variety of processes including induction of pro-inflammatory cytokines and respiratory neutrophil influx via production of chemoattractants (Didon et al. 2011). In the lung epithelium some of these CEBPB-regulated inflammatory response genes include *IL6*, *IL8 (CXCL8)*, *IL1ß*, growth regulated oncogene (*GRO*α) and serum amyloid A (*SAA*) (Poli 1998; Mukaida, Mahe, and Matsushima 1990; Cassel and Nord 2003).

Another study has also revealed a role for lung CEBPB in driving LPS-induced airway neutrophilia and inflammation via control of CXCL1 expression (Cassel and Nord 2003; Roos et al. 2012).
These studies confirm our data, which show similar effects in the skin. Additionally, our data also reveal novel intrinsic effects of CEBPB on neutrophils activation and migration, since CEBPB-KO in neutrophil-like cells hampered their ability to migrate efficiently towards an IL-8 gradient.

4.5.2. CEBPB effects on ECM organization and cell adhesion

The role of CEBPB within the context of ECM organization has not been well-described so far. Here, I identify CEBPB to be central regulating the expression of various ECM and cell adhesion genes, a function that is quite important in the skin to maintain skin homeostasis. Specifically, under IL-22, CEBPB is involved in the positive regulation of these processes. IL-22 alone is responsible for tissue homeostasis and wound repair and is therefore a main trigger for ECM production, activating the expression of various ECM and adhesion genes (McGee et al. 2013; Shabgah et al. 2017). IL-22 can also induce the expression of different extracellular matrix (ECM)-degrading enzymes like the matrix metalloproteinases (MMP)-1 and -3, which are required for epithelial migratory capacity during tissue repair (Wolk et al. 2006) and were found to be downregulated in the CEBPB-KO, indicating that CEBPB loss likely inhibits keratinocytes migration. Therefore, CEBPB acts under this stimulus as an activator in these processes, again underlining a potential role in physiological wound repair in the skin, an interesting aspect for further functional validation. In contrast, under Pso-TCS stimulation, many ECM genes were upregulated upon CEBPB loss, indicating that under psoriatic inflammation, where IL-22 is present in combination with other dominating inflammatory cytokines (e.g. IL-17A, TNF-α, IFN-γ), CEBPB functions rather in the repression of pathogenic ECM remodeling by inhibiting different MMPs, as well as suppressing cell adhesion molecules (e.g. VCAM1, ITGAM), which are known to be upregulated in skin inflammation to mediate the attachment and extravasation of more immune cells.

4.5.3. CEBPB as a driver of acanthosis- effects on keratinocytes proliferation and differentiation

Keratinization, which stands collectively for the processes of keratinocytes proliferation and differentiation, was significantly dysregulated upon loss of CEBPB under both homeostatic and Pso-type conditions.

Proliferation

Our results show that various hyperproliferation-associated KRTs (e.g. KRT6A/B, KRT16, KRT17) were under the regulation of CEBPB for their gene expression. Indeed, these KRTs were strongly suppressed in 3D skin equivalents lacking CEBPB under Pso-TCS stimulation, and represent with the exception of

KRT17, which has been already associated with CEBPB in context of breast cancer (Jinesh, Flores, and Brohl 2018), novel targets of CEBPB that have not been described so far. Moreover, our sc RNASeq results imply the potential involvement of CEBPB in keratinocytes cell cycle checkpoints (e.g. G1/S and G2/M). Similar effects for CEBPB as a cell cycle checkpoint regulator able to mediate cell cycle arrest has been described for renal epithelial cells (N. Yang et al. 2021).

In literature, both positive and negative effects have been described for the role of CEBPB in cell proliferation in different tissues. Pro-proliferative effects have been described for stem cell proliferation in the mammary gland and for the mitotic clonal expansion of preadipocytes during adipogenesis (LaMarca et al. 2010; Chen et al. 2021). Moreover, CEBPB was found to be crucial for the cell cycle acceleration in the life-threatening condition of LPS-induced emergency granulopoiesis, where CEBPB-KO mice failed to increase their circulating neutrophils (Sánchez et al. 2017). In primary human endometrial stromal cells (HESCs) CEBPB was found to promote proliferation by regulating several key cell cycle-factors during the G1-S transition (Wei Wang et al. 2012). They describe the regulation of cyclin D, E, and A, as well as CDKs 2,4 and CDC25C, confirming our results in keratinocytes. In contrast, anti-proliferative function was demonstrated for chondrocytes and cardiomyocytes (Ushijima et al. 2014; Boström et al. 2010). Similarly, mouse models focusing on the skin, showed contradictory results. In contrast to our data, anti-proliferative effects on keratinocytes are reported in some mouse models lacking CEBPB (House et al. 2010; Lopez et al. 2009; S. Zhu et al. 1999).

Differentiation

The early differentiation markers KRT1 and KRT10 were downregulated in the CEBPB-KO keratinocytes under Pso-TCS, implying CEBPB's function as a positive regulator of these keratins expression in the human skin. Indeed, these results are confirmed by findings from mouse models, where *Cebpb* -/- mice showed decreased expression of both KRT 1 and KRT10, but not of involucrin and loricrin in the epidermis, suggesting that CEBPB plays an important role in the early events of keratinocytes differentiation to impose growth arrest and induce expression of early differentiation markers (S. Zhu et al. 1999). On the other hand, terminal differentiation genes were upregulated upon loss of CEBPB, indicating a potential negative involvement of CEBPB in the late cornification process of keratinocytes, both under steady state and psoriatic microenvironment. CEBPB has been described to mediate its effects on keratinocytes differentiation also in combination with CREB and c-Jun (Rozenberg et al. 2013). Besides keratinocytes differentiation, CEBPB is required for sebocytes differentiation in the mouse skin, underlining that CEBPB might be interesting to study in the context of sebocytes and HS as well (House et al. 2010).

Acanthosis

Acanthosis as a result of hyperproliferation and dysregulated differentiation is a characteristic hallmark of chronic skin inflammation mainly for type 3 CISDs, but also in other diseases like LP and AD. Our results identify CEBPB as a key factor for promoting acanthosis, likely due to its described effects on keratinization pathways. So far, besides STAT3 (Caruso et al. 2009; Calautti, Avalle, and Poli 2018), not much is known about the transcriptional machinery underlying the process of acanthosis in the skin, hence highlighting the importance of the identified CEBPB-acanthosis axis. With respect to acanthosis, the potential physiological role of CEBPB is likely in mediating wound healing, given that psoriasis can be viewed as a constant healing wound under cytokine stress. Epidermal hyperplasia has been also described in mouse models, however with contradictory results. In one study, Cebpb-KO (*Cebpb -/-*) showed a mild epidermal hyperplasia (S. Zhu et al. 1999), whereas in another study Cebpb-KO was shown to reduce the epidermal thickness of the skin and LIP knockin in these mice (*Cebpb -/L*) could rescue this phenotype (Bégay et al. 2018). Another study using LIP overexpressing mice (LIP OE R26LIP) confirmed this role for Cebpb-LIP in increasing the numbers of PCNA+ proliferating cells and inducing acanthosis (Ackermann et al. 2019). Therefore, one limitation in this study, is the use of CEBPB-KO without rescue experiments with the respective isoforms, which is critical given that total CEBPB has effects on both proliferation and differentiation. Investigation of CEBPB isoform-specific function especially within keratinization is therefore needed. Indeed, in monocytes, cells predominantly overexpressing LAP*, but not those overexpressing LIP exhibited a reduced proliferation (Gutsch et al. 2011). In other cells, like adipocytes, gastric cells and hematopoietic stem cells (HSCs), the CEBPB isoforms were found to be sequentially upregulated to control the proliferation and differentiation balance (Regalo et al. 2016; Sato et al. 2020) . For instance, during the hematopoietic stress response, early upregulation of LIP promoted cell-cycle entry expanding the HSCs pool, whereas subsequent differentiation of amplified HSCs was then mediated by LAP/LAP*. Thus, besides the stimulus, also cell-dependent and temporal regulation is critical for CEBPB's final effects on the processes of proliferation and differentiation.

4.5.4. CEBPB as a novel driver of mitochondrial metabolism and metabolic fitness in keratinocytes

Although metabolic hyperactivation has been described as an important mechanism in Psoriasis/ type 3 disease pathology, it is relatively understudied compared to other disease aspects. Metabolism has been investigated more in the context of pso-associated comorbidities (e.g obesity, metabolic syndrome), rather than on the molecular level in keratinocytes, which has only recently become a

focus in the field (X. Zhou et al. 2022). Cellular metabolism in keratinocytes does not only affect the supply of energy required for efficient keratinocyte proliferation, but is also involved in a variety of inflammatory immune responses. Here, I focused on intrinsic CEBPB-mediated metabolic effects in primary human keratinocytes. In sum, our data demonstrate that CEBPB-deficient keratinocytes undergo extensive metabolic reprogramming leading to enhanced oxidative stress and downregulated mitochondrial respiration, ATP production and metabolic fitness.

We identified a series of metabolic genes regulated by CEBPB in keratinocytes and involved in different psoriasis-relevant metabolic pathways like prostaglandin synthesis, lipid metabolism, urea cycle and mitochondrial respiration. The urea cycle with its two key enzymes ARG1 and ASS1, which were strongly downregulated by loss of CEBPB under Pso-type conditions, has recently been implicated in the Psoriasis disease pathogenesis. ARG1 was shown to be induced by CEBPB in murine keratinocytes, where it drives polyamine production, which is a novel metabolic mechanism that promotes self-RNA sensing by Dendritic Cells (DCs) in Psoriasis (Lou et al. 2020). Moreover, ARG1 overexpression in psoriatic skin promotes keratinocytes hyperproliferation by limiting iNOS activity (Bruch-Gerharz et al. 2003). CEBPB has been described to contribute to breast cancer progression metabolically via ASS1 (M. Liu et al. 2022).

The functional validation of this metabolic transcriptional reprograming by ATP, Seahorse and MitoTracker assays showed strong stimulus-dependency, with strongest effects being observed under the unstimulated (US) condition, followed by the pso-type stimuli IL-17A+ TNF-α, IL-17A alone, and to less extent Pso-TCS, whereas no effects were observed with type 1/ 2 stimuli, underlining the well-established role of metabolism specifically in the type 3 pattern of CISDs. These results reveal a crucial role for CEBPB in the ATP production and mitochondrial respiration of human keratinocytes under steady-state (US), thus describing a new physiological role for CEBPB in healthy skin. CEBPB regulates these processes also under stress and type 3 inflammation, however to a weaker extent, implying that the IL-17A+TNF-α stimulus is likely inducing compensatory metabolic mechanisms in the cells that are missing under homeostasis.

Mitochondria and ROS

Mitochondria are central in cellular energy metabolism and responsible for the generation of the majority of intracellular ATP by mitochondrial respiration. Mitochondrial damage and dysfunction of the mitochondrial electron transport chain (ETC) impacts various disease-relevant cellular processes beyond energy balance, such as cell signaling, ROS production and apoptosis (Bell et al. 2007; L. R. Stein and Imai 2012; Green and Reed 1998). Another important consequence of ETC dysfunction is the

inhibition of cell proliferation, one of the main pathogenic mechanisms driving Psoriasis (Wheaton et al. 2014; Han et al. 2008; Birsoy et al. 2015).

In this project, I revealed a previously unknown role for CEBPB in the regulation of mitochondrial ETC. Various ETC genes are positively regulated by CEBPB in keratinocytes. In fact, all key parameters of mitochondrial respiratory function (ATP production, Basal and Maximal respiration) and metabolic fitness (SRC) were strongly downregulated by loss of CEBPB. In line, functional mitochondrial density of keratinocytes was also reduced in the CEBPB-KO, providing one potential mechanism to explain the observed dysfunction in mitochondrial respiration. The effects of CEBPB on mitochondrial metabolism can therefore be explained by two potential ways, either directly by affecting the gene expression of various mitochondrial components, both structural and functional, or indirectly via the regulation of other pathways that can lead to lower mitochondrial function and fitness. One such pathway is the oxidative stress (OS) pathway. In healthy cells, there is a balance between reactive oxygen species (ROS) production and removal by antioxidant mechanisms (Go and Jones 2017; Hu et al. 2022). Disruption of this balance, however, leads to the accumulation of ROS, putting the organism in a state of oxidative stress, finally leading to cell, organelle and tissue damage (Liguori et al. 2018). The role of ROS in the skin's metabolism and its downstream effects on various skin diseases has been well described (Pleńkowska, Gabig-Cimińska, and Mozolewski 2020; Hu et al. 2022).

OS is characteristic in the pathogenesis of Psoriasis, where ROS overproduction contributes to inflammation and abnormal proliferation in keratinocytes, with antioxidants being proposed as therapeutics (F. Xu et al. 2019; Qiang Zhou, Mrowietz, and Rostami-Yazdi 2009; Hu et al. 2022; Wroński and Wójcik 2022; Wuyuntana Wang et al. 2019). Similar effects of OS on keratinocytes and melanocytes have been described for the pathogenesis of Rosacea and Vitiligo, respectively (Y. Zhang et al. 2022; Y. Wang, Li, and Li 2019). In the latter, ROS-mediated cell damage has been shown to contribute to the generation of autoantigens, a mechanism that is likely involved in other autoimmune skin disorders as well. In this project, I show increased oxidative stress in keratinocytes upon loss of CEBPB and hypothesize that this underlies the observed reduction in MitoTracker-quantified mitochondrial density due to ROS-mediated mitochondrial damage (mitophagy). In fact, CEBPB has been described as a ROS responsive transcription factor in the context of cancer (Lei et al. 2020) and inhibition of a CEBPB-dependent axis was shown to decrease mitochondrial ROS generation in epithelial cell lines (J. Xu et al. 2021). CEBPB was shown to be central for ROS neutralization in highly proliferating cells (e.g. tumor cells), where it acts on antioxidative enzymes. Our results reveal a similar role for CEBPB in both steady-state proliferating keratinocytes, as well as hyperproliferating

keratinocytes under psoriatic conditions. Here, I show that CEBPB represses genes involved in ROS generation (e.g. *PRODH, NOXA1*), while inducing genes critical for ROS removal like *SOD2*, hence implying an overall increased oxidative stress in keratinocytes upon loss of CEBPB. In fact, the superoxide dismutase 2 (SOD2) reduction in keratinocytes lead to ROS accumulation and ROS-mediated inflammation in Psoriasis (Y. Zhang et al. 2022), further confirming our results.

Mouse models of CEBPB metabolic effects

One well-established role for CEBPB in mitochondria, is its function in mitochondrial ß-oxidation to control fatty acid metabolism (Du et al. 2019). CEBPB-kockout mice have reduced plasma triglycerides, free fatty acids (FFA) and leptin levels (Millward et al. 2007). CEBPB has been associated with obesity and metabolic disorders, where it mediates fat accumulation in the liver and adipose tissue, with Cebpb-deficient mice showing reduced fat mass and body weight (Zhao et al. 2017; Chen et al. 2021; Z. Wu et al. 1995; J.-W. Zhang et al. 2004; Ackermann et al. 2019). CEBPB loss also lead to decreased liver fat content conferring a protective effect against the development of hepatic steatosis, and thereby lowering the risk for obesity and diabetes (Shaikh Mizanoor Rahman et al. 2007; Schroeder-Gloeckler et al. 2007). Moreover, reducing CEBPB conferred protection from HFD-induced systemic inflammation and insulin resistance, proposing it as an attractive therapeutic target for ameliorating obesity-induced inflammatory responses (Shaikh M. Rahman et al. 2012). On the other hand, LIP-overexpressing mice showed a cancer-type metabolic phenotype with increased mitochondrial respiration and cellular hyperproliferation, further highlighting the role of such metabolic reprogramming in driving tissue hyperplasia in tumors (Ackermann et al. 2019) and likely also in Psoriasis. In contrast, a reduced expression of CEBPB-LIP in mice has been found to ameliorate metabolic health in ageing (Müller et al. 2018). Based on these findings, as well as internal pre-liminary data (not shown), LIP could be coined as the metabolically “harmful” CEBPB isoform. Finally, it would be interesting to check the effects of CEBPB on glycolysis in keratinocytes as well, especially under stress (aerobic glycolysis), since CEBPB has been described to regulate glycolysis in other tissues and in cancer (W. Li et al. 2018; Z. Wang et al. 2022; Ackermann et al. 2019). Nevertheless, in contrast to mitochondrial respiration, glycolysis has been already studied intrinsically in keratinocytes and its inhibition has been proposed as a novel treatment strategy for Psoriasis (Z. Zhang et al. 2018).

In conclusion, our results highlight CEBPB as a novel potent metabolic transcription factor in keratinocytes, intervening with cellular metabolism on various levels.

4.6. CEBPB in Atopic Dermatitis

A hallmark of AD is an increased colonization of the skin with *Staphylococcus aureus* due to the action of type 2 cytokines in downregulating epidermal AMP production, thus inhibiting cutaneous immunity and skin barrier function (Ong et al. 2002; S. Eyerich et al. 2011). Upregulation of AMPs upon loss of CEBPB specifically under type 2 inflammatory conditions, might therefore be beneficial for AD patients to rescue the compromised AMP production and host defense. Interestingly, the 'IL4+IL13 signaling' pathway and its associated genes were upregulated in the CEBPB-KO under US condition, but downregulated under AD-TCS stimulation, implying that under steady-state CEBPB acts suppressive, whereas under an ongoing type 2 inflammation, it might be involved in positively regulating IL-4+IL-13 signaling. Also, in literature the role of CEBPB on this pathway is rather contradictory. On the one hand, CEBPB has been shown to negatively regulate IL-4+IL-13 signaling during ER stress (Arensdorf and Rutkowski 2013) and to inhibit IL-13 in CD4+ T cells (Bruhn et al. 2012). On the other hand, CEBPB has been described to drive the expression of cytokine receptors for IL4 *(IL4ra)* and IL13 (*IL13ra*) (Ruffell et al. 2009; Huber et al. 2012; Bruhn et al. 2012). That CEBPB is rather immune suppressive under type 2 microenvironment, is supported by other studies on myeloid cells, showing within macrophage polarization that CEBPB promotes the M2 ("healer") fate under IL-4 and IL-13 stimuli (Chawla 2010; N. Wang, Liang, and Zen 2014). These findings further underline the ability of CEBPB to mediate immune activating or suppressive functions depending mainly on the present stimuli, but also on the cell type. Studies focusing specifically on the function of the single isoforms might therefore be helpful to gain a better understanding of these complex functions.

4.7. CEBPB in Lichen Planus

4.7.1. CEBPB as a regulator of the IFN-γ response and type 1 inflammatory secretome in keratinocytes

CEBPB has been associated to IFN-γ in previous studies (Nagi-Miura et al. 2013; P et al. 2016; Th et al. 2011). In line with this, IFN-γ response genes were enriched among downregulated genes upon loss of CEBPB. For instance, CEBPB has been assigned an important role as an effector transcription factor downstream of IFNγ in immune responses. A study profiling murine *Cebpb -/-* bone marrow macrophages has identified a number of IFNγ-responsive genes that specifically rely on Cebpb for their expression such as *irf9* and the death-associated protein kinase 1 *(dapk1)* (Xiao et al. 2001; S. K. Roy et al. 2000; P et al. 2016), similar to our results, where I identified the *DAPK1* isoform *(DAPK2)* and other IRF members *(*e.g. *IRF1)* to be positively regulated by CEBPB in human keratinocytes under type

1 inflammation. Other studies have shown that CEBPB-dependent gene expression in response to IFN-γ is specifically regulated by a MEKK1-MEK1-ERK1/2 pathway, where CEBPB utilizes the IFNγ-response element GATE for the transcriptional activation of its targets (Weihua, Kolla, and Kalvakolanu 1997; Akira and Kishimoto 1997; Sanjit K. Roy et al. 2002). Interestingly, many of the IFNγ-response genes that have been identified in this project to be dependent on CEBPB for their expression, have been described in the molecular signature of interface dermatitis (ID), which was generated from the top regulated genes of LE/LP patients (Lauffer et al. 2018). These included *IRF1* (as a hub gene in LE/LP), *ICAM1, CXCL9, CXCL10, CXCL11, ISG20, IFIT2, IL12B, IL18BP* and *CCL19.* Thus, our results reveal a novel role for CEBPB as a central regulator upstream of the ID gene signature in keratinocytes.

Besides IFN-γ signaling, other key signaling pathways like TNF, NFκB, JAK-STAT, TLR and IL-1 family signaling, as well as complement cascades were found to be positively regulated by CEBPB under lichenoid-type inflammation. As previously mentioned, the association of CEBPB with those pathways has been described in literature. In contrast, CEBPB-KO upregulated genes under type 1 stimulation were not as abundant like in other stimuli, indicating that CEBPB is likely a positive regulator rather than a repressor of gene expression under type 1 inflammation. Nevertheless, some type 2-relevant factors were found to be upregulated. This potential shift towards a type 2 phenotype is also supported by mouse studies showing a complete loss of the type 1 immune response in *Cebpb -/-* mice. Here, within the CD4 T-cell repertoire, Th1 cells were strongly decreased, whereas their Th2 counterparts were markedly enhanced, thereby skewing the cellular immunity towards a prevailing Th2-type response (Screpanti et al. 1995).

4.7.2. CEBPB as a key driver of keratinocytes cell death pathways

Apoptotic cell death

Different cell death pathways were found to be suppressed in the CEBPB-KO. Our results reveal a pro-apoptotic role for CEBPB in keratinocytes, where it drives the expression of various pro-apoptotic genes, while inhibiting anti-apoptotic ones. CEBPB-KO keratinocytes were resistant to apoptosis under a cell death-triggering lichenoid microenvironment. Consistently, murine *Cebpb -/-* macrophages failed to undergo apoptosis upon IFN-γ treatment, confirming our data (Gade et al. 2012; Xiao et al. 2001). Importantly, CEBPB has been assigned both pro- and anti-apoptotic functions in literature. It has been shown to promote apoptosis in multiple tumor cells like melanoma and leukemia (Qing Zhou et al. 2021; Shao et al. 2021; X. Yang et al. 2015; K. Zhang et al. 2010). Furthermore, it promoted apoptosis in in smooth muscle cells, chondrocytes and vascular endothelial cells (Luo et al. 2022; J. Zhang et al. 2020; Feng et al. 2019). In contrast, another *Cebpb -/-* mouse model showed increased

apoptosis rates of peripheral blood monocytes (Tamura et al. 2015). A similar anti-apoptotic effect of CEBPB has been described also for neutrophils (Akagi et al. 2008). Another study implicates CEBPB in upregulating autophagy of oxLDL-treated macrophages, while reducing their apoptosis (Zahid et al. 2020). Except for one study focusing on carcinogenic cell death, where *Cebpb -/-* mice exhibited increased carcinogen-mediated apoptosis in epidermal keratinocytes (Sterneck et al. 2006), not much is known on how CEBPB regulates apoptosis specifically in the skin. Altogether, these findings indicate that the outcome of CEBPB on apoptosis depends, similar to the other described processes, on the cell type, but also largely on the apoptosis trigger with differing effects for IFNγ-, carcinogen-, hypoxia- and OS-induced apoptosis.

Inflammasome-mediated cell death

Inflammasomes are key signalling platforms that are triggered by a range of substances during infections, tissue injury or metabolic stress, and in return activate the highly pro-inflammatory cytokines interleukin-1β (IL-1β) and IL-18 by a Caspase 1-mediated mechanism (Martinon, Burns, and Tschopp 2002; Latz, Xiao, and Stutz 2013). In addition, inflammasome activation causes a rapid, pro-inflammatory form of cell death called pyroptosis (Miao, Rajan, and Aderem 2011). Unlike apoptosis, pyroptosis results in cellular lysis releasing cytosolic contents to the extracellular space, hence contributing to immune cell recruitment and tissue inflammation. While appropriate inflammasome activation is vital for host defense and tissue homeostasis, aberrant inflammasome activation can cause uncontrolled tissue responses contributing to various diseases, including autoinflammatory disorders and cancer (Zheng, Liwinski, and Elinav 2020).

'Inflammasomes' as pathway and key inflammasome components like *AIM2, MEFV, NOD and CASP1* were found to be positively regulated by CEBPB in keratinocytes under type 1 inflammatory conditions. 'NOD-like receptors (NLRs) signaling', which functions upstream of Caspase-1 to form the inflammasome (Martinon, Burns, and Tschopp 2002), as well as *IL1B* expression and IL-1β protein secretion was also suppressed in the CEBPB-KO, further underlining the potential role of CEBPB in keratinocytes inflammasome activation. Our results are in line with various literature findings associating CEBPB with inflammasome pathway. CEBPB deletion in macrophages and adipocytes rendered them defective in inflammasome activation (Shaikh M. Rahman et al. 2012). Moreover, CEBPB was found to be critical for hepatic inflammasome activation by hepatotoxins resulting in liver injury (Buck, Solis-Herruzo, and Chojkier 2016). CEBPB knockdown in mice inhibited NLRP3 inflammasome-mediated caspase-1 signaling, suppressing the secretion of IL-1β and IL-18. CEBPB was also shown to contribute to tissue injury via NLRP3 inflammasome-mediated pyroptosis (X.-G. Dai et

al. 2020; D. Wu et al. 2022). A recent study has implicated the CEBPB-regulated inflammasome in the pathogenesis of systemic lupus erythematosus (SLE). Interestingly, knockdown of *CEBPB* could inhibit NLRP3 inflammasome activation and pyroptosis via regulating *Pim-1* expression (X. Wang et al. 2022). Given our data on PIM1 expression in keratinocytes, this CEBPB-PIM1 axis could be interesting to validate in context of inflammasomes and apoptosis in cutaneous Lupus and Lichen. Importantly, all these studies implicate CEBPB only in the TNF-NLRP inflammasome (Latz, Xiao, and Stutz 2013), whereas our results reveal an additional novel role for CEBPB in the regulation of IFNγ-dependent absent in melanoma 2 (AIM2) inflammasomes as well. It would therefore be interesting to functionally validate this pathway, which would represent a novel inflammasome-mediated cell death pathway in lichen/ lupus pathogenesis.

In general, more analysis is needed to pin-point the forms of cell death mediated by CEBPB downstream of type 1 cytokines in keratinocytes. However, based on our data, I would hypothesize that CEBPB likely contributes to epidermal injury in cutaneous lichen and lupus by acting on various pathways of both inflammatory (e.g. inflammasomes) and non-inflammatory (e.g. apoptosis) nature.

4.8. CEBPB in correlation with clinical attributes and transcriptional profiles in CISD patients

Correlation with clinical attributes and enrichment analysis with patients gene expression confirm the relevance of our *in vitro* generated data in patients. Indeed, our results showing strong positive correlation of CEBPB levels in the lesional skin with the key clinical disease attributes of 'acanthosis' and 'neutrophils' in CISD and 'Interface dermatitis' in LE/LP patients, underline the molecular connection of CEBPB to these features. Moreover, these results lead to the tempting hypothesis of blocking CEBPB with direct effects on these attributes and amelioration of their clinical scores, which can be expected from the correlation analysis, where low levels of CEBPB are correlated with low severity for these attributes. Enrichment of CEBPB positively regulated targets in the lesional skin of Pso and LE/LP patients, gives further strong evidence for the pathological role of CEBPB in those diseases via regulation of key transcriptional signatures and coins CEBPB as disease driver in Pso and LE/LP. Whereas the enrichment results observed in AD patients for CEBPB-negatively regulated targets, indicate that CEBPB rather acts as a repressor instead of a disease driver in AD. Importantly, this enrichment was observed for both 2D and 3D generated gene signatures, confirming on the one hand that both models were convenient and clinically relevant for studying keratinocytes gene expression and transcriptomic changes under immunogenic conditions, and confirming on the other

hand, the disease/ clinical-relevance of those CEBPB-dependent signatures that were generated by two different biological models with clear patient enrichment observed in both cases.

4.9. CEBPB disease associations- In the skin and beyond

In this study, I revealed the association of CEBPB with the key inflammatory skin diseases Psoriasis, Lichen and AD and described the potential role of CEBPB in each of these diseases. However, CEBPB has been described in various other diseases, especially in context of cytokine-induced autoimmune pathology and IL-17A-associated diseases like rheumatoid arthritis (RA), multiple sclerosis (MS) or EAE and type 17 asthma, as well as in obesity and cancer.

One of the best-studied examples for the tissue-specific roles of CEBPB in inflammation is provided by the lung, where CEBPB activity was described in inflammatory disorders such a chronic bronchitis, pulmonary fibrosis, LPS-induced neutrophilia, type 17 asthma and chronic obstructive pulmonary disease (COPD) (Mori et al. 2015; Roos et al. 2012; S.-S. Liu et al. 2019; Borger et al. 2007). CEBPB was shown to be a critical transcription factor in neutrophilic corticosteroid (CS)-resistant asthma by mediating IL-17A and GC-dependent synergistic induction of *LCN2* and *SAA* (Hong et al. 2022), two targets that were also found to be regulated by CEBPB in our data in keratinocytes.

Similar to our data in Psoriasis, CEBPB is central driver in the pathogenesis of Th17-dependent autoimmunity in EAE/MS. Here, *Cebpb -/-* mice were resistant to EAE with defects in Th17 cell priming and reduced immune cell infiltration into CNS. Mechanistically, CEBPB was found to regulate the IL23R expression in APCs and T-cells (Simpson-Abelson et al. 2017). In line, CEBPB levels were upregulated in human brain tissue of MS patients (Lock et al. 2002). In RA, CEBPB was assigned a role in suppressing cell apoptosis and driving hypoxia-induced cell proliferation of rheumatoid arthritis fibroblast-like synoviocytes (RA-FLS) via promoting G_1/S transition of the cell cycle (Yu et al. 2019), similar to our results implicating CEBPB in cell cycle regulation in psoriatic keratinocytes.

In cancer, CEBPB can have both tumor suppressor and oncogenic effects. Its function as a tumor suppressor comes from its central role in Oncogene-induced senescence (OIS), which is an intrinsic tumor suppression mechanism (Basu et al. 2018), whereas its pro-oncogenic functions are mediated by its pro-proliferative effects on various tumor cells (Sterken et al. 2022; D. Li et al. 2018). CEBPB was shown to promote epithelial cancer-associated inflammation and to drive breast cancer development by promoting cell migration, invasion and epithelial to mesenchymal transition (EMT) (Lee et al. 2021; Sterken et al. 2022; X.-Z. Liu et al. 2022). In addition, CEBPB has been assigned a main role as a pro-

leukemogenic transcription factor and is involved in the pathogenesis of various blood cancers, such as AML and B-cell acute lymphoblastic leukemia (BCP-ALL) (Lechner et al. 2011; Marigo et al. 2010; Abdel Ghani et al. 2022; Kurata et al. 2021). In fact, BCP-ALL is the only disease that has been directly associated with CEBPB mutations so far (Akasaka et al. 2007). Additionally, CEBPB has been assigned a central role in cell lymphoma (ALCL) (Bonzheim et al. 2013) and non-small cell lung cancer progression (NSCLC) (T. Lu et al. 2022), as well as in promoting chemoresistance in colorectal cancer (CRC) and sarcoma, with CEBPB high copy number tumors being associated with worse clinical outcome (D. Wang et al. 2019; Gardiner et al. 2017).

Finally, in the skin, CEBPB has been shown to drive tumorigenic skin hyperplasia. Here, *Cebpb -/-* mice were completely resistant to both Ras-mediated (Songyun Zhu et al. 2002) and carcinogen-induced skin tumor development (Sterneck et al. 2006). CEBPB has been also assigned critical roles in the pathogenesis of melanoma (Swoboda et al. 2021; Vidarsdottir et al. 2020).

4.10. Conclusion and Working model for CEBPB role in skin inflammation

In conclusion, in this project, I have identified CEBPB as a novel master transcription factor in keratinocytes and a key regulator of Psoriasis and Lichen disease pathology. Based on our results, I propose the following model for the role of CEBPB in the pathogenic epithelial response (Figure 44). CEBPB is upregulated in the lesional skin of Psoriasis and Lichen patients by the action of Th17/Th22-relevant (type 3) and Th1-relevant (type 1) cytokines, where it acts as a regulatory node to drive key pathways of disease pathology. In Psoriasis, it drives keratinocytes hyperproliferation, mitochondrial metabolism and metabolic fitness, contributing to the development of acanthosis. Additionally, it drives the early event of keratinocytes differentiation, AMP production and the secretion of neutrophil chemoattracting factors, as well as other type 3-relevant pro-inflammatory cytokines and chemokines. It is critical for neutrophil infiltration into the skin, acting both on the keratinocyte and neutrophil levels. In Lichen, CEBPB regulates the IFNγ-response, as well as IFN-γ, TNF and IL-1 signaling and contributes to the lichenoid skin inflammation by favoring the secretion of type 1-related inflammatory factors, which in return potentiate immune cell infiltration. It contributes to the development of interface dermatitis by promoting keratinocytes apoptosis and other cell death pathways, likely inflammasome-mediated ones. Thus, I unravel CEBPB as a pleiotropic activator of skin inflammation downstream of IL-17A, TNF-α, IL-22 and IFN-γ, and propose it as a novel inflammatory checkpoint in the human skin with a unique mode of action (MOA).

Our study is hence the most comprehensive study to completely dissect this multi-functional transcription factor in the human skin inflammation on a global level, investigating the transcriptomic signature, regulated secretome, metabolism and functional effects on cell survival, proliferation and differentiation, all in a stimulus-dependent manner, finally connecting these findings to clinically relevant disease attributes in CISD patients.

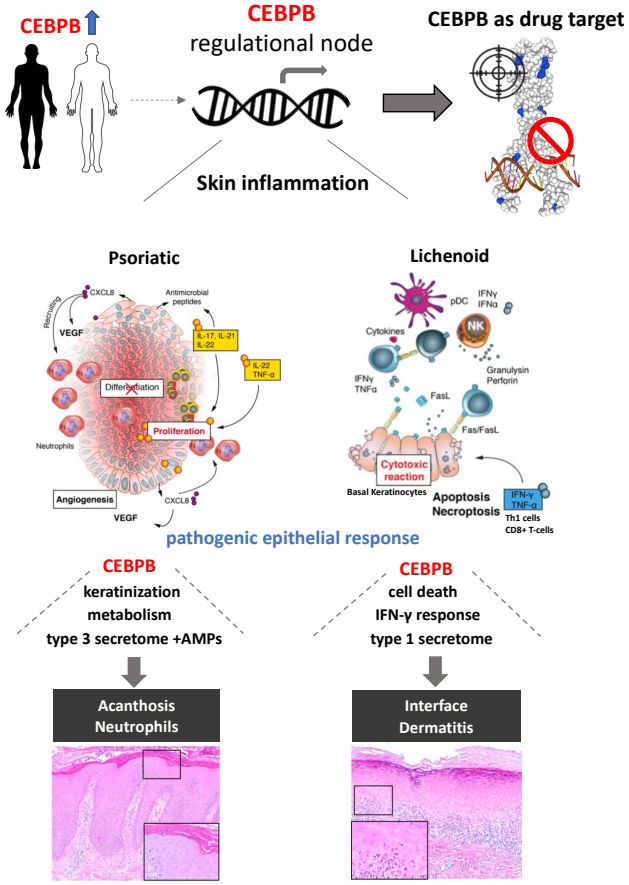

Figure 44: CEBPB is a novel master transcription factor in keratinocytes and a key regulator of Psoriasis and Lichen disease pathologies. Proposed model for the function of CEBPB in regulating the pathogenic epithelial response. CEBPB is upregulated in the lesional skin of Pso and LP patients, where it acts as a regulational node to drive skin inflammation via transcriptional reprograming of keratinocytes under cytokine stress. In psoriatic skin inflammation, CEBPB promotes keratinocytes proliferation and early differentiation, while inhibiting terminal differentiation, and mediates neutrophil infiltration. It supports the metabolic hyperactivation of keratinocytes by acting on mitochondrial metabolism and increasing the cells metabolic fitness in response to oxidative stress. AMP production and type 3-relevant factors depend on CEBPB for their secretion. In lichenoid skin inflammation, CEBPB drives IFN-γ response, type 1 factors secretion and different cell death pathways like apoptosis. These keratinocyte-intrinsic molecular mechanisms contribute to the development of the clinical attributes of 'acanthosis', 'neutrophil infiltrates' and 'interface dermatitis' in Psoriasis and Lichen, respectively. Adapted and modified from (Eyerich and Eyerich 2018).

4.11. Clinical implications and potential of CEBPB as a drug target

Transcription factors (TFs) own great therapeutic potential and have recently moved away from the stigma of being “undruggable”. Successful examples of targeting TFs can be seen with MYC, STAT3, p53 and HIF1A (Lambert et al. 2018; Bushweller 2019; Guo, Wisniewski, and Ji 2014). Based on the results of this project, it is therefore tempting to hypothesize that CEBPB might be a promising therapeutic target in skin inflammation, especially due to its unique mode-of-action (MOA). CEBPB targeting might represent an interesting causative therapy to address diseases more specifically based on their clinical features. For instance, the described MOA of CEBPB in Psoriasis, can be an interesting therapeutic target not only for Psoriasis patients, but also for other patients suffering from certain pathologies with acanthosis, excessive neutrophil infiltration or metabolic hyperactivation, both in the skin and beyond the skin. This is of particular interest especially for those CISDs with limited therapy options available. Potential advantages of targeting CEBPB compared to other existing therapies, might be the broader application spectrum, lower cost of small molecules as drug class compared to antibody-based drugs and better tissue penetration (Slivka et al. 2019; Eyerich and Eyerich 2018). Potential high risk of side effects and tissue specificity represent two potential disadvantages linked to targeting CEBPB. As already described, CEBPB has been implicated in an extremely wide variety of diseases. Therefore, targeting CEBPB beyond the skin could be beneficial for many patients. Indeed, CEBPB as a target is a hot topic in the field of cancer, where CEBPB targeting anti-cancer agents have been tested as a proof-of-principle (Qing Zhou et al. 2021; Abdel Ghani et al. 2022).

4.12. Outlook

Although there has been a clear progress in the development of biologic therapeutics for common CISDs, most of these therapies still have substantial numbers of non-responders and causative treatments are largely lacking. Therefore, a better understanding of the disease pathogenesis at the molecular level is crucial for filling this gap representing an important task in the field for the next era of diagnostics and therapy. This project is a contribution to expanding this molecular view of CISDs and providing novel insights into the transcriptional regulation of the pathogenic epithelial response.

Finally, when setting out to examine the functions of CEBPB in future studies, it is important to bear in mind that CEBPB carries out its crucial roles in inflammation by affecting both the immune effector cells, as well as regulating the target cells in various tissues. Hence, it will be necessary to tease out tissue-specific and temporal roles of CEBPB in response to different stimuli.

Also, the different roles of the CEBPB isoforms within the regulation of cutaneous inflammation, will surely require more extensive research. Besides the isoform-specific function of CEBPB, other open questions that remain to be addressed include the function of CEBPB in other cell subsets in the skin and the role of CEBPB post-translational modifications, given their importance in regulating CEBPB activity. A deeper insight into these mechanisms might be helpful for assessing CEBPB as a therapeutic target in inflammatory skin disorders.

5. References

Abdel Ghani, Luca, Maria V. Yusenko, Daria Frank, Ramkumar Moorthy, John C. Widen, Wolfgang Dörner, Cyrus Khandanpour, Daniel A. Harki, and Karl-Heinz Klempnauer. 2022. "A Synthetic Covalent Ligand of the C/EBPβ Transactivation Domain Inhibits Acute Myeloid Leukemia Cells." *Cancer Letters* 530 (April): 170–80. https://doi.org/10.1016/j.canlet.2022.01.024.

Ackermann, Tobias, Götz Hartleben, Christine Müller, Guido Mastrobuoni, Marco Groth, Britt A. Sterken, Mohamad A. Zaini, et al. 2019. "C/EBPβ-LIP Induces Cancer-Type Metabolic Reprogramming by Regulating the Let-7/LIN28B Circuit in Mice." *Communications Biology* 2: 208. https://doi.org/10.1038/s42003-019-0461-z.

Aghamajidi, Azin, Ehsan Raoufi, Gilda Parsamanesh, Ahmad Jalili, Mohammad Salehi-Shadkami, Marjan Mehrali, and Monireh Mohsenzadegan. 2021. "The Attentive Focus on T Cell-Mediated Autoimmune Pathogenesis of Psoriasis, Lichen Planus and Vitiligo." *Scandinavian Journal of Immunology* 93 (4): e13000. https://doi.org/10.1111/sji.13000.

Akagi, Tadayuki, Takayuki Saitoh, James O'Kelly, Shizuo Akira, Adrian F. Gombart, and H. Phillip Koeffler. 2008. "Impaired Response to GM-CSF and G-CSF, and Enhanced Apoptosis in C/EBPbeta-Deficient Hematopoietic Cells." *Blood* 111 (6): 2999–3004. https://doi.org/10.1182/blood-2007-04-087213.

Akasaka, Takashi, Theodore Balasas, Lisa J. Russell, Kei-ji Sugimoto, Aneela Majid, Renata Walewska, E. Loraine Karran, et al. 2007. "Five Members of the CEBP Transcription Factor Family Are Targeted by Recurrent IGH Translocations in B-Cell Precursor Acute Lymphoblastic Leukemia (BCP-ALL)." *Blood* 109 (8): 3451–61. https://doi.org/10.1182/blood-2006-08-041012.

Akira, S., H. Isshiki, T. Sugita, O. Tanabe, S. Kinoshita, Y. Nishio, T. Nakajima, T. Hirano, and T. Kishimoto. 1990. "A Nuclear Factor for IL-6 Expression (NF-IL6) Is a Member of a C/EBP Family." *The EMBO Journal* 9 (6): 1897–1906. https://doi.org/10.1002/j.1460-2075.1990.tb08316.x.

Akira, S., and T. Kishimoto. 1997. "NF-IL6 and NF-Kappa B in Cytokine Gene Regulation." *Advances in Immunology* 65: 1–46.

Alam, T., M. R. An, R. C. Mifflin, C. C. Hsieh, X. Ge, and J. Papaconstantinou. 1993. "Trans-Activation of the Alpha 1-Acid Glycoprotein Gene Acute Phase Responsive Element by Multiple Isoforms of C/EBP and Glucocorticoid Receptor." *The Journal of Biological Chemistry* 268 (21): 15681–88.

Albanesi, C., and S. Pastore. 2010. "Pathobiology of Chronic Inflammatory Skin Diseases: Interplay Between Keratinocytes and Immune Cells as a Target for Anti-Inflammatory Drugs." *Current Drug Metabolism* 11 (3): 210–27. https://doi.org/10.2174/138920010791196328.

Albanesi, Cristina, Claudia Scarponi, Maria L. Giustizieri, and Giampiero Girolomoni. 2005. "Keratinocytes in Inflammatory Skin Diseases." *Current Drug Targets. Inflammation and Allergy* 4 (3): 329–34. https://doi.org/10.2174/1568010054022033.

Antonini, Dario, Anna Sirico, Edith Aberdam, Raffaele Ambrosio, Carmen Campanile, Sharmila Fagoonee, Fiorella Altruda, Daniel Aberdam, Janice L. Brissette, and Caterina Missero. 2015. "A Composite Enhancer Regulates P63 Gene Expression in Epidermal Morphogenesis and in Keratinocyte Differentiation by Multiple Mechanisms." *Nucleic Acids Research* 43 (2): 862–74. https://doi.org/10.1093/nar/gku1396.

Arensdorf, Angela M., and D. Thomas Rutkowski. 2013. "Endoplasmic Reticulum Stress Impairs IL-4/IL-13 Signaling through C/EBPβ-Mediated Transcriptional Suppression." *Journal of Cell Science* 126 (Pt 17): 4026–36. https://doi.org/10.1242/jcs.130757.

Atwood, A. A., and L. Sealy. 2010. "Regulation of C/EBPbeta1 by Ras in Mammary Epithelial Cells and the Role of C/EBPbeta1 in Oncogene-Induced Senescence." *Oncogene* 29 (45): 6004–15. https://doi.org/10.1038/onc.2010.336.

Augustin, M., J.M. Alvaro-Gracia, M. Bagot, O. Hillmann, P.C.M. van de Kerkhof, G. Kobelt, M. Maccarone, L. Naldi, and H. Schellekens. 2012. "A Framework for Improving the Quality of Care for People with Psoriasis: Improving Care for People with Psoriasis." *Journal of the European Academy of Dermatology and Venereology* 26 (July): 1–16. https://doi.org/10.1111/j.1468-3083.2012.04576.x.

Basu, Sandip K., Mesfin Gonit, Jacqueline Salotti, Jiji Chen, Atharva Bhat, Myriam Gorospe, Benoit Viollet, Kevin P. Claffey, and Peter F. Johnson. 2018. "A RAS-CaMKKβ-AMPKα2 Pathway Promotes Senescence by Licensing Post-Translational Activation of C/EBPβ through a Novel 3'UTR Mechanism." *Oncogene* 37 (26): 3528–48. https://doi.org/10.1038/s41388-018-0190-7.

Bégay, Valérie, Christian Baumeier, Karin Zimmermann, Arnd Heuser, and Achim Leutz. 2018. "The C/EBPβ LIP Isoform Rescues Loss of C/EBPβ Function in the Mouse." *Scientific Reports* 8 (1): 8417. https://doi.org/10.1038/s41598-018-26579-y.

Bell, Eric L., Tatyana A. Klimova, James Eisenbart, Carlos T. Moraes, Michael P. Murphy, G.R. Scott Budinger, and Navdeep S. Chandel. 2007. "The Qo Site of the Mitochondrial Complex III Is Required for the Transduction of Hypoxic Signaling via Reactive Oxygen Species Production." *The Journal of Cell Biology* 177 (6): 1029–36. https://doi.org/10.1083/jcb.200609074.

Bernard, François-Xavier, Franck Morel, Magalie Camus, Nathalie Pedretti, Christine Barrault, Julien Garnier, and Jean-Claude Lecron. 2012. "Keratinocytes under Fire of Proinflammatory Cytokines: Bona Fide Innate Immune Cells Involved in the Physiopathology of Chronic Atopic Dermatitis and Psoriasis." *Journal of Allergy* 2012 (November): 1–10. https://doi.org/10.1155/2012/718725.

Berrier, A., G. Siu, and K. Calame. 1998. "Transcription of a Minimal Promoter from the NF-IL6 Gene Is Regulated by CREB/ATF and SP1 Proteins in U937 Promonocytic Cells." *Journal of Immunology (Baltimore, Md.: 1950)* 161 (5): 2267–75.

Bikle, Daniel D, Zhongjian Xie, and Chia-Ling Tu. 2012. "Calcium Regulation of Keratinocyte Differentiation." *Expert Review of Endocrinology & Metabolism* 7 (4): 461–72. https://doi.org/10.1586/eem.12.34.

Birsoy, Kıvanç, Tim Wang, Walter W. Chen, Elizaveta Freinkman, Monther Abu-Remaileh, and David M. Sabatini. 2015. "An Essential Role of the Mitochondrial Electron Transport Chain in Cell Proliferation Is to Enable Aspartate Synthesis." *Cell* 162 (3): 540–51. https://doi.org/10.1016/j.cell.2015.07.016.

Black, Antony P. B., Michael R. Ardern-Jones, Victoria Kasprowicz, Paul Bowness, Louise Jones, Abigail S. Bailey, and Graham S. Ogg. 2007. "Human Keratinocyte Induction of Rapid Effector Function in Antigen-Specific Memory CD4+ and CD8+ T Cells." *European Journal of Immunology* 37 (6): 1485–93. https://doi.org/10.1002/eji.200636915.

Boch, Katharina, Ewan A. Langan, Khalaf Kridin, Detlef Zillikens, Ralf J. Ludwig, and Katja Bieber. 2021. "Lichen Planus." *Frontiers in Medicine* 8: 737813. https://doi.org/10.3389/fmed.2021.737813.

Boehncke, Wolf-Henning, and Michael P Schön. 2015. "Psoriasis." *The Lancet* 386 (9997): 983–94. https://doi.org/10.1016/S0140-6736(14)61909-7.

Bonzheim, Irina, Martin Irmler, Margit Klier-Richter, Julia Steinhilber, Nataša Anastasov, Sabine Schäfer, Patrick Adam, et al. 2013. "Identification of C/EBPβ Target Genes in ALK+ Anaplastic Large Cell Lymphoma (ALCL) by Gene Expression Profiling and Chromatin Immunoprecipitation." *PloS One* 8 (5): e64544. https://doi.org/10.1371/journal.pone.0064544.

Borger, Peter, Hisako Matsumoto, Sarah Boustany, Mikael M. C. Gencay, Janette K. Burgess, Greg G. King, Judith L. Black, Michael Tamm, and Michael Roth. 2007. "Disease-Specific Expression and Regulation of CCAAT/Enhancer-Binding Proteins in Asthma and Chronic Obstructive Pulmonary Disease." *The Journal of Allergy and Clinical Immunology* 119 (1): 98–105. https://doi.org/10.1016/j.jaci.2006.07.056.

Bos, J. D., and M. L. Kapsenberg. 1993. "The Skin Immune System: Progress in Cutaneous Biology." *Immunology Today* 14 (2): 75–78. https://doi.org/10.1016/0167-5699(93)90062-P.

Boström, Pontus, Nina Mann, Jun Wu, Pablo A. Quintero, Eva R. Plovie, Daniela Panáková, Rana K. Gupta, et al. 2010. "C/EBPβ Controls Exercise-Induced Cardiac Growth and Protects against Pathological Cardiac Remodeling." *Cell* 143 (7): 1072–83. https://doi.org/10.1016/j.cell.2010.11.036.

Bretz, J. D., S. C. Williams, M. Baer, P. F. Johnson, and R. C. Schwartz. 1994. "C/EBP-Related Protein 2 Confers Lipopolysaccharide-Inducible Expression of Interleukin 6 and Monocyte Chemoattractant Protein 1 to a Lymphoblastic Cell Line." *Proceedings of the National Academy of Sciences of the United States of America* 91 (15): 7306–10. https://doi.org/10.1073/pnas.91.15.7306.

Bruch-Gerharz, Daniela, Oliver Schnorr, Christoph Suschek, Karl-Friedrich Beck, Josef Pfeilschifter, Thomas Ruzicka, and Victoria Kolb-Bachofen. 2003. "Arginase 1 Overexpression in Psoriasis: Limitation of Inducible Nitric Oxide Synthase Activity as a Molecular Mechanism for Keratinocyte Hyperproliferation." *The American Journal of Pathology* 162 (1): 203–11. https://doi.org/10.1016/S0002-9440(10)63811-4.

Bruhn, Sören, Mark Katzenellenbogen, Mika Gustafsson, Andrea Krönke, Birte Sönnichsen, Huan Zhang, and Mikael Benson. 2012. "Combining Gene Expression Microarray- and Cluster Analysis with Sequence-Based Predictions to Identify Regulators of IL-13 in Allergy." *Cytokine* 60 (3): 736–40. https://doi.org/10.1016/j.cyto.2012.08.009.

Buck, M., V. Poli, P. van der Geer, M. Chojkier, and T. Hunter. 1999. "Phosphorylation of Rat Serine 105 or Mouse Threonine 217 in C/EBP Beta Is Required for Hepatocyte Proliferation Induced by TGF Alpha." *Molecular Cell* 4 (6): 1087–92. https://doi.org/10.1016/s1097-2765(00)80237-3.

Buck, M., H. Turler, and M. Chojkier. 1994. "LAP (NF-IL-6), a Tissue-Specific Transcriptional Activator, Is an Inhibitor of Hepatoma Cell Proliferation." *The EMBO Journal* 13 (4): 851–60. https://doi.org/10.1002/j.1460-2075.1994.tb06328.x.

Buck, Martina, Jose Solis-Herruzo, and Mario Chojkier. 2016. "C/EBPβ-Thr217 Phosphorylation Stimulates Macrophage Inflammasome Activation and Liver Injury." *Scientific Reports* 6 (April): 24268. https://doi.org/10.1038/srep24268.

Bushweller, John H. 2019. "Targeting Transcription Factors in Cancer - from Undruggable to Reality." *Nature Reviews. Cancer* 19 (11): 611–24. https://doi.org/10.1038/s41568-019-0196-7.

Cain, Derek W., Emily G. O'Koren, Matthew J. Kan, Mandy Womble, Gregory D. Sempowski, Kristen Hopper, Michael D. Gunn, and Garnett Kelsoe. 2013. "Identification of a Tissue-Specific, C/EBPβ-Dependent Pathway of Differentiation for Murine Peritoneal Macrophages." *Journal of Immunology (Baltimore, Md.: 1950)* 191 (9): 4665–75. https://doi.org/10.4049/jimmunol.1300581.

Calautti, Enzo, Lidia Avalle, and Valeria Poli. 2018. "Psoriasis: A STAT3-Centric View." *International Journal of Molecular Sciences* 19 (1): 171. https://doi.org/10.3390/ijms19010171.

Calkhoven, C. F., C. Müller, and A. Leutz. 2000. "Translational Control of C/EBPalpha and C/EBPbeta Isoform Expression." *Genes & Development* 14 (15): 1920–32.

Candi, Eleonora, Rainer Schmidt, and Gerry Melino. 2005. "The Cornified Envelope: A Model of Cell Death in the Skin." *Nature Reviews. Molecular Cell Biology* 6 (4): 328–40. https://doi.org/10.1038/nrm1619.

Cao, Z., R. M. Umek, and S. L. McKnight. 1991. "Regulated Expression of Three C/EBP Isoforms during Adipose Conversion of 3T3-L1 Cells." *Genes & Development* 5 (9): 1538–52. https://doi.org/10.1101/gad.5.9.1538.

Cardinaux, J. R., I. Allaman, and P. J. Magistretti. 2000. "Pro-Inflammatory Cytokines Induce the Transcription Factors C/EBPbeta and C/EBPdelta in Astrocytes." *Glia* 29 (1): 91–97.

Caruso, Roberta, Elisabetta Botti, Massimiliano Sarra, Maria Esposito, Carmine Stolfi, Laura Diluvio, Maria Laura Giustizieri, et al. 2009. "Involvement of Interleukin-21 in the Epidermal Hyperplasia of Psoriasis." *Nature Medicine* 15 (9): 1013–15. https://doi.org/10.1038/nm.1995.

Cassel, Tobias N., and Magnus Nord. 2003. "C/EBP Transcription Factors in the Lung Epithelium." *American Journal of Physiology. Lung Cellular and Molecular Physiology* 285 (4): L773-781. https://doi.org/10.1152/ajplung.00023.2003.

Chawla, Ajay. 2010. "Control of Macrophage Activation and Function by PPARs." *Circulation Research* 106 (10): 1559–69. https://doi.org/10.1161/CIRCRESAHA.110.216523.

Chen, Keren, Junyan Zhang, Feng Liang, Qi Zhu, Shufang Cai, Xian Tong, Zuyong He, Xiaohong Liu, Yaosheng Chen, and Delin Mo. 2021. "HMGB2 Orchestrates Mitotic Clonal Expansion by Binding to the Promoter of C/EBPβ to Facilitate Adipogenesis." *Cell Death & Disease* 12 (7): 666. https://doi.org/10.1038/s41419-021-03959-3.

Chiricozzi, Andrea, Kristine E. Nograles, Leanne M. Johnson-Huang, Judilyn Fuentes-Duculan, Irma Cardinale, Kathleen M. Bonifacio, Nicholas Gulati, et al. 2014. "IL-17 Induces an Expanded Range of Downstream Genes in Reconstituted Human Epidermis Model." *PloS One* 9 (2): e90284. https://doi.org/10.1371/journal.pone.0090284.

Choudhury, Mahua, Ishtiaq Qadri, Shaikh Mizanoor Rahman, Jill Schroeder-Gloeckler, Rachel C. Janssen, and Jacob E. Friedman. 2011. "C/EBPβ Is AMP Kinase Sensitive and up-Regulates PEPCK in Response to ER Stress in Hepatoma Cells." *Molecular and Cellular Endocrinology* 331 (1): 102–8. https://doi.org/10.1016/j.mce.2010.08.014.

Chung, Wen-Hung, Shuen-Iu Hung, Jui-Yung Yang, Shih-Chi Su, Shien-Ping Huang, Chun-Yu Wei, See-Wen Chin, et al. 2008. "Granulysin Is a Key Mediator for Disseminated Keratinocyte Death in Stevens-Johnson Syndrome and Toxic Epidermal Necrolysis." *Nature Medicine* 14 (12): 1343–50. https://doi.org/10.1038/nm.1884.

Cornelissen, Christian, Yvonne Marquardt, Katharina Czaja, Jörg Wenzel, Jorge Frank, Juliane Lüscher-Firzlaff, Bernhard Lüscher, and Jens M. Baron. 2012. "IL-31 Regulates Differentiation and Filaggrin Expression in Human Organotypic Skin Models." *The Journal of Allergy and Clinical Immunology* 129 (2): 426–33, 433.e1-8. https://doi.org/10.1016/j.jaci.2011.10.042.

Cortez, Dolores M., Marc D. Feldman, Srinivas Mummidi, Anthony J. Valente, Bjorn Steffensen, Matthew Vincenti, Jeffrey L. Barnes, and Bysani Chandrasekar. 2007. "IL-17 Stimulates MMP-1 Expression in Primary Human Cardiac Fibroblasts via P38 MAPK- and ERK1/2-Dependent C/EBP-Beta , NF-KappaB, and AP-1 Activation." *American Journal of Physiology. Heart and Circulatory Physiology* 293 (6): H3356-3365. https://doi.org/10.1152/ajpheart.00928.2007.

Dai, Jun, Ajinkya Kumbhare, Dima Youssef, Zhi Q. Yao, Charles E. McCall, and Mohamed El Gazzar. 2017. "Expression of C/EBPβ in Myeloid Progenitors during Sepsis Promotes Immunosuppression." *Molecular Immunology* 91 (November): 165–72. https://doi.org/10.1016/j.molimm.2017.09.008.

Dai, Xin-Gui, Qiong Li, Tao Li, Wei-Bo Huang, Zhen-Hua Zeng, Yang Yang, Ze-Peng Duan, Yu-Jing Wang, and Yu-Hang Ai. 2020. "The Interaction between C/EBPβ and TFAM Promotes Acute Kidney Injury via Regulating NLRP3 Inflammasome-Mediated Pyroptosis." *Molecular Immunology* 127 (November): 136–45. https://doi.org/10.1016/j.molimm.2020.08.023.

Del Duca, Ester, Paola Morelli, Luigi Bennardo, Cosimo Di Raimondo, and Steven Paul Nisticò. 2020. "Cytokine Pathways and Investigational Target Therapies in Hidradenitis Suppurativa." *International Journal of Molecular Sciences* 21 (22): 8436. https://doi.org/10.3390/ijms21228436.

Della Vella, Fedora, Dorina Lauritano, Giuseppe Pannone, Raffaele Del Prete, Dario Di Stasio, Maria Contaldo, and Massimo Petruzzi. 2021. "Prevalence of HPV in Patients Affected by Oral Lichen Planus: A Prospective Study Using Two Different Chair-Side Sampling Methods." *Journal of Oral Pathology & Medicine: Official Publication of the International Association of Oral Pathologists and the American Academy of Oral Pathology* 50 (7): 716–22. https://doi.org/10.1111/jop.13164.

Descombes, P., and U. Schibler. 1991. "A Liver-Enriched Transcriptional Activator Protein, LAP, and a Transcriptional Inhibitory Protein, LIP, Are Translated from the Same MRNA." *Cell* 67 (3): 569–79. https://doi.org/10.1016/0092-8674(91)90531-3.

Desvergne, Béatrice, Liliane Michalik, and Walter Wahli. 2006. "Transcriptional Regulation of Metabolism." *Physiological Reviews* 86 (2): 465–514. https://doi.org/10.1152/physrev.00025.2005.

Didon, Lukas, Jenny L. Barton, Abraham B. Roos, Gordon J. Gaschler, Carla M. T. Bauer, Tove Berg, Martin R. Stämpfli, and Magnus Nord. 2011. "Lung Epithelial CCAAT/Enhancer-Binding Protein-β Is Necessary for the Integrity of Inflammatory Responses to Cigarette Smoke." *American Journal of Respiratory and Critical Care Medicine* 184 (2): 233–42. https://doi.org/10.1164/rccm.201007-1113OC.

Dillon, Stacey R., Cindy Sprecher, Angela Hammond, Janine Bilsborough, Maryland Rosenfeld-Franklin, Scott R. Presnell, Harald S. Haugen, et al. 2004. "Interleukin 31, a Cytokine Produced by Activated T Cells, Induces Dermatitis in Mice." *Nature Immunology* 5 (7): 752–60. https://doi.org/10.1038/ni1084.

Ding, Hui, Jinjun Chen, Jingping Qin, Ruhua Chen, and Zili Yi. 2021. "TGF-β-Induced α-SMA Expression Is Mediated by C/EBPβ Acetylation in Human Alveolar Epithelial Cells." *Molecular Medicine (Cambridge, Mass.)* 27 (1): 22. https://doi.org/10.1186/s10020-021-00283-6.

Divakaruni, Ajit S., Alexander Paradyse, David A. Ferrick, Anne N. Murphy, and Martin Jastroch. 2014. "Analysis and Interpretation of Microplate-Based Oxygen Consumption and PH Data." *Methods in Enzymology* 547: 309–54. https://doi.org/10.1016/B978-0-12-801415-8.00016-3.

Du, Chenghua, Pan Pan, Yan Jiang, Qiuli Zhang, Jinsuo Bao, and Chang Liu. 2016. "Microarray Data Analysis to Identify Crucial Genes Regulated by CEBPB in Human SNB19 Glioma Cells." *World Journal of Surgical Oncology* 14 (1): 258. https://doi.org/10.1186/s12957-016-0997-z.

Du, Qianqian, Zheqiong Tan, Feng Shi, Min Tang, Longlong Xie, Lin Zhao, Yueshuo Li, et al. 2019. "PGC1α/CEBPB/CPT1A Axis Promotes Radiation Resistance of Nasopharyngeal Carcinoma through Activating Fatty Acid Oxidation." *Cancer Science* 110 (6): 2050–62. https://doi.org/10.1111/cas.14011.

Dunn, S. M., L. S. Coles, R. K. Lang, S. Gerondakis, M. A. Vadas, and M. F. Shannon. 1994. "Requirement for Nuclear Factor (NF)-Kappa B P65 and NF-Interleukin-6 Binding Elements in the Tumor Necrosis Factor Response Region of the Granulocyte Colony-Stimulating Factor Promoter." *Blood* 83 (9): 2469–79.

Duprez, Estelle, Katharina Wagner, Heike Koch, and Daniel G. Tenen. 2003. "C/EBPbeta: A Major PML-RARA-Responsive Gene in Retinoic Acid-Induced Differentiation of APL Cells." *The EMBO Journal* 22 (21): 5806–16. https://doi.org/10.1093/emboj/cdg556.

Eckert, R L, and E A Rorke. 1989. "Molecular Biology of Keratinocyte Differentiation." *Environmental Health Perspectives* 80 (March): 109–16.

Egawa, Gyohei, and Kenji Kabashima. 2016. "Multifactorial Skin Barrier Deficiency and Atopic Dermatitis: Essential Topics to Prevent the Atopic March." *The Journal of Allergy and Clinical Immunology* 138 (2): 350-358.e1. https://doi.org/10.1016/j.jaci.2016.06.002.

Eichner, R., T. T. Sun, and U. Aebi. 1986. "The Role of Keratin Subfamilies and Keratin Pairs in the Formation of Human Epidermal Intermediate Filaments." *The Journal of Cell Biology* 102 (5): 1767–77. https://doi.org/10.1083/jcb.102.5.1767.

Eyerich, K., and S. Eyerich. 2018. "Immune Response Patterns in Non-Communicable Inflammatory Skin Diseases." *Journal of the European Academy of Dermatology and Venereology: JEADV* 32 (5): 692–703. https://doi.org/10.1111/jdv.14673.

Eyerich, Kilian, Sara J. Brown, Bethany E. Perez White, Reiko J. Tanaka, Robert Bissonette, Sandipan Dhar, Thomas Bieber, et al. 2019. "Human and Computational Models of Atopic Dermatitis: A Review and Perspectives by an Expert Panel of the International Eczema Council." *The Journal of Allergy and Clinical Immunology* 143 (1): 36–45. https://doi.org/10.1016/j.jaci.2018.10.033.

Eyerich, Kilian, Stefanie Eyerich, and Tilo Biedermann. 2015. "The Multi-Modal Immune Pathogenesis of Atopic Eczema." *Trends in Immunology* 36 (12): 788–801. https://doi.org/10.1016/j.it.2015.10.006.

Eyerich, Stefanie, Kilian Eyerich, Andrea Cavani, and Carsten Schmidt-Weber. 2010. "IL-17 and IL-22: Siblings, Not Twins." *Trends in Immunology* 31 (9): 354–61. https://doi.org/10.1016/j.it.2010.06.004.

Eyerich, Stefanie, Kilian Eyerich, Claudia Traidl-Hoffmann, and Tilo Biedermann. 2018. "Cutaneous Barriers and Skin Immunity: Differentiating A Connected Network." *Trends in Immunology* 39 (4): 315–27. https://doi.org/10.1016/j.it.2018.02.004.

Eyerich, Stefanie, Anna T. Onken, Stephan Weidinger, Andre Franke, Francesca Nasorri, Davide Pennino, Martine Grosber, et al. 2011. "Mutual Antagonism of T Cells Causing Psoriasis and Atopic Eczema." *New England Journal of Medicine* 365 (3): 231–38. https://doi.org/10.1056/NEJMoa1104200.

Farley, Sherry M., Lisa J. Wood, and Mihail S. Iordanov. 2011. "An Epidermotypic Model of Interface Dermatitis Reveals Individual Functions of Fas Ligand and Gamma Interferon in Hypergranulosis, Cytoid Body Formation, and Gene Expression." *The American Journal of Dermatopathology* 33 (3): 244–50. https://doi.org/10.1097/DAD.0b013e3181f1b200.

Feng, Yu, Qingchu Li, Yinxiang Wu, Nana Zhao, Lu Li, Li Li, and Liming Zhao. 2019. "Blocking C/EBP β Protects Vascular Endothelial Cells from Injury Induced by Intermittent Hypoxia." *Sleep & Breathing = Schlaf & Atmung* 23 (3): 953–62. https://doi.org/10.1007/s11325-018-1759-7.

Finlay, Andrew Y. 2009. "The Burden of Skin Disease: Quality of Life, Economic Aspects and Social Issues." *Clinical Medicine* 9 (6): 592–94. https://doi.org/10.7861/clinmedicine.9-6-592.

Furue, Masutaka, Kazuhisa Furue, Gaku Tsuji, and Takeshi Nakahara. 2020. "Interleukin-17A and Keratinocytes in Psoriasis." *International Journal of Molecular Sciences* 21 (4): 1275. https://doi.org/10.3390/ijms21041275.

Gade, Padmaja, Girish Ramachandran, Uday B. Maachani, Mark A. Rizzo, Tetsuya Okada, Ron Prywes, Alan S. Cross, Kazutoshi Mori, and Dhananjaya V. Kalvakolanu. 2012. "An IFN-γ-Stimulated ATF6-C/EBP-β-Signaling Pathway Critical for the Expression of Death Associated Protein Kinase 1 and Induction of Autophagy." *Proceedings of the National Academy of Sciences of the United States of America* 109 (26): 10316–21. https://doi.org/10.1073/pnas.1119273109.

Gade, Padmaja, Sanjit K. Roy, Hui Li, Shreeram C. Nallar, and Dhananjaya V. Kalvakolanu. 2008. "Critical Role for Transcription Factor C/EBP-Beta in Regulating the Expression of Death-Associated Protein Kinase 1." *Molecular and Cellular Biology* 28 (8): 2528–48. https://doi.org/10.1128/MCB.00784-07.

Gardiner, Jamie D., Lisa M. Abegglen, Xiaomeng Huang, Bryce E. Carter, Elizabeth A. Schackmann, Marcus Stucki, Christian N. Paxton, et al. 2017. "C/EBPβ-1 Promotes Transformation and Chemoresistance in Ewing Sarcoma Cells." *Oncotarget* 8 (16): 26013–26. https://doi.org/10.18632/oncotarget.14847.

Garzorz-Stark, Natalie, Richa Batra, Felix Lauffer, Manja Jargosch, Caroline Pilz, Sophie Roenneberg, Alexander Schäbitz, et al. 2020. "Identifying Hidden Drivers of Heterogeneous Inflammatory Diseases." bioRxiv. https://doi.org/10.1101/2020.07.25.221309.

Ghoreschi, Kamran, Arian Laurence, Xiang-Ping Yang, Cristina M. Tato, Mandy J. McGeachy, Joanne E. Konkel, Haydeé L. Ramos, et al. 2010. "Generation of Pathogenic T(H)17 Cells in the Absence of TGF-β Signalling." *Nature* 467 (7318): 967–71. https://doi.org/10.1038/nature09447.

Gilliet, Michel, and Roberto Lande. 2008. "Antimicrobial Peptides and Self-DNA in Autoimmune Skin Inflammation." *Current Opinion in Immunology* 20 (4): 401–7. https://doi.org/10.1016/j.coi.2008.06.008.

Go, Young-Mi, and Dean P. Jones. 2017. "Redox Theory of Aging: Implications for Health and Disease." *Clinical Science (London, England : 1979)* 131 (14): 1669–88. https://doi.org/10.1042/CS20160897.

Grassi, M., F. Capello, L. Bertolino, Z. Seia, and M. Pippione. 2009. "Identification of Granzyme B-Expressing CD-8-Positive T Cells in Lymphocytic Inflammatory Infiltrate in Cutaneous Lupus Erythematosus and in Dermatomyositis." *Clinical and Experimental Dermatology* 34 (8): 910–14. https://doi.org/10.1111/j.1365-2230.2009.03297.x.

Green, D. R., and J. C. Reed. 1998. "Mitochondria and Apoptosis." *Science (New York, N.Y.)* 281 (5381): 1309–12. https://doi.org/10.1126/science.281.5381.1309.

Griffiths, Christopher E. M., April W. Armstrong, Johann E. Gudjonsson, and Jonathan N. W. N. Barker. 2021. "Psoriasis." *The Lancet* 397 (10281): 1301–15. https://doi.org/10.1016/S0140-6736(20)32549-6.

Guo, Liang, Xi Li, and Qi-Qun Tang. 2015. "Transcriptional Regulation of Adipocyte Differentiation: A Central Role for CCAAT/Enhancer-Binding Protein (C/EBP) β." *The Journal of Biological Chemistry* 290 (2): 755–61. https://doi.org/10.1074/jbc.R114.619957.

Guo, Wenxing, John A. Wisniewski, and Haitao Ji. 2014. "Hot Spot-Based Design of Small-Molecule Inhibitors for Protein–Protein Interactions." *Bioorganic & Medicinal Chemistry Letters* 24 (11): 2546–54. https://doi.org/10.1016/j.bmcl.2014.03.095.

Gutsch, Romina, Judith D. Kandemir, Daniel Pietsch, Christian Cappello, Johann Meyer, Kathrin Simanowski, René Huber, and Korbinian Brand. 2011. "CCAAT/Enhancer-Binding Protein Beta Inhibits Proliferation in Monocytic Cells by Affecting the Retinoblastoma Protein/E2F/Cyclin E Pathway but Is Not Directly Required for Macrophage Morphology." *The Journal of Biological Chemistry* 286 (26): 22716–29. https://doi.org/10.1074/jbc.M110.152538.

Han, Yong Hwan, Suhn Hee Kim, Sung Zoo Kim, and Woo Hyun Park. 2008. "Antimycin A as a Mitochondrial Electron Transport Inhibitor Prevents the Growth of Human Lung Cancer A549 Cells." *Oncology Reports* 20 (3): 689–93.

Hay, Roderick J., Nicole E. Johns, Hywel C. Williams, Ian W. Bolliger, Robert P. Dellavalle, David J. Margolis, Robin Marks, et al. 2014. "The Global Burden of Skin Disease in 2010: An Analysis of the Prevalence and Impact of Skin Conditions." *The Journal of Investigative Dermatology* 134 (6): 1527–34. https://doi.org/10.1038/jid.2013.446.

Henes, Joerg C., Eva Ziupa, Michael Eisfelder, Annette Adamczyk, Bjoern Knaudt, Felix Jacobs, Juergen Lux, et al. 2014. "High Prevalence of Psoriatic Arthritis in Dermatological Patients with Psoriasis: A Cross-Sectional Study." *Rheumatology International* 34 (2): 227–34. https://doi.org/10.1007/s00296-013-2876-z.

Hirai, Hideyo, Asumi Yokota, Akihiro Tamura, Atsushi Sato, and Taira Maekawa. 2015. "Non-Steady-State Hematopoiesis Regulated by the C/EBPβ Transcription Factor." *Cancer Science* 106 (7): 797–802. https://doi.org/10.1111/cas.12690.

Hirai, Hideyo, Pu Zhang, Tajhal Dayaram, Christopher J. Hetherington, Shin-ichi Mizuno, Jiro Imanishi, Koichi Akashi, and Daniel G. Tenen. 2006. "C/EBPbeta Is Required for 'emergency' Granulopoiesis." *Nature Immunology* 7 (7): 732–39. https://doi.org/10.1038/ni1354.

Ho, Allen W., and Thomas S. Kupper. 2019. "T Cells and the Skin: From Protective Immunity to Inflammatory Skin Disorders." *Nature Reviews Immunology* 19 (8): 490–502. https://doi.org/10.1038/s41577-019-0162-3.

Hong, Lingzi, Tomasz Herjan, Katarzyna Bulek, Jianxin Xiao, Suzy A. A. Comhair, Serpil C. Erzurum, Xiaoxia Li, and Caini Liu. 2022. "Mechanisms of Corticosteroid Resistance in Type 17 Asthma." *Journal of Immunology (Baltimore, Md.: 1950)* 209 (10): 1860–69. https://doi.org/10.4049/jimmunol.2200288.

House, John S., Songyun Zhu, Rakesh Ranjan, Keith Linder, and Robert C. Smart. 2010. "C/EBPalpha and C/EBPbeta Are Required for Sebocyte Differentiation and Stratified Squamous Differentiation in Adult Mouse Skin." *PloS One* 5 (3): e9837. https://doi.org/10.1371/journal.pone.0009837.

Howell, Michael D., Byung Eui Kim, Peisong Gao, Audrey V. Grant, Mark Boguniewicz, Anna Debenedetto, Lynda Schneider, Lisa A. Beck, Kathleen C. Barnes, and Donald Y. M. Leung. 2007. "Cytokine Modulation of Atopic Dermatitis Filaggrin Skin Expression." *The Journal of Allergy and Clinical Immunology* 120 (1): 150–55. https://doi.org/10.1016/j.jaci.2007.04.031.

Hsu, W., T. K. Kerppola, P. L. Chen, T. Curran, and S. Chen-Kiang. 1994. "Fos and Jun Repress Transcription Activation by NF-IL6 through Association at the Basic Zipper Region." *Molecular and Cellular Biology* 14 (1): 268–76. https://doi.org/10.1128/mcb.14.1.268-276.1994.

Hu, Jingyi, Qiong Bian, Xiaolu Ma, Yihua Xu, and Jianqing Gao. 2022. "A Double-Edged Sword: ROS Related Therapies in the Treatment of Psoriasis." *Asian Journal of Pharmaceutical Sciences* 17 (6): 798–816. https://doi.org/10.1016/j.ajps.2022.10.005.

Huber, René, Daniel Pietsch, Thomas Panterodt, and Korbinian Brand. 2012. "Regulation of C/EBPβ and Resulting Functions in Cells of the Monocytic Lineage." *Cellular Signalling* 24 (6): 1287–96. https://doi.org/10.1016/j.cellsig.2012.02.007.

Ioannides, D., E. Vakirlis, L. Kemeny, B. Marinovic, C. Massone, R. Murphy, A. Nast, et al. 2020. "European S1 Guidelines on the Management of Lichen Planus: A Cooperation of the European Dermatology Forum with the European Academy of Dermatology and Venereology." *Journal of the European Academy of Dermatology and Venereology: JEADV* 34 (7): 1403–14. https://doi.org/10.1111/jdv.16464.

Jinesh, Goodwin G., Elsa R. Flores, and Andrew S. Brohl. 2018. "Chromosome 19 MiRNA Cluster and CEBPB Expression Specifically Mark and Potentially Drive Triple Negative Breast Cancers." *PloS One* 13 (10): e0206008. https://doi.org/10.1371/journal.pone.0206008.

Kabashima, Kenji, Tetsuya Honda, Florent Ginhoux, and Gyohei Egawa. 2019. "The Immunological Anatomy of the Skin." *Nature Reviews Immunology* 19 (1): 19–30. https://doi.org/10.1038/s41577-018-0084-5.

Kishimoto, Megumi, Mayumi Komine, Miho Sashikawa-Kimura, Tuba Musarrat Ansary, Koji Kamiya, Junichi Sugai, Makiko Mieno, et al. 2021. "STAT3 Activation in Psoriasis and Cancers." *Diagnostics (Basel, Switzerland)* 11 (10): 1903. https://doi.org/10.3390/diagnostics11101903.

Koning, Heleen D. de, Anna Simon, Patrick L. J. M. Zeeuwen, and Joost Schalkwijk. 2012. "Pattern Recognition Receptors in Infectious Skin Diseases." *Microbes and Infection* 14 (11): 881–93. https://doi.org/10.1016/j.micinf.2012.03.004.

Krueger, G. G., and G. Stingl. 1989. "Immunology/Inflammation of the Skin--a 50-Year Perspective." *The Journal of Investigative Dermatology* 92 (4 Suppl): 32S-51S. https://doi.org/10.1111/1523-1747.ep13074960.

Kupper, Thomas S., and Robert C. Fuhlbrigge. 2004. "Immune Surveillance in the Skin: Mechanisms and Clinical Consequences." *Nature Reviews Immunology* 4 (3): 211–22. https://doi.org/10.1038/nri1310.

Kurata, Morito, Iichiro Onishi, Tomoko Takahara, Yukari Yamazaki, Sachiko Ishibashi, Ryo Goitsuka, Daisuke Kitamura, et al. 2021. "C/EBPβ Induces B-Cell Acute Lymphoblastic Leukemia and Cooperates with BLNK Mutations." *Cancer Science* 112 (12): 4920–30. https://doi.org/10.1111/cas.15164.

Lai, Yuping, and Richard L. Gallo. 2009. "AMPed up Immunity: How Antimicrobial Peptides Have Multiple Roles in Immune Defense." *Trends in Immunology* 30 (3): 131–41. https://doi.org/10.1016/j.it.2008.12.003.

LaMarca, Heather L., Adriana P. Visbal, Chad J. Creighton, Hao Liu, Yiqun Zhang, Fariba Behbod, and Jeffrey M. Rosen. 2010. "CCAAT/Enhancer Binding Protein Beta Regulates Stem Cell Activity and Specifies Luminal Cell Fate in the Mammary Gland." *Stem Cells (Dayton, Ohio)* 28 (3): 535–44. https://doi.org/10.1002/stem.297.

Lambert, Mélanie, Samy Jambon, Sabine Depauw, and Marie-Hélène David-Cordonnier. 2018. "Targeting Transcription Factors for Cancer Treatment." *Molecules : A Journal of Synthetic Chemistry and Natural Product Chemistry* 23 (6): 1479. https://doi.org/10.3390/molecules23061479.

Latz, Eicke, T. Sam Xiao, and Andrea Stutz. 2013. "Activation and Regulation of the Inflammasomes." *Nature Reviews. Immunology* 13 (6): 10.1038/nri3452. https://doi.org/10.1038/nri3452.

Lauffer, Felix, Manja Jargosch, Linda Krause, Natalie Garzorz-Stark, Regina Franz, Sophie Roenneberg, Alexander Böhner, et al. 2018. "Type I Immune Response Induces Keratinocyte Necroptosis and Is Associated with Interface Dermatitis." *Journal of Investigative Dermatology* 138 (8): 1785–94. https://doi.org/10.1016/j.jid.2018.02.034.

Lebre, Maria C., Angelic M. G. van der Aar, Lisa van Baarsen, Toni M. M. van Capel, Joost H. N. Schuitemaker, Martien L. Kapsenberg, and Esther C. de Jong. 2007. "Human Keratinocytes Express Functional Toll-like Receptor 3, 4, 5, and 9." *The Journal of Investigative Dermatology* 127 (2): 331–41. https://doi.org/10.1038/sj.jid.5700530.

Lechner, Melissa G., Carolina Megiel, Sarah M. Russell, Brigid Bingham, Nicholas Arger, Tammy Woo, and Alan L. Epstein. 2011. "Functional Characterization of Human Cd33+ and Cd11b+ Myeloid-Derived Suppressor Cell Subsets Induced from Peripheral Blood Mononuclear Cells Co-Cultured with a Diverse Set of Human Tumor Cell Lines." *Journal of Translational Medicine* 9 (June): 90. https://doi.org/10.1186/1479-5876-9-90.

LeClair, K. P., M. A. Blanar, and P. A. Sharp. 1992. "The P50 Subunit of NF-Kappa B Associates with the NF-IL6 Transcription Factor." *Proceedings of the National Academy of Sciences of the United States of America* 89 (17): 8145–49. https://doi.org/10.1073/pnas.89.17.8145.

Lee, Lil-Li, Su-Jung Kim, Young-Il Hahn, Jeong-Hoon Jang, Soma Saeidi, and Young-Joon Surh. 2021. "Stabilization of C/EBPβ through Direct Interaction with STAT3 in H-Ras Transformed Human Mammary Epithelial Cells." *Biochemical and Biophysical Research Communications* 546 (March): 130–37. https://doi.org/10.1016/j.bbrc.2021.02.011.

Lefterova, Martina I., Yong Zhang, David J. Steger, Michael Schupp, Jonathan Schug, Ana Cristancho, Dan Feng, et al. 2008. "PPARgamma and C/EBP Factors Orchestrate Adipocyte Biology via Adjacent Binding on a Genome-Wide Scale." *Genes & Development* 22 (21): 2941–52. https://doi.org/10.1101/gad.1709008.

Lei, Kecheng, Yiyuan Xia, Xiao-Chuan Wang, Eun Hee Ahn, Lingjing Jin, and Keqiang Ye. 2020. "C/EBPβ Mediates NQO1 and GSTP1 Anti-Oxidative Reductases Expression in Glioblastoma, Promoting Brain Tumor Proliferation." *Redox Biology* 34 (July): 101578. https://doi.org/10.1016/j.redox.2020.101578.

Li, Congxin, François Cesbron, Michael Oehler, Michael Brunner, and Thomas Höfer. 2018. "Frequency Modulation of Transcriptional Bursting Enables Sensitive and Rapid Gene Regulation." *Cell Systems* 6 (4): 409-423.e11. https://doi.org/10.1016/j.cels.2018.01.012.

Li, D., J. Liu, S. Huang, X. Bi, B. Wang, Q. Chen, H. Chen, and X. Pu. 2018. "CCAAT Enhancer Binding Protein β Promotes Tumor Growth and Inhibits Apoptosis in Prostate Cancer by Methylating Estrogen Receptor β." *Neoplasma* 65 (1): 34–41. https://doi.org/10.4149/neo_2018_161205N620.

Li, Dan, Jin Li, Chunlei Li, Qianming Chen, and Hong Hua. 2017. "The Association of Thyroid Disease and Oral Lichen Planus: A Literature Review and Meta-Analysis." *Frontiers in Endocrinology* 8: 310. https://doi.org/10.3389/fendo.2017.00310.

Li, Wei, Takashi Tanikawa, Ilona Kryczek, Houjun Xia, Gaopeng Li, Ke Wu, Shuang Wei, et al. 2018. "Aerobic Glycolysis Controls Myeloid-Derived Suppressor Cells and Tumor Immunity via a Specific CEBPB Isoform in Triple-Negative Breast Cancer." *Cell Metabolism* 28 (1): 87-103.e6. https://doi.org/10.1016/j.cmet.2018.04.022.

Liguori, Ilaria, Gennaro Russo, Francesco Curcio, Giulia Bulli, Luisa Aran, David Della-Morte, Gaetano Gargiulo, et al. 2018. "Oxidative Stress, Aging, and Diseases." *Clinical Interventions in Aging* 13 (April): 757–72. https://doi.org/10.2147/CIA.S158513.

Liu, Min, Runmei Li, Min Wang, Ting Liu, Qiuru Zhou, Dong Zhang, Jian Wang, Meng Shen, Xiubao Ren, and Qian Sun. 2022. "PGAM1 Regulation of ASS1 Contributes to the Progression of Breast Cancer through the CAMP/AMPK/CEBPB Pathway." *Molecular Oncology* 16 (15): 2843–60. https://doi.org/10.1002/1878-0261.13259.

Liu, Shan-Shan, Xiao-Xi Lv, Chang Liu, Jie Qi, Yun-Xuan Li, Xu-Peng Wei, Ke Li, et al. 2019. "Targeting Degradation of the Transcription Factor C/EBPβ Reduces Lung Fibrosis by Restoring Activity of the Ubiquitin-Editing Enzyme A20 in Macrophages." *Immunity* 51 (3): 522-534.e7. https://doi.org/10.1016/j.immuni.2019.06.014.

Liu, Xiao-Zheng, Anastasiia Rulina, Man Hung Choi, Line Pedersen, Johanna Lepland, Sina T. Takle, Noelly Madeleine, et al. 2022. "C/EBPB-Dependent Adaptation to Palmitic Acid Promotes Tumor Formation in Hormone Receptor Negative Breast Cancer." *Nature Communications* 13 (1): 69. https://doi.org/10.1038/s41467-021-27734-2.

Lock, Christopher, Guy Hermans, Rosetta Pedotti, Andrea Brendolan, Eric Schadt, Hideki Garren, Annette Langer-Gould, et al. 2002. "Gene-Microarray Analysis of Multiple Sclerosis Lesions Yields New Targets Validated in Autoimmune Encephalomyelitis." *Nature Medicine* 8 (5): 500–508. https://doi.org/10.1038/nm0502-500.

Lodi, G., R. Pellicano, and M. Carrozzo. 2010. "Hepatitis C Virus Infection and Lichen Planus: A Systematic Review with Meta-Analysis." *Oral Diseases* 16 (7): 601–12. https://doi.org/10.1111/j.1601-0825.2010.01670.x.

Lopez, Rodolphe G., Susana Garcia-Silva, Susan J. Moore, Oksana Bereshchenko, Ana B. Martinez-Cruz, Olga Ermakova, Elke Kurz, Jesus M. Paramio, and Claus Nerlov. 2009. "C/EBPalpha and Beta Couple Interfollicular Keratinocyte Proliferation Arrest to Commitment and Terminal Differentiation." *Nature Cell Biology* 11 (10): 1181–90. https://doi.org/10.1038/ncb1960.

Lou, Fangzhou, Yang Sun, Zhenyao Xu, Liman Niu, Zhikai Wang, Siyu Deng, Zhaoyuan Liu, et al. 2020. "Excessive Polyamine Generation in Keratinocytes Promotes Self-RNA Sensing by Dendritic Cells in Psoriasis." *Immunity* 53 (1): 204-216.e10. https://doi.org/10.1016/j.immuni.2020.06.004.

Lu, Tao, Ming Li, Mengnan Zhao, Yiwei Huang, Guoshu Bi, Jiaqi Liang, Zhencong Chen, et al. 2022. "Metformin Inhibits Human Non-Small Cell Lung Cancer by Regulating AMPK-CEBPB-PDL1 Signaling Pathway." *Cancer Immunology, Immunotherapy: CII* 71 (7): 1733–46. https://doi.org/10.1007/s00262-021-03116-x.

Lu, Yong-Chen, Ira Kim, Elizabeth Lye, Fang Shen, Nobutaka Suzuki, Shinobu Suzuki, Steve Gerondakis, et al. 2009. "Differential Role for C-Rel and C/EBPbeta/Delta in TLR-Mediated Induction of Proinflammatory Cytokines." *Journal of Immunology (Baltimore, Md.: 1950)* 182 (11): 7212–21. https://doi.org/10.4049/jimmunol.0802971.

Luo, Bao-Ying, Jie Zhou, Dan Guo, Qian Yang, Qin Tian, Dun-Peng Cai, Rui-Mei Zhou, et al. 2022. "Methamphetamine Induces Thoracic Aortic Aneurysm/Dissection through C/EBPβ." *Biochimica Et Biophysica Acta. Molecular Basis of Disease* 1868 (9): 166447. https://doi.org/10.1016/j.bbadis.2022.166447.

Macosko, Evan Z., Anindita Basu, Rahul Satija, James Nemesh, Karthik Shekhar, Melissa Goldman, Itay Tirosh, et al. 2015. "Highly Parallel Genome-Wide Expression Profiling of Individual Cells Using Nanoliter Droplets." *Cell* 161 (5): 1202–14. https://doi.org/10.1016/j.cell.2015.05.002.

Marigo, Ilaria, Erika Bosio, Samantha Solito, Circe Mesa, Audry Fernandez, Luigi Dolcetti, Stefano Ugel, et al. 2010. "Tumor-Induced Tolerance and Immune Suppression Depend on the C/EBPbeta Transcription Factor." *Immunity* 32 (6): 790–802. https://doi.org/10.1016/j.immuni.2010.05.010.

Martin, Praxedis, Jérémie D. Goldstein, Loïc Mermoud, Alejandro Diaz-Barreiro, and Gaby Palmer. 2021. "IL-1 Family Antagonists in Mouse and Human Skin Inflammation." *Frontiers in Immunology* 12. https://www.frontiersin.org/articles/10.3389/fimmu.2021.652846.

Martinon, Fabio, Kimberly Burns, and Jürg Tschopp. 2002. "The Inflammasome: A Molecular Platform Triggering Activation of Inflammatory Caspases and Processing of ProIL-Beta." *Molecular Cell* 10 (2): 417–26. https://doi.org/10.1016/s1097-2765(02)00599-3.

Martinon, Fabio, Annick Mayor, and Jürg Tschopp. 2009. "The Inflammasomes: Guardians of the Body." *Annual Review of Immunology* 27: 229–65. https://doi.org/10.1146/annurev.immunol.021908.132715.

Matsui, Takeshi, and Masayuki Amagai. 2015. "Dissecting the Formation, Structure and Barrier Function of the Stratum Corneum." *International Immunology* 27 (6): 269–80. https://doi.org/10.1093/intimm/dxv013.

Matsumoto, M., Y. Sakao, and S. Akira. 1998. "Inducible Expression of Nuclear Factor IL-6 Increases Endogenous Gene Expression of Macrophage Inflammatory Protein-1 Alpha, Osteopontin and CD14 in a Monocytic Leukemia Cell Line." *International Immunology* 10 (12): 1825–35. https://doi.org/10.1093/intimm/10.12.1825.

Matsusaka, T., K. Fujikawa, Y. Nishio, N. Mukaida, K. Matsushima, T. Kishimoto, and S. Akira. 1993. "Transcription Factors NF-IL6 and NF-Kappa B Synergistically Activate Transcription of the Inflammatory Cytokines, Interleukin 6 and Interleukin 8." *Proceedings of the National Academy of Sciences of the United States of America* 90 (21): 10193–97. https://doi.org/10.1073/pnas.90.21.10193.

McGee, Heather M., Barbara Schmidt, Carmen J. Booth, George D. Yancopoulos, David M. Valenzuela, Andrew J. Murphy, Sean Stevens, Richard A. Flavell, and Valerie Horsley. 2013. "Interleukin-22 Promotes Fibroblast- Mediated Wound Repair in the Skin." *The Journal of Investigative Dermatology* 133 (5): 1321–29. https://doi.org/10.1038/jid.2012.463.

Mehrel, T., D. Hohl, J. A. Rothnagel, M. A. Longley, D. Bundman, C. Cheng, U. Lichti, M. E. Bisher, A. C. Steven, and P. M. Steinert. 1990. "Identification of a Major Keratinocyte Cell Envelope Protein, Loricrin." *Cell* 61 (6): 1103–12. https://doi.org/10.1016/0092-8674(90)90073-n.

Miao, Edward A., Jayant V. Rajan, and Alan Aderem. 2011. "Caspase-1 Induced Pyroptotic Cell Death." *Immunological Reviews* 243 (1): 206–14. https://doi.org/10.1111/j.1600-065X.2011.01044.x.

Millward, Carrie A., Jason D. Heaney, David S. Sinasac, Eric C. Chu, Ilya R. Bederman, Danielle A. Gilge, Stephen F. Previs, and Colleen M. Croniger. 2007. "Mice with a Deletion in the Gene for CCAAT/Enhancer-Binding Protein Beta Are Protected against Diet-Induced Obesity." *Diabetes* 56 (1): 161–67. https://doi.org/10.2337/db06-0310.

Mink, S., S. Jaswal, O. Burk, and K. H. Klempnauer. 1999. "The V-Myb Oncoprotein Activates C/EBPbeta Expression by Stimulating an Autoregulatory Loop at the C/EBPbeta Promoter." *Biochimica Et Biophysica Acta* 1447 (2–3): 175–84. https://doi.org/10.1016/s0167-4781(99)00168-2.

Moll, R., W. W. Franke, D. L. Schiller, B. Geiger, and R. Krepler. 1982. "The Catalog of Human Cytokeratins: Patterns of Expression in Normal Epithelia, Tumors and Cultured Cells." *Cell* 31 (1): 11–24. https://doi.org/10.1016/0092-8674(82)90400-7.

Mori, Michiko, Leif Bjermer, Jonas S. Erjefält, Martin R. Stampfli, and Abraham B. Roos. 2015. "Small Airway Epithelial-C/EBPβ Is Increased in Patients with Advanced COPD." *Respiratory Research* 16: 133. https://doi.org/10.1186/s12931-015-0297-0.

Mukaida, N., Y. Mahe, and K. Matsushima. 1990. "Cooperative Interaction of Nuclear Factor-Kappa B- and Cis-Regulatory Enhancer Binding Protein-like Factor Binding Elements in Activating the Interleukin-8 Gene by pro-Inflammatory Cytokines." *The Journal of Biological Chemistry* 265 (34): 21128–33.

Müller, Christine, Laura M. Zidek, Tobias Ackermann, Tristan de Jong, Peng Liu, Verena Kliche, Mohamad Amr Zaini, et al. 2018. "Reduced Expression of C/EBPβ-LIP Extends Health and Lifespan in Mice." *ELife* 7 (June): e34985. https://doi.org/10.7554/eLife.34985.

Nagi-Miura, Noriko, Daisuke Okuzaki, Kosuke Torigata, Minami A. Sakurai, Akihiko Ito, Naohito Ohno, and Hiroshi Nojima. 2013. "CAWS Administration Increases the Expression of Interferon γ and Complement Factors That Lead to Severe Vasculitis in DBA/2 Mice." *BMC Immunology* 14 (September): 44. https://doi.org/10.1186/1471-2172-14-44.

Natsuka, S., S. Akira, Y. Nishio, S. Hashimoto, T. Sugita, H. Isshiki, and T. Kishimoto. 1992. "Macrophage Differentiation-Specific Expression of NF-IL6, a Transcription Factor for Interleukin-6." *Blood* 79 (2): 460–66.

Nestle, Frank O., Paola Di Meglio, Jian-Zhong Qin, and Brian J. Nickoloff. 2009. "Skin Immune Sentinels in Health and Disease." *Nature Reviews Immunology* 9 (10): 679–91. https://doi.org/10.1038/nri2622.

Nestle, Frank O., Daniel H. Kaplan, and Jonathan Barker. 2009. "Psoriasis." *New England Journal of Medicine* 361 (5): 496–509. https://doi.org/10.1056/NEJMra0804595.

Niehof, M., S. Kubicka, L. Zender, M. P. Manns, and C. Trautwein. 2001. "Autoregulation Enables Different Pathways to Control CCAAT/Enhancer Binding Protein Beta (C/EBP Beta) Transcription." *Journal of Molecular Biology* 309 (4): 855–68. https://doi.org/10.1006/jmbi.2001.4708.

Niehof, M., K. Streetz, T. Rakemann, S. C. Bischoff, M. P. Manns, F. Horn, and C. Trautwein. 2001. "Interleukin-6-Induced Tethering of STAT3 to the LAP/C/EBPbeta Promoter Suggests a New Mechanism of Transcriptional Regulation by STAT3." *The Journal of Biological Chemistry* 276 (12): 9016–27. https://doi.org/10.1074/jbc.M009284200.

Noda, Shinji, James G. Krueger, and Emma Guttman-Yassky. 2015. "The Translational Revolution and Use of Biologics in Patients with Inflammatory Skin Diseases." *Journal of Allergy and Clinical Immunology* 135 (2): 324–36. https://doi.org/10.1016/j.jaci.2014.11.015.

Ong, Peck Y., Takaaki Ohtake, Corinne Brandt, Ian Strickland, Mark Boguniewicz, Tomas Ganz, Richard L. Gallo, and Donald Y. M. Leung. 2002. "Endogenous Antimicrobial Peptides and Skin Infections in Atopic Dermatitis." *The New England Journal of Medicine* 347 (15): 1151–60. https://doi.org/10.1056/NEJMoa021481.

Ossipow, V., P. Descombes, and U. Schibler. 1993. "CCAAT/Enhancer-Binding Protein MRNA Is Translated into Multiple Proteins with Different Transcription Activation Potentials." *Proceedings of the National Academy of Sciences of the United States of America* 90 (17): 8219–23. https://doi.org/10.1073/pnas.90.17.8219.

Otsuka, Atsushi, Takashi Nomura, Pawinee Rerknimitr, Judith A. Seidel, Tetsuya Honda, and Kenji Kabashima. 2017. "The Interplay between Genetic and Environmental Factors in the Pathogenesis of Atopic Dermatitis." *Immunological Reviews* 278 (1): 246–62. https://doi.org/10.1111/imr.12545.

P, Gade, Kimball As, DiNardo Ac, Gangwal P, Ross Dd, Boswell Hs, Keay Sk, and Kalvakolanu Dv. 2016. "Death-Associated Protein Kinase-1 Expression and Autophagy in Chronic Lymphocytic Leukemia Are Dependent on Activating Transcription Factor-6 and CCAAT/Enhancer-Binding Protein-β." *The Journal of Biological Chemistry* 291 (42). https://doi.org/10.1074/jbc.M116.725796.

Palmer, Colin N. A., Alan D. Irvine, Ana Terron-Kwiatkowski, Yiwei Zhao, Haihui Liao, Simon P. Lee, David R. Goudie, et al. 2006. "Common Loss-of-Function Variants of the Epidermal Barrier Protein Filaggrin Are a Major Predisposing Factor for Atopic Dermatitis." *Nature Genetics* 38 (4): 441–46. https://doi.org/10.1038/ng1767.

Parisi, Rosa, Deborah P. M. Symmons, Christopher E. M. Griffiths, Darren M. Ashcroft, and Identification and Management of Psoriasis and Associated ComorbidiTy (IMPACT) project team. 2013. "Global Epidemiology of Psoriasis: A Systematic Review of Incidence and Prevalence." *The Journal of Investigative Dermatology* 133 (2): 377–85. https://doi.org/10.1038/jid.2012.339.

Pasparakis, Manolis, Ingo Haase, and Frank O. Nestle. 2014. "Mechanisms Regulating Skin Immunity and Inflammation." *Nature Reviews Immunology* 14 (5): 289–301. https://doi.org/10.1038/nri3646.

Patel, Devang N., Carter A. King, Steven R. Bailey, Jeffrey W. Holt, Kaliyamurthi Venkatachalam, Alok Agrawal, Anthony J. Valente, and Bysani Chandrasekar. 2007. "Interleukin-17 Stimulates C-Reactive Protein Expression in Hepatocytes

and Smooth Muscle Cells via P38 MAPK and ERK1/2-Dependent NF-KappaB and C/EBPbeta Activation." *The Journal of Biological Chemistry* 282 (37): 27229–38. https://doi.org/10.1074/jbc.M703250200.

Pleńkowska, Joanna, Magdalena Gabig-Cimińska, and Paweł Mozolewski. 2020. "Oxidative Stress as an Important Contributor to the Pathogenesis of Psoriasis." *International Journal of Molecular Sciences* 21 (17): 6206. https://doi.org/10.3390/ijms21176206.

Poli, V. 1998. "The Role of C/EBP Isoforms in the Control of Inflammatory and Native Immunity Functions." *The Journal of Biological Chemistry* 273 (45): 29279–82. https://doi.org/10.1074/jbc.273.45.29279.

Poli, V., and R. Cortese. 1989. "Interleukin 6 Induces a Liver-Specific Nuclear Protein That Binds to the Promoter of Acute-Phase Genes." *Proceedings of the National Academy of Sciences of the United States of America* 86 (21): 8202–6. https://doi.org/10.1073/pnas.86.21.8202.

Poli, V., F. P. Mancini, and R. Cortese. 1990. "IL-6DBP, a Nuclear Protein Involved in Interleukin-6 Signal Transduction, Defines a New Family of Leucine Zipper Proteins Related to C/EBP." *Cell* 63 (3): 643–53. https://doi.org/10.1016/0092-8674(90)90459-r.

Prpić Massari, L., M. Kastelan, F. Gruber, G. Laskarin, V. Sotosek Tokmadzić, N. Strbo, G. Zamolo, G. Zauhar, and D. Rukavina. 2004. "Perforin Expression in Peripheral Blood Lymphocytes and Skin-Infiltrating Cells in Patients with Lichen Planus." *The British Journal of Dermatology* 151 (2): 433–39. https://doi.org/10.1111/j.1365-2133.2004.06086.x.

Quaranta, Maria, Bettina Knapp, Natalie Garzorz, Martina Mattii, Venu Pullabhatla, Davide Pennino, Christian Andres, et al. 2014. "Intraindividual Genome Expression Analysis Reveals a Specific Molecular Signature of Psoriasis and Eczema." *Science Translational Medicine* 6 (244): 244ra90. https://doi.org/10.1126/scitranslmed.3008946.

Rahman, Shaikh M., Rachel C. Janssen, Mahua Choudhury, Karalee C. Baquero, Rebecca M. Aikens, Becky A. de la Houssaye, and Jacob E. Friedman. 2012. "CCAAT/Enhancer-Binding Protein β (C/EBPβ) Expression Regulates Dietary-Induced Inflammation in Macrophages and Adipose Tissue in Mice." *The Journal of Biological Chemistry* 287 (41): 34349–60. https://doi.org/10.1074/jbc.M112.410613.

Rahman, Shaikh Mizanoor, Jill M. Schroeder-Gloeckler, Rachel C. Janssen, Hua Jiang, Ishtiaq Qadri, Kenneth N. Maclean, and Jacob E. Friedman. 2007. "CCAAT/Enhancing Binding Protein Beta Deletion in Mice Attenuates Inflammation, Endoplasmic Reticulum Stress, and Lipid Accumulation in Diet-Induced Nonalcoholic Steatohepatitis." *Hepatology (Baltimore, Md.)* 45 (5): 1108–17. https://doi.org/10.1002/hep.21614.

Ramji, Dipak P., and Pelagia Foka. 2002. "CCAAT/Enhancer-Binding Proteins: Structure, Function and Regulation." *The Biochemical Journal* 365 (Pt 3): 561–75. https://doi.org/10.1042/BJ20020508.

Ray, A., M. Hannink, and B. K. Ray. 1995. "Concerted Participation of NF-Kappa B and C/EBP Heteromer in Lipopolysaccharide Induction of Serum Amyloid A Gene Expression in Liver." *The Journal of Biological Chemistry* 270 (13): 7365–74. https://doi.org/10.1074/jbc.270.13.7365.

Regalo, Goncalo, Susann Förster, Carlos Resende, Bianca Bauer, Barbara Fleige, Wolfgang Kemmner, Peter M. Schlag, Thomas F. Meyer, José C. Machado, and Achim Leutz. 2016. "C/EBPβ Regulates Homeostatic and Oncogenic Gastric Cell Proliferation." *Journal of Molecular Medicine (Berlin, Germany)* 94 (12): 1385–95. https://doi.org/10.1007/s00109-016-1447-7.

Reynolds, Gary, Peter Vegh, James Fletcher, Elizabeth F. M. Poyner, Emily Stephenson, Issac Goh, Rachel A. Botting, et al. 2021. "Developmental Cell Programs Are Co-Opted in Inflammatory Skin Disease." *Science* 371 (6527): eaba6500. https://doi.org/10.1126/science.aba6500.

Robinson, G. W., P. F. Johnson, L. Hennighausen, and E. Sterneck. 1998. "The C/EBPbeta Transcription Factor Regulates Epithelial Cell Proliferation and Differentiation in the Mammary Gland." *Genes & Development* 12 (12): 1907–16. https://doi.org/10.1101/gad.12.12.1907.

Roos, Abraham B., Jenny L. Barton, Anna Miller-Larsson, Benita Dahlberg, Tove Berg, Lukas Didon, and Magnus Nord. 2012. "Lung Epithelial-C/EBPβ Contributes to LPS-Induced Inflammation and Its Suppression by Formoterol." *Biochemical and Biophysical Research Communications* 423 (1): 134–39. https://doi.org/10.1016/j.bbrc.2012.05.096.

Roos, Abraham B., and Magnus Nord. 2012. "The Emerging Role of C/EBPs in Glucocorticoid Signaling: Lessons from the Lung." *The Journal of Endocrinology* 212 (3): 291–305. https://doi.org/10.1530/JOE-11-0369.

Roy, S. K., S. J. Wachira, X. Weihua, J. Hu, and D. V. Kalvakolanu. 2000. "CCAAT/Enhancer-Binding Protein-Beta Regulates Interferon-Induced Transcription through a Novel Element." *The Journal of Biological Chemistry* 275 (17): 12626–32. https://doi.org/10.1074/jbc.275.17.12626.

Roy, Sanjit K., Junbo Hu, Qingjun Meng, Ying Xia, Paul S. Shapiro, Sekhar P. M. Reddy, Leonidas C. Platanias, et al. 2002. "MEKK1 Plays a Critical Role in Activating the Transcription Factor C/EBP-Beta-Dependent Gene Expression in Response to IFN-Gamma." *Proceedings of the National Academy of Sciences of the United States of America* 99 (12): 7945–50. https://doi.org/10.1073/pnas.122075799.

Rozenberg, Julian M., Paramita Bhattacharya, Raghunath Chatterjee, Kimberly Glass, and Charles Vinson. 2013. "Combinatorial Recruitment of CREB, C/EBPβ and c-Jun Determines Activation of Promoters upon Keratinocyte Differentiation." *PloS One* 8 (11): e78179. https://doi.org/10.1371/journal.pone.0078179.

Ruddy, Matthew J., Grace C. Wong, Xikui K. Liu, Hiroyasu Yamamoto, Soji Kasayama, Keith L. Kirkwood, and Sarah L. Gaffen. 2004a. "Functional Cooperation between Interleukin-17 and Tumor Necrosis Factor-Alpha Is Mediated by CCAAT/Enhancer-Binding Protein Family Members." *The Journal of Biological Chemistry* 279 (4): 2559–67. https://doi.org/10.1074/jbc.M308809200.

Ruffell, Daniela, Foteini Mourkioti, Adriana Gambardella, Peggy Kirstetter, Rodolphe G. Lopez, Nadia Rosenthal, and Claus Nerlov. 2009. "A CREB-C/EBPβ Cascade Induces M2 Macrophage-Specific Gene Expression and Promotes Muscle

Injury Repair." *Proceedings of the National Academy of Sciences of the United States of America* 106 (41): 17475–80. https://doi.org/10.1073/pnas.0908641106.

Sabat, Robert, Kerstin Wolk, Lucie Loyal, Wolf-Dietrich Döcke, and Kamran Ghoreschi. 2019. "T Cell Pathology in Skin Inflammation." *Seminars in Immunopathology* 41 (3): 359–77. https://doi.org/10.1007/s00281-019-00742-7.

Sahu, Sanjaya Kumar, Manish Kumar, Sohini Chakraborty, Srijon Kaushik Banerjee, Ranjeet Kumar, Pushpa Gupta, Kuladip Jana, et al. 2017. "MicroRNA 26a (MiR-26a)/KLF4 and CREB-C/EBPβ Regulate Innate Immune Signaling, the Polarization of Macrophages and the Trafficking of Mycobacterium Tuberculosis to Lysosomes during Infection." *PLoS Pathogens* 13 (5): e1006410. https://doi.org/10.1371/journal.ppat.1006410.

Sánchez, Ángela, Carlos Relaño, Araceli Carrasco, Constanza Contreras-Jurado, Antonio Martín-Duce, Ana Aranda, and Susana Alemany. 2017. "Map3k8 Controls Granulocyte Colony-Stimulating Factor Production and Neutrophil Precursor Proliferation in Lipopolysaccharide-Induced Emergency Granulopoiesis." *Scientific Reports* 7 (1): 5010. https://doi.org/10.1038/s41598-017-04538-3.

Sano, Shigetoshi, Keith Syson Chan, Steve Carbajal, John Clifford, Mary Peavey, Kaoru Kiguchi, Satoshi Itami, Brian J. Nickoloff, and John DiGiovanni. 2005. "Stat3 Links Activated Keratinocytes and Immunocytes Required for Development of Psoriasis in a Novel Transgenic Mouse Model." *Nature Medicine* 11 (1): 43–49. https://doi.org/10.1038/nm1162.

Satake, Sakiko, Hideyo Hirai, Yoshihiro Hayashi, Nobuaki Shime, Akihiro Tamura, Hisayuki Yao, Satoshi Yoshioka, et al. 2012. "C/EBPβ Is Involved in the Amplification of Early Granulocyte Precursors during Candidemia-Induced 'Emergency' Granulopoiesis." *Journal of Immunology (Baltimore, Md.: 1950)* 189 (9): 4546–55. https://doi.org/10.4049/jimmunol.1103007.

Sato, Atsushi, Naoka Kamio, Asumi Yokota, Yoshihiro Hayashi, Akihiro Tamura, Yasuo Miura, Taira Maekawa, and Hideyo Hirai. 2020. "C/EBPβ Isoforms Sequentially Regulate Regenerating Mouse Hematopoietic Stem/Progenitor Cells." *Blood Advances* 4 (14): 3343–56. https://doi.org/10.1182/bloodadvances.2018022913.

Satoh, Takashi, Katsuhiro Nakagawa, Fuminori Sugihara, Ryusuke Kuwahara, Motooki Ashihara, Fumihiro Yamane, Yosuke Minowa, et al. 2017. "Identification of an Atypical Monocyte and Committed Progenitor Involved in Fibrosis." *Nature* 541 (7635): 96–101. https://doi.org/10.1038/nature20611.

Schäbitz, A., C. Hillig, M. Mubarak, M. Jargosch, A. Farnoud, E. Scala, N. Kurzen, et al. 2022. "Spatial Transcriptomics Landscape of Lesions from Non-Communicable Inflammatory Skin Diseases." *Nature Communications* 13 (1): 7729. https://doi.org/10.1038/s41467-022-35319-w.

Schäkel, K., M. P. Schön, and K. Ghoreschi. 2016. "[Pathogenesis of psoriasis]." *Der Hautarzt; Zeitschrift Fur Dermatologie, Venerologie, Und Verwandte Gebiete* 67 (6): 422–31. https://doi.org/10.1007/s00105-016-3800-8.

Schroeder-Gloeckler, Jill M., Shaikh Mizanoor Rahman, Rachel C. Janssen, Liping Qiao, Jianhua Shao, Michael Roper, Stephanie J. Fischer, et al. 2007. "CCAAT/Enhancer-Binding Protein Beta Deletion Reduces Adiposity, Hepatic Steatosis, and Diabetes in Lepr(Db/Db) Mice." *The Journal of Biological Chemistry* 282 (21): 15717–29. https://doi.org/10.1074/jbc.M701329200.

Screpanti, I., L. Romani, P. Musiani, A. Modesti, E. Fattori, D. Lazzaro, C. Sellitto, S. Scarpa, D. Bellavia, and G. Lattanzio. 1995. "Lymphoproliferative Disorder and Imbalanced T-Helper Response in C/EBP Beta-Deficient Mice." *The EMBO Journal* 14 (9): 1932–41. https://doi.org/10.1002/j.1460-2075.1995.tb07185.x.

Sebastian, Thomas, Radek Malik, Sara Thomas, Julien Sage, and Peter Frederick Johnson. 2005. "C/EBPbeta Cooperates with RB:E2F to Implement Ras(V12)-Induced Cellular Senescence." *The EMBO Journal* 24 (18): 3301–12. https://doi.org/10.1038/sj.emboj.7600789.

Segre, Julia A. 2006. "Epidermal Barrier Formation and Recovery in Skin Disorders." *The Journal of Clinical Investigation* 116 (5): 1150–58. https://doi.org/10.1172/JCI28521.

Shabgah, Arezoo Gowhari, Jamshid Gholizadeh Navashenaq, Omid Gohari Shabgah, Hamed Mohammadi, and Amirhossein Sahebkar. 2017. "Interleukin-22 in Human Inflammatory Diseases and Viral Infections." *Autoimmunity Reviews* 16 (12): 1209–18. https://doi.org/10.1016/j.autrev.2017.10.004.

Shao, Keke, Weilin Pu, Jianfeng Zhang, Shicheng Guo, Fei Qian, Ingrid Glurich, Qing Jin, et al. 2021. "DNA Hypermethylation Contributes to Colorectal Cancer Metastasis by Regulating the Binding of CEBPB and TFCP2 to the CPEB1 Promoter." *Clinical Epigenetics* 13 (1): 89. https://doi.org/10.1186/s13148-021-01071-z.

Shen, Fang, Zihua Hu, Jaya Goswami, and Sarah L. Gaffen. 2006. "Identification of Common Transcriptional Regulatory Elements in Interleukin-17 Target Genes." *The Journal of Biological Chemistry* 281 (34): 24138–48. https://doi.org/10.1074/jbc.M604597200.

Shen, Fang, Matthew J. Ruddy, Pascale Plamondon, and Sarah L. Gaffen. 2005. "Cytokines Link Osteoblasts and Inflammation: Microarray Analysis of Interleukin-17- and TNF-Alpha-Induced Genes in Bone Cells." *Journal of Leukocyte Biology* 77 (3): 388–99. https://doi.org/10.1189/jlb.0904490.

Shengyuan, Liu, Yao Songpo, Wei Wen, Tian Wenjing, Zhang Haitao, and Wang Binyou. 2009. "Hepatitis C Virus and Lichen Planus: A Reciprocal Association Determined by a Meta-Analysis." *Archives of Dermatology* 145 (9): 1040–47. https://doi.org/10.1001/archdermatol.2009.200.

Simpson-Abelson, Michelle R., Erin E. Childs, M. Carolina Ferreira, Shrinivas Bishu, Heather R. Conti, and Sarah L. Gaffen. 2015. "C/EBPβ Promotes Immunity to Oral Candidiasis through Regulation of β-Defensins." *PLoS ONE* 10 (8): e0136538. https://doi.org/10.1371/journal.pone.0136538.

Simpson-Abelson, Michelle R., Gerard Hernandez-Mir, Erin E. Childs, J. Agustin Cruz, Amanda C. Poholek, Ansuman Chattopadhyay, Sarah L. Gaffen, and Mandy J. McGeachy. 2017. "CCAAT/Enhancer-Binding Protein β Promotes Pathogenesis of EAE." *Cytokine* 92 (April): 24–32. https://doi.org/10.1016/j.cyto.2017.01.005.

Slivka, Peter F., Chen-Lin Hsieh, Alex Lipovsky, Steven D. Pratt, John Locklear, Marian T. Namovic, Heath A. McDonald, et al. 2019. "Small Molecule and Pooled CRISPR Screens Investigating IL17 Signaling Identify BRD2 as a Novel Contributor to Keratinocyte Inflammatory Responses." *ACS Chemical Biology* 14 (5): 857–72. https://doi.org/10.1021/acschembio.8b00260.

Smink, Jeske J., and Achim Leutz. 2010. "Rapamycin and the Transcription Factor C/EBPbeta as a Switch in Osteoclast Differentiation: Implications for Lytic Bone Diseases." *Journal of Molecular Medicine (Berlin, Germany)* 88 (3): 227–33. https://doi.org/10.1007/s00109-009-0567-8.

Sontheimer, Richard D. 2009. "Lichenoid Tissue Reaction/Interface Dermatitis: Clinical and Histological Perspectives." *The Journal of Investigative Dermatology* 129 (5): 1088–99. https://doi.org/10.1038/sj.jid.2009.42.

Sperling, Tanya, Monika Ołdak, Barbara Walch-Rückheim, Claudia Wickenhauser, John Doorbar, Herbert Pfister, Magdalena Malejczyk, Sławomir Majewski, Andrew C. Keates, and Sigrun Smola. 2012. "Human Papillomavirus Type 8 Interferes with a Novel C/EBPβ-Mediated Mechanism of Keratinocyte CCL20 Chemokine Expression and Langerhans Cell Migration." *PLoS Pathogens* 8 (7): e1002833. https://doi.org/10.1371/journal.ppat.1002833.

Stein, B., and A. S. Baldwin. 1993. "Distinct Mechanisms for Regulation of the Interleukin-8 Gene Involve Synergism and Cooperativity between C/EBP and NF-Kappa B." *Molecular and Cellular Biology* 13 (11): 7191–98. https://doi.org/10.1128/mcb.13.11.7191-7198.1993.

Stein, Liana Roberts, and Shin-ichiro Imai. 2012. "The Dynamic Regulation of NAD Metabolism in Mitochondria." *Trends in Endocrinology & Metabolism*, Special Issue: The evolving role of mitochondria in metabolism, 23 (9): 420–28. https://doi.org/10.1016/j.tem.2012.06.005.

Sterken, Britt A., Tobias Ackermann, Christine Müller, Hidde R. Zuidhof, Gertrud Kortman, Alejandra Hernandez-Segura, Mathilde Broekhuis, Diana Spierings, Victor Guryev, and Cornelis F. Calkhoven. 2022. "C/EBPβ Isoform-Specific Regulation of Migration and Invasion in Triple-Negative Breast Cancer Cells." *NPJ Breast Cancer* 8 (1): 11. https://doi.org/10.1038/s41523-021-00372-z.

Sterneck, E., S. Zhu, A. Ramirez, J. L. Jorcano, and R. C. Smart. 2006. "Conditional Ablation of C/EBP Beta Demonstrates Its Keratinocyte-Specific Requirement for Cell Survival and Mouse Skin Tumorigenesis." *Oncogene* 25 (8): 1272–76. https://doi.org/10.1038/sj.onc.1209144.

Sterry, W., B. E. Strober, A. Menter, and International Psoriasis Council. 2007. "Obesity in Psoriasis: The Metabolic, Clinical and Therapeutic Implications. Report of an Interdisciplinary Conference and Review." *The British Journal of Dermatology* 157 (4): 649–55. https://doi.org/10.1111/j.1365-2133.2007.08068.x.

Steven, A. C., M. E. Bisher, D. R. Roop, and P. M. Steinert. 1990. "Biosynthetic Pathways of Filaggrin and Loricrin--Two Major Proteins Expressed by Terminally Differentiated Epidermal Keratinocytes." *Journal of Structural Biology* 104 (1–3): 150–62. https://doi.org/10.1016/1047-8477(90)90071-j.

Swift, Joseph, and Gloria Coruzzi. 2017. "A Matter of Time - How Transient Transcription Factor Interactions Create Dynamic Gene Regulatory Networks." *Biochimica et Biophysica Acta* 1860 (1): 75–83. https://doi.org/10.1016/j.bbagrm.2016.08.007.

Swoboda, Alexander, Robert Soukup, Oliver Eckel, Katharina Kinslechner, Bettina Wingelhofer, David Schörghofer, Christina Sternberg, et al. 2021. "STAT3 Promotes Melanoma Metastasis by CEBP-Induced Repression of the MITF Pathway." *Oncogene* 40 (6): 1091–1105. https://doi.org/10.1038/s41388-020-01584-6.

Takeshita, Junko, Sungat Grewal, Sinéad M. Langan, Nehal N. Mehta, Alexis Ogdie, Abby S. Van Voorhees, and Joel M. Gelfand. 2017. "Psoriasis and Comorbid Diseases: Epidemiology." *Journal of the American Academy of Dermatology* 76 (3): 377–90. https://doi.org/10.1016/j.jaad.2016.07.064.

Tamura, Akihiro, Hideyo Hirai, Asumi Yokota, Atsushi Sato, Tsukimi Shoji, Takahiro Kashiwagi, Masaki Iwasa, Aya Fujishiro, Yasuo Miura, and Taira Maekawa. 2015. "Accelerated Apoptosis of Peripheral Blood Monocytes in Cebpb-Deficient Mice." *Biochemical and Biophysical Research Communications* 464 (2): 654–58. https://doi.org/10.1016/j.bbrc.2015.07.045.

Tanaka, T., S. Akira, K. Yoshida, M. Umemoto, Y. Yoneda, N. Shirafuji, H. Fujiwara, S. Suematsu, N. Yoshida, and T. Kishimoto. 1995. "Targeted Disruption of the NF-IL6 Gene Discloses Its Essential Role in Bacteria Killing and Tumor Cytotoxicity by Macrophages." *Cell* 80 (2): 353–61. https://doi.org/10.1016/0092-8674(95)90418-2.

Tengku-Muhammad, T. S., T. R. Hughes, H. Ranki, A. Cryer, and D. P. Ramji. 2000. "Differential Regulation of Macrophage CCAAT-Enhancer Binding Protein Isoforms by Lipopolysaccharide and Cytokines." *Cytokine* 12 (9): 1430–36. https://doi.org/10.1006/cyto.2000.0711.

Th, Huang, Uthe Jj, Bearson Sm, Demirkale Cy, Nettleton D, Knetter S, Christian C, Ramer-Tait Ae, Wannemuehler Mj, and Tuggle Ck. 2011. "Distinct Peripheral Blood RNA Responses to Salmonella in Pigs Differing in Salmonella Shedding Levels: Intersection of IFNG, TLR and MiRNA Pathways." *PloS One* 6 (12). https://doi.org/10.1371/journal.pone.0028768.

Tong, Philip L., Ben Roediger, Natasha Kolesnikoff, Maté Biro, Szun S. Tay, Rohit Jain, Lisa E. Shaw, Michele A. Grimbaldeston, and Wolfgang Weninger. 2015. "The Skin Immune Atlas: Three-Dimensional Analysis of Cutaneous Leukocyte Subsets by Multiphoton Microscopy." *The Journal of Investigative Dermatology* 135 (1): 84–93. https://doi.org/10.1038/jid.2014.289.

Tsukada, Junichi, Yasuhiro Yoshida, Yoshihiko Kominato, and Philip E. Auron. 2011. "The CCAAT/Enhancer (C/EBP) Family of Basic-Leucine Zipper (BZIP) Transcription Factors Is a Multifaceted Highly-Regulated System for Gene Regulation." *Cytokine* 54 (1): 6–19. https://doi.org/10.1016/j.cyto.2010.12.019.

Ushijima, Takahiro, Ken Okazaki, Hidetoshi Tsushima, and Yukihide Iwamoto. 2014. "CCAAT/Enhancer-Binding Protein β Regulates the Repression of Type II Collagen Expression during the Differentiation from Proliferative to Hypertrophic Chondrocytes." *The Journal of Biological Chemistry* 289 (5): 2852–63. https://doi.org/10.1074/jbc.M113.492843.

Vallejo, M., D. Ron, C. P. Miller, and J. F. Habener. 1993. "C/ATF, a Member of the Activating Transcription Factor Family of DNA-Binding Proteins, Dimerizes with CAAT/Enhancer-Binding Proteins and Directs Their Binding to CAMP Response Elements." *Proceedings of the National Academy of Sciences of the United States of America* 90 (10): 4679–83. https://doi.org/10.1073/pnas.90.10.4679.

Veremeyko, Tatyana, Amanda W. Y. Yung, Daniel C. Anthony, Tatyana Strekalova, and Eugene D. Ponomarev. 2018. "Early Growth Response Gene-2 Is Essential for M1 and M2 Macrophage Activation and Plasticity by Modulation of the Transcription Factor CEBPβ." *Frontiers in Immunology* 9: 2515. https://doi.org/10.3389/fimmu.2018.02515.

Vičić, Marijana, Nika Hlača, Marija Kaštelan, Ines Brajac, Vlatka Sotošek, and Larisa Prpić Massari. 2023. "Comprehensive Insight into Lichen Planus Immunopathogenesis." *International Journal of Molecular Sciences* 24 (3): 3038. https://doi.org/10.3390/ijms24033038.

Vidarsdottir, Linda, Rita Valador Fernandes, Vasilios Zachariadis, Ishani Das, Elin Edsbäcker, Ingibjorg Sigvaldadottir, Alireza Azimi, et al. 2020. "Silencing of CEBPB-AS1 Modulates CEBPB Expression and Resensitizes BRAF-Inhibitor Resistant Melanoma Cells to Vemurafenib." *Melanoma Research* 30 (5): 443–54. https://doi.org/10.1097/CMR.0000000000000675.

Volz, Thomas, Susanne Kaesler, and Tilo Biedermann. 2012. "Innate Immune Sensing 2.0 - from Linear Activation Pathways to Fine Tuned and Regulated Innate Immune Networks." *Experimental Dermatology* 21 (1): 61–69. https://doi.org/10.1111/j.1600-0625.2011.01393.x.

Wang, Dan, Li Yang, Weina Yu, Qian Wu, Jingyao Lian, Feng Li, Shasha Liu, et al. 2019. "Colorectal Cancer Cell-Derived CCL20 Recruits Regulatory T Cells to Promote Chemoresistance via FOXO1/CEBPB/NF-KB Signaling." *Journal for Immunotherapy of Cancer* 7 (1): 215. https://doi.org/10.1186/s40425-019-0701-2.

Wang, Jen-Hung, and Sung-Jen Hung. 2021. "Lichen Planus Associated with Hepatitis B, Hepatitis C, and Liver Cirrhosis in a Nationwide Cohort Study." *Journal of the American Academy of Dermatology* 84 (4): 1085–86. https://doi.org/10.1016/j.jaad.2020.07.073.

Wang, Nan, Hongwei Liang, and Ke Zen. 2014. "Molecular Mechanisms That Influence the Macrophage M1-M2 Polarization Balance." *Frontiers in Immunology* 5: 614. https://doi.org/10.3389/fimmu.2014.00614.

Wang, Wei, Robert N. Taylor, Indrani C. Bagchi, and Milan K. Bagchi. 2012. "Regulation of Human Endometrial Stromal Proliferation and Differentiation by C/EBPβ Involves Cyclin E-Cdk2 and STAT3." *Molecular Endocrinology (Baltimore, Md.)* 26 (12): 2016–30. https://doi.org/10.1210/me.2012-1169.

Wang, Wuyuntana, null Yuhai, Huan Wang, null Chasuna, and null Bagenna. 2019. "Astilbin Reduces ROS Accumulation and VEGF Expression through Nrf2 in Psoriasis-like Skin Disease." *Biological Research* 52 (1): 49. https://doi.org/10.1186/s40659-019-0255-2.

Wang, Xiaoyang, Weili Cheng, Xiaopan Chen, Yanan Gong, Guangjie Wang, Xiaoxue Zhang, and Yuanyuan Qi. 2022. "Inhibition of CEBPB Attenuates Lupus Nephritis via Regulating Pim-1 Signaling." *Mediators of Inflammation* 2022: 2298865. https://doi.org/10.1155/2022/2298865.

Wang, Yinghan, Shuli Li, and Chunying Li. 2019. "Perspectives of New Advances in the Pathogenesis of Vitiligo: From Oxidative Stress to Autoimmunity." *Medical Science Monitor: International Medical Journal of Experimental and Clinical Research* 25 (February): 1017–23. https://doi.org/10.12659/MSM.914898.

Wang, Zhengrong, Jinghuan Pang, Lingyan Wang, Qinhui Dong, and Dan Jin. 2022. "CEBPB Regulates the Bile Acid Receptor FXR to Accelerate Colon Cancer Progression by Modulating Aerobic Glycolysis." *Journal of Clinical Laboratory Analysis* 36 (11): e24703. https://doi.org/10.1002/jcla.24703.

Wassermann-Dozorets, Rina, and Menachem Rubinstein. 2017. "C/EBPβ LIP Augments Cell Death by Inducing Osteoglycin." *Cell Death & Disease* 8 (4): e2733. https://doi.org/10.1038/cddis.2017.155.

Wedel, A., and H. W. Ziegler-Heitbrock. 1995. "The C/EBP Family of Transcription Factors." *Immunobiology* 193 (2–4): 171–85. https://doi.org/10.1016/s0171-2985(11)80541-3.

Weihua, X., V. Kolla, and D. V. Kalvakolanu. 1997. "Interferon Gamma-Induced Transcription of the Murine ISGF3gamma (P48) Gene Is Mediated by Novel Factors." *Proceedings of the National Academy of Sciences of the United States of America* 94 (1): 103–8. https://doi.org/10.1073/pnas.94.1.103.

Wheaton, William W., Samuel E. Weinberg, Robert B. Hamanaka, Saul Soberanes, Lucas B. Sullivan, Elena Anso, Andrea Glasauer, et al. 2014. "Metformin Inhibits Mitochondrial Complex I of Cancer Cells to Reduce Tumorigenesis." *ELife* 3 (May): e02242. https://doi.org/10.7554/eLife.02242.

Williams, S. C., N. D. Angerer, and P. F. Johnson. 1997. "C/EBP Proteins Contain Nuclear Localization Signals Imbedded in Their Basic Regions." *Gene Expression* 6 (6): 371–85.

Williams, S. C., C. A. Cantwell, and P. F. Johnson. 1991. "A Family of C/EBP-Related Proteins Capable of Forming Covalently Linked Leucine Zipper Dimers in Vitro." *Genes & Development* 5 (9): 1553–67. https://doi.org/10.1101/gad.5.9.1553.

Wolk, Kerstin, Ellen Witte, Elizabeth Wallace, Wolf-Dietrich Döcke, Stefanie Kunz, Khusru Asadullah, Hans-Dieter Volk, Wolfram Sterry, and Robert Sabat. 2006. "IL-22 Regulates the Expression of Genes Responsible for Antimicrobial Defense, Cellular Differentiation, and Mobility in Keratinocytes: A Potential Role in Psoriasis." *European Journal of Immunology* 36 (5): 1309–23. https://doi.org/10.1002/eji.200535503.

Wroński, Adam, and Piotr Wójcik. 2022. “Impact of ROS-Dependent Lipid Metabolism on Psoriasis Pathophysiology.” *International Journal of Molecular Sciences* 23 (20): 12137. https://doi.org/10.3390/ijms232012137.

Wu, Dan, Yanqiong Zhang, Chunhui Zhao, Qiuyue Li, Junhong Zhang, Jiaxin Han, Zhijian Xu, et al. 2022. “Disruption of C/EBPβ-Clec7a Axis Exacerbates Neuroinflammatory Injury via NLRP3 Inflammasome-Mediated Pyroptosis in Experimental Neuropathic Pain.” *Journal of Translational Medicine* 20 (1): 583. https://doi.org/10.1186/s12967-022-03779-9.

Wu, Z., Y. Xie, N. L. Bucher, and S. R. Farmer. 1995. “Conditional Ectopic Expression of C/EBP Beta in NIH-3T3 Cells Induces PPAR Gamma and Stimulates Adipogenesis.” *Genes & Development* 9 (19): 2350–63. https://doi.org/10.1101/gad.9.19.2350.

Xiao, W., L. Wang, X. Yang, T. Chen, D. Hodge, P. F. Johnson, and W. Farrar. 2001. “CCAAT/Enhancer-Binding Protein Beta Mediates Interferon-Gamma-Induced P48 (ISGF3-Gamma) Gene Transcription in Human Monocytic Cells.” *The Journal of Biological Chemistry* 276 (26): 23275–81. https://doi.org/10.1074/jbc.M010047200.

Xu, Fengli, Jixiang Xu, Xia Xiong, and Yongqiong Deng. 2019. “Salidroside Inhibits MAPK, NF-KB, and STAT3 Pathways in Psoriasis-Associated Oxidative Stress via SIRT1 Activation.” *Redox Report: Communications in Free Radical Research* 24 (1): 70–74. https://doi.org/10.1080/13510002.2019.1658377.

Xu, Jiang, Linqing Liu, Lin Gan, Yuanyuan Hu, Ping Xiang, Yan Xing, Jie Zhu, and Shandong Ye. 2021. “Berberine Acts on C/EBPβ/LncRNA Gas5/MiR-18a-5p Loop to Decrease the Mitochondrial ROS Generation in HK-2 Cells.” *Frontiers in Endocrinology* 12: 675834. https://doi.org/10.3389/fendo.2021.675834.

Yamamoto, Seiji, Tomoko Hagihara, Yoshiyuki Horiuchi, Akira Okui, Shotaro Wani, Tokuyuki Yoshida, Takao Inoue, et al. 2017. “Mediator Cyclin-Dependent Kinases Upregulate Transcription of Inflammatory Genes in Cooperation with NF-KB and C/EBPβ on Stimulation of Toll-like Receptor 9.” *Genes to Cells: Devoted to Molecular & Cellular Mechanisms* 22 (3): 265–76. https://doi.org/10.1111/gtc.12475.

Yang, Ni, Hai Wang, Rui Zhang, Zequn Niu, Shaowei Zheng, and Zhengliang Zhang. 2021. “C/EBP β Mediates the Aberrant Inflammatory Response and Cell Cycle Arrest in Lps-Stimulated Human Renal Tubular Epithelial Cells by Regulating NF-KB Pathway.” *Archives of Medical Research* 52 (6): 603–10. https://doi.org/10.1016/j.arcmed.2021.03.008.

Yang, Xuejun, Tongde Du, Xiang Wang, Yingqiu Zhang, Wanglai Hu, Xiaofeng Du, Lin Miao, and Chuanchun Han. 2015. “IDH1, a CHOP and C/EBPβ-Responsive Gene under ER Stress, Sensitizes Human Melanoma Cells to Hypoxia-Induced Apoptosis.” *Cancer Letters* 365 (2): 201–10. https://doi.org/10.1016/j.canlet.2015.05.027.

Yu, Shanshan, Ying Lu, Ming Zong, Qi Tan, and Lieying Fan. 2019. “Hypoxia-Induced MiR-191-C/EBPβ Signaling Regulates Cell Proliferation and Apoptosis of Fibroblast-like Synoviocytes from Patients with Rheumatoid Arthritis.” *Arthritis Research & Therapy* 21 (1): 78. https://doi.org/10.1186/s13075-019-1861-7.

Zahid, M. D. Khurshidul, Michael Rogowski, Christopher Ponce, Mahua Choudhury, Naima Moustaid-Moussa, and Shaikh M. Rahman. 2020. “CCAAT/Enhancer-Binding Protein Beta (C/EBPβ) Knockdown Reduces Inflammation, ER Stress, and Apoptosis, and Promotes Autophagy in OxLDL-Treated RAW264.7 Macrophage Cells.” *Molecular and Cellular Biochemistry* 463 (1–2): 211–23. https://doi.org/10.1007/s11010-019-03642-4.

Zenz, Rainer, Robert Eferl, Clemens Scheinecker, Kurt Redlich, Josef Smolen, Helia B. Schonthaler, Lukas Kenner, Erwin Tschachler, and Erwin F. Wagner. 2008. “Activator Protein 1 (Fos/Jun) Functions in Inflammatory Bone and Skin Disease.” *Arthritis Research & Therapy* 10 (1): 201. https://doi.org/10.1186/ar2338.

Zhang, Jiang-Wen, Qi-Qun Tang, Charles Vinson, and M. Daniel Lane. 2004. “Dominant-Negative C/EBP Disrupts Mitotic Clonal Expansion and Differentiation of 3T3-L1 Preadipocytes.” *Proceedings of the National Academy of Sciences of the United States of America* 101 (1): 43–47. https://doi.org/10.1073/pnas.0307229101.

Zhang, Jinlong, Jiawei Jiang, Guofeng Bao, Guanhua Xu, Lingling Wang, Jiajia Chen, Chu Chen, et al. 2020. “Interaction between C/EBPβ and RUNX2 Promotes Apoptosis of Chondrocytes during Human Lumbar Facet Joint Degeneration.” *Journal of Molecular Histology* 51 (4): 401–10. https://doi.org/10.1007/s10735-020-09891-8.

Zhang, Kaiji, Jian Li, Wentong Meng, Hongyun Xing, and Yiming Yang. 2010. “C/EBPβ and CHOP Participate in Tanshinone IIA-Induced Differentiation and Apoptosis of Acute Promyelocytic Leukemia Cells in Vitro.” *International Journal of Hematology* 92 (4): 571–78. https://doi.org/10.1007/s12185-010-0686-6.

Zhang, Y., and W. N. Rom. 1993. “Regulation of the Interleukin-1 Beta (IL-1 Beta) Gene by Mycobacterial Components and Lipopolysaccharide Is Mediated by Two Nuclear Factor-IL6 Motifs.” *Molecular and Cellular Biology* 13 (6): 3831–37. https://doi.org/10.1128/mcb.13.6.3831-3837.1993.

Zhang, Yiya, Yangfan Li, Lei Zhou, Xin Yuan, Yaling Wang, Qing Deng, Zhili Deng, et al. 2022. “Nav1.8 in Keratinocytes Contributes to ROS-Mediated Inflammation in Inflammatory Skin Diseases.” *Redox Biology* 55 (August): 102427. https://doi.org/10.1016/j.redox.2022.102427.

Zhang, Zhuzhen, Zhenzhen Zi, Eunice E. Lee, Jiawei Zhao, Diana C. Contreras, Andrew P. South, E. Dale Abel, et al. 2018. “Differential Glucose Requirement in Skin Homeostasis and Injury Identifies a Therapeutic Target for Psoriasis.” *Nature Medicine* 24 (5): 617–27. https://doi.org/10.1038/s41591-018-0003-0.

Zhao, Nai-Qian, Xiao-Yan Li, Li Wang, Zi-Ling Feng, Xi-Fen Li, Yan-Fang Wen, and Jin-Xiang Han. 2017. “Palmitate Induces Fat Accumulation by Activating C/EBPβ-Mediated G0S2 Expression in HepG2 Cells.” *World Journal of Gastroenterology* 23 (43): 7705–15. https://doi.org/10.3748/wjg.v23.i43.7705.

Zheng, Danping, Timur Liwinski, and Eran Elinav. 2020. “Inflammasome Activation and Regulation: Toward a Better Understanding of Complex Mechanisms.” *Cell Discovery* 6 (1): 1–22. https://doi.org/10.1038/s41421-020-0167-x.

Zheng, Yan, Dimitry M. Danilenko, Patricia Valdez, Ian Kasman, Jeffrey Eastham-Anderson, Jianfeng Wu, and Wenjun Ouyang. 2007. “Interleukin-22, a T(H)17 Cytokine, Mediates IL-23-Induced Dermal Inflammation and Acanthosis.” *Nature* 445 (7128): 648–51. https://doi.org/10.1038/nature05505.

Zhou, Qiang, Ulrich Mrowietz, and Martin Rostami-Yazdi. 2009. “Oxidative Stress in the Pathogenesis of Psoriasis.” *Free Radical Biology & Medicine* 47 (7): 891–905. https://doi.org/10.1016/j.freeradbiomed.2009.06.033.

Zhou, Qing, Xiotian Sun, Nicolas Pasquier, Parvaneh Jefferson, Trang T. T. Nguyen, Markus D. Siegelin, James M. Angelastro, and Lloyd A. Greene. 2021. “Cell-Penetrating CEBPB and CEBPD Leucine Zipper Decoys as Broadly Acting Anti-Cancer Agents.” *Cancers* 13 (10): 2504. https://doi.org/10.3390/cancers13102504.

Zhou, Xue, Youdong Chen, Lian Cui, Yuling Shi, and Chunyuan Guo. 2022. “Advances in the Pathogenesis of Psoriasis: From Keratinocyte Perspective.” *Cell Death & Disease* 13 (1): 1–13. https://doi.org/10.1038/s41419-022-04523-3.

Zhu, S., H. S. Oh, M. Shim, E. Sterneck, P. F. Johnson, and R. C. Smart. 1999. “C/EBPbeta Modulates the Early Events of Keratinocyte Differentiation Involving Growth Arrest and Keratin 1 and Keratin 10 Expression.” *Molecular and Cellular Biology* 19 (10): 7181–90. https://doi.org/10.1128/MCB.19.10.7181.

Zhu, Songyun, Kyungsil Yoon, Esta Sterneck, Peter F. Johnson, and Robert C. Smart. 2002. “CCAAT/Enhancer Binding Protein-Beta Is a Mediator of Keratinocyte Survival and Skin Tumorigenesis Involving Oncogenic Ras Signaling.” *Proceedings of the National Academy of Sciences of the United States of America* 99 (1): 207–12. https://doi.org/10.1073/pnas.012437299.

Żychowska, Magdalena, Zdzislaw Woźniak, and Wojciech Baran. 2021. “Immunohistochemical Analysis of the Expression of Selected Cell Lineage Markers (CD4, CD8, CD68, c-Kit, Foxp3, CD56, CD20) in Cutaneous Variant of Lichen Planus.” *International Journal of Dermatology* 60 (9): 1097–1101. https://doi.org/10.1111/ijd.15437.